STUDIES OF POLYCYCLIC AROMATIC HYDROCARBONS IN DUNGENESS CRABS: BIOMONITORING, PHYSIOLOGICALLY BASED TOXICOKINETIC MODEL, AND HUMAN HEALTH RISK ASSESSMENT

by

Curtis Van Eickhoff
P.B.D. Simon Fraser University, 1991
B.Sc. University of British Columbia, 1988

THESIS SUBMITTED IN PARTIAL FULFILLMENT OF
THE REQUIREMENTS FOR THE DEGREE OF

DOCTOR OF PHILOSOPHY

In the Department
of
Biological Sciences

SIMON FRASER UNIVERSITY
Fall 2004

APPROVAL

Name: Curtis Eickhoff

Degree: Doctor of Philosophy

Title of Thesis:

Studies of polycyclic aromatic hydrocarbons in Dungeness crabs: Biomonitoring, physiologically based toxicokinetic model, and human health risk assessment

Examining Committee:

Chair: Dr. E. Elle

Dr. F.C.P. Law, Professor, Senior Supervisor
Department of Biological Sciences, S.F.U.

Dr. R.A. Nicholson, Associate Professor
Department of Biological Sciences, S.F.U.

Dr. C.J. Kennedy, Associate Professor
Department of Biological Sciences, S.F.U.

Dr. M.M. Moore, Associate Professor
Department of Biological Sciences, S.F.U.
Public Examiner

Dr. K.J. Hall, Professor
Department of Civil Engineering and
Institute for Resources and Environment, U.B.C.
External Examiner

December 8th, 2004
Date Approved

SIMON FRASER UNIVERSITY

PARTIAL COPYRIGHT LICENCE

ABSTRACT

Polycyclic aromatic hydrocarbons (PAH) are ubiquitous pollutants released into the environment from the incomplete combustion of organic material and petrochemical sources. PAH are persistent molecules that partition into sediments and biota in the aquatic environment. PAH such as benzo[a]pyrene, are of concern because they are metabolised into potentially carcinogenic chemicals that can cause tumours in fish and mammals.

The purpose of this research was three-fold, (1) to explore the use of the dungeness crab for monitoring PAH in the aquatic environment, (2) to adapt a physiologically based toxicokinetic (PBTK) model to describe the disposition of benzo[a]pyrene in the dungeness crab, and (3) to examine the lifetime cancer risk to humans associated with the consumption of PAH contaminated crabs.

Kitimat Arm is an aquatic ecosystem in British Columbia, contaminated with PAH by industrial processes. Dungeness crabs were collected at several sites within this fjord, and concentrations of PAH were determined in the crabs by GC/MS. A synchronous fluorescence spectroscopy assay was adapted to screen crab haemolymph samples for pyrene and it's metabolites. PAH could be readily determined in the tissues of crabs and tissue concentrations decreased with distance from the source of the PAH contamination. Therefore, crabs were an effective tool for monitoring PAH contamination in the fjord.

A PBTK model was adapted to describe the disposition of benzo[a]pyrene in the dungeness crab. The model was composed of seven compartments representing the major tissues of the crab. The flux of benzo[a]pyrene in each compartment was described by algebraic and mass-balance differential equations, coded into Visual Basic and solved numerically by an Excel spreadsheet. The model was implemented with parameters, calibrated, and validated using data obtained empirically. The model successfully predicted benzo[a]pyrene concentrations in the tissue compartments after simulated exposures to benzo[a]pyrene by intravascular, oral and water exposure routes.

A human health risk assessment was conducted to evaluate the lifetime cancer risk associated with consumption of PAH contaminated crabs from Kitimat Arm. Deterministic and stochastic risk assessment models were implemented. There was an excess cancer risk associated with consumption of crabs from Hospital Beach, an area near the source of PAH contamination.

DEDICATION

This thesis is dedicated to my family, friends, and co-workers who always believed in my ability to complete this project; and in particular to my father, Manfred Eickhoff, who anticipated my completion of this work with even greater intensity than myself.

My thesis is also dedicated to the late Bill Reid, the great Haida artist who created many inspiring works and polished the places that didn't show.

ACKNOWLEDGEMENTS

I would like to thank my committee members for all of their assistance, Drs. Francis C.P. Law, Russell Nicholson, Chris Kennedy, and Frank Gobas. In particular, Dr. Francis Law gave me the freedom to shape my studies and thesis while providing a great deal of wisdom, support and mutual respect. Also thanks go to my defense examiners Drs. Margo Moore and Ken Hall for their detailed and insightful edits to my thesis.

I would also like acknowledge my labmates: Kim Mark, Thomas Achenbach, Dr. Rostam Namdari, Lorne Sampson, Dr. S. Abedini, Y.T. He, S.X. He, and Dr. Meng for their assistance and cooperation in the laboratory. There are too many collegues to mention with whom I learned and enjoyed the graduate student's experience.

I owe a large debt of gratitude to Dr. Walter Cretney who accommodated me on field trips to Kitimat on Institute of Ocean Sciences research vessels C.S.S. Endeavor and C.S.S. Vector. I would also like to thank the crews for their role in my studies.

I would like to acknowledge the efforts of Dr. Jim McKinley who reviewed my thesis chapters and other Vizon SciTec Inc. (formerly BC Research) staff who encouraged and supported me along this long journey.

I shared a common thesis burden with Karen Kinnee as well as lots of love, respect and mutual admiration along the way.

Finally, I would like to recognise the love and support of my family, Mary, Manfred, and Lewis Eickhoff.

TABLE OF CONTENTS

LIST OF FIGURES

LIST OF TABLES

LIST OF ABBREVIATIONS AND ACRONYMS

ANOVA	Analysis of Variance
ANT	Anthracene
BA	Benz[*a*]anthracene
BaP TEF	Benzo[*a*]pyrene Toxic Equivalent Factors
BAP	Benzo[*a*]pyrene
BF	Benzofluoranthenes
CRY	Chrysene
DMF	Dimethyl formamide
EDL	Estimated Detection Limit
ESSDL	Estimated Sample Specific Detection Limit
FLR	Fluoranthene
GC/MS	Gas Chromatography Mass Spectrometry
GC-MSD	Gas Chromatograph - Mass Selective Detector
HHRA	Human Health Risk Assessment
HPAH	High molecular weight PAH
HPLC	High performance liquid chromatography
IPM	Individual PAH Model
Kow	Octanol/water partition coefficient
LADD	Lifetime Average Daily Dose
LPAH	Low Molecular Weight PAH
MSC	Mixture of Standard Composition
OME	Ontario Ministry of Environment
PAH	Polycyclic Aromatic Hydrocarbon
PBTK	Physiologically Based Toxicokinetic Model
PHN	Phenanthrene
PYR	Pyrene

SD	Standard Deviation
SE	Standard Error
SFS	Synchronous Fluorescence Spectrometry
SIM	Selective Ion Monitoring
TIC	Total Ion Chromatograph
USEPA	US Environmental Protection Agency
WMM	Whole Mixture Model

CHAPTER 1
GENERAL INTRODUCTION

1.1 Introduction

PAH are a group of ubiquitous environmental pollutants. They are generated from the incomplete combustion of organic matter but are ultimately stored in the aquatic environment. PAH are generated as a complex mixture of heterocyclic ringed hydrocarbons, made up of hundreds of different molecules. Most PAH in the marine environment are associated with particulate materials such as black carbon (soot) and appear resistant to degradation and desorption (McGroddy and Farrington, 1995). PAH may also be associated with tars and oils in highly contaminated environments.

1.1.1 Polycyclic Aromatic Hydrocarbons

PAH have been studied as potential human carcinogens for many years. The initial discovery of the link between PAH and cancer is credited to Sir Percivall Pott who reported an increased incidence of scrotal cancer among English chimney sweepers (Bjorseth and Becher, 1986). In the 1930s, PAH were identified as the cause of the carcinogenicity associated with soot and tar (OME, 1997).

PAH may cause other types of toxic effects including skin and eye irritation, immunotoxicity, and developmental toxicity (OME, 1997). However, these effects have

been demonstrated at high experimental doses, while the carcinogenic effects are assumed to occur at very low doses.

Concern about PAH in the aquatic environment is largely related to their persistence in the environment and carcinogenic potential in fish and invertebrates. Some PAH are potent carcinogens for both aquatic and terrestrial animals. PAH are poorly water soluble, lipophilic molecules that partition readily into organic matter. PAH adsorb to particles of organic material in the air or water column, and ultimately settle into soil and sediments. Thus, an unusually high prevalence of oral, dermal and hepatic neoplasms have been observed in bottom-dwelling fish caught in PAH-contaminated waters and sediments (Couch and Harshbarger, 1985). However, the carcinogenicity of PAH appears to vary with the chemical composition of the mixture, the associated matrix, and the bioavailability of the PAH to animals (McGroddy and Farrington, 1995; Krahn et al., 1986; Krahn et al., 1987). Despite the large number of studies on the environmental fate and effects of PAH, very few biomarkers of PAH exposure have been reported for invertebrates in the marine environment. Therefore, this research was conducted to examine the crab, (*Cancer magister* Dana), as an effective species for biomonitoring PAH on the Pacific Coast of North America.

1.1.2 Crabs as Biomonitors

The dungeness crab can be used as a tool for monitoring the presence of polycyclic aromatic hydrocarbons (PAH) in marine and estuarine environments. Generally, fish have been most commonly used to monitor PAH exposure in aquatic life. However, it is often difficult to determine PAH concentrations in fish tissues because

these compounds are readily metabolised and eliminated by fish. Also, fish move around from place to place quickly, and are often only exposed to contaminants for short periods of time.

Mussels have also been used extensively for biomonitoring a variety of contaminants including metals, PAH, and chlorinated organics such as pesticides and dioxins and furans. The Mussel Watch Project has been running since 1986 and involves numerous sites in the United States and around the world. In the year 2000, it was one of the largest, longest running monitoring programs ever conducted (National Status and Trends Program, 2000).

The crab was seen as an alternative to the more commonly studied fish and bivalve species as a biomonitoring tool. While crabs are also important fisheries species, they have several differences that might be seen as attributes for biomonitoring. First, crabs are generally not as mobile as fish, and are intimately associated with sediments that may be contaminated with persistent chemicals such as PAH. Second, crabs and other invertebrates likely have a lower metabolic capacity than fish (Dunn and Fee, 1979). Therefore, it may be expected that PAH may be more readily determined in the tissues of crabs than fish. Also, crabs are considered to have tissues that are richer in fat than fish. Environmental contaminants that are poorly water soluble such as PAH may be expected to accumulate more readily in the fatty tissues of the crab, rather than the leaner muscle of the fish.

The dungeness crab has been used as a species for monitoring dioxins and furan contamination released from pulp mills and other sources on the Pacific Coast (PTI,

1991; Bright *et al.,* 1999; Yunker and Cretney, 1996; Yunker *et al.,* 2002), and it has been shown that crabs can accumulate these persistent, fat soluble compounds in the hepatopancreas (Yunker and Cretney, 1996). Therefore, the dungeness crab was selected as a potentially ideal species for further study in biomonitoring PAH contamination in coastal environments. While mussels and other bivalves may also be well suited to biomonitoring PAH, I saw an opportunity to investigate the utility of the dungeness crab a species that has seen limited use as a biomonitor.

1.1.3 Dungeness Crab

The dungeness crab, (*Cancer magister,* Dana) is found along the Pacific coast of North America. It ranges from the northern shores of the Aleutian Islands in Alaska, to south of San Francisco in California. The dungeness crab preferentially inhabits eel-grass beds and muddy to sandy bottoms, from the low intertidal zone to depths in excess of 600 ft. The dungeness crab is one of the most commercially important shellfish species harvested in many coastal communities.

While crabs measuring approximately 25.5 cm (10 inches) across the back have been harvested off the coast of Washington, the crab seldom exceeds 20 cm (8 inches) and averages just under 18 cm (7 inches) of shell width. The legal harvestable size of male dungeness crabs in British Columbia is 16.4 cm. The dungeness crab has white-tipped claws and a brownish shell.

The dungeness crab eats a wide variety of marine organisms. Stomachs of ocean crabs have been found to contain clams, fish, and crabs, as well as other items, including starfish, worms, squid, snails, and eggs from fish or crabs. The dungeness crab is also

cannibalistic, a fact which has been observed in the laboratory and borne out by examination of stomach contents.

The dungeness crab is also preyed upon by a number of organisms, including fish such as dogfish, hake, halibut, ling cod, sculpins, and wolf eel. The crab is consumed extensively by the octopus, cuttlefish, sea otters, and, of course, humans.

1.1.4 Kitimat Arm

Kitimat Arm was selected as an ideal location to examine the effectiveness of the crab as a biomonitoring tool. Kitimat Arm is part of a large group of fjords located on the northern coast of British Columbia, Canada (Figure 1.1).

Figure 1.1 Map of British Columbia (adapted from Magellan Geographix, 1995)

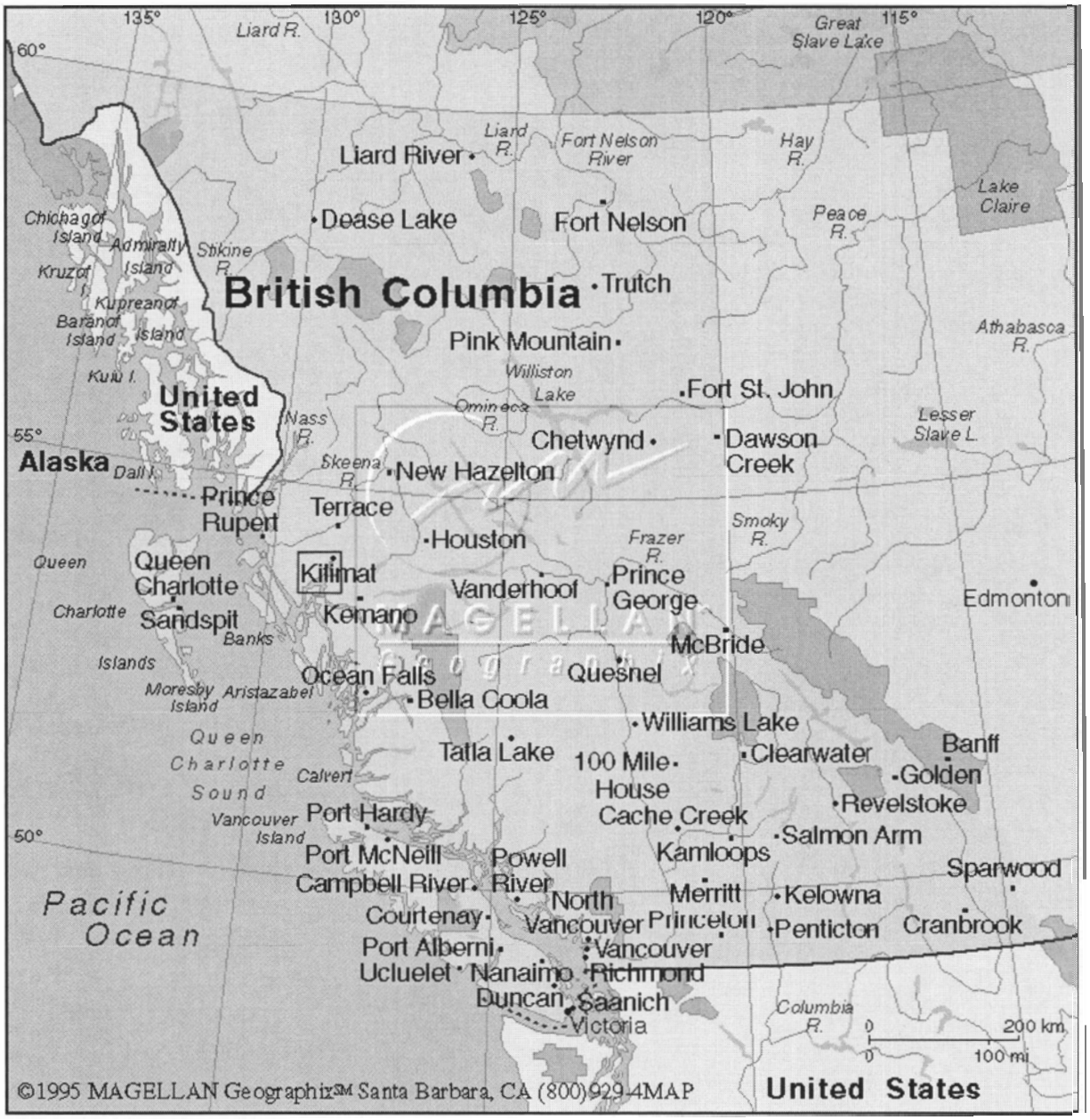

The head of Kitimat Arm is the site of considerable industrial activity including an aluminium smelter, a methanol plant and a pulp mill terminal (Figure 1.2).

Figure 1.2 Kitimat Arm and Douglas Channel, BC, Canada.

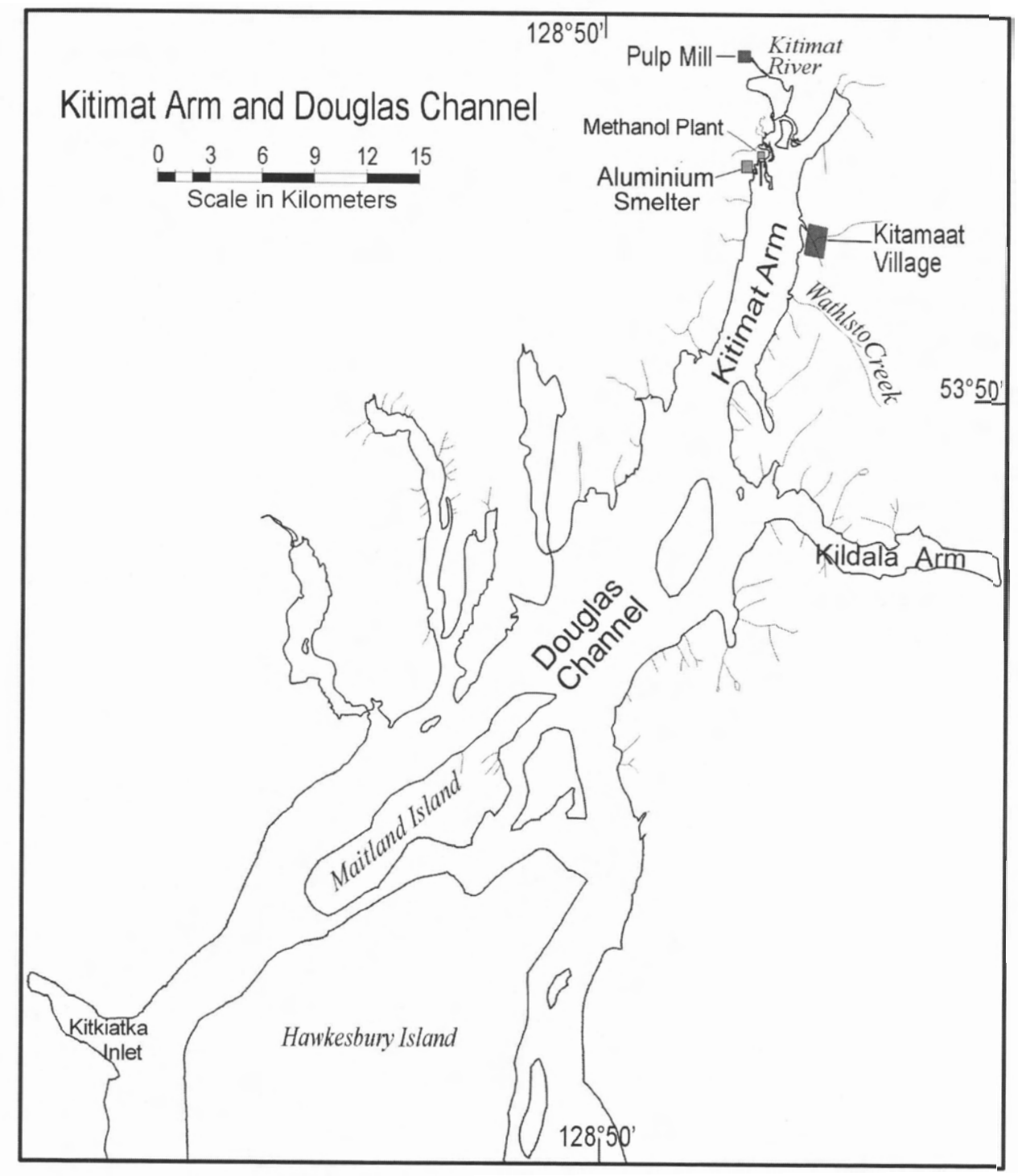

The aluminium smelter is alleged to be the primary source of PAH input into the marine environment through loss of green coke during transport to the smelter and

release of PAH in airborne emissions, waterborne effluents, and surface runoff (Simpson et al., 1996; EVS, 1992).

The town of Kitimat, BC, is situated about four miles from the head of Kitimat Arm. An aboriginal settlement, Kitamaat Village, is located on the eastern shore of Kitimat Arm (Figure 1.2). The largest tribe of aboriginal people settled there is known as the Haisla Nation. The Haisla people subsist on many indigenous aquatic organisms in Kitimat Arm including salmonids, halibut, seaweed, shrimp, seals, and crabs (Kitamaat Village Council, 1996).

1.1.5 Risk Assessment

Risk assessment is the characterisation of the potential adverse health effects of human exposures to environmental hazards (NAS, 1983). The risk assessment process can be divided into four main steps: hazard identification, dose-response assessment, exposure assessment, and risk characterisation. The hazard identification determines if human exposure to an agent could cause an increase in the incidence of an adverse health condition such as cancer or birth defects, etc. Dose-response assessment is the process of characterising the relationship between exposure of a population to an agent and the incidence of adverse health effects. Exposure assessment refers to the process of measuring or estimating the intensity, frequency, and duration of exposure to an agent in the environment (NAS, 1983). Risk characterisation involves the estimation of health effect incidences due to exposure to an agent described by the exposure assessment.

I decided to conduct a human health risk assessment to determine if there was a potential for adverse health effects due to the consumption of PAH contaminated crabs

collected from Kitimat Arm. This seemed to be a very logical use of the crab tissue data describing PAH contamination obtained from the biomonitoring studies. The risk assessment was designed to determine if the local aboriginal population located in Kitamaat Village were at a risk of increased cancer incidence. Presumably, the local peoples who subsist on crabs and other foods obtained from this environment would be at the greatest risk of adverse effects due to the consumption of contaminated crabs.

1.1.6 PBTK Model

Physiologically based pharmacokinetic (PBPK) models have been traditionally developed and used to describe the disposition of drugs in test animal models and humans. More recently, this modelling technique has been used to study the uptake, disposition, and elimination of drugs and antibiotics in fish. Physiologically based toxicokinetic models (PBTK) models have also been developed to predict the tissue concentrations of environmental contaminants in fish species, and to examine the uptake of these chemicals from the water. The PBTK model offers the risk assessor the ability to predict tissue concentrations in an organism based on the concentrations of a given chemical in the environment. Therefore, the PBTK model may used as a tool for predicting tissue concentration data for environmental and human health risk assessments. The PBTK model is a powerful tool because it is scalable and adaptable. A PBTK model developed for one species may be adapted by changing basic physiological parameters so that it can be used to predict tissue concentrations in another species. While this flexibility was initially designed for dealing with differences in scale between

pharmaceutical test models such as rodents, and humans, it lends itself to adaptation for more environmentally relevant species such as fish.

While PBTK models have been previously developed to describe the disposition of PAH such as pyrene in fish, this modelling approach has not been adapted to invertebrate species. Therefore, I chose to determine if a PBTK model designed to describe the disposition of PAH in fish, could be adapted to predict tissue concentrations of benzo[a]pyrene in the dungeness crab.

1.1.7 Benzo[a]pyrene

Benzo[a]pyrene was selected as the model PAH for the development of the PBTK model because it has been shown to be a carcinogenic in numerous animal studies, and is the best characterised PAH in terms of toxicity (U.S. EPA, 1991a). Figure 1.3 shows the structure of benzo[a]pyrene.

Figure 1.3 Structure of benzo[a]pyrene

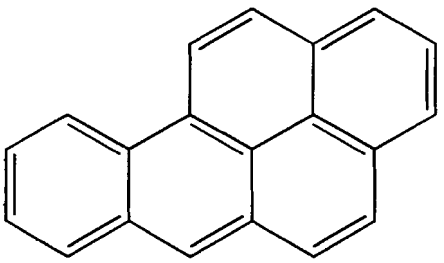

In addition, benzo[a]pyrene is the reference to which all other carcinogenic PAH are compared for risk assessments (Nisbet and LaGoy, 1992; OME, 1997). Both the U.S. Environmental Protection Agency and the Ontario Ministry of Environment relate toxic equivalency or relative potency of carcinogenic PAH to benzo[a]pyrene (Nisbet and

LaGoy, 1992; OME, 1997). The physical and chemical properties of benzo[a]pyrene are summarised in Table 1.1.

Table 1.1 Physical and chemical properties of benzo[a]pyrene[1]

Property	Value
Molecular weight	252.3
Melting point	179°C
Boiling point	310 - 313°C
Vapour pressure	7.0 E-7 Pa
Density	1.351 g/cm^3
Log Kow	6.1
Water solubility	3.8 μg/L

[1](Data source: OME, 1997)

Benzo[a]pyrene is a poorly water soluble PAH with a relatively high octanol water partition coefficient or log Kow. Thus it commonly adsorbs to organic material in the air or in water. Compounds with a high log Kow such as benzo[a]pyrene may be absorbed by aquatic organisms through the diet, or by gill uptake (Gobas and MacKay, 1987; McElroy and Sisson, 1989; Gobas et al. 1993). Benzo[a]pyrene is a relatively stable and persistent molecule that can often be determined in soils, sediments, and biota that have been contaminated with PAH.

1.2 Research Objectives

The purpose of this research was three-fold, (1) to explore the use of the dungeness crab for monitoring PAH in the aquatic environment, (2) to adapt a physiologically based toxicokinetic (PBTK) model to describe the disposition of

benzo[a]pyrene in the dungeness crab, and (3) to determine the lifetime cancer risk to humans associated with the consumption of PAH contaminated crabs.

The remaining chapters of this thesis address these three objectives. Chapters 2 and 3 examine the use of the dungeness crab as a biological tool for monitoring PAH in a coastal estuarine and marine environment. Chapters 4 and 5 describe laboratory experiments conducted to examine the toxicokinetics of benzo[a]pyrene in the dungeness crab for the development, calibration, and validation of the PBTK model for describing the disposition of benzo[a]pyrene in the crab. Finally, Chapters 6 and 7 address the potential for adverse human health effects associated with the consumption of PAH contaminated crabs collected from Kitimat Arm.

CHAPTER 2
DETERMINATION OF POLYCYCLIC AROMATIC HYDROCARBONS IN DUNGENESS CRABS OF KITIMAT ARM, BC.

2.1 Introduction:

Polycyclic aromatic hydrocarbon contaminants in the sediments and biota of Kitimat Arm have been the subject of a number of studies (Simpson *et al.*, 1996; EVS, 1992; Cretney *et al.*, 1983; 6. EVS, 1995; 7. EVS, 1998; Paine *et al.*, 1996). Although these studies have generally demonstrated elevated levels of PAH in the sediments, few studies have demonstrated significant levels of PAH contaminants in biota. Thus, although PAH have been found in the tissues of crabs (W. Cretney, personal communication, Institute of Ocean Studies, Sydney, BC, Canada, 1996), other researchers have concluded that there is limited bioavailability of PAH to the biota of Kitimat Arm (EVS, 1998; Paine *et al.*, 1996). Since elevated levels of PAH in sediments may cause adverse effects to sediment-dwelling organisms, it is important to investigate the extent of PAH contamination in the dungeness crabs of Kitimat Arm. PAH-contaminated crabs are also a public health concern from the human consumers' perspective.

Various species of crabs have been used to monitor PAH exposure around the world. Off the coast of North America, concentrations of PAH have been determined in the blue crab, *Callinectes sapidus*, collected from Chesapeake Bay, (Mothershead, 1991;

Hale, 1988; Anon., 1990); in the rock crab, *Cancer irroratus*, in New York Bight and Long Island Sound (Humason and Gadbois, 1982; Pancirov and Brown, 1977); in the snow crab, *Chionoecetes opilio* and the spider crab, *Hyas coarctatus*, on the coast of Newfoundland (Hellou *et al.*, 1994). Other species have been used to biomonitor PAH elsewhere such as the swim crab, *Polybius henslowi*, on the Northern coast of France and Spain (Baumard *et al.*, 1998); and the mud crab, *Scylla serrata*, obtained from the Brisbane River estuary in Australia (Kayal and Connell, 1995).

Two hypotheses were formed at the outset of this study. First, the dungeness crab could be used to effectively biomonitor PAH in Kitimat Arm. To test this hypothesis, tissues would be collected from crabs caught in Kitimat Arm for analysis by GC-MS. The second hypothesis was that the concentrations of PAH determined in the crab tissues would decrease with increasing distance from the smelter, the alleged source of PAH input to the aquatic environment.

This chapter describes the determination of 10 different PAH analytes in the hepatopancreas and muscle tissues of crabs collected from various sites within Kitimat Arm, BC, Canada. The levels and isomer distribution patterns of the PAH analytes in crabs from different sampling sites were examined to gain a better understanding of the bioavailability and fate of PAH in the crabs and to provide further evidence for the source(s) of PAH contamination in the area.

2.2 Materials And Methods

2.2.1 Study Area

Crabs were collected from five different sites at or around Kitimat Arm, BC, Canada: Hospital Beach (53°59.60'N, 128°41.58'W), Kitamaat Village (53°59.22'N, 128°39.25'W, 53°59.15'N, 128°39.30'W), Wathlsto Creek (53°57.09'N, 128°39.64'W), and one site each from Kildala Arm (53°50.52'N, 128°30.32'W) and Kitkiatka Inlet (53°38.1'N, 129°15.5'W) (Figure 2.1). These sites were chosen based on their potential for collection of crabs and proximity to the smelter. The Hospital Beach site located on the western side of Kitimat Arm is the closest to the effluent outfall of the aluminium smelter. The Kitamaat Village and Wathlsto Creek sites located on the eastern side of Kitimat Arm are further away from the smelter. Kildala Arm, BC, Canada and Kitkiatka Inlet, BC, Canada, were selected as "clean" reference sites.

2.2.2 Sample Collection

Legal size, male dungeness crabs were caught at five different sites (Figure 2.1) using round, stainless steel, commercial crab traps (Ladner Crab Traps, Ladner, BC, Canada) at a depth of 15-50 m on four separate dates: March 1994, May 1995, May 1996 and October 1996. Table 2.1 summarises the sampling locations, dates and catch results of these expeditions. Kitkiatka Inlet was only visited in March 1994.

Table 2.1 Number of crabs collected at each sampling date and location in British Columbia, Canada.

Sample Date	Hospital Beach	Kitamaat Village	Wathlsto Creek	Kildala* Arm	Kitkiatka* Inlet
March 1994	-	20	-	-	15
May 1995	20	18	12	-	-
May 1996	26	3	6	15	-
October 1996	20	15	2	15	-
Total	66	56	20	30	15

* reference sites

The crabs (n = 187) were weighed (744 ● 10 g, mean + standard error) and the carapace width between the tips of the tenth antennal spines (17.6 ● 0.1 cm, mean ± standard error) was measured. Crabs were dissected on site to remove muscle and hepatopancreas tissues. Tissues were frozen immediately at –20°C for subsequent analysis in the laboratory at Simon Fraser University, Burnaby, BC, Canada.

Figure 2.1 Map of Kitimat Arm showing crab collection sites.

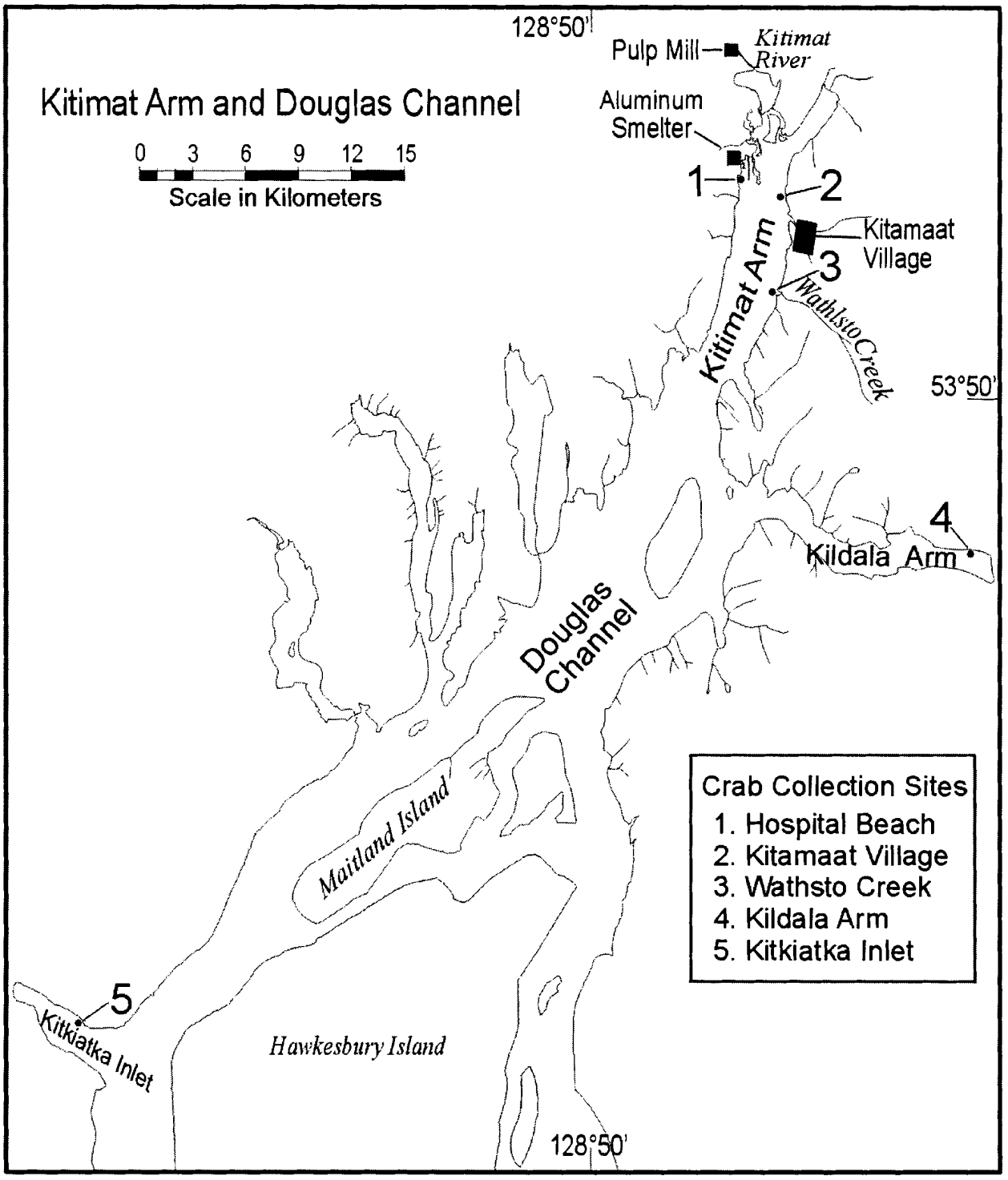

2.2.3 Sample Preparation

The tissue samples were homogenised individually using a model PT 10/35 Polytron homogeniser (Brinkman Company, Rexdale, ON, Canada). Excised muscle samples were solid, and required 0.9% saline (2:1 wt tissue/wt saline) for homogenisation, while the hepatopancreas samples were soft and could be homogenised without added saline. An aliquot of the homogenate equivalent to 5 g hepatopancreas or 15 g muscle was weighed separately in a 50 ml conical centrifuge tube with a Teflon-lined screw cap. Tissue samples were spiked separately with a solution containing the following deuterated internal PAH standards: acenaphthene-d_{10}, fluorene-d_{10}, anthracene-d_{10}, fluoranthene-d_{10}, pyrene-d_{10}, benz[*a*]anthracene-d_{12}, benzo[*b*]fluoranthene-d_{12}, benzo[*k*]fluoranthene-d_{12}, benzo[*a*]pyrene-d_{12} (CDN Isotopes, Pointe Claire, PQ, Canada), phenanthrene-d_{10}, and chrysene-d_{12}, (Aldrich Chemical Company, Milwaukee, WI, USA). Acenaphthene-d_{10}, fluorene-d_{10} and benzofluoranthenes-d_{12} were not included in the spiking solution used to analyse the PAH analytes in muscle tissues.

Each muscle homogenate was further split equally into two 50-ml conical centrifuge tubes before saponification. Both the hepatopancreas and muscle homogenates were saponified and extracted according to the procedure reported by the Axys Group (Axys Group, 1995) with recommendations from G. Brooks (personal communication Axys Group, Sydney, BC, Canada, 1997) and modifications. Briefly, about 1 ml of 50% w/v KOH and 7 ml of high performance liquid chromatography (HPLC) grade methanol were added to the homogenate. The mixture was refluxed at approximately 78°C for 1 hour in a recirculating water bath. The samples were removed and vortexed after 20 and 40 minutes of refluxing. After a 1-hour saponification, distilled, deionised H_2O (8 ml)

was added to each sample. The procedure was repeated once. At the conclusion of a 2-hour saponification, the samples were allowed to cool to room temperature before being shaken with 22 ml of pentane for 15 min. Each saponified muscle homogenate was extracted in two separate tubes due to volume restrictions. However, each hepatopancreas tissue sample could be extracted in a single tube. The pentane layer was removed from each tube. The extraction procedure was repeated twice with freshly added pentane. The extracts were combined into one tube per sample and reduced to about 6 ml under a gentle stream of N_2. One ml of iso-octane was added to minimise PAH loss through vaporization before volume reduction. The extracts were washed with 2 ml of 0.1 M HCl to remove the contaminants with basic pH. The organic extract was removed and reduced to 1 ml prior to silica gel column cleanup.

Sample cleanup was performed by liquid chromatography using a 205 x 14 mm glass column packed with 1 cm sodium sulphate and 10 cm 230-400 mesh Silica Gel 60 (Sigma-Aldrich Canada, Mississauga, ON, Canada). Column packing materials were mixed with pentane to form slurries and degassed before being added to the column. The packed column was rinsed with 1 bed volume of pentane before use. After adding the tissue extract, the column was rinsed with 12 ml of pentane and eluted with 15 ml of methylene chloride. The methylene chloride eluate was collected and evaporated down to near dryness with a gentle stream of N_2. A solution of methylene chloride (50 µl) containing the deuterated recovery standards (naphthalene-d_8, acenaphthylene-d_8 and benzo[ghi]perylene-d_{12}) was added, and the volume was adjusted to 100 µl prior to GC/MS-selective ion monitoring (SIM) analysis.

2.2.4 GC/MS-SIM Analysis

Gas chromatography mass spectrometry was used to determine the concentrations of the following U.S. EPA priority PAH in the crab tissues: acenaphthene, fluorene, phenanthrene, anthracene, fluoranthene, pyrene, chrysene, benz[*a*]anthracene, benzo[*b*]fluoranthene and benzo[*k*]fluoranthene, and benzo[*a*]pyrene. An aliquot (1 µl) of the methylene chloride extract (see above) was injected directly into an Hewlett Packard 5980 Series II gas chromatograph (Hewlett Packard Canada, Mississauga, ON, Canada). The GC was fitted with an HP 5971 mass selective detector (MSD) and a 30 m x 0.25 mm (i.d.) HP-5 MS capillary column (cross-linked 5% phenyl methyl silicone; 0.25 µm film thickness). The GC oven was temperature-programmed for an initial temperature of 70°C, held for 2 min, increased to 100°C in 1 min, held for 3 min and then raised to 300°C in 20 min. The injector and MSD temperature were set to 250°C and 280°C, respectively. Helium was the carrier gas and flowed at a rate of 40-45 ml/min. A split-less injection mode was used in the analysis.

The GC/MS system was operated in the electron impact (EI) mode and the electron energy was set at 70 eV. Initial mass calibration was performed according to the specification of Hewlett Packard Canada (Mississauga, ON, Canada). Two characteristic ions for each analyte were acquired using the SIM mode. Data from GC/MS analyses were processed with the HP G1034C MS ChemStation (Version C.03.00) on a 486 100 MHz computer to integrate the ion pair peaks.

A total of four ions were monitored for each PAH analyte in the sample extract; one ion pair from the deuterated standard and the other from the analyte. The ion pair of

each PAH analyte consisted of the molecular ion and a fragment ion at 1/2 of the molecular weight. A summary of the ion pairs used in the SIM analysis is summarised in Table 2.2. While all ion pairs were integrated and used in calculating recoveries, only the molecular ions were used in concentration determination.

Table 2.2 Ion pairs for selective ion monitoring in gas chromatography mass spectrometric analysis

Analyte Compound	Data Acquisition Start Time (minutes)	Ion Pairs			
		Deuterated Standard		Analyte	
		Molecular Ion	½ Molecular Ion	Molecular Ion	½ Molecular Ion
Naphthalene*	9.00	136	68	128	64
Acenaphthylene*	13.00	160	80	152	76
Acenaphthene*	14.01	164	82	154	77
Fluorene*	15.30	176	88	166	83
Phenanthrene*	18.00	188	94	178	89
Anthracene*	18.80	188	94	178	89
Fluoranthene†	21.00	212	106	202	101
Pyrene†	22.00	212	106	202	101
Benz[*a*]anthracene†	24.60	240	120	228	114
Chrysene†	25.60	240	120	228	114
Benzofluoranthenes†	28.60	264	132	252	126
Benzo[*a*]pyrene†	28.80	264	132	252	126
Benzo(*ghi*)perylene†	34.50	288	144	276	138

* Low molecular weight PAH, (LPAH); †high molecular weight PAH, (HPAH).

2.2.5 Analytical Quality Assurance and Quality Control

A calibration curve for each PAH analyte was prepared using serial dilutions of the EPA 610 PAH standard mixture (Supelco Co., Division of Sigma-Aldrich Canada, Mississauga, ON, Canada). Six different standard concentrations were prepared, each

containing the recovery and the surrogate standards for the relative response factor (RRF) calculation. The retention times and integrity of the surrogate standards were examined visually after each GC/MSD-SIM analysis. A test mixture was also prepared by adding known amounts of pyrene, benz[*a*]anthracene and benzo[a]pyrene to a blank hepatopancreas homogenate. This was used to check GC separation and MS sensitivity. The samples were prepared by other personnel in the laboratory and analysed blindly by the primary author. A test mixture sample, a method blank and a calibration standard were included with each set of 10-20 tissue extract samples.

The PAH analytes in the tissue extracts were identified by comparison to the retention times and mass ratios of the standard mixture. PAH concentrations were calculated from the relative response factor, RRF, according to EPA 600 Series method 1624 (Revision B) for isotope dilution GC/MS (US EPA, 1984). Background of the non-deuterated standards was subtracted from the calculated concentrations. Quantitation was performed using a technique that self-corrected concentrations by recoveries of the deuterated standards. Mean (± standard error) recoveries of spiked deuterated PAH surrogate standards were as follows: acenaphthene (63 ± 1%), phenanthrene (88 ± 2%), anthracene (87 ± 2%), fluoranthene (90 ± 2%), pyrene (96 ± 2%), benz[a]anthracene (92 ± 2%) chrysene (89 ± 1%), benzofluoranthenes (86 ± 2%) and benzo[*a*]pyrene (76 ± 1%); while the recoveries of blind spiked unlabeled pyrene, benz[*a*]anthracene and benzo[*a*]pyrene in quality control samples were 81%, 67%, and 87%, respectively. No PAH analyte peaks were observed in the procedural blanks. Sample specific estimated detection limits (EDL) were also determined for each PAH analyte using the U.S. EPA 8290 method (US EPA, 1994). The EDL of the PAH analytes were found to range from

0.1- 0.3 ng/g for the hepatopancreas and 0.01-0.09 ng/g for the muscle. These quality control results show that the GC/MSD-SIM system met all the acceptance criteria of the U.S. EPA method (US EPA, 1984) and that the PAH analysis was precise and sensitive.

The benzo[*b*]fluoranthene and benzo[*k*]fluoranthene peaks co-eluted under the chromatographic conditions employed in this study. Therefore, they were integrated together and reported as a single value for benzofluoranthenes. Despite efforts to minimise photolytic degradation, relative recoveries of the photolytically-sensitive PAH such as acenaphthene-d_{10} and benzofluoranthene-d_{12} were low. Therefore, acenaphthene analyte concentration was determined reliably in about half of the hepatopancreas samples. Neither acenaphthene nor benzofluoranthenes were determined in the muscle because of rapid photolytic degradation of the deuterated surrogate standards. Also, fluorene was not determined in hepatopancreas and muscle tissues due to low recoveries.

2.2.6 Statistical Analysis

PAH tissue concentration data were analysed statistically using version 6.12 SAS for Windows (SAS Institute, Cary, NC, USA). Mixed model analysis of variance (ANOVA) was used to resolve the difference in sample size for the PAH concentrations in the hepatopancreas dataset. Hypotheses were tested at the alpha = 0.05 significance level. Each PAH analyte was analysed with respect to the date and location of sample collection. The data from Kitkiatka Inlet was excluded from the statistical analysis since they were obtained on only one occasion. In addition, acenaphthene was excluded since it could not be determined in all tissue samples due to degradation of the deuterated surrogate standard. Tissue PAH concentrations that were less than the EDL were

included in the analysis to avoid left censoring of the data (Porter *et al.*, 1988; Newman *et al.*, 1989). The data were log transformed before analysis as they were found to be log normally distributed. PAH concentration correlation analysis between the hepatopancreas and muscle of crabs was performed on non-transformed data using Microsoft Excel 97 SR2.

2.3 Results

A total ion chromatograph (TIC) obtained by GC-MS shows the PAH determined in the crab tissues collected from Kitimat Arm (Figure 2.2).

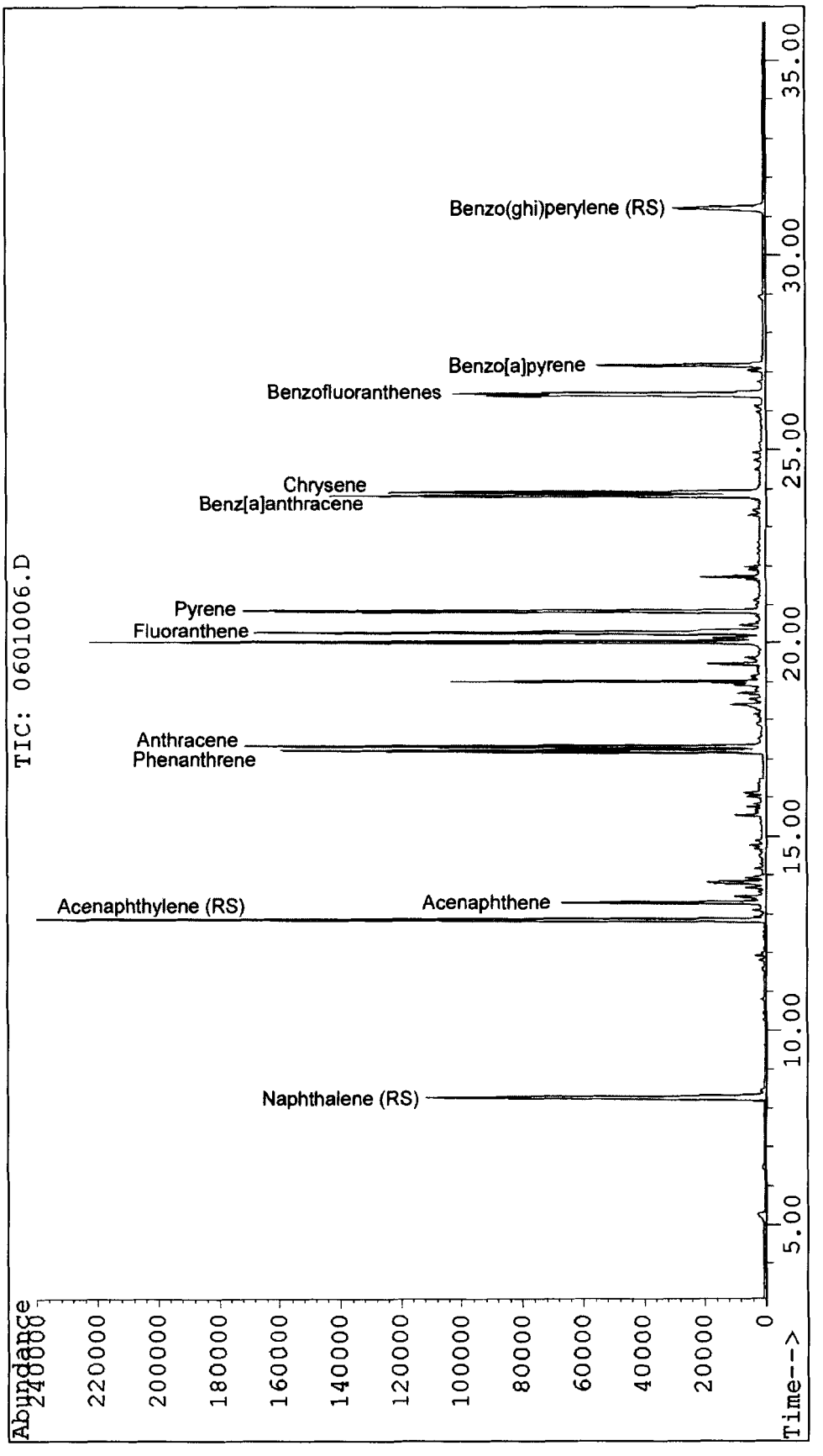

Figure 2.2 Total ion chromatograph showing PAH determined in crab tissues. RS = recovery standard.

All measured concentrations of PAH determined in crab tissues are presented in Appendix A. The mean concentration of each PAH analyte in the hepatopancreas tissue of crabs from different sites is shown in Figure 2.3.

Figure 2.3 Mean PAH concentrations in the hepatopancreas of crabs at different sampling sites in Kitimat Arm Douglas Channel, BC, Canada (1994-1996). Error bars indicate standard error of the mean (SEM). Value at top of error bar indicates upper SEM value.

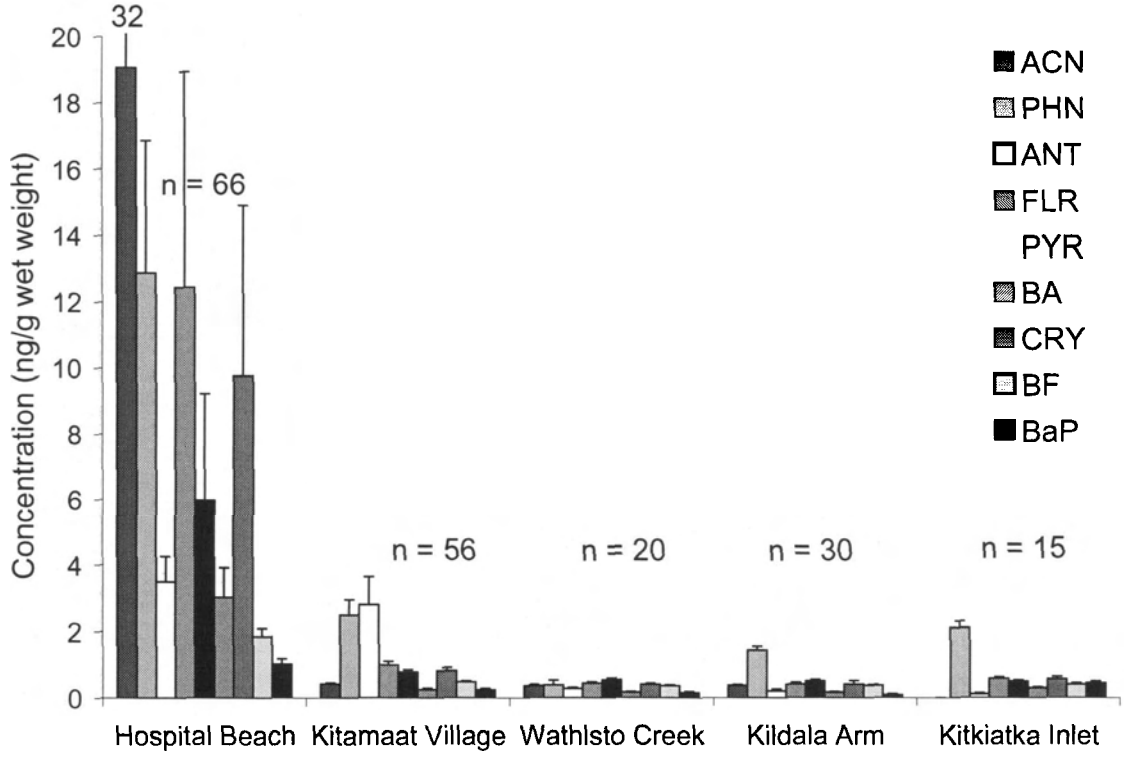

PAH concentrations in the hepatopancreas of crabs collected from May 1995 to October 1996 are displayed in Table 2.3.

Table 2.3 Mean concentrations of PAH in hepatopancreas of crabs collected in Douglas Channel, BC Canada, arithmetic means ± standard error

Mean PAH concentration (ng/g wet weight)									
Site	ACN	PHN	ANT	FLR	PYR	BA	CRY	BF	BAP
				March 1994					
Kitamaat Village	-	2.29 ± 0.30	0.92 ± 0.67	0.74 ± 0.12	0.71 ± 0.08	0.20 ± 0.02	0.53 ± 0.08	0.50 ± 0.03	0.33 ± 0.02
Kitkiatka Inlet	-	2.12 ± 0.19	0.12 ± 0.02	0.59 ± 0.06	0.51 ± 0.04	0.27 ± 0.04	0.53 ± 0.08	0.40 ± 0.04	0.43 ± 0.06
				May 1995					
Hospital Beach	-	0.05 ± 0.01	2.32 ± 0.42	5.06 ± 0.81	1.36 ± 0.20	3.83 ± 1.25	3.67 ± 1.08	2.03 ± 0.29	0.98 ± 0.30
Kitamaat Village	-	0.02 ± 0.002	0.50 ± 0.12	0.63 ± 0.09	0.52 ± 0.05	0.31 ± 0.20	0.80 ± 0.23	0.40 ± 0.04	0.23 ± 0.05
Wathlsto Creek	-	0.02 ± 0.003	0.17 ± 0.06	0.33 ± 0.06	0.45 ± 0.10	0.09 ± 0.02	0.33 ± 0.04	0.28 ± 0.04	0.25 ± 0.04
				May 1996					
Hospital Beach	29.1 ± 22.9	13.7 ± 2.28	1.48 ± 0.28	3.79 ± 1.11	1.38 ± 0.22	0.58 ± 0.22	1.38 ± 0.34	1.03 ± 0.11	0.76 ± 0.26
Kitamaat Village	0.28 ± 0.06	0.97 ± 0.13	0.11 ± 0.07	0.53 ± 0.04	0.64 ± 0.21	0.27 ± 0.05	0.51 ± 0.05	0.45 ± 0.05	0.003 ± 0.0005
Wathlsto Creek	0.34 ± 0.04	0.22 ● 0.16	0.23 ± 0.04	0.56 ± 0.10	0.62 ± 0.09	0.24 ± 0.03	0.43 ± 0.11	0.44 ± 0.06	0.003 ± 0.001
Kildala Arm	0.24 ± 0.03	1.16 ± 0.18	0.20 ± 0.10	0.51 ± 0.09	0.64 ± 0.06	0.22 ± 0.05	0.41 ± 0.35	0.59 ± 0.13	0.29 ± 0.18
				October 1996					
Hospital Beach	0.36 ± 0.04	24.6 ± 12.4	7.14 ± 2.26	29.3 ± 21.2	15.7 ± 10.5	3.00 ± 2.59	20.5 ± 16.9	2.58 ± 0.63	0.82 ± 0.28
Kitamaat Village	0.42 ± 0.04	5.42 ± 1.26	7.77 ± 2.67	1.61 ± 0.30	1.00 ± 0.19	0.11 ± 0.02	0.99 ± 0.31	0.55 ± 0.03	0.20 ± 0.03
Wathlsto Creek	0.46	1.80	0.28	0.36	0.33	0.15	0.41	0.47	0.24
Kildala Arm	0.49 ± 0.02	1.44 ± 0.09	0.06 ± 0.01	0.21 ± 0.04	0.31 ± 0.04	0.11 ± 0.01	0.38 ± 0.05	0.35 ± 0.01	0.12 ± 0.02

Among the PAH analytes in the hepatopancreas, acenaphthene had the highest concentration. A high level of phenanthrene also was found in the hepatopancreas of crabs caught at different sites. A comparison of PAH analyte concentrations in different sampling sites by ANOVA showed that anthracene and pyrene tissue concentrations of Hospital Beach samples were significantly higher than those of Kildala Arm (t=3.34, p=0.023, t=2.7, p=0.038); and fluoranthene and benzo[*a*]pyrene tissue concentrations of crabs from Hospital Beach were significantly higher than those of Wathlsto creek (t=3.73, p=0.0047, t=2.21, p=0.0286) and Kildala arm (t=4.5, p=0.005, t=2.41, p=0.0171). In contrast, benz[*a*]anthracene, benzofluoranthenes and chrysene concentrations of Hospital Beach samples were not found to be significantly different to those of the other sites. The site-specific tissue concentration data were analysed further by gradient analysis. Results of the ANOVA analysis showed that fluoranthene (p=0.0034) and benzo[a]pyrene (p=0.0152) concentrations significantly decreased in the hepatopancreas of crabs caught at an increasing distance down the Arm from Hospital Beach. PAH concentrations in the hepatopancreas of the two reference sites, Kildala Arm and Kitkiatka Inlet appeared similar. No significant differences in PAH concentrations were found at these sites using the ANOVA test (Figure 2.3, Figure 2.4) despite of the fact that these sites were far apart (Figure 2.1). At both sites, phenanthrene was found to be the predominant PAH in the hepatopancreas (Figure 2.3).

Total PAH (TPAH) concentrations in hepatopancreas samples were calculated as the sum of all PAH analytes determined. Figure 2.4 shows that mean TPAH concentrations in the crabs of Hospital Beach were the highest among all sites. The

TPAH concentration at Kitamaat Village was significantly different from those of Wathlsto Creek and Kildala Arm, but not Kitkiatka Inlet ($F=45.97$, $p<0.0001$).

Figure 2.4 Mean total PAH (TPAH) concentrations in the hepatopancreas of crabs at different sampling sites in Douglas Channel, BC, Canada (1994-1996). Error bars indicate standard error of the mean (SEM).

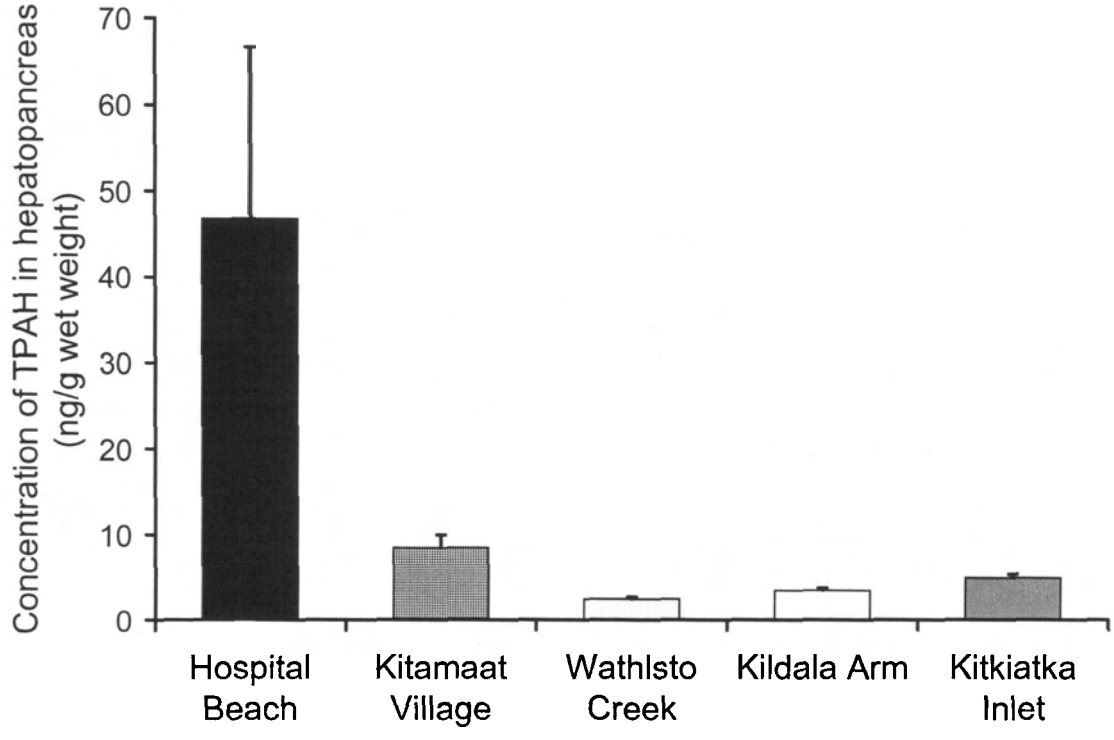

A number of crabs, (19), were also analysed for PAH analytes in the muscle (Figure 2.5). These crabs were selected from crabs caught either at Hospital Beach or near Kitamaat Village which were suspected to have high concentrations of PAH in the tissue. As with the hepatopancreas data, PAH concentrations in the muscle of crabs from Hospital Beach were high and variable, but were not statistically different from the crabs from Kitamaat Village (Figure 2.5). A summary of all concentrations determined in muscle tissues is presented in Table A-6 in Appendix A.

Figure 2.5 PAH concentrations in the muscle of selected crabs at different sampling sites in Kitimat Arm Douglas Channel, BC, Canada (1994-1996). Error bars indicate standard error of the mean (SEM).

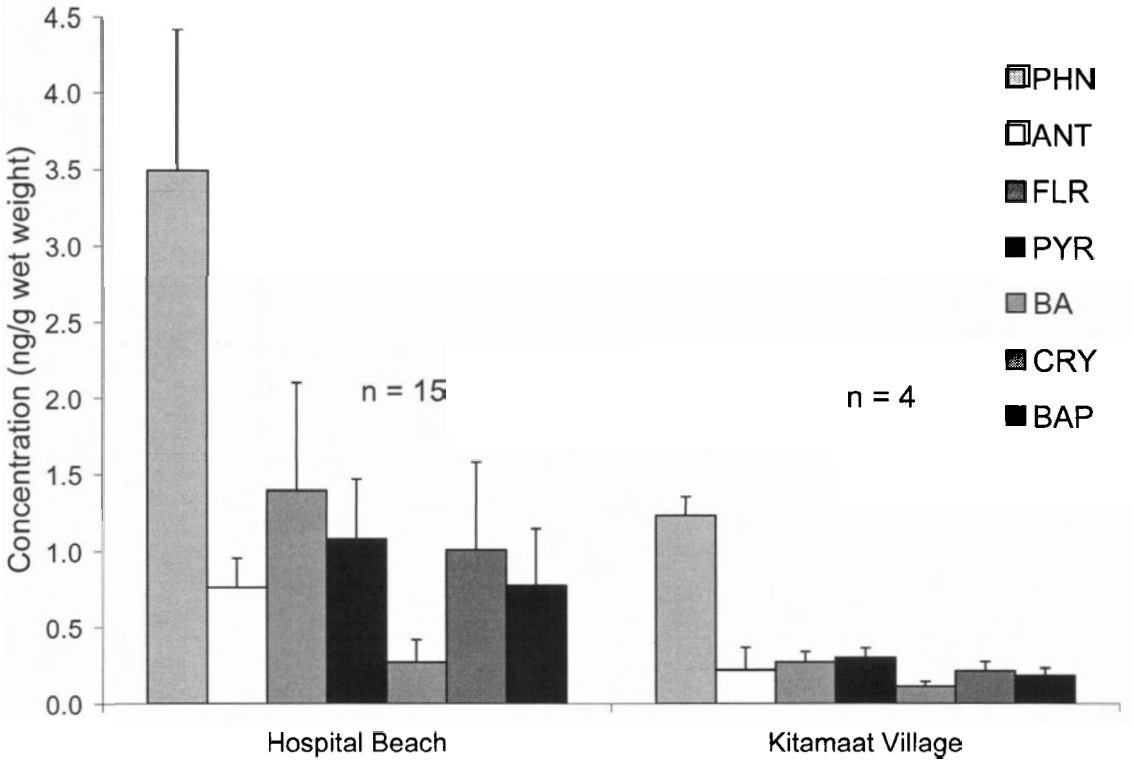

2.4 Discussion

In the present study, PAH-contaminated crabs were found throughout the Kitimat and Kildala Arms and down the Douglas Channel as far as Kitkiatka Inlet. These results show that the PAH contaminants in Kitimat Arm are detectable in crab tissues and therefore, bioavailable to the crabs. The highest tissue PAH concentrations are found in crabs caught near Hospital Beach, which is very close to the effluent discharge of the smelter's waste lagoons. Paine *et al.* (1996) suggested that there is limited PAH bioavailability to the dungeness crabs in Kitimat Arm since they found few PAH-contaminated crabs, and only in the Inner Harbour. A plausible explanation for the discrepancy in results between Paine *et al.* (1996) and the present study may be related to

the less sensitive analytical procedure employed by Paine *et al.* (1996). For example, the detection limits of PAH analytes in my study range from 0.1-0.3 μg/kg whereas those of Paine *et al.* (1996) ranged from 5-20 μg/kg. Because most of the PAH concentrations in the crab tissues were below 10 μg/kg (Figure 2.4, Figure 2.5), the analytical method used by Paine *et al.* (1996) was not sensitive enough to detect the PAH in the crab tissues. However, one might conclude that PAH bioavailability is low in crabs since only a low level of PAH is found in the tissues as compared to that in the sediments. However, the bioavailability of PAH cannot be fully appreciated based on the concentrations of parent compounds in the tissues alone because crabs are able to metabolise PAH (Eickhoff *et al.*, 1995; Lee and Conner, 1982; Lee *et al.*, 1976). For example, parent PAH are difficult to detect in groundfish such as the starry flounder (Namdari, 1998) because fish are capable of rapidly metabolising PAH such as pyrene, which is conjugated to form pyrene-1-glucuronide, and excreted in the bile. Therefore, it is often more effective to monitor the metabolites of PAH instead of the unchanged PAH in the bile of fish. Although invertebrates such as crabs do not metabolise PAH as quickly as fish, a significant level of metabolic activity also takes place in the invertebrates. The synchronous fluorescence spectrometry method (Ariese *et al.*, 1993) described in Chapter 3 was adapted to screen for pyrene-1-glucoside and 1-hydroxypyrene in the haemolymph of crabs (Paine *et al.*, 1996; Eickhoff *et al.*, 1995; Eickhoff *et al.*, 2003).

These results show that tissue PAH concentrations were generally higher in crabs caught off Hospital Beach than those caught in other sites (Figure 2.4, Figure 2.5). This is consistent with the findings of previous studies that sediment PAH concentrations are the highest when they are sampled close to the smelter but decline sharply in concentrations

at sites further down the Arm (Simpson *et al.*, 1996; Paine *et al.*, 1996). A similar observation was also reported in the marine sediments near a Norwegian aluminium smelter in the Sunndalsfjord (Næs *et al.*, 1999). This Norwegian smelter is also set at the head of a long fjord remarkably similar in geography to Kitimat Arm.

The hypothesis that a PAH concentrations in crab tissues should be highest in concentrations near the head of the Arm at Hospital Beach, with lower concentrations further down Kitimat Arm, and the lowest levels at Kildala Arm and Kitkiatka Inlet was tested. However, Figure 2.3 - Figure 2.5 show that generally, PAH concentrations are highest at Hospital Beach, the site closest to the smelter, and at a much lower level at other sites throughout Douglas Channel (ANOVA, Tukey-Kramer, $a=0.05$, $p<0.0001$). We have been unable to demonstrate a significant concentration gradient of PAH concentrations in crab tissues although there is a significant tissue concentration difference between Hospital Beach and the reference sites. The total concentration of all PAH analytes (TPAH) determined in the tissues at all sites over time reflects the same trend (Figure 2.4), although there was a significant difference between the TPAH concentration in crab hepatopancreas from Kitamaat Village compared to Wathlsto Creek and Kildala Arm, (ANOVA, Tukey-Kramer, $a=0.05$, $p<0.0001$). My inability to demonstrate a spatial difference in concentration for these PAH analytes could be explained by the fact that the PAH emissions from the smelter are evenly distributed by the atmosphere over a very large area, and that cycling of PAH may occur throughout Douglas Channel. It is quite possible that the background level of PAH is comparable or perhaps greater than those attributed to the smelter's current emissions.

Kildala Arm and Kitkiatka Inlet were chosen to represent "clean" reference sites. However, PAH levels in the hepatopancreas of crabs collected from these sites were similar to those collected from Wathlsto creek in Kitimat Arm (Figure 2.2). Aerial transport of PAH from the smelter, cycling of contaminants throughout Douglas Channel, as well as local logging operations and boat traffic may account for the PAH found in the crabs from these "clean" sites.

The PAH concentrations in crab tissues were quite variable. This is especially evident in the crabs caught in Hospital Beach (Figure 2.3 - Figure 2.5). The variability in tissue PAH concentration appears to parallel that of the sediments and may have resulted from the randomness of soot, coal dust, and tar balls deposition or pitch spillage near the smelter (Simpson *et al.*, 1996; EVS, 1992).

My results show that low molecular weight PAH (LPAH), including naphthalene, acenaphthene, fluorene, phenanthrene, and anthracene (Simpson *et al.*, 1996) were often found at a higher concentrations than high molecular weight PAH (HPAH) (fluoranthene, pyrene, chrysene, benzo[*a*]anthracene, benzofluoranthenes, and benzo[*a*]pyrene) in crab tissues. For example, LPAH, such as acenaphthene and phenanthrene, are found at high concentrations in the hepatopancreas of crabs (Figure 2.3 and Figure 2.4). This is consistent with the finding that a relatively high level of LPAH was found in the crab tissues in an earlier study conducted in Kitimat Arm (Paine *et al.*, 1996). Acenaphthene or phenanthrene was often the predominant PAH determined in crab tissues from Kitimat Arm. Phenanthrene was also determined at high concentrations in crabs particularly at Hospital Beach, and was also the most prominent PAH determined in the tissues of two crab species, the snow crab, *Chionoecetes opilio* and the spider crab, *Hyas coarctatus*,

collected from Conception Bay, Newfoundland (Hellou *et al.*, 1994). Moreover, high concentrations of LPAH such as phenanthrene, and anthracene, and HPAH, fluoranthene and pyrene, were determined in the tissues of *Polybius henslowi*, an edible crab species caught on the coast of France and Spain in the North Atlantic (Baumard *et al.*, 1998). This study also found that both LPAH and HPAH accumulated in the tissues of crabs, but HPAH such as benz[*a*]anthracene, benzofluoranthenes, and benzo[*a*]pyrene did not accumulate to the same degree as the LPAH and other HPAH such as fluoranthene, pyrene, and chrysene.

In contrast, higher levels of HPAH than LPAH were reported in the sediments collected throughout Kitimat Arm (Simpson *et al.*, 1996). Since LPAH are more water-soluble and therefore are less tightly bound to the organic materials of sediments than HPAH, crabs may be exposed to higher concentrations of LPAH than HPAH in water. This hypothesis is further supported by the finding that phenanthrene is found at a high concentration in the sediment and is the only LPAH detected in the pore waters (EVS, 1998). Baumard *et al.* (1998) reported a high ratio of phenanthrene to anthracene in crab tissues, and stated that phenanthrene is 20 times more water soluble than anthracene and therefore more available in the water column for uptake by crabs. Hellou *et al.* (1994) stated that composition of diet, bioavailability of contaminants, differences in PAH distribution and location, and metabolism are factors which are involved in the differential accumulation of high and low molecular weight PAH by crabs. My results are consistent with the observations of these studies. Phenanthrene is also detectable in crab tissues at Kitkiatka Inlet. This suggests that phenanthrene may be more mobile due to it's solubility than some of the other PAH.

Figure 2.6 shows the relationship between the water solubility of PAH analytes and their concentrations in the hepatopancreas of crabs collected near Hospital Beach. Generally, the higher the water solubility of the PAH, the higher the concentration in the hepatopancreas (Figure 2.6).

Figure 2.6 Mean concentration of analyte PAH in the hepatopancreas of crabs collected from Hospital Beach (1994-1996) vs. water solubility. Regression Lines: Group 1 – solid line, r^2 = 0.845; Group 2 – short dash, r^2 = 0.985; Group 3 – long dash, r^2 = 0.999. Error bars indicate standard error of the mean (SEM).

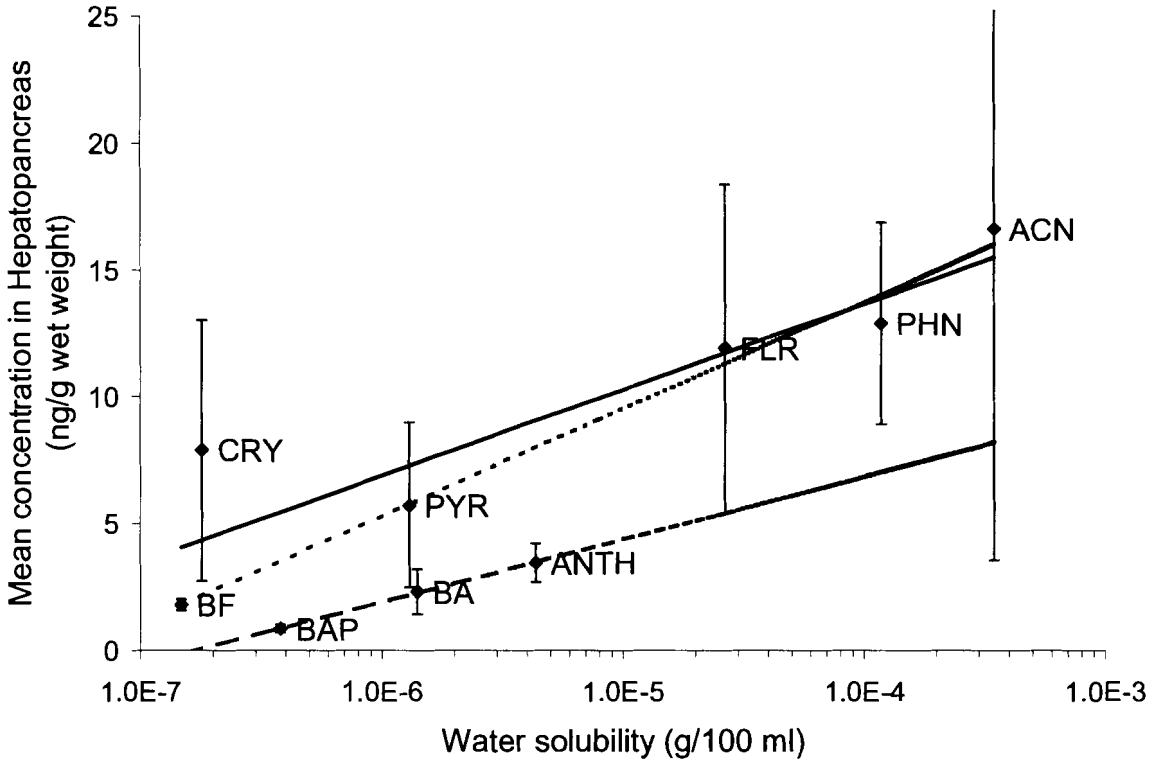

PAH can be classified into two groups based on their structure and the log-linear relationship between water solubility and hepatopancreas concentrations (Figure 2.7). Group 1 is comprised of PAH which contain a two ringed naphthalene structural subunit, acenaphthene, phenanthrene chrysene, pyrene, fluoranthene, and benzofluoranthenes; while Group 2 compounds, anthracene, benz[*a*]anthracene and benzo[*a*]pyrene, are based

on a three ringed anthracene structural subunit. Chrysene may be somewhat of an exception, as it appears to be concentrated in the hepatopancreas at a higher concentration relative to other PAH in group 1 with equal or greater water solubility.

Figure 2.7 Chemical structures of PAH analytes, Group 1 includes PAH based on a 2 ring subunit (naphthalene) and Group 2 includes PAH based on a 3 ring structural subunit (anthracene).

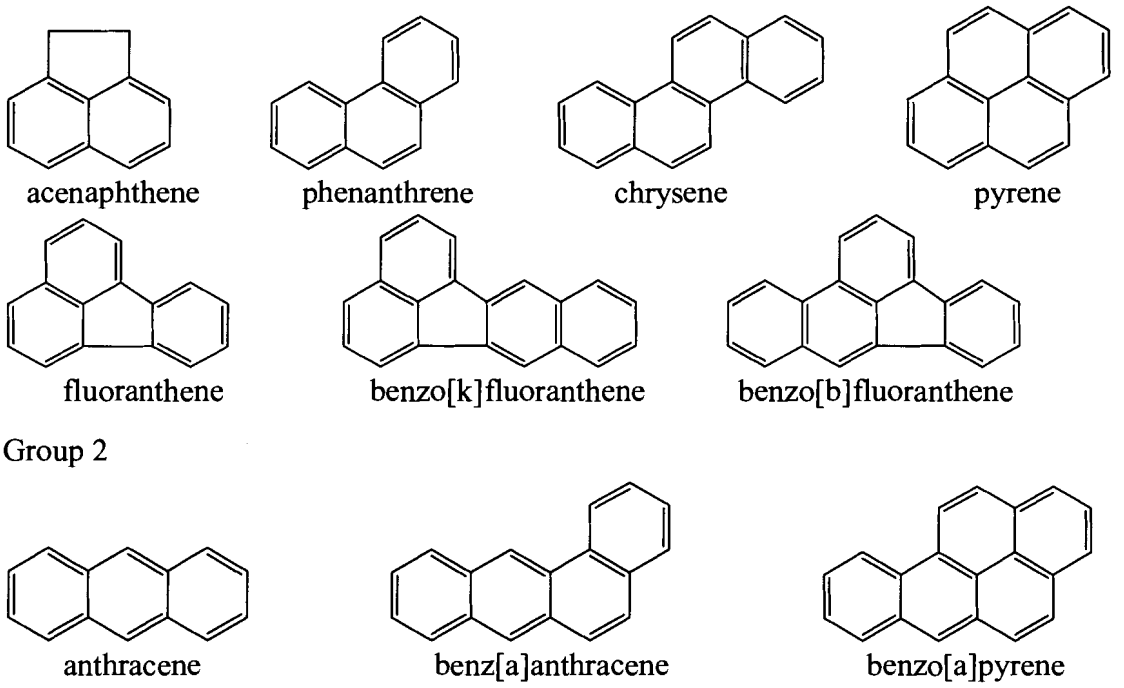

Indeed, if regression lines are fit through the concentration vs. water solubility data, the correlation, r^2, between the group 1 compounds, ($r^2 = 0.845$) improves if chrysene is not included, $r^2 = 0.986$ (Figure 2.6). There is a similarly strong correlation between the group 2 compounds ($r^2 = 0.999$). These observations indicate that the water solubility of PAH appears to be an important factor in differential exposure and bioconcentration of PAHs by dungeness crabs. While the relationships between water solubility, chemical structure, and tissue concentration is interesting and may be useful

for prediction of relative tissue concentrations, they are very simplistic. In fact, the concentration of PAH in the tissues of crabs is also influenced by the relative absorption, distribution, metabolism and excretion rates of each PAH in the crab. For example, pyrene and benzo[*a*]pyrene are metabolised and excreted at different rates by the dungeness crab.

Since the hepatopancreas of male crabs contains a larger amount of lipid than the muscle, (6.6% and 0.9% wet weight respectively) (Allen, 1971), the hepatopancreas is expected to accumulate a higher level of PAH on a wet weight basis. As shown in Figure 2.8, mean PAH analyte concentrations are greater in the hepatopancreas than in the muscle of selected crabs.

Figure 2.8 Mean concentrations of PAH determined in hepatopancreas and muscle tissues of selected crabs. Error bars indicate standard error of the mean (SEM). Value at top of error bar indicates upper SEM value.

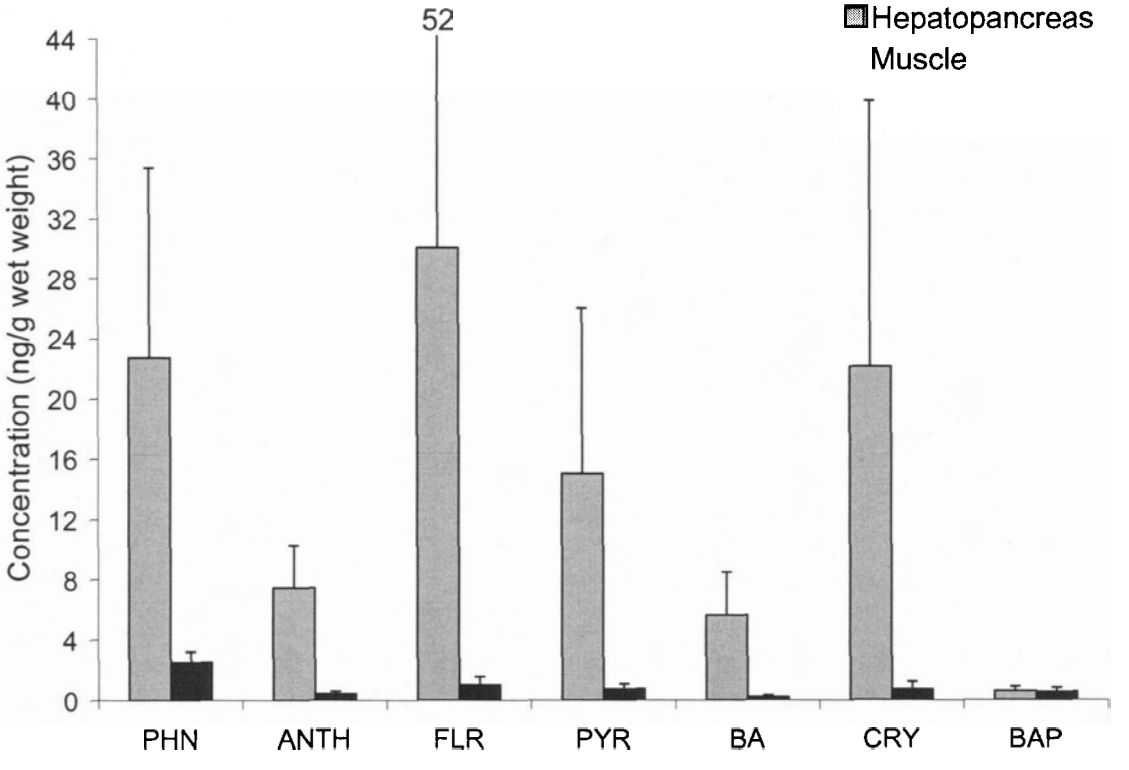

The muscle tissue analysis was performed on 19 crabs, which had particularly high concentrations of PAH in the hepatopancreas. The muscle tissue of these crabs was selected for analysis because crabs that had high levels of PAH in the hepatopancreas would be expected to have detectable levels of PAH in the muscle.

The hepatopancreas/muscle concentration ratios (Table 2.4) also reflect the higher concentration of PAH analytes in the hepatopancreas.

Table 2.4 Concentration ratios and correlation coefficients for concentrations of PAH determined in hepatopancreas and muscle samples from selected crabs collected at Hospital Beach.

Parameter	PHN	ANT	FLR	PYR	BA	CRY	BAP
Mean ratio of hepatopancreas/ muscle concentrations	5	16	18	10	35	20	2
Hepatopancreas :muscle correlation coefficient (r^2)	0.09	0.63	0.31	0.34	0.07	-0.40	0.62
Site specific concentration differences	+	+	+	+	0	0	+
Molecular weight	178	178	202	202	228	228	252
Water solubility (g/100ml)	1.18E-4	4.34E-6	2.65E-5	1.3E-6	1.4E-6	1.8E-7	3.8E-7
log Kow*	4.5	4.45	5.2	5.2	5.6	5.9	6.3

*(Mackay *et al.*, 1991)

Hellou *et al.* (1994) also reported higher mean concentrations of PAH in the hepatopancreas compared to the muscle of crabs. In another study conducted with blue crabs, *Callinectes sapidus*, from the Elizabeth River and Chesapeake Bay, PAH burdens in the hepatopancreas were found to be generally 2-4 fold greater than muscle burdens from the same crabs on a wet weight basis (Mothershead *et al.*, 1991).

While the PAH levels appear to be clearly higher in the hepatopancreas, only the mean concentration of anthracene in the muscle of crabs was found to be significantly different to that of the hepatopancreas using Student's t-test and one way analysis of variance ($t=2.477$, $p=0.0181$). Probably, the statistical tests were unable to resolve the difference in PAH analyte concentrations between these tissues due to a large variability in the hepatopancreas dataset and a small sample size of 19 crabs which had PAH determined in both hepatopancreas and muscle tissues. Similarly, the hepatopancreas/muscle concentration ratios of PAH at Hospital Beach were likely distorted by one or two extreme outlying values of the dataset.

Statistical analysis was performed to examine the correlation between the concentrations of individual PAH in the hepatopancreas and that of the muscle taken from the same crabs. In general, there was a poor correlation between PAH concentrations in the hepatopancreas and muscle tissues (Table 2.4). This may be due to the fact that the hepatopancreas data are confounded by the outlying values and a relatively small sample size of muscle values. If the extreme outlying values in the data set are excluded, reasonably good correlations between the hepatopancreas and muscle tissue concentrations can be found for the following PAH analytes (correlation coefficients, r^2): anthracene (0.63) and benzo[a]pyrene (0.62), pyrene (0.34) and fluoranthene (0.31) (Table 2.4). However, phenanthrene (0.09) and benz[a]anthracene (0.07) display a low PAH concentration correlation between the hepatopancreas and muscle tissues and chrysene shows a negative correlation (-0.40).

It is interesting that ANT, BAP, FLR, PYR, and PHN, which display a difference in concentration between the sample sites, also show a positive correlation of PAH

concentrations between hepatopancreas and muscle tissues. In contrast, BA and CRY, which do not display a concentration differences in the sample sites, show a very low correlation of PAH concentrations between hepatopancreas and muscle tissues. These results indicate that the PAH analytes in Kitimat Arm vary markedly in their bioavailabilities, which cannot be determined solely by their molecular weights and log Kow values (Table 2.4). Thus, the accumulation of PAH analytes by crab tissues may be determined by a number of factors including PAH distribution in sediments, pore water and prey PAH concentrations, water solubility and binding of PAH analytes to organic sediment particles, and the toxicokinetics of individual PAH analytes in the crab.

While tissue lipid concentrations may influence the relative concentrations of PAH in the muscle and hepatopancreas, lipid analysis was not performed on the tissues in this study. In retrospect, lipid analysis may have greatly enhanced this study by allowing for the normalisation of contaminant concentrations based on lipid content, because dungeness crabs may exhibit significant seasonal and annual variations in lipid levels. Unfortunately, the influence of lipid tissue content on the apparent temporal trends in PAH concentrations cannot be examined for this dataset.

The concentrations of PAHs determined in the hepatopancreas and muscle of dungeness crabs collected in Kitimat Arm are much lower that those of blue crabs collected from the Elizabeth River, an industrial area with one of the highest recorded PAH loads recorded in the world (Mothershead *et al.*, 1991). Concentrations of total resolvable PAHs in the hepatopancreas of the blue crabs were between 2,900-11,000 μg/kg, while concentrations of total PAH determined in dungeness crabs collected from sites in Kitimat Arm ranged from 0.7-308 μg/kg. Similar total PAH concentrations levels,

<5-1,100 μg/kg were previously determined in blue crabs collected in South Chesapeake Bay (Hale, 1988). Concentrations of total PAH between 55.5-123.1 μg/kg have been determined in tissues of mud crabs collected in the Brisbane River estuary on the coast of Australia (Kayal and Connell, 1995). It should be noted that the TPAH concentrations reported in the present study are based solely on the 10 PAH analytes determined.

Since crabs are in close contact with sediments, it is reasonable to hypothesize that concentrations of PAH in crabs generally reflect the sediments in Kitimat Arm. Indeed, Chris Simpson found that "levels (of PAH) are highest in the head of Kitimat Arm – especially in the vicinity of the aluminium smelter, and decline rapidly with increasing distance from the smelter" (Simpson, 1996). Concentrations of total PAH in Inner Harbour sediments ranged from 12 – 528 μg/g dry weight, while sediment concentrations near Kitamaat Village ranged in concentration between 9.3 – 20 μg/g dry weight (Simpson, 1996). The concentration of TPAH at one site in Kildala Arm was 1.0 μg/g dry weight while the concentration of a sediment sample obtained from Kitkiatka Inlet was 1.4 μg/g dry weight (Simpson, 1996). One of the sources of PAH input into Kitimat Arm from the smelter, B Lagoon had TPAH concentrations of 10,000 μg/g dry weight in the sediments (Simpson, 1996). Previous work by Cretney *et al.* (1983), also demonstrated the same spacial pattern of PAH in Kitimat Arm that is reflected by the levels of PAH contamination in the crab tissues. While concentrations of PAH in crab tissues are 2-3 orders of magnitude lower than those found in sediments, the PAH concentrations in the crab tissues reflect the concentrations observed in the sediments. Concentrations in crab tissues are lower than those found in the sediments most likely due to factors involving uptake, metabolism, and elimination of the PAH in crabs.

The dungeness crab seems to be an effective indicator species for monitoring PAH exposure to biota in Kitimat Arm for the following reasons. Firstly, crabs can be readily caught at many sites in the Arm. Secondly, detectable levels of PAH are present in the muscle and the hepatopancreas. Crabs are an important benthic species of Kitimat Arm, and do not move about from one area to another as quickly as many fish species. Finally, crabs do not metabolise and excrete PAH from their tissues as rapidly as fish (Dunn and Fee, 1979). Therefore, PAH levels in crabs may reflect differences in the relative amount and bioavailability of PAH at different sites, particularly between Hospital Beach, and other sites downstream in Douglas Channel.

The study area focused mainly on sites along the eastern side of Kitimat Arm such as Kitamaat Village and Wathlsto Creek (Figure 2.1). These sites have been chosen based on the potential of catching crabs, distance from the smelter, and proximity to human settlement. Future studies should determine the concentrations of PAH in crabs on the western side of Kitimat Arm. As suggested by Simpson *et al.* (1996), waterborne PAH-laden particles and atmospheric emissions tend to be deposited along the western side by prevailing currents and winds. This was reflected in studies by Cretney *et al.,* (1983) and Simpson *et al.,* (1996) that showed higher PAH concentrations in the sediments on the western side of Kitimat Arm.

2.5 Conclusions

In summary, this study has demonstrated that PAH in Kitimat Arm and Douglas Channel are bioavailable to dungeness crabs. Concentrations of PAH in the tissues were the highest and the most variable in crabs collected from the site close to the smelter and

dropped off sharply to a lower level along the eastern side of the arm and reference sites. Levels of PAH at reference sites were not significantly different from sites in Kitimat Arm that were closer to the smelter. Water solubility and chemical structure appear to be important factors that affect PAH exposure and bioconcentration by crabs. Hepatopancreas PAH concentrations were higher and more variable than those in the muscle tissues. Overall, this study has shown that dungeness crabs can be used to monitor tissue concentrations of parent PAH in biota in estuarine and marine environments such as Kitimat Arm.

CHAPTER 3
SCREENING PYRENE METABOLITES IN THE HAEMOLYMPH OF DUNGENESS CRABS USING SYNCHRONOUS FLUORESCENCE SPECTROMETRY (SFS): METHOD DEVELOPMENT AND APPLICATION

3.1 Introduction:

Despite the large number of studies on the environmental fate and effects of PAH, very few biomarkers of PAH exposure have been reported for invertebrates in the marine environment. Typically, PAH are determined in tissues of aquatic organisms using analytical tools such as GC/MS or HPLC-Fluorescence.

Ariese *et al.*, (1993) first used SFS as a biomonitoring tool to screen for pyrene-1-glucuronide in fish bile. In recent years, SFS also has been used increasingly to screen for PAH in various sample matrices including seawater (Santana Rodriguez *et al.*, 1993), fish bile (Ariese *et al.*, 1993; Eickhoff *et al.*, 1995; Fragoso *et al.*, 1999), terrestrial isopods (Stroomberg *et al.*, 1999), and crab haemolymph (Eickhoff *et al.*, 1995; Paine *et al.*, 1996). A spectrofluorometric assay may be conducted either by scanning both the excitation and emission monochromator of a spectrofluorometer simultaneously with a constant wavelength difference (the SFS approach) or by scanning the emission monochromator and keeping the excitation wavelength fixed (the fixed wavelength approach) (Ariese *et al.*, 1993; Lin *et al.*, 1994). The SFS method usually results in a much simpler fluorescence spectrum than the fixed wavelength method because SFS has

the ability to reduce the spectral interferences from other chemicals with similar excitation and emission wavelengths and provides a single peak for quantification. In this case, a constant wavelength difference of $\lambda = 37$ nm is selective for pyrene and its metabolites because other potentially interfering compounds or PAH do not produce spectral bands in the resulting spectra. Therefore, the SFS method has been successfully adapted to obtain separate fluorescent peaks to determine pyrene and pyrene metabolites in the haemolymph of crabs without relying on chromatographic separation.

While GC/MS is a highly sensitive and selective instrument for PAH separation, detection and analysis, a laborious and expensive extraction step is often required to clean up tissue samples prior to analysis. SFS has several advantages over the more traditional GC/MS method in analysing PAH-related chemicals in the tissues of aquatic organisms. For example, my SFS assay uses the haemolymph of crabs to selectively screen for both pyrene and pyrene metabolites. The volume of haemolymph in crabs is large and can be easily obtained with a syringe from the arthroidal membrane of a leg joint. Sample preparation is fast, requiring only a short centrifugation treatment rather than a long extraction and clean-up process. Therefore, a large number of haemolymph samples can be processed quickly. Scanning of haemolymph samples by SFS is also rapid. It takes only 2-3 minutes to analyse a haemolymph sample. Finally, the SFS method can be used together with a non-destructive haemolymph collection method, which allows the release of crabs back into the environment if they are not required for further study.

The SFS method also has several advantages over the high performance liquid chromatography-fluorescence (HPLC-F) method developed by Krahn *et al.*(1986) for monitoring PAH in fish bile (Krahn *et al.*, 1986). The HPLC-F method requires an

enzyme hydrolysis and extraction step to prepare the samples (Ariese *et al.*, 1993, Krahn *et al.*, 1986) whereas enzyme hydrolysis is not used in this SFS method. Moreover, the HPLC-F method involves the summation of chromatographic peaks at different wavelength pairs for individual PAH. It should be noted that the majority of the HPLC-F peaks are unidentified as they are assumed to represent a particular parent PAH or PAH metabolite based on retention time (RT) of the chromatogram. Since chemicals other than the target PAH may fluoresce at the monitoring wavelengths in the HPLC-F (Krahn *et al.*, 1986), total fluorescence is just an arbitrary number if it is not calibrated or validated with an independent standard. This can make inter-laboratory comparison of HPLC-F results difficult due to dependence on sample treatment and instrument parameters. In contrast, the SFS method is selective for pyrene and its metabolites and is calibrated with 1-hydroxypyrene as an independent standard.

The objectives of this study were: 1) to develop a new rapid screening method by adapting the SFS method to screen crab haemolymph for PAH-exposure; 2) to apply the SFS method for detecting pyrene and its metabolites in the haemolymph of crabs caught in Kitimat Arm; and 3) to compare the results of this technique to tissue concentrations determined by GC/MS.

The SFS method (Ariese *et al.*, 1993) was adapted to monitor pyrene and its metabolites in the haemolymph of PAH-exposed crabs. To validate the method, we exposed crabs to pyrene in the laboratory. Enzymatic hydrolysis experiments were conducted and HPLC-F analysis was used to identify the pyrene metabolites in the haemolymph. The haemolymph samples were also analysed by the SFS method and HPLC-F to quantitate the concentration of pyrene metabolites and parent pyrene

respectively, in the haemolymph. Once validated by the laboratory generated samples, the SFS assay was applied to the analysis of field samples obtained from Kitimat Arm.

3.2 Materials And Methods

3.2.1 Chemicals

Pyrene and 1-hydroxypyrene were purchased from Aldrich Chemical Company, Milwaukee, WI, USA. Sulfatase (arylsulfatase, aryl-sulfate sulfohydrolase, phenolsulfatase; EC 3.1.6.1) from *Aerobacter aerogenes*, β-glucosidase (EC 3.2.1.21), β-glucuronidase (type B-10 from bovine liver), Trizma® buffer (Sigma Chemical Company, St. Louis, MI, USA), *p*-nitrophenyl sulfate potassium salt, salicin, trichloroacetic acid, sodium acetate trihydrate, potassium biphthalate sodium hydroxide buffer and sodium citrate buffer were obtained from Sigma Chemical Company, St. Louis, MI, USA. All chemicals were used without prior purification. HPLC grade ethanol and water were obtained from Fisher Scientific, Vancouver, BC, Canada. These solvents were used to prepare 66% and 50% ethanol solutions for spectrofluorometric measurements.

3.2.2 Laboratory Studies

3.2.2.1 Treatment of Crabs in the Laboratory

Three adult male dungeness crabs (mean weight 0.886 kg) were obtained locally at the Dollarton Crab Shack, North Vancouver, BC, Canada. The crabs were kept in a large refrigerated tank at 10°C in 27‰ seawater at Simon Fraser University, Burnaby, BC, Canada and fed chopped fish for a week before experimentation. After each crab was

administered a single dose of pyrene (2 mg/kg) intravascularly via the arthroidal membrane of a leg joint, they were held in separate aquaria in a temperature-controlled room at 10±1°C in 27‰ seawater. Seawater was changed daily. Haemolymph samples (1 ml) were taken via the arthroidal membrane of a different leg joint from that used for dosing, using 1-ml disposable syringes at time intervals up to 100 hours post-dosing. The experiment was terminated at 100 hours at which time the crabs were bled by sectioning a walking leg and 15 ml of haemolymph was collected before the crabs were euthanised.

3.2.2.2 Determination of Glucuronic Acid and Sulfate Conjugated Metabolites

Aliquots of the haemolymph (2 ml) were extracted with 8 ml of hexane to remove unchanged pyrene and unconjugated pyrene metabolites. Trichloroacetic acid was added (5 μl) to breakdown gel formation at the solvent interface. The hexane layer was removed. A further 4 ml of hexane was added to the remaining aqueous phase and extracted as above. The hexane layer was again removed. Two extraction steps were found to be sufficient to remove all unchanged pyrene and unconjugated pyrene metabolites. The remaining aqueous layer was blown gently with N_2 to remove any hexane that might still be remaining. Water-soluble, conjugated pyrene metabolites in the aqueous layer were hydrolysed with each specific enzyme in 5 ml of sodium citrate buffer (pH 6.8) as follows: To hydrolyse the glucuronic acid conjugated metabolites, a 1 ml aliquot of β-glucuronidase enzyme resuspended in HPLC grade water was added to the sodium citrate buffered solution (Sigma, 1994). This mixture was incubated at 37°C for 21 hours. Sulfate conjugated pyrene metabolites were hydrolysed by mixing an aliquot of the sodium citrate buffered solution (5 ml) with 27.5 units of sulfatase in 1.5 ml

of potassium biphthalate sodium hydroxide buffer (0.05 M, pH 5.0). The mixture was incubated for 23 hours at 37°C according to methods supplied with the enzyme. These enzyme mediated reactions have been previously shown to hydrolyse pyrene or benzo[a]pyrene conjugates (Kennedy *et al.,* 1989; Namdari, 1998; Seubert and Kennedy, 1997).

3.2.2.3 Examination of Unknown Metabolite

An aliquot of haemolymph (5 ml) was deproteinised with 66% ethanol (15 ml) in a 50-ml polypropylene centrifuge tube. The mixture was refrigerated for 20 minutes at 4°C and centrifuged at 9000 rpm at 4°C for 20 min using a Sorvall RC-5B refrigerated superspeed centrifuge Sorvall Instruments, Wilmington, DE, USA. The supernatant was decanted and dried under a Jouan RC10 centrifugal evaporator, Canberra Packard Canada, Mississauga, ON, Canada. The residues were resuspended in 3 ml of 100 mM sodium acetate buffer (pH 5.0). To hydrolyse the glucose conjugated metabolite(s), an aliquot of the sodium citrate buffered solution (3 ml) was mixed with 10 units of β-glucosidase in 1 ml of buffer. The mixture was incubated at 37°C for 24 hours.

3.2.2.4 Extraction of Incubated Mixture

At the conclusion of the incubation, the enzymatic reactions were stopped with an equal volume of hexane containing benz[*a*]anthracene, the internal standard. The reaction mixture was mixed on a mechanical shaker and the hexane layer was removed. The extraction was repeated once because two extraction steps were found to be sufficient to remove all unchanged pyrene and unconjugated pyrene metabolites. The hexane extracts

were combined and evaporated with N_2. The residues were redissolved in acetonitrile (2 ml) and analysed by HPLC.

3.2.2.5 High Performance Liquid Chromatography

Both conjugated and unconjugated metabolites of pyrene were qualitatively identified initially by comparing their retention time with those of the authentic chemicals, pyrene, 1-hydroxypyrene, and 1-pyrene glucoside, in a Hewlett-Packard 1050 high performance liquid chromatograph (HPLC) Hewlett-Packard Canada, Mississauga, ON, Canada. The HPLC was equipped with a Hypersil 5 ODS 100 mm x 4.6 mm column, a Hypersil 5 C18 30 mm x 4.6 mm guard column Phenomenex, Torrence, CA, USA, and an Hewlett-Packard 1046A fluorescence detector. The excitation and emission wavelengths of the detector were set at 230 nm and 400 nm, respectively. A gradient mobile phase was used to resolve pyrene from its metabolites: solvent A was composed of HPLC grade water containing 0.005% acetic acid and solvent B was 100% methanol. The initial solvent ratio was 95% A and 5% B. The proportion of Solvent B was increased at a linear rate over 15 minutes to 100%, held for 10 min, and returned to initial solvent proportions over 5 minutes.

3.2.3 Field Studies

3.2.3.1 Sampling Location and Date

Legal size, male dungeness crabs were caught at a depth of 15-40 m from Kitimat Arm and Douglas Channel with round, stainless steel, commercial crab traps (Ladner Crab Traps, Ladner, BC, Canada). The following are specific sites of sampling: Hospital

Beach (53°59.60'N, 128°41.58'W), Kitamaat Village (53°59.22'N, 128°39.25'W - 53°59.15'N, 128°39.30'W), Wathlsto Creek (53°57.09'N, 128°39.64'W) (Figure 2.1). The two reference sites were Kildala Arm (53°50.52'N, 128°30.32'W) and Kitkiatka Inlet (53°38.1'N, 129°15.5'W). The crabs were collected on four separate occasions; March 1994, May 1995, May 1996 and October 1996. Because of sampling and time constraints, and inequalities in catch success, all sites were not sampled equally. Table 2.1 lists the locations, dates and catch results. Whenever possible, at least 15 crabs were collected from each site for statistical analysis. The crabs were weighed (mean, standard error 744 ± 10 g) and the carapace width (between the tips of the tenth antennal spines) was measured (mean, standard error 17.6 ± 0.1 cm), prior to the removal of haemolymph for subsequent analysis.

3.2.3.2 Collection of Haemolymph Samples

The crabs were bled individually by sectioning a walking leg at the segment above the dactyl tip. Haemolymph samples were collected from each crab separately in 22 ml glass scintillation vials. The crabs were dissected and hepatopancreas tissues were removed and stored individually in glass vials. All tissues were stored at –20°C for subsequent SFS or GC/MS analysis (Eickhoff *et al.*, 2003a). The study by Ariese *et al.* (1993), stated that the pyrene metabolite conjugates are quite stable at -20°C. My own studies showed that prepared samples were stable for up to 4 weeks when stored at 4°C, but decomposition of the conjugates took place after approximately one month of storage.

3.2.4 Synchronous Fluorescence Spectrometry

An aliquot of haemolymph sample (1 ml) from pyrene-exposed crabs in the laboratory or from crabs caught in Kitimat Arm was deproteinated with 3 ml of pre-chilled ethanol (66%) in a 10-ml polypropylene centrifuge tube. The mixture was kept at 4°C for 20 minutes before being centrifuged at 9000 rpm at 4°C for 20 min in a Sorvall RC-5B Refrigerated Superspeed Centrifuge Sorvall Instruments, Wilmington, DE, USA. The supernatant was decanted into a 7-ml glass vial and refrigerated at 4°C prior to analysis.

The sample extracts were warmed to room temperature before analysis. Each extract was vortexed thoroughly before being decanted into a 1-cm quartz cuvette and scanned on a Perkin Elmer LS 50 Luminescence Spectrometer Perkin Elmer, Norwalk, CT, UK. Both monochromators were scanned synchronously at a fixed wavelength difference ($\Delta\lambda$) of 37 nm from 300-400 nm. Excitation and emission slit widths were both set at 5 nm. Net Peak Area (NPA) was integrated from 330-351 nm using background subtraction to quantify unchanged pyrene and pyrene metabolites in the haemolymph extract. Peak integration was performed using the FL Data Manager software Perkin Elmer, Beaconsfield, Buckinghamshire, UK, on an IBM PS2 computer, model 50Z IBM Corp., Armonk, NY, USA. Authentic pyrene and 1-hydroxypyrene were used as fluorescence standards. A standard curve was prepared for the spectrofluorometer using 1-hydroxypyrene standard concentrations ranging from 1.2 E-9 – 4.9 E-8 M. Fluorescence units were expressed as nanograms of 1-hydroxypyrene equivalents per ml of haemolymph. The detection limit was 0.02 ng of 1-hydroxypyrene equivalents/ml

haemolymph. The detection limit was determined as 3 times the baseline NPA or "baseline noise" of a blank sample.

3.2.5 Statistical Analysis

Spectrometric results from different sites or dates were compared. Differences in 1-hydroxypyrene equivalents were analysed using SAS version 6.12 for Windows SAS Institute Inc., Cary, NC, USA. Both the mixed model analysis of variance (Proc Mixed) and the multiple comparison tests (Tukey-Kramer least squares means) were used to examine the differences in haemolymph 1-hydroxypyrene equivalents between sites or dates. Mixed model analysis of variance (ANOVA) was used to resolve the differences in sample size and collection date of the sites. The contrast test was used to determine if a gradient in concentrations between sites was present. Correlation analysis was preformed using Proc Corr and Microsoft Excel 97 SR-2. Data was log transformed prior to analysis because both 1-hydroxypyrene equivalent values and hepatopancreas PAH concentrations were found to be log normally distributed.

3.3 Results

3.3.1 SFS Assay Adaptation

SFS analysis of the haemolymph of crabs exposed to pyrene in the laboratory revealed a number of peaks in the spectrum representing unchanged pyrene, 1-hydroxypyrene and an unknown pyrene metabolite(s). As expected, the pyrene metabolite profiles in the haemolymph were found to vary with the post-dosing time. For example, within one hour after dosing, only one spectrographic peak represented by pyrene was

found by SFS in the spectrum at 355 nm. At 100 hours post-dosing, however, an unknown metabolite peak which had a maximum fluorescence by SFS at 344 nm together with pyrene (335 nm) was observed in the spectrum. Figure 3.1 shows a spectrograph with two peaks obtained from the haemolymph of a crab 100 hours after dosing.

Figure 3.1 Synchronous fluorescence spectrograph of crab haemolymph extract from a laboratory dosed crab showing pyrene (P) and an unknown metabolite (M) 100 hours post dose.

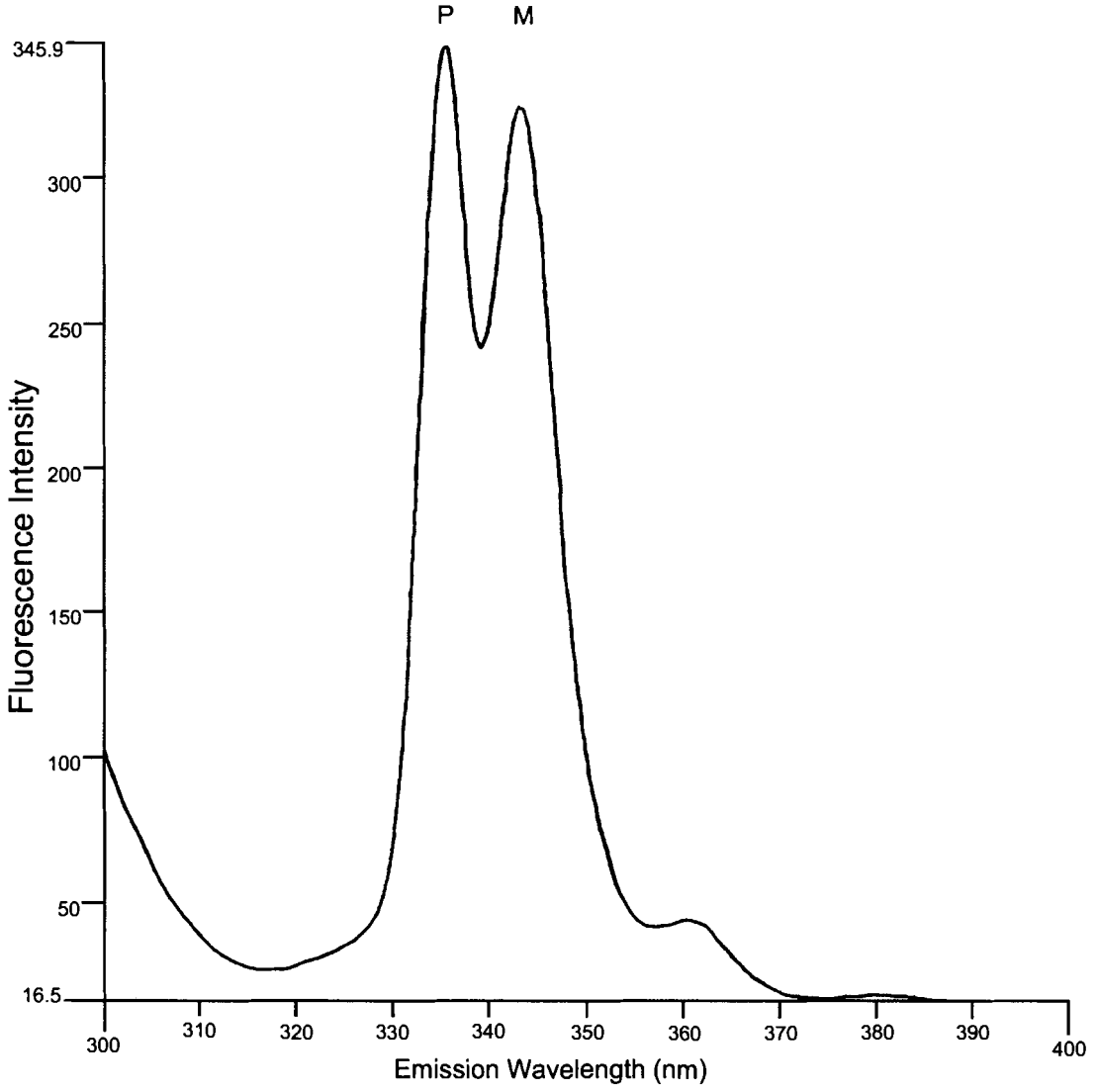

One peak corresponds to pyrene, while the identity of the molecule which produced the second peak is unknown. An overlay of the unknown metabolite peak in relation to the pyrene and 1-hydroxypyrene peaks in 50% ethanol is shown (Figure 3.2).

Figure 3.2 Overlay of synchronous fluorescence spectrographs of crab haemolymph extracts showing pyrene, 1-OH pyrene, and the unknown conjugated metabolite.

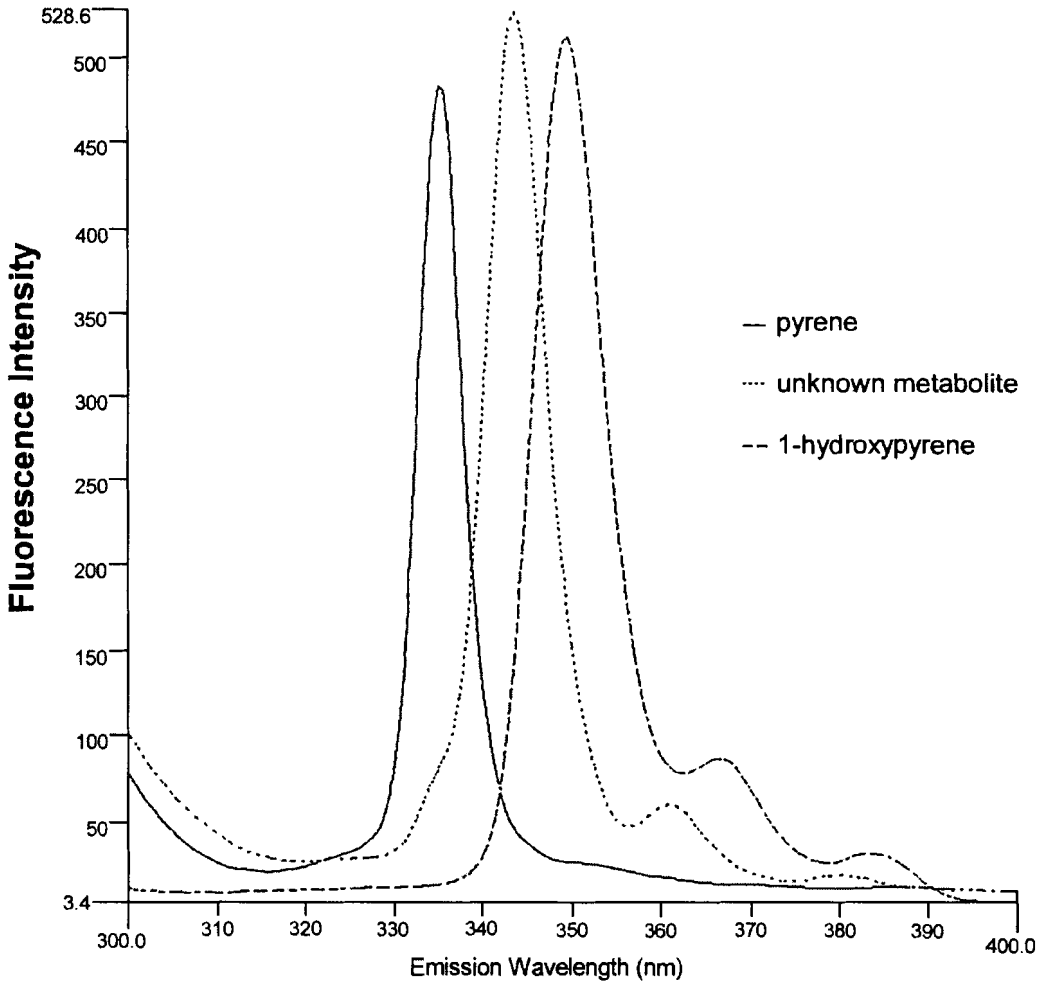

Pyrene, the unknown metabolite and 1-hydroxypyrene had maximum fluorescence in the SFS spectrum at 335 nm, 344 nm, and 349 nm, respectively. Bile was obtained from the gall bladder of a starry flounder, (*Platichthys stellatus*) exposed to

pyrene in the laboratory by R. Namdari. I analysed the bile using the SFS technique. The bile contained mainly pyrene-1-glucuronide (Ariese *et al.*, 1993; Namdari, 1998) which had maximum fluorescence at 342.5 nm in the SFS assay (Figure 3.3).

Figure 3.3 SFS scan of bile obtained from starry flounder exposed to pyrene.

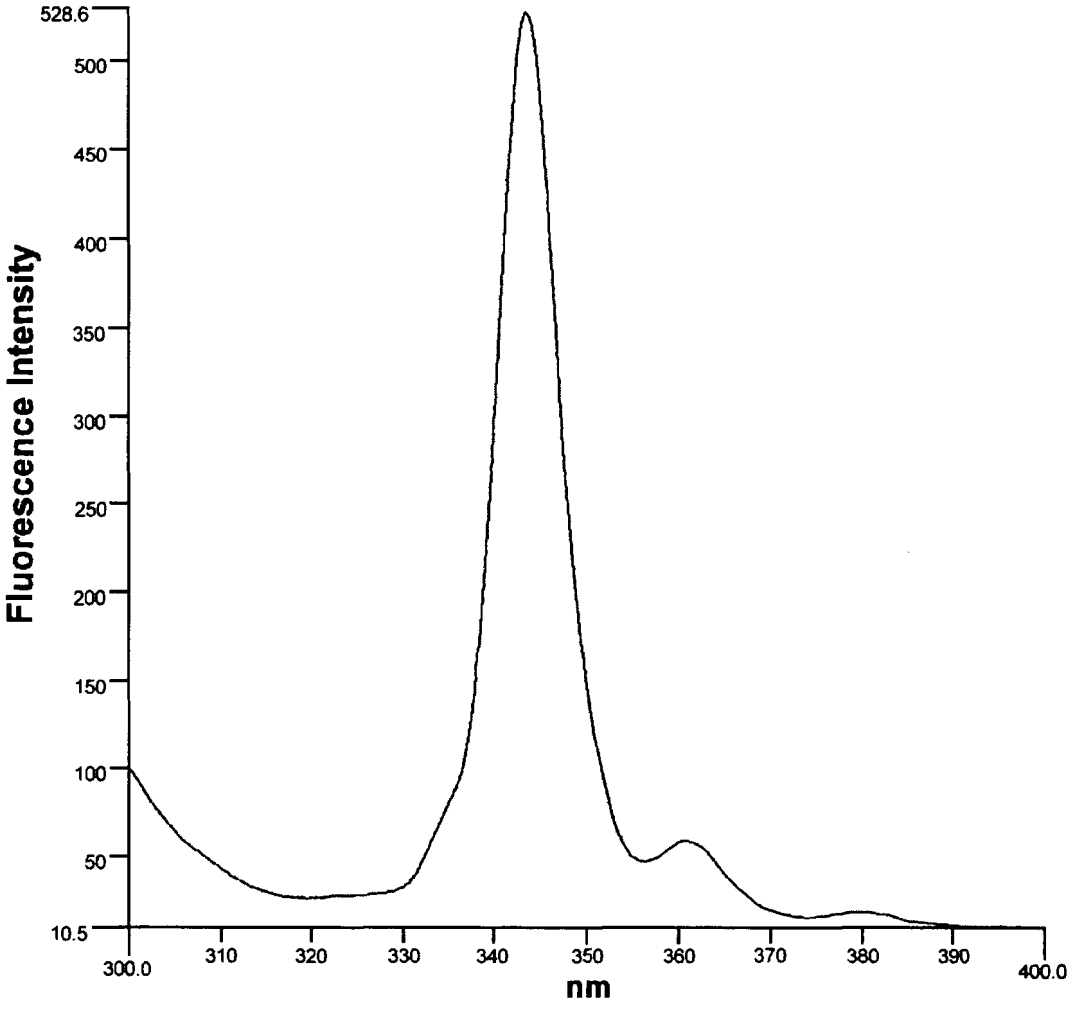

Based on the results of these studies, the unknown pyrene metabolite in the haemolymph of crabs was determined to be neither 1-hydroxypyrene nor pyrene-1-glucuronide.

3.3.1.1 Identity of Unknown Pyrene Metabolite Peak

The identity of the unknown metabolite in the haemolymph was characterized further using reverse phase HPLC equipped with a fluorescence detector. A typical HPLC chromatogram of the haemolymph extracts shows 4 peaks: a large polar peak representing the unknown metabolite(s), the benz[*a*]anthracene internal standard peak, and two smaller peaks co-eluting with the 1-hydroxypyrene and pyrene standards (Figure 3.4a).

Figure 3.4 Chromatograph of pyrene metabolites extracted from haemolymph a) before and, b) after glucosidase treatment.

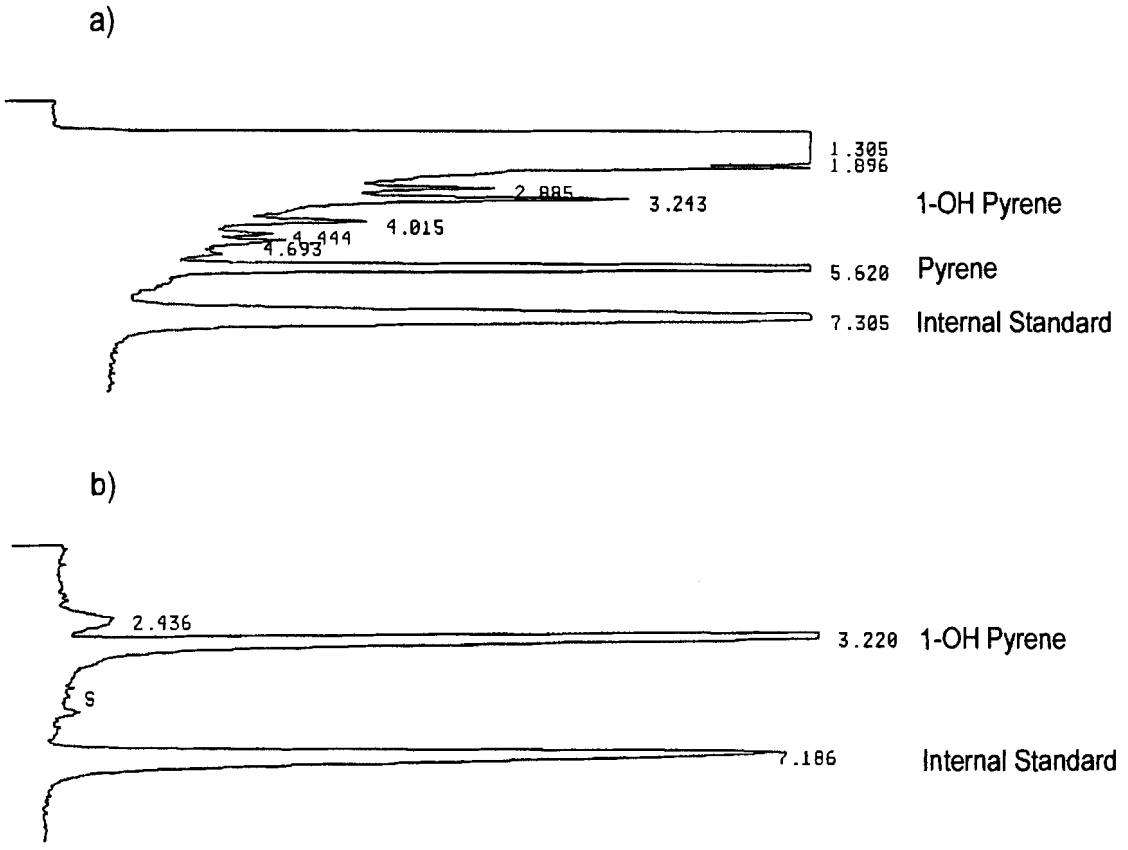

Pre-treatment of haemolymph with β-glucosidase reduced or eliminated the unknown metabolite peak (RT 1-1.9 min) with a concomitant increase in the size of the 1-hydroxypyrene peak (RT 3.2 min) (Figure 3.4b). Pre-treatment of the haemolymph with sulfatase produced a much smaller yield of 1-hydroxypyrene, and β-glucuronidase pre-treatment had no effect on the unknown pyrene metabolite at all (data not shown). These results show that the dungeness crabs preferentially conjugate 1-hydroxypyrene with glucose to form the glucoside conjugate(s) and that the SFS assay is able to distinguish the carbohydrate moiety in the conjugated metabolite.

3.3.2 Use of SFS Assay to Monitor Pyrene Metabolites in Laboratory Dosed Crabs

The SFS assay was used to monitor pyrene metabolites in the haemolymph of crabs exposed to pyrene in the laboratory. The uptake and elimination of pyrene was measured by HPLC, and the increase in pyrene metabolite was measured by SFS. Thus the concentrations of pyrene and metabolites in the haemolymph were monitored in three crabs dosed intravascularly with 2 mg/kg pyrene (Figure 3.5).

Figure 3.5 Concentration of pyrene determined by high performance liquid chromatography (ng pyrene/ml) and pyrene metabolites determined by synchronised fluorescence spectroscopy (ng 1-OH pyrene equivalents/ml) in haemolymph over time.

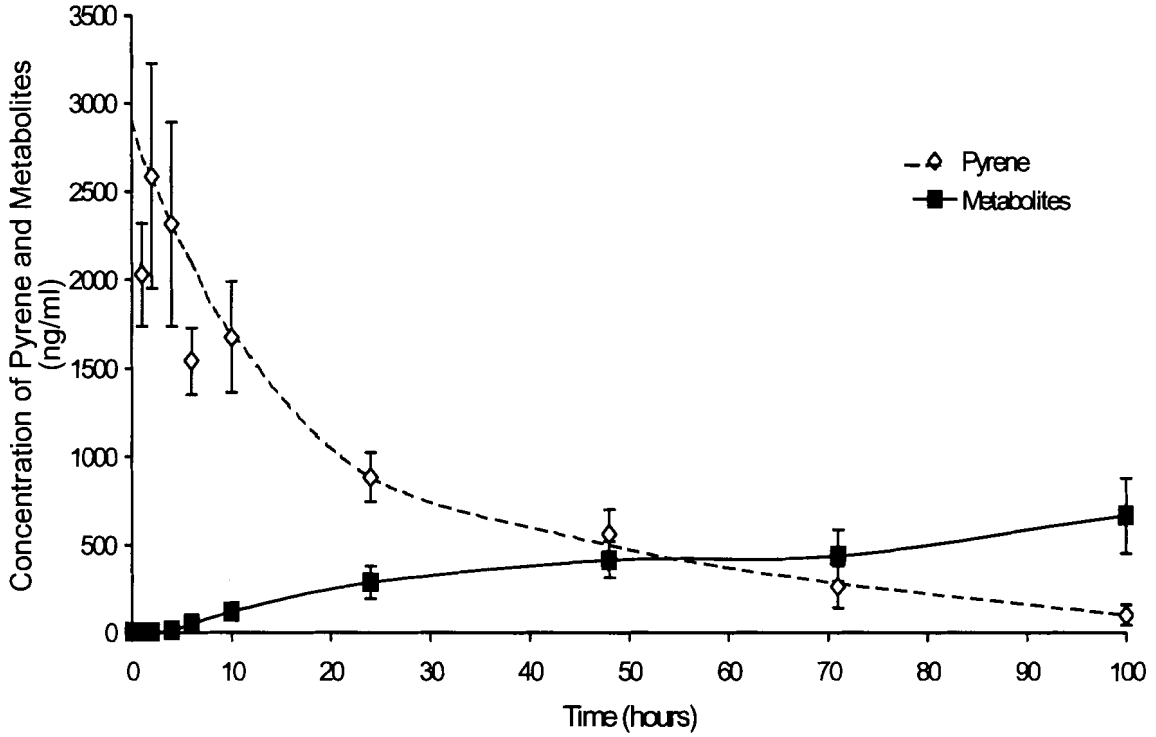

The pyrene haemolymph concentration vs. time curve appears to show a two compartment elimination phase following an intravascular dose. As the concentration of pyrene decreases in the haemolymph, the concentration of pyrene metabolites increases to a maximum of 670 ng/ml after 100 hours.

3.3.3 Use of SFS for Screening Field Samples

The SFS assay was also used to screen for pyrene metabolites in the haemolymph of PAH-exposed crabs in Kitimat Arm. A typical scan of the haemolymph (Figure 3.6) shows the pyrene-1-glucoside peak.

Figure 3.6 Synchronous fluorescence spectrograph of crab haemolymph field sample extract showing pyrene-1-glucoside peak.

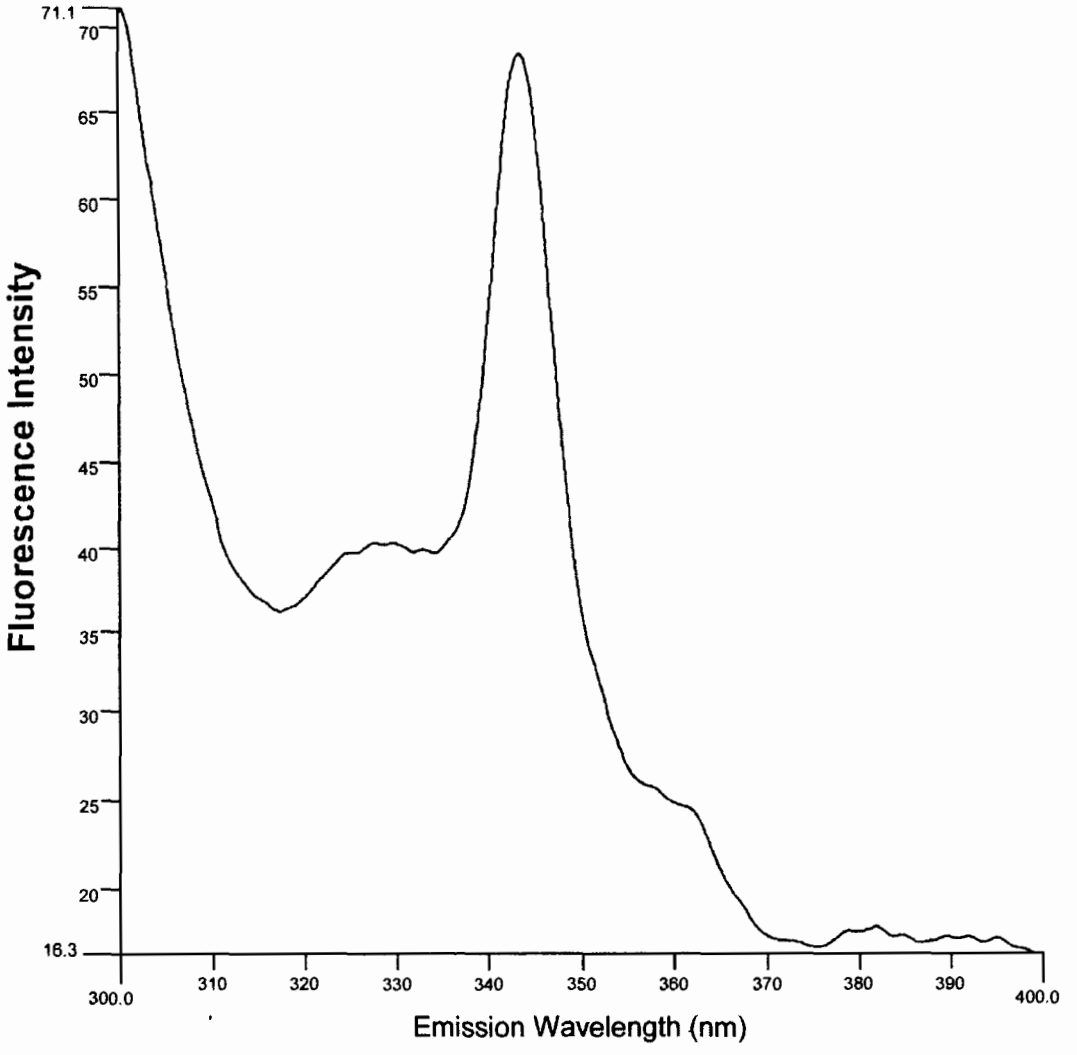

The concentration of pyrene metabolite in the haemolymph of these crabs was generally the highest at Hospital Beach, the site closest to the aluminium smelter, although the level of pyrene-related fluorescence was quite variable and appeared to change with time particularly at the Kitamaat Village site. (Figure 3.7).

Figure 3.7 Mean 1-OH pyrene equivalents in samples from Kitimat Arm with respect to sampling time. Error bars indicate standard error the mean (SEM).

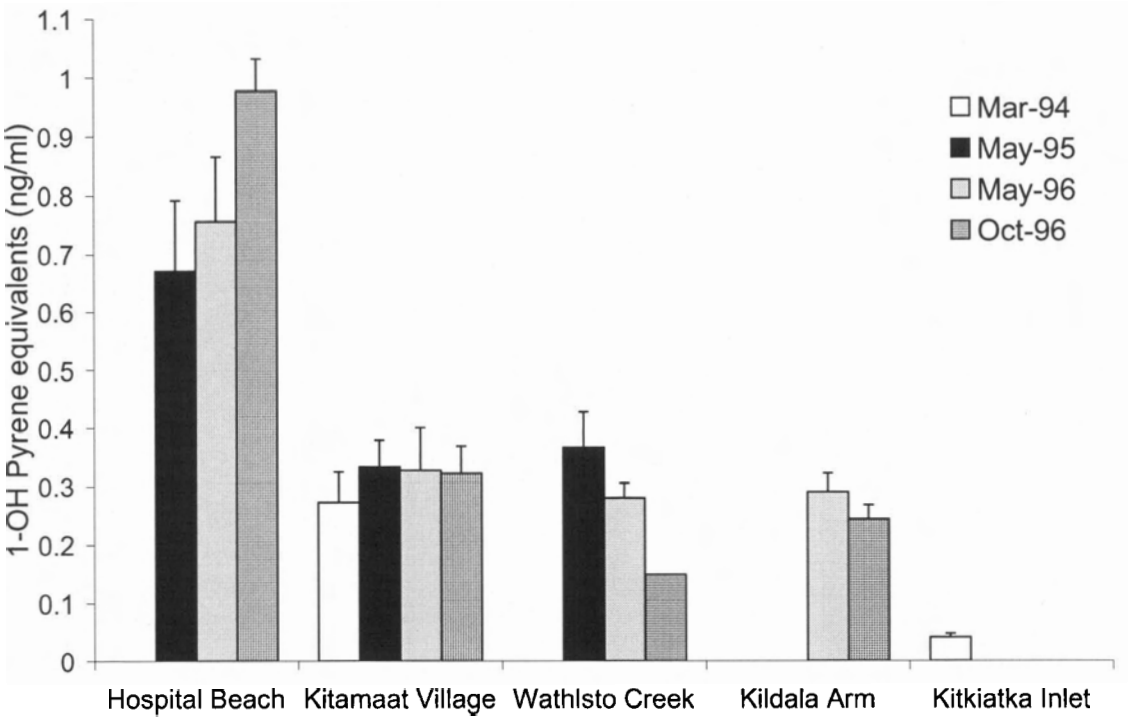

Indeed, there were significant differences in the 1-hydroxypyrene equivalent concentrations over time (ANOVA, $p<0.05$). The mean concentration of 1-hydroxypyrene equivalents in the haemolymph of crabs at each site (Figure 3.8) showed a marked difference in concentration (ANOVA, $p<0.05$) from a high level near the source of pollution to a lower level at various distances from the source. Multiple comparison tests using the Tukey-Kramer least squares means analysis confirmed that there were three significantly different ($p<0.05$) levels of 1-hydroxypyrene equivalent concentrations, denoted as A, B and C in Figure 3.8. The error bars in Figure 3.7 and Figure 3.8 represent the standard error of the mean, and show the variability in SFS measurements. Therefore, variability in 1-hydroxypyrene equivalents is the highest in Hospital Beach samples and decreases with distance from the smelter (Figure 3.8).

Figure 3.8 Mean fluorescence values of haemolymph extracts from sampling sites in Kitimat Arm including all sampling times for each site. Error bars indicate standard error the mean (SEM).

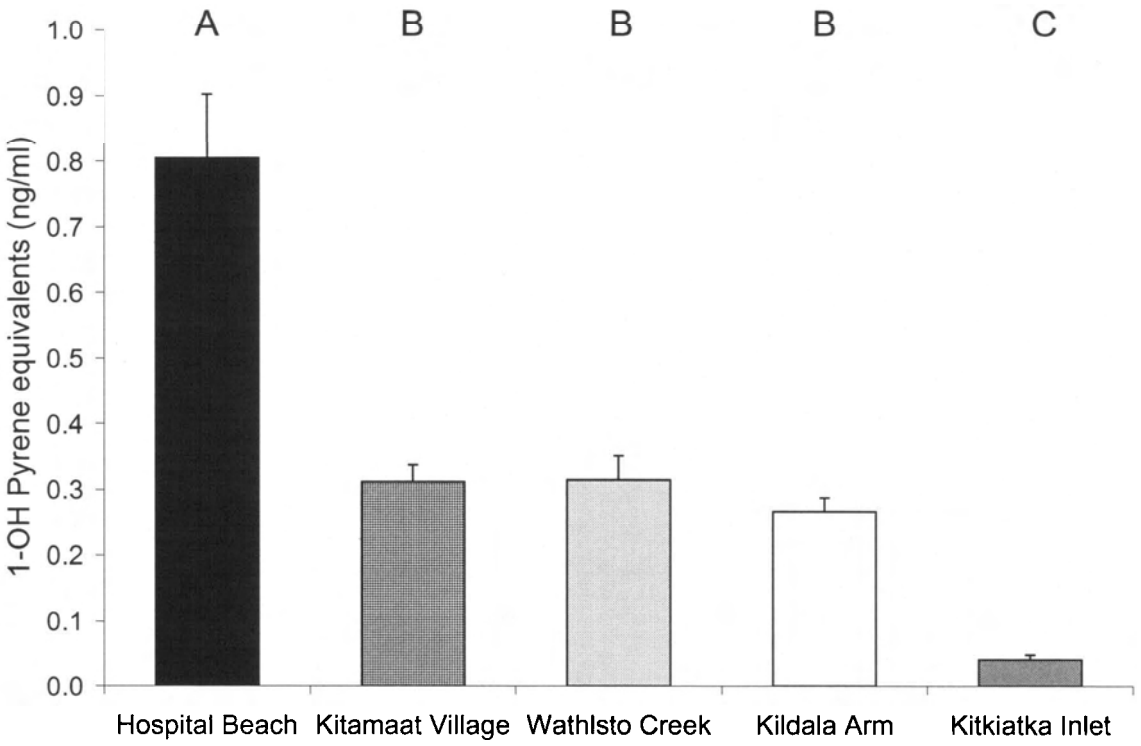

3.3.4 Comparison of PAH Concentrations Obtained by SFS and GC/MS

When the log concentration of 1-OH pyrene equivalents in the haemolymph was plotted against the log concentration of individual PAH in the hepatopancreas of each crab (Eickhoff *et al.*, 2003a), the fluorescence responses in individual crabs were found to weakly correlate with the GC/MS determined pyrene level in the hepatopancreas (r=0.30, p<0.05) (Figure 3.9). This data was plotted on a log scale because both data sets were found to be log normally distributed.

Figure 3.9 Correlation of log concentration of 1-hydroxypyrene equivalents in haemolymph and log pyrene concentrations in the hepatopancreas.

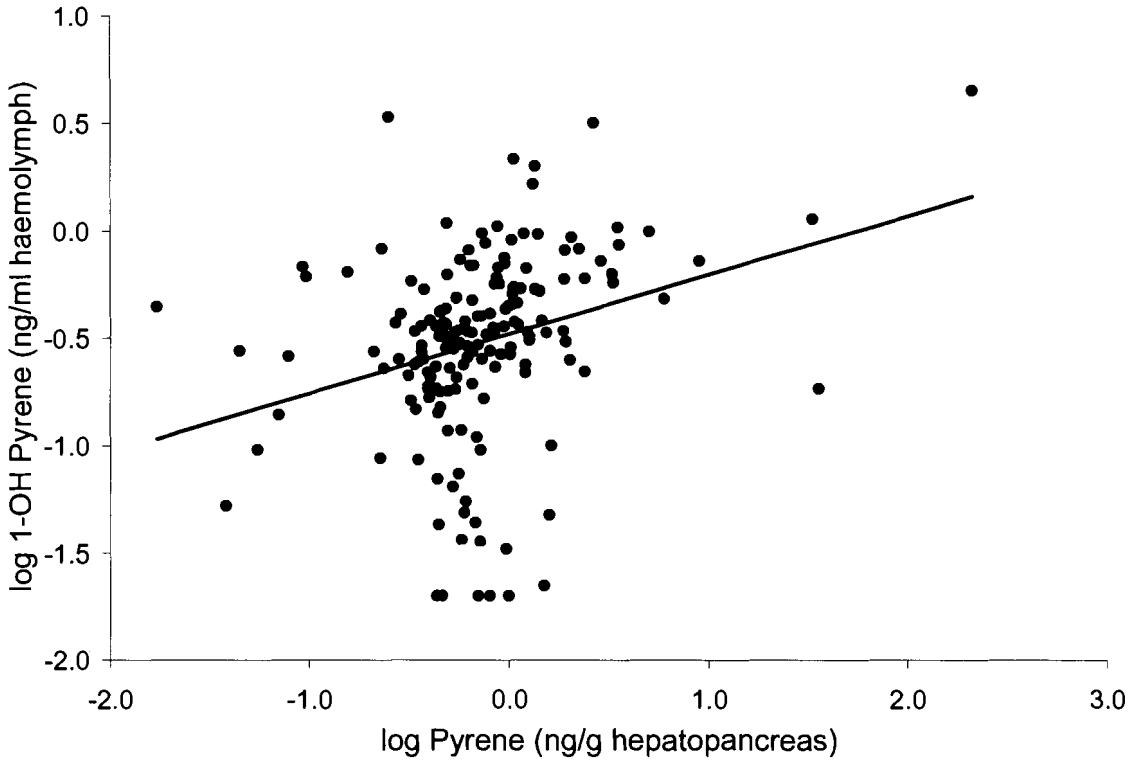

There was a somewhat stronger positive correlation between the concentration of 1-OH pyrene equivalents in the haemolymph in individual crabs and the TPAH concentration in the hepatopancreas (r=0.39, p<0.05) (Figure 3.10). It should be noted that TPAH is a sum of the phenanthrene, anthracene, fluoranthene, pyrene, chrysene, benz[a]anthracene, benzo[b]fluoranthene, benzo[k]fluoranthene, and benzo[a]pyrene concentrations determined by GC/MS in the hepatopancreas of each crab.

Figure 3.10 Correlation of log concentration of 1-hydroxypyrene equivalents in haemolymph and log total PAH (TPAH) concentrations in the hepatopancreas.

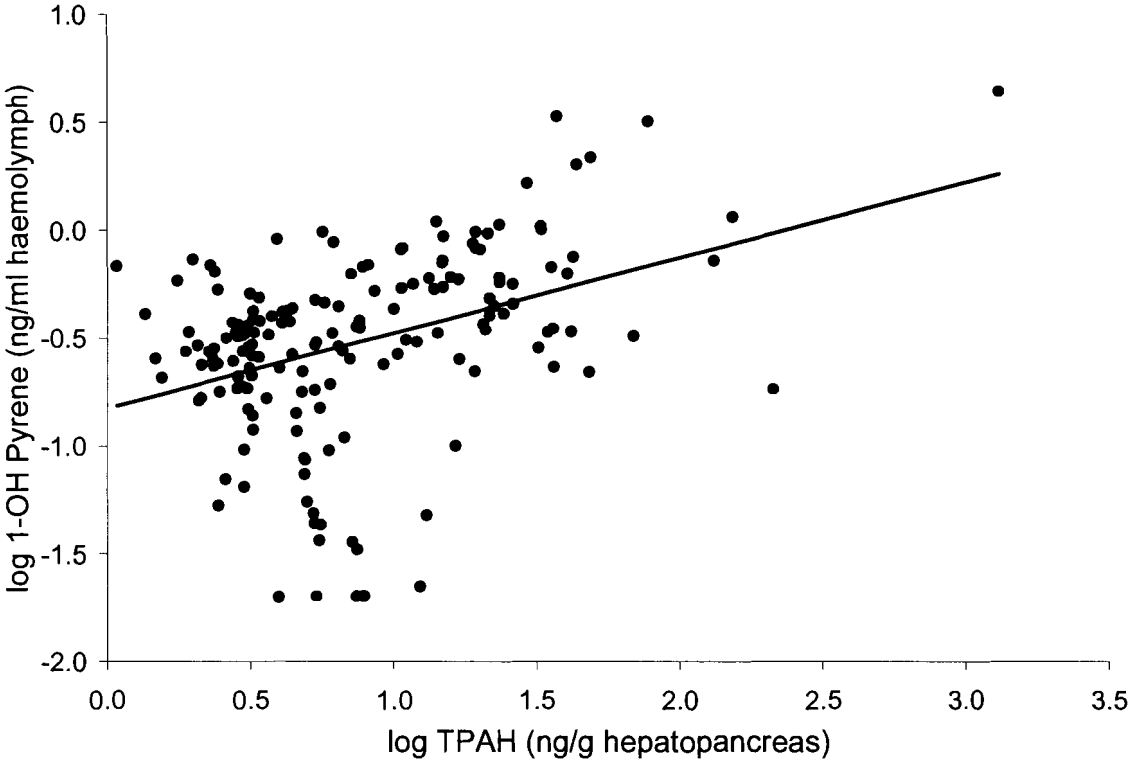

3.4 Discussion

3.4.1 Glycosylation of Pyrene by Dungeness Crab

Results of this study indicate that dungeness crabs are capable of metabolising pyrene to 1-hydroxypyrene and pyrene-1-glucoside, which can be detected semi-quantitatively in the haemolymph using SFS. These results are consistent with a previous report that the American lobster (*Homarus americanus*) converts benzo[*a*]pyrene to benzo[*a*]pyrene-1-glucoside (Li and James, 1993, 2000). Pyrene and other PAH such as fluoranthene are often found at relatively high concentrations in PAH-contaminated water or sediments (Giger and Blumer, 1974). Pyrene therefore serves as a good indicator for the presence of other PAH in the aquatic environment and is easier to monitor than other

PAH indicators such as fluoranthene because pyrene has high fluorescence and is more readily detectable by fluorescence analytical techniques.

3.4.2 Adaptations of SFS Method for Screening Crab Haemolymph Samples

3.4.2.1 Rationale

The SFS method of Ariese *et al.* (1993) has been used to screen for pyrene metabolites in the bile of fish. However, this SFS assay could not be adapted directly without modification to analyse the haemolymph of crabs since fish and crabs are different physiologically (Bone *et al.,* 1995; Bliss, 1982) and in the pathways of pyrene biotransformation (Ariese *et al.,* 1993; James, 1989; Kennedy *et al.,* 1989; Li and James, 1993, 2000; Namdari, 1998). To compensate for these differences, the following three modifications were made to the SFS fish bile assay:

(i) Changes in Monitoring Wavelengths

First, the monitoring wavelengths were modified. The wavelengths used to quantify the fluorescence peak were modified to reflect the difference in the type and number of pyrene metabolite peaks produced in crabs and fish. Previous studies have shown that different carbohydrate substrates are used to conjugate 1-hydroxypyrene metabolite in fish and invertebrates. For example, English sole *(Parophrys vetulus)*, flounder *(Platichthys flesus)*, and starry flounder *(Platichthys stellatus)* conjugate 1-hydroxypyrene primarily with uridine diphospho glucuronic acid (UDPGA) (Ariese *et al.*, 1993; Namdari, 1998; Krahn *et al.*, 1984). In contrast, invertebrates such as the lobster, *Homarus americanus* (Li and James, 1993) and other crustaceans (James, 1987) use uridine diphospho glucose (UDPG) co-substrates to form glucoside metabolites. The

current study suggests strongly that dungeness crabs also use UDP-glucose to form pyrene-1-glucoside from 1-hydroxypyrene. Since pyrene-1-glucoside and pyrene-1-glucuronide had maximum fluorescence at different wavelengths; 344 nm and 342.5 nm respectively, the SFS assay for the haemolymph was modified accordingly. In addition, although there is typically only one SFS peak representing pyrene-1-glucuronide in the bile of flounder (Ariese *et al.*, 1993), several SFS peak representing pyrene and pyrene metabolites may be present in the haemolymph of crabs (Figure 3.1). Because unchanged pyrene fluoresces maximally at 335 nm in the SFS assay, crab haemolymph is scanned from 330-351 nm instead of the reported 335-356 nm for fish bile flounder (Ariese *et al.*, 1993).

(ii) Change in Calibration Units

Secondly, the calibration unit also has been modified. As mentioned before, little or no unchanged pyrene is typically found in the bile of pyrene-exposed fish flounder (Ariese *et al.*, 1993; Namdari, 1998). Therefore, the fluorescent response of fish bile is calibrated against 1-hydroxypyrene standard and the results are expressed as pyrene-1-glucuronide units after correcting for the difference in molecular weight and fluorescence yield of 1-hydroxypyrene and pyrene-1-glucuronide. In contrast, both unchanged pyrene and pyrene metabolites are found in the haemolymph of crabs and the fluorescent peaks of pyrene and pyrene metabolites often cannot be resolved completely (Figure 3.1). Therefore, the SFS assay for the haemolymph of crabs is calibrated against the 1-hydroxypyrene standard and the results are reported as 1-hydroxypyrene equivalent units.

(iii) Changes in Sample Preparation

Finally, a modification has been made to sample dilution and preparation. The flounder converts pyrene rapidly to pyrene-1-glucuronide and excretes the metabolites

into the bile (Namdari, 1998). We have observed that crabs metabolise pyrene relatively slowly, therefore, both unchanged pyrene and pyrene metabolites can be found in the haemolymph. The volume of bile is usually less than 1 ml in fish, and therefore, pyrene metabolites can be detected readily after diluting the bile by as much as 1/500. In contrast, the volume of the haemolymph in crabs is very large; it is estimated to comprise 35.7% of the dungeness crab's body weight (Allen, 1971). Since pyrene metabolite concentrations in the haemolymph are likely to be very low, a much smaller dilution factor is used in the SFS assay (1/4 as compared to 1/500 in fish bile). Furthermore, in order to prepare an optically transparent solution for fluorescence spectrometry, haemolymph proteins and macromolecules were precipitated with chilled ethanol (Autrup, 1979). A 66% ethanol solution (chilled to 4°C) was used to deproteinise the haemolymph so that the final ethanol concentration was 50%, the same percentage used in the fish bile assay (Ariese *et al.*, 1993).

3.4.3 Effectiveness of SFS Assay

3.4.3.1 Comparison of Results with Other Studies

Results of my field study show that SFS is an effective tool for monitoring exposure of dungeness crabs to PAH. Pyrene-associated fluorescent response in the haemolymph of crabs is found to decrease to a lower level with distance from the aluminium smelter, the alleged source of PAH pollution in Kitimat Arm and Douglas Channel. My results are in agreement with those of a previous SFS study on juvenile salmon in Kitimat Arm, which showed the highest pyrene-related fluorescent response in bile from fish collected close to the aluminium smelter (EVS, 1995). Similarly, the

concentrations of individual PAH analytes in the sediments were high near the smelter but are at lower, but similar concentrations at sites further down the Arm (Paine *et al.*, 1996; Simpson *et al.*, 1996) as seen in the haemolymph samples. A recent study near an aluminium smelter in Norway also has reported a similar pattern of PAH concentrations in sediments and indicator organisms (Næs *et al.*, 1999) Similar concentration profiles of individual PAH analytes have also been found in the hepatopancreas of crabs at Kitimat Arm (Eickhoff *et al.*, 2003a). It appears that the concentration of PAH in the crabs are representative of the concentration of PAH in the sediments, and that movement of crabs between sampling areas is unlikely due to separation of muddy, sandy areas favoured by crabs by rocky areas that are uninhabited by dungeness crabs. Therefore the crab represents an effective biomonitor for PAH in contaminated sediments.

3.4.3.2 Variability in 1-OH Pyrene Equivalents in the Haemolymph

A large variability in fluorescence measurements was observed among crabs collected from Hospital Beach, the site closest to the aluminium smelter (Figure 3.7 and Figure 3.8). The variability in 1-OH pyrene equivalent concentrations is consistent with the hypothesis that Kitimat Arm is contaminated by random deposition of PAH in soot, coal dust, and tar balls or the accidental spillage of pitch (EVS, 1991). This observation is also consistent with the variability in PAH concentrations determined in the hepatopancreas and muscle by GC/MS. Therefore, the SFS method is also capable of demonstrating that crabs experience varying levels of exposure to PAH contaminated materials.

3.4.3.3 Comparison of Results Obtained by GC/MS and SFS

A high concentration of PAH analytes have been observed in the hepatopancreas tissue of crabs collected near the aluminium smelter (Eickhoff *et al.*, 2003a). The variability in the hepatopancreas PAH concentrations in the hepatopancreas and muscle appear to parallel that of the pyrene-associated fluorescent responses in the haemolymph. Correlation analysis was performed, comparing either the concentrations of pyrene or TPAH in the hepatopancreas with the concentration of 1-OH pyrene equivalents in the haemolymph for individual crabs collected from all sites. A positive but low correlation was found between pyrene-associated fluorescence in the haemolymph and the concentration of pyrene in the hepatopancreas whereas the correlation between pyrene-associated fluorescence in the haemolymph and TPAH in the hepatopancreas was stronger (Figure 3.9 and Figure 3.10). An explanation for the low correlation between the SFS and GC/MS results is not readily available but may be related to a comparison of different PAH within the tissues of individual crabs, rather than a comparison of the tissue concentrations related to site specific exposure levels for each group of crabs. Further, the correlation between SFS and GC/MS results may be low because of the differences in the toxicokinetics of individual PAH in crabs and the target analytes of the analytical method. The toxicokinetics of PAH in crabs or other animals is rather complicated and involves the interplay of PAHs with the biochemistry and physiology of crabs. Because of the high Kow of PAHs and the relatively high lipid content of the hepatopancreas, PAHs are readily absorbed by crabs and accumulate in the hepatopancreas. However, since the mixed-function oxidases activities in the hepatopancreas of crabs are relatively low, pyrene is metabolised slowly to 1-

hydroxypyrene and pyrene-1-glucoside. As a result, a relatively high concentration of unchanged pyrene is found in the hepatopancreas, since pyrene concentration is determined mainly by uptake, and absorption from water and food, metabolism, and elimination rates of pyrene, and may also be affected by feeding and respiration rates. On the other hand, only low levels of pyrene metabolites are present in the haemolymph, and these levels are determined by the rate of pyrene metabolism in the hepatopancreas, any uptake or metabolism by other tissues, and the rate of metabolite elimination in the antennal gland including the urinary bladder. Since the rates of absorption, metabolism and elimination could vary with the individual PAH and with the post-exposure time, it is not surprising that a relatively low correlation exists between pyrene-related fluorescence in the haemolymph and the concentration of pyrene or TPAH in the hepatopancreas. Correlation with TPAH levels may be stronger because pyrene may be eliminated faster than other PAH in the hepatopancreas, while other PAH may remain longer. Therefore, the SFS analysis of pyrene and metabolites may be a better indicator of short-term exposure, while analysis of more persistent parent compounds by GC/MS may be a better monitor for long term exposure. Finally, there are differences in target analytes and tissues used for analysis between the two analytical methods. The SFS analysis measures the combined fluorescent responses of pyrene and pyrene metabolites in the haemolymph, while the GC/MS method was used to determine the concentration of individual parent PAH compounds in the hepatopancreas.

However, despite the apparent weak statistical correlation between the levels of pyrene metabolites measured by SFS and pyrene and TPAH determined by GC/MS in individual crabs, the SFS method is an effective method to monitor crabs exposed to

PAHs in the marine environment. The SFS assay is equally capable of differentiating between different levels of PAH exposure within Kitimat Arm when compared with the GC/MS method but at a lower cost in time and effort.

3.4.3.4 SFS as a Biomonitoring Tool

The SFS assay provides a simple, rapid, and effective method for monitoring both pyrene and pyrene metabolites in the haemolymph of crabs exposed to pyrene. This assay is capable of resolving the difference between pyrene, 1-hydroxypyrene and conjugated pyrene metabolites such as pyrene-1-glucuronide and pyrene-1-glucoside. We have demonstrated that concentrations of pyrene metabolites can be monitored in the haemolymph of crabs exposed to pyrene. Thus, this assay can be a powerful tool to study the toxicokinetics of pyrene in the crab, or other aquatic invertebrates.

The dungeness crab seems to be an excellent indicator species for monitoring PAH pollutants in Kitimat Arm or other geographical locations on the Pacific coast for the following reasons. Firstly, crabs can be readily caught at many sites in the Arm. Secondly, detectable levels of pyrene and pyrene metabolites are present in the haemolymph. Finally, the crab, which has economic importance, is a benthic invertebrate which does not move about from one area to another as quickly as most fish species. Therefore, pyrene-related fluorescent response in the haemolymph of crabs may reflect the bioavailability of PAHs at a particular site.

3.4.4 Other Potential Applications of SFS Method

The SFS method may be used to monitor the exposure of crab species other than the dungeness crabs in other geographic locations. These crab species may include the snow crab, *Chionoecetes opilio*, and spider crab, *Hyas coarctatus,* which are important species in both the northern Atlantic and Pacific oceans to support fisheries in Alaska, the Bering Sea, and the Gulf of St. Lawrence (Hellou *et al.*, 1994). Similarly, the edible crab, *Cancer pagurus,* is an important fisheries species on the Atlantic coast of Europe; while the blue crab, *Callinectes sapidus* Rathbun has been frequently used as a biomonitor on the Atlantic and Gulf coasts (Mothershead *et al.*, 1991; Hale, 1988; Anon, 1990).

3.4.5 Future Studies

The field study has focused mainly on sites along the eastern side of Kitimat Arm such as Kitamaat Village and Wathlsto Creek (Figure 2.1). These sites have been chosen based on limited knowledge of the sub-populations of crabs in this area, the habitat of crabs, distance from the smelter, and proximity to human settlement. Further studies should be conducted with crabs on the western side of Kitimat Arm. Waterborne PAH-laden particles and atmospheric emissions tend to be deposited along the western side by prevailing currents and winds (Simpson *et al.*, 1996). Unfortunately, my past attempts to catch crabs in this area have been hampered by rocky terrain, which is unsuitable habitat for the dungeness crab. We have subsequently identified some potential sites on the western side of Kitimat Arm for crab sampling.

Future studies could involve conducting a tag and release study to examine the motility of crabs in Kitimat Arm. Sub-populations of crabs may be localised in small

areas with favourable sandy or muddy bottoms surrounded by rocky areas throughout this fjord. Therefore, tagging and recapturing crabs may determine if the tagged crabs have moved from one site to another. PAH exposure may also be assessed on the western side of the Arm. SFS may be used to monitor the exposure of crabs to PAHs for this purpose. Haemolymph samples can be removed without endangering the health of animals, which are released and can be re-sampled upon recapture. This would provide a unique opportunity to assess the temporal levels of PAH exposure in individual animals.

3.5 Summary

In summary, a rapid screening method has been adapted for monitoring exposure of dungeness crabs to PAHs using SFS. This rapid screening assay is capable of resolving different exposure levels between geographically distinct sites in a PAH-contaminated environment. Also, the pyrene-associated fluorescent response in the haemolymph of crabs generally parallels the concentration profile of PAH in crab tissues determined by GC/MS. Therefore, SFS is an effective semi-quantitative method for biomonitoring PAH exposure in the crab.

CHAPTER 4
EMPIRICAL STUDIES
FOR THE DEVELOPMENT OF THE PBTK MODEL

4.1 Introduction

Physiologically based toxicokinetic (PBTK) models involve the embodiment of anatomical, physiological, and biochemical parameters that can be used to describe the disposition of toxic chemicals in a biological organism. These parameters are obtained from the literature or from laboratory experiments. This chapter describes the experiments that were conducted to parameterise, calibrate, and validate the PBTK model adapted to describe the disposition of benzo[a]pyrene in the dungeness crab.

The objectives of this study were to provide empirical data to parameterise, calibrate, and validate the PBTK model. Experiments were conducted to examine the toxicokinetics, bioavailability, and tissue distribution of benzo[a]pyrene in the crab following three routes of exposure: intra-vascular, oral bolus dose, and water borne exposure. Partition coefficients for the PBTK model were estimated using an *in vitro* method. A body composition analysis was performed to estimate tissue volumes for the PBTK model. The results of these experiments are presented and discussed.

In addition to the experiments for the PBTK model, the elimination of benzo[a]pyrene and metabolites in the urine was examined, and the major solvent extractable metabolites were identified.

4.2 Materials and Methods

4.2.1 Crabs

Dungeness crabs (*Cancer magister*) were obtained commercially from a local seafood retailer (Dollarton Crab Shack). Crabs were maintained in a recirculating, temperature controlled 490 L seawater tank located in an indoor aquatic facility at Simon Fraser University. The crabs were acclimated to aerated 100% seawater at a temperature of 9 °C and a salinity of 29 ± 1 ppt for one or two weeks before experiments. Crabs were fed biweekly with a mixed diet of chopped fish and previously frozen clam meat but were fasted for three days prior to an experiment. The seawater in the tank was changed after feeding to remove uneaten food and animal waste. Seawater used in the holding tank and for experiments was filtered using a paper and charcoal filter apparatus to remove impurities.

4.2.2 Chemicals

Unlabeled benzo[a]pyrene, (3,4-benzpyrene), and polyoxyethylene sorbitan monooleate (Tween 80) were obtained from Sigma Chemical Co. (St. Louis, MO). 1,2-Benzanthracene was purchased from Aldrich Chemical Co. (Milwaukee, WI). (7,10-^{14}C)Benzo[a]pyrene (specific activity 63 mCi/mmol) was purchased from Amersham Canada Ltd. (Oakville, ON). ^{14}C-labelled benzo[a]pyrene was purified by thin layer chromatography (TLC) on silica-gel plates using 9:1 pentane:benzene as the developing solvent. The radiochemical purity of the ^{14}C-labeled benzo[a]pyrene exceeded 99% as determined by TLC. Unlabeled benzo[a]pyrene purity was found to exceed 99% by high pressure liquid chromatography (HPLC) and was used without further purification.

HPLC grade organic solvents were obtained from Caledon Laboratories Ltd. Radioactivity was determined using Biodegradable Counting Scintillant, BCS supplied by Amersham Canada Ltd., Oakville, ON, or Carbon 14 Cocktail from the R.J. Harvey Instrument Corporation, Hillsdale, NJ. All other chemicals were of analytical grade or better. Benzo[a]pyrene metabolite standards, benzo[a]pyrene-trans-7,8-dihydrodiol, and benzo[a]pyrene-trans-9,10-dihydrodiol were obtained from Midwest Research Institute, Kansas City, MO.

4.2.3 Toxicokinetic Studies with Crabs

4.2.3.1 Toxicokinetics of Benzo[a]pyrene in Crabs Following Intravascular Injection

To facilitate intravascular dosing and haemolymph sampling, a septum was formed on the dorsal carapace of crabs. A 1-2 mm hole was carefully bored into the carapace above the pericardial cavity using a Dremel® drill fitted with a small burr bit to ensure the integrity of the hypodermis (skin) below the shell. This hole was covered with dental dam affixed with cyanoacrylate glue to form a septum. ^{14}C-labeled benzo[a]pyrene was dissolved in mulgofen with "cold" benzo[a]pyrene (specific activity 0.924 mg/μCi) and diluted with 0.9% saline. An aliquot of the solution, (2 mg/kg or 1 ml/kg) was injected as a single bolus into the pericardial chamber of each crab. At 1, 2, 4, 8, 18, 24, 29, 48, 75, 96, 144, 192, 240 and 480 hours following dosing, 1 ml haemolymph samples were withdrawn from crabs through the septum. Each 1 ml haemolymph sample was mixed with 1 ml of 50 mg/ml N-ethyl maleimide to prevent clotting and all samples were frozen until analysis. Crabs were maintained at 9°C in a 490 L refrigerated seawater tank. Seawater (29 ± 1‰) was continuously recirculated (approx. 22 L/min) and filtered with

an Omnifilter charcoal cartridge to remove any excreted parent chemical, metabolites and waste products. Sets of three crabs were sacrificed on each of days 1, 2, and 4 post dosing. Sets of two crabs were sacrificed on each of days 8 and 20. Crabs were euthanised by freezing on dry ice and were kept frozen at –28°C until tissues were dissected for analysis.

4.2.3.2 Toxicokinetics of Benzo[a]pyrene in Crabs Following Single Oral Bolus Dose

In order to study oral bioavailability and tissue disposition, crabs were administered with a single oral bolus dose of benzo[a]pyrene. Crabs were administered a dose of 2 mg/kg (1mg/ml) ^{14}C-labelled benzo[a]pyrene (specific activity 0.964 mg/μCi) in the first of two experiments. In the second experiment, crabs were administered a more environmentally relevant 100 fold lower dose of non-radiolabelled benzo[a]pyrene 20 μg/kg (10 μg/ml). Benzo[a]pyrene was dissolved in mulgofen (0.1% w/v), suspended in 0.9% saline, and thoroughly mixed with a clam homogenate before dosing. A red food colouring dye was incorporated into the dose for detection of regurgitation. Crabs were gavaged directly into the stomach using a gavage needle fitted to a 2 ml glass Hamilton syringe. No regurgitation was observed following dose administration. Haemolymph samples were taken from the membrane at the base of a walking leg at certain time points post-dosing. Crabs were maintained in recirculated seawater as described above. Sets of three crabs were euthanised by quick freezing in a plastic bag on dry ice at predetermined time points after dosing and were kept frozen at –28 °C until dissected for tissue analysis.

4.2.3.3 Toxicokinetics of Benzo[a]pyrene in Crabs Following Water-borne Exposure

Crabs were exposed to benzo[a]pyrene in seawater to examine the uptake, elimination and tissue disposition of this chemical from the water medium. Water-borne exposures were conducted in glass aquaria tanks equipped with an aerator, two large stir bars (7.2 x 1.2 cm) and a stainless steel grid to prevent the animals from interfering with the stirring motion as depicted in Figure 4.1.

Figure 4.1 Exposure system for water-borne benzo[a]pyrene experiments with crab *in situ*.

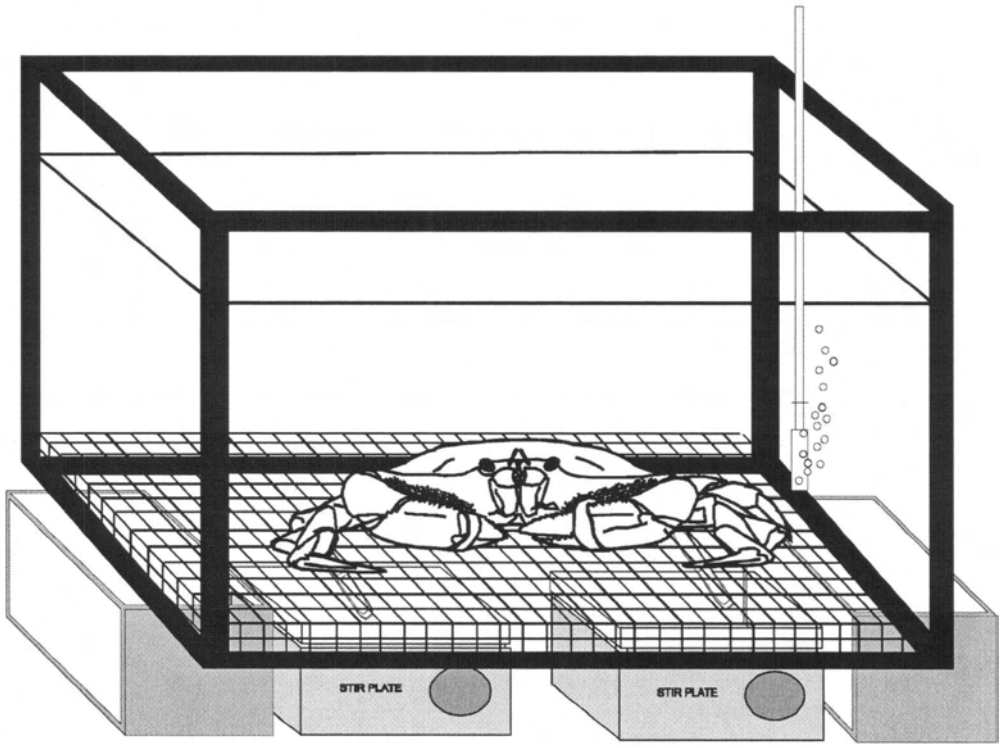

Experiments were conducted at 9 °C in a temperature controlled room. Separate experiments were conducted with two different nominal concentrations of benzo[a]pyrene in seawater, 20 µg/L and 2 µg/L. Prior to experiments, a stock solution of benzo[a]pyrene was prepared with the universal solvent, dimethyl-formamide (DMF). In

addition, 0.5 ml of Tween 80 was added to 16 L of 29 ppt seawater in the exposure tanks. The 3.1 E-3 % v/v Tween 80/seawater solution was stirred for a period of 12 hours prior to the addition of a 100 µl aliquot of the stock solution. The seawater solution was then stirred for a 24 hour period prior to exposure. A 3 ml water sample was taken at either end of each tank using clean glass volumetric pipettes 1 hour and 24 hours after addition of chemical to determine the concentration of chemical in the water prior to exposure. Water samples were also taken during the exposure phase at certain times concurrent with haemolymph samples. Haemolymph samples were taken from the arthroidal membrane at the base of the legs. Crabs were individually exposed to benzo[a]pyrene for a period of 72 hours and were then transferred to 16 L of clean seawater in fresh tanks to monitor elimination. Seawater was changed daily during the depuration phase of the experiment. Sets of three crabs were euthanised on dry ice at certain time points after dosing and were kept frozen at –28 °C until dissected for tissue analysis.

4.2.4 Urinary Excretion and *In Vivo* Metabolism

The *in vivo* metabolism and excretion of benzo[a]pyrene in the urine was examined using a published urine collection method (Eickhoff and Law, 1995) adapted from two previous methods for measuring urinary flow rates, Holliday (1977) and Wheatley (1985). Sets of three crabs were administered 2 mg/kg doses of ^{14}C-labelled benzo[a]pyrene by two different routes; intravascular and oral (specific activities 0.925, 0.964 mg/µCi) as described previously. Crabs were maintained in separate glass aquaria containing approximately 12 L of 29 ± 1 ppt seawater which completely covered the

crab's carapace to a level of about 1 cm from the bottom of the collection vessel (Figure 4.2).

Figure 4.2 Crab fitted with urine collection vessel in experiment tank

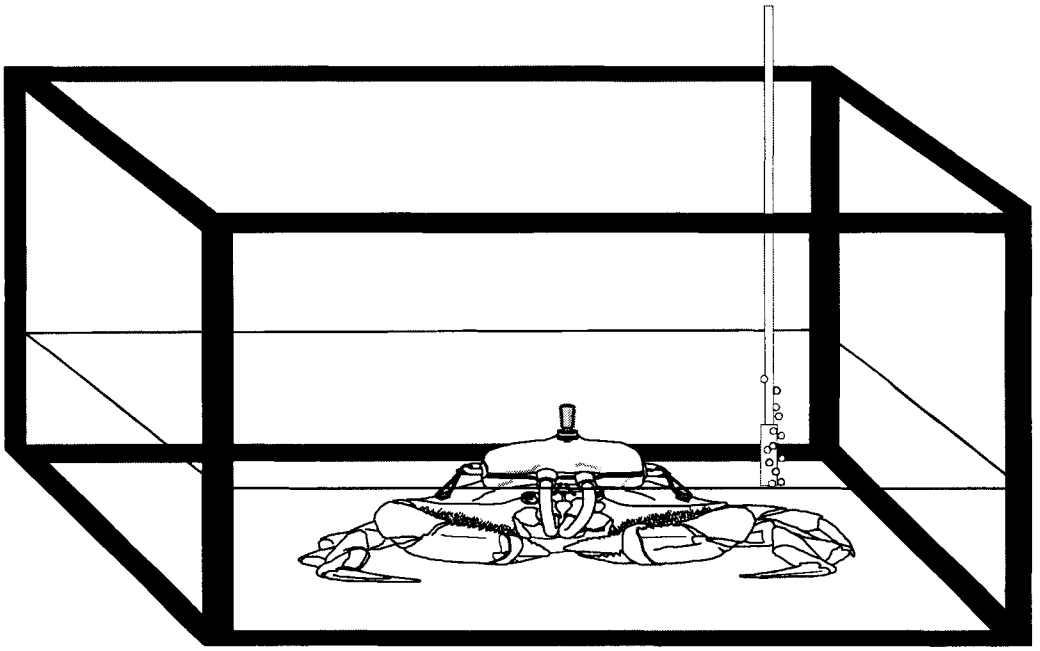

The static seawater was changed daily. Haemolymph was sampled via the pericardial chamber to minimise handling and disruption of crabs. Urine was collected daily at regular time intervals using a disposable 10 ml syringe and a 21 gauge needle fitted with a 10 - 12 cm length of PE 100 polyethylene tubing. Urine volumes were measured in graduated cylinders tubes and were subsequently transferred to disposable 50 ml glass centrifuge tubes. Collection vessels were rinsed with 10 ml of ethanol following each sample. The ethanol rinse was added to urine samples which were frozen at –28 °C prior to analysis. Urine flow rates were calculated by dividing the volume of urine excreted by the appropriate time interval. Parent BaP and metabolites were

determined and characterised in pooled urine samples using the analytical methods described below.

4.2.4.1 Urine Collection System

Urine collection vessels were rectangular shaped, hand blown glass globes, approximately 50 - 60 ml in volume. The reusable glass vessels conformed to the contours of the dorsal carapace Figure 4.3.

Figure 4.3 Exploded view of urine collection system

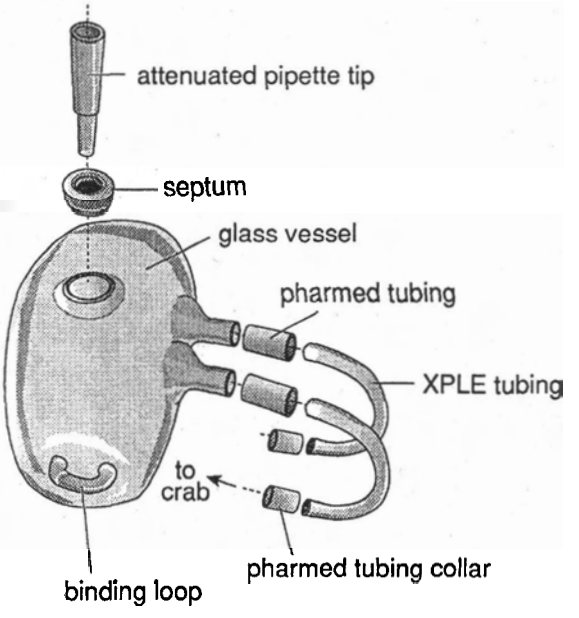

Two entry tubes (ID 3/16"), at the front of the vessel were connected with heat moulded 7 - 8 cm long XPLE collection tubes (ID 1/8", OD 1/4") using tight fitting Pharmed® (Norton) (ID 3/16") tubing collars. Collection tubes were secured to the crab with short (2 cm) Pharmed attachment collars as detailed below. At the top of each collection vessel was a sampling port fitted with a modified 10.25 mm Vacutainer®

septum (Becton Dickinson, Rutherford, New Jersey). The septum was shortened and bored to accommodate an attenuated 2-200 µl polypropylene pipette tip used to guide a sampling syringe.

4.2.4.2 Attachment of Urine Collectors

Crabs were kept on crushed ice for 15 to 20 minutes before being fitted with catheters. External catheters were mounted around both nephropores (external urinary ducts) on the epistome (also called the third antennal segment which refers to the antennal sternal plate forming the anterior part of the buccal frame). The epistome was cleared of epibiota (small hair-like processes), cleansed with acetone and primed with a glue accelerant. Sutures on the epistome around both nephropores were filled with cyanoacrylate glue (Hot Stuff®, Satellite City, Simi, California) to prevent catheter leakage at the base. A rim of glue was built up around both nephropores to obtain a good seal with the tubing. Short attachment collars, (≈1.5 cm), of flexible Pharmed® tubing, were fixed with cyanoacrylate glue around each nephropore, taking care not to occlude the operculae. A previously heat moulded collection tube was then pressed into each collar so that it curved upward between the eye stalks of the crab and connected with the glass vessel. Collection tubes were connected to the glass collection vessel with a Pharmed® tubing collar. The collection vessel was placed on the surface of the dorsal carapace, marginally posterior to the cephalic ridge. To stabilise the vessel, rubber bands were fixed to the attachment points (Figure 4.3) and were glued to the carapace of the crab. Chelae were banded so that the crab could not remove or interfere with the collection device. A dungeness crab fitted with a urine collector is shown in Figure 4.4.

Figure 4.4 Urine collection system fitted to a dungeness crab.

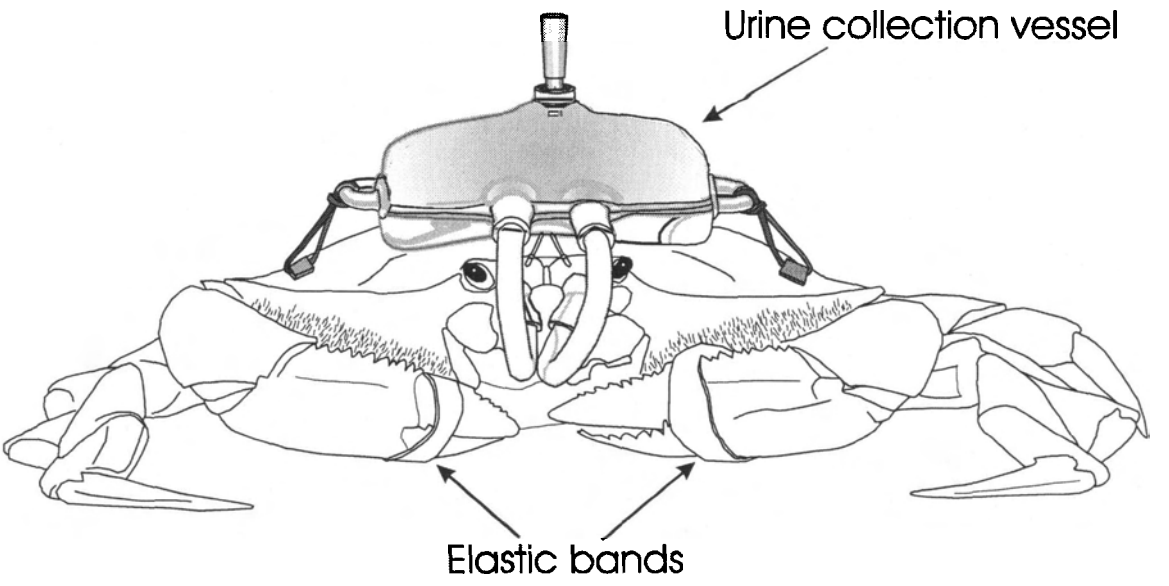

The catheters displaced the third maxillipeds slightly, but did not produce obvious signs of stress in the crabs. Catheterised crabs were able to evacuate freely, as the tubing did not impair the flow of urine, or create a capillary force to draw urine out of the bladder. Crabs could remain catheterised for a period of 2 weeks or more, over which time samples could be taken without any obvious signs of degeneration in the experimental animal.

When the urine collection system was fitted to crabs, the glue seal surrounding each nephropore was tested with a food colour preparation to ensure the patency of the attachment collars. This test was administered by pressing a length of XPLE tubing into the attachment collar glued around each nephropore. A low pressure was applied to a food colouring solution in a 30 ml syringe fitted to the tubing in order to detect the presence of any leaks.

4.2.4.3 Patency Tests of Assembled Collection Systems

Two different patency tests were performed on the collection system which was assembled but not attached to crabs. The collars normally glued around crab nephropores were plugged with ground glass stoppers. The tests are described as follows: a) The first test used a dye to test for leakage from the collection system under ambient conditions. A urine collecting system containing 22 ml of 41.5 μg/ml Fast Green FCF dye was immersed in 340 ml of distilled water at room temperature (25°). After 96 hours, the surrounding water was tested for the presence of dye with a spectrophotometeric assay (Eickhoff and Law, 1995). b) A second test was conducted to test the resistance of the collection system to osmotic pressure. A collection system containing 25 ml of 31 ppt saline solution was placed in 400 ml of distilled water. After 96 hours, the volume and salinity of the saline solution in the urine collector and the immersion water outside the collector were measured (Eickhoff and Law, 1995).

4.2.5 Crab Dissection and Body Composition Analysis

Following toxicokinetic experiments, crabs were reweighed and the weights were recorded. A total of 67 crabs ranging from 571 – 922 g were dissected for the estimation of tissue volumes. Tissues including the muscle, hypodermis, gills, hepatopancreas, testes, bladder, stomach, intestine, and heart were excised, rinsed with deionised, distilled water, patted dry on a paper towel, and weighed to the nearest thousandth of a gram. The mass of each tissue was recorded. The chitinous parts of the cardiac stomach were excised from the membrane prior to mass determination. Tissue volumes for the PBTK model were calculated for each tissue as a percentage of the total body mass of each crab.

The volume of haemolymph was calculated as 35.7% of the total body mass. The total amount of muscle tissue was calculated as 23.2% of the total body mass based on the body composition of a subset of crabs. For this subset of six crabs, the entire muscle tissue was excised from the carapace and the mass was determined. Crab tissues were subsequently analysed to determine the concentration of benzo[a]pyrene. Tissues that were not extracted immediately were frozen at -28°C.

4.2.6 Determination of *in vitro* Partition Coefficients

The tissue:tris buffered saline (TBS) partition coefficient was determined for each of nine tissues: bladder, gill, muscle, hepatopancreas, heart, haemolymph, gastrointestinal tract (gut), hypodermis (skin), and testes for each concentration. Additionally, haemolymph:seawater partitioning was examined using autoclaved 29 ppt seawater rather than TBS. *In vitro* partition coefficients were determined using a dialysis membrane method adapted from the *in vitro* methods of Jepson *et al.* (1994) and Sato and Nakajima (1979) described in Andersen *et al.* (1984). Tissues from four freshly euthanised crabs were excised and pooled. Tissues were homogenised in TBS pH 7.4 at a ratio of 4:1 tissue:buffer.

Dialysis tubing (Spectra/Por®, #3 MWCO 3500 Molecular porous membrane tubing, 18.5 mm, Spectrum®, Laguna Hills, CA) was pre-cut to 6.5 cm lengths, soaked in distilled water for 15 minutes, and heated to 80 °C while stirring for 30 minutes in a 10 mM sodium bicarbonate solution. Dialysis tubing was then transferred to a 10 mM sodium EDTA solution and soaked for 30 minutes, stirred in distilled water for 30 min @ 80 °C, allowed to cool and conditioned in TBS for prior to use.

Homogenised tissues were added to dialysis tubing as follows; one end of each dialysis tube was tightly tied with 2-0 non-sterile, non-absorbable, surgical suture (Ethicon Inc.). Two glass beads were placed in the bottom of the bag and a 2.000 g aliquot of freshly homogenised tissue was weighed into each bag using a bench top balance. Dialysis bags were sealed by carefully tying the open end with 2-0 silk to prevent the inclusion of air bubbles. Excess suture was cut off, but one length was kept long to suspend the dialysis bags in TBS buffer solution. Bags were dialysed in TBS for 48 hours prior to experiments to clear molecules below the 3500 molecular weight cut off (MWCO).

Mixtures of ^{14}C-benzo[a]pyrene and non-radiolabelled benzo[a]pyrene were prepared in methylene chloride in 2 ml volumetric flasks, blown down with a gentle stream of nitrogen, redissolved in 100 µl of Tween 80, and resuspended in TBS to a final volume of 2 ml. Two stock solutions were formulated so that amounts of 100 ng or 1000 ng of ^{14}C-benzo[a]pyrene (specific activity 224, 23.0 µCi/mg respectively) could be added in a 48 µL aliquot to each test vial for test concentrations of 50 and 500 ng/ml. Aliquots were added to vials using a 50 µl Hamilton syringe and were analysed by LSC and HPLC to determine the concentration and specific activity of ^{14}C-benzo[a]pyrene.

Into each 22 ml test vial (Supelco), 20 ml of TBS was pipetted. A micro stirring bar (Fisher) and a dialysis bag containing 2g of homogenised tissue were then added. A 48 µL aliquot of chemical was added to the TBS in each vial which was sealed with a Teflon lined cap. Dialysis bags were suspended in test vials with 2-0 silk suture so that the bag was submerged in buffer but was not disturbed by the stir bar at the bottom of the

vial as depicted in Figure 4.5a. Vials were placed randomly in groups of nine onto stir plates as shown in Figure 4.5b.

Figure 4.5 Dialysis vial set-up for *in vitro* partition coefficient determination a)detailed diagram of vial containing tissue dialysis bag, b) vials set-up on stir plate

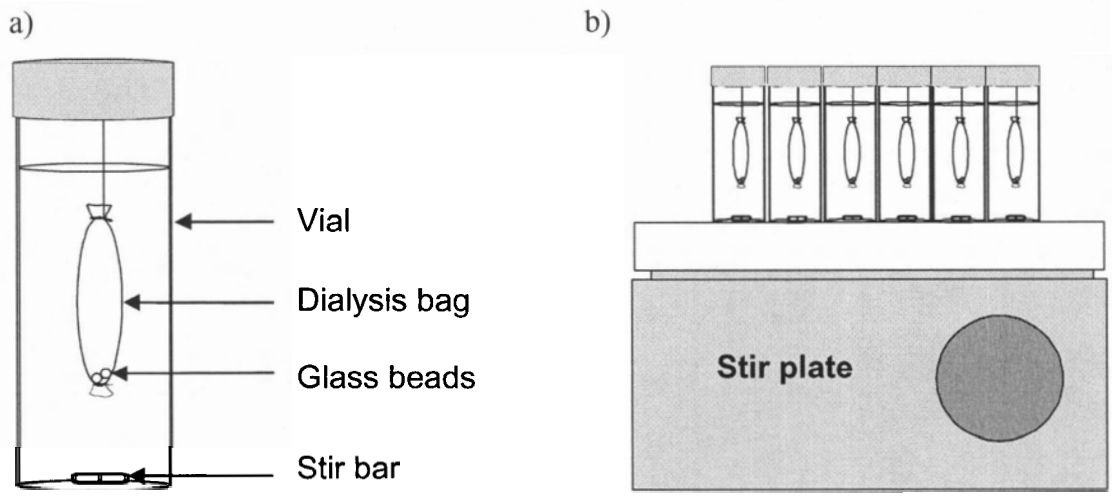

Reference vials consisting of dialysis bags filled with 2 g of TBS were tested at both concentrations and with both TBS and seawater. Control vials were also prepared which contained all components except dialysis bags. Four replicates were run for each tissue, reference and control at each test concentration. The experiment was conducted at 9 °C in a temperature controlled room. Vials were stirred continuously for a period of 14 days. At the end of the test, 2 ml aliquots were taken from each vial using 2 ml glass volumetric pipettes. Aliquots were added to scintillation vials with 15 ml of liquid scintillation cocktail. Vials were counted for 10 minutes using a Beckman LS 8000 liquid scintillation counter.

The concentration of benzo[a]pyrene was calculated based on the DPM measured in each medium by scintillation counting. The concentration of benzo[a]pyrene in the

tissues was calculated as the difference in the concentration of benzo[a]pyrene in the TBS of the control vial without dialysis bag minus the concentration of benzo[a]pyrene in the TBS of each vial with dialysis bag. The tissue:TBS partition coefficient was calculated as the benzo[a]pyrene concentration in each tissue over the concentration of benzo[a]pyrene in the TBS. Tissue:haemolymph partition coefficients were calculated as the tissue:TBS partition coefficient over the haemolymph:TBS partition coefficient.

4.2.7 Determination of Benzo[a]pyrene in Crab Tissues and Seawater

4.2.7.1 Extraction of Haemolymph Samples

Haemolymph samples (1ml) were added to 1ml of 50 mg/ml N-ethyl maleimide to prevent clotting. Each sample was spiked with a 10 ml aliquot of a stock benzanthracene internal standard solution. Haemolymph was deproteinised and extracted with 6 ml of HPLC grade acetonitrile. Samples were shaken in 15 ml disposable conical glass tubes closed with PFTE lined screw caps for 30 minutes and were then centrifuged for 10 minutes at 3500 rpm to pellet the denatured protein and macromolecules. Supernatant aliquots were pipetted directly into 2 ml autosampler vials for HPLC analysis. Low analyte concentration supernatants were concentrated using a Jouan RC10.22 Centrivap (Jouan Inc. Winchester, VA), resuspended with 1 ml acetonitrile, and pipetted into 2 ml autosampler vials.

4.2.7.2 Extraction of Benzo[a]pyrene from Tissue Samples

Excised crab tissues including muscle, bladder, hypodermis, gastrointestinal tract, testes and carcass were weighed and homogenised 1:1 with 0.9% saline using a Polytron

homogeniser (Brinkman Co., Rexdale, Ont.). Hepatopancreas samples were homogenised either 4:1 tissue:saline with 0.9% saline, or with no saline added. Homogenised tissue aliquots (2, 4, or 5g) were weighed into 50 ml disposable glass centrifuge tubes sealed with PFTE lined screw caps. Homogenate aliquots were spiked with 20 μL of a 2 ng/μL benzanthracene internal standard stock solution. Samples were allowed to sit for 30 minutes and were then saponified.

Saponification was performed by adding 0.6 ml of 50% w/v KOH and 5 ml of HPLC grade methanol. Samples were refluxed in a recirculating heated water bath at 78 °C for 1 hour and were vortexed at 20 minute intervals. Samples were removed from heat and 5 ml of distilled water was added prior to a further hour of reflux at 78 °C and periodic vortexing at 20 and 40 minutes.

Saponified samples were allowed to cool to room temperature and were then extracted with 22 ml of pentane. Samples were shaken for 30 minutes on a mechanical shaker and centrifuged at 3500 rpm for 10 minutes to separate the aqueous and organic layers. The extraction was repeated twice and extracts were pooled separately in 50 ml centrifuge tube and were concentrated with a gentle stream of N_2 in 1 ml of octanol prior to liquid chromatography column cleanup.

Sample cleanups were performed by liquid chromatography using 205 X 14 mm glass columns. Sodium sulphate was added to a height of 1cm in a followed by 230-400 mesh Silica Gel 60 to a total height of 10 cm. Both column packing materials were added in degassed pentane slurries and the packed columns were rinsed with 1 bed volume of pentane. Samples were added to columns, rinsed with 12 ml of pentane and then eluted

with 15 ml of methylene chloride. Column eluates were concentrated with N_2, resuspended with 2 ml of acetonitrile and placed in autosampler vials for HPLC analysis. Recoveries of benzo[a]pyrene from each tissue type were determined by spiking clean tissues with known amounts of analyte and internal standard.

4.2.7.3 Extraction of Benzo[a]pyrene from Seawater

Seawater samples were placed in 15 ml disposable glass centrifuge tubes. Samples were spiked with 10 μL of a 2 ng/μL benzanthracene internal standard stock solution. Samples were extracted with 9 ml of pentane, shaken for 15 minutes on a mechanical shaker, and centrifuged at 3000 rpm for 5 minutes. This extraction was repeated twice and extracts were combined and evaporated under a gentle stream of N_2. Extracts were resuspended with 1 ml of acetonitrile and placed in 2 ml autosampler vials for HPLC analysis.

4.2.7.4 Analytical Method for the Determination of Benzo[a]pyrene

An aliquot of sample extract was injected into a Hewlett-Packard High Pressure Liquid Chromatograph (HPLC) Model 1050 equipped with a Vydac PAH column (5 μm, 250 x 4.5 mm), C18 cartridge guard column and pre-column filter assembly. The column assembly was eluted with an isocratic acetonitrile:water (90%:10%) mobile phase at a flow rate of 1 ml/minute. An Hewlett Packard 1046A programmable fluorescence detector was linked with an Hewlett Packard 3396 Series II integrator to record and analyse chromatograms. The excitation and emission wavelengths of the detector were set at 280 and 430 nm, respectively. The detector was calibrated using at least five

benzo[a]pyrene concentration standards prepared with the benzanthracene internal standard stock solution. Calibration curves were prepared by plotting the ratios of analyte over internal standard peak areas versus analyte concentration. Calibration curves were analysed by linear regression using Microsoft Excel® spreadsheet software on a PC computer. An example of a typical calibration curve is presented in Figure 4.6.

Figure 4.6 Typical calibration curve for the determination of benzo[a]pyrene by HPLC

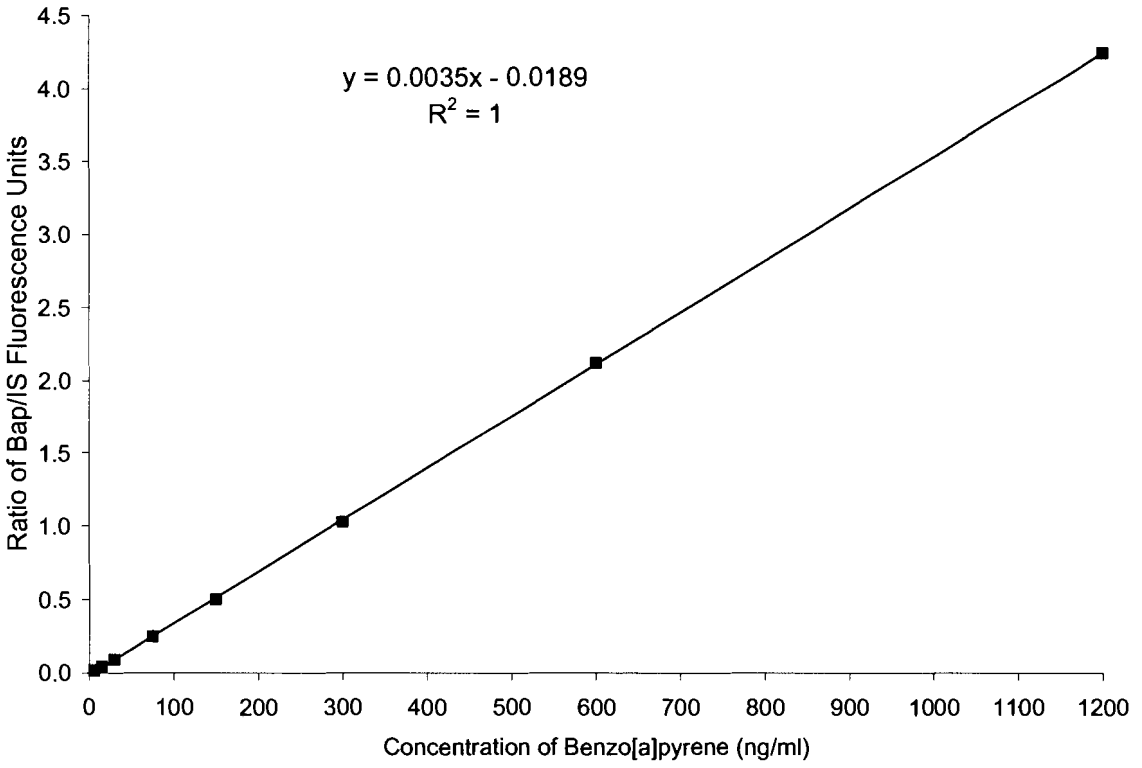

4.2.8 Analytical Methods for Determination of Benzo[a]pyrene Metabolites in Urine

4.2.8.1 High Performance Liquid Chromatography

Urine samples were thawed and a 1 ml aliquot of each urine sample was analysed by LSC for total radioactivity. Urine samples were individually treated to evaporate

added ethanol and reduce sample volume to approximately 10 ml using a Jouan RC10.22 Centrivap (Jouan Inc. Winchester, VA). The 10 ml urine aliquots were extracted 3 times with 25 ml of ethyl acetate in 50 ml glass centrifuge tubes. The extracts were collected and blown down under a gentle stream of nitrogen. The extracts were resuspended with 2 ml of reagent grade alcohol. A 0.5 ml aliquot of each extract was counted for radioactivity. The remaining 1.5 ml was placed in an HPLC autosampler vial for metabolite analysis. The aqueous phase of each urine sample was resuspended to 10 ml following extraction. A 0.5 ml aliquot was counted for determination of radioactivity.

The remaining aqueous fractions were hydrolysed by acidification with HCl and heating in a boiling water bath for 1 hr. The hydrolysed fractions were then extracted three times with a three fold volume of ethyl acetate. Aliquots of the ethyl acetate extracts and aqueous layers were analysed by LSC. Ethyl acetate extracts of hydrolysed and non-hydrolysed aqueous fractions were pooled separately, concentrated using a gentle flow of N_2 and resuspended in acetonitrile. Extracts were analysed using an Hewlett Packard HP1090 liquid chromatograph equipped with a reverse phase Zorbax ODS column, Diode Array Detector (DAD) and a Gilson fraction collector (model FC204). Injected samples were eluted at a flow of 1 ml/min with a non-linear gradient solvent system (Varanasi et al. 1986) as shown in Table 4.1. Solvent A consisted of 0.005% v/v glacial acetic acid in deionised, distilled water while Solvent B was HPLC grade acetonitrile.

Table 4.1 Timetable for non-linear gradient mobile phase

Time (minutes)	% Solvent A	% Solvent B
0 – 0.5	80	20
0.5 – 12.5	80 – 40	20 – 60
12.5 – 24.5	40 – 30	60 – 70
24.5 – 34.5	30 – 0	70 – 100
34.5 – 42.5	0	100

Fractions were collected at 0.5 minute intervals in 7 ml vials analysed by liquid scintillation counting (LSC). Peaks were identified by comparison with retention times of the following metabolite standards run under identical conditions: 3-hydroxybenzo[a]pyrene, 9-hydroxybenzo[a]pyrene, benzo[a]pyrene-4,5-dione, benzo[a]pyrene-*trans*-7,8-dihydrodiol, benzo[a]pyrene-*trans*-9,10-dihydrodiol (Midwest Research Institute, Kansas City, MO). UV absorbance of eluted metabolites and metabolite standards was monitored at a wavelength of 280 nm.

4.2.8.2 Gas Chromatography Mass Spectrometry

Fractions corresponding to the retention times of radiolabelled metabolite peaks were isolated using the HPLC method described above. The fractions obtained from several HPLC runs were pooled and reacted with trimethyl sulfoxide (TMS) to form derivatives in ethyl acetate. Aliquots were injected into an Hewlett Packard 5980 Series II GC fitted with an HP-5 M.S. cross-linked 5% Ph Me silicone 30 m x 0.25 mm GC column with a 0.25 μm film thickness (Hewlett Packard). The column was connected to the ion source of an Hewlett Packard 5971 Mass Selective Detector (MSD). The GC oven was programmed as follows: the initial temperature was 200 °C and increased at a rate of 8°C/minute to 280 °C and held for 10 minutes. The injector temperature was set to 250°C

and the MSD to 280°C. A splitless injection sequence was used and the carrier gas was He with a flow rate of 40-45 ml/min. The mass spectrometer was operated in the Electron Impact mode (EI) and the electron energy was set at 70 eV. Chromatographic data was acquired and Selective Ion Monitoring (SIM) was performed using Hewlett Packard G1034C Version C.03.00 MS ChemStation and Standalone Data Analysis software on a PC computer to analyse total ion chromatograms. Metabolites were identified using a library composed of benzo[a]pyrene metabolite standards including 3-hydroxy-benzo[a]pyrene, 6-hydroxy-benzo[a]pyrene, 9-hydroxy-benzo[a]pyrene, benzo[a]pyrene-trans-4,5-dihydrodiol, benzo[a]pyrene-cis-7,8-dihydrodiol, benzo[a]pyrene-r-7,t-8,c-9,t-10-tetrahydrotetrol, benzo[a]pyrene-trans-7,8-dihydrodiol, benzo[a]pyrene-trans-9,10-dihydrodiol, benzo[a]pyrene-3,6-dione, benzo[a]pyrene-1,6-dione, (Midwest Research Institute, Kansas City, MO) and cis-7,8-dihydroxy-7,8-dihydrobenzo[a]pyrene (Chemsyn Science Laboratories, Lenexa, KS) that were derivatised using TMS and run under the same conditions as unknown metabolite analytes.

4.2.9 Determination of Radioactivity

Radioactivity in liquid samples such as urine, haemolymph, tissue extracts, seawater, buffer samples, and dose aliquots was determined by liquid scintillation counting (LSC). Sample aliquots were pipetted separately into 20 ml scintillation vials. After addition of 10 ml of BCS scintillation cocktail, samples were vortexed. Radioactivity in each vial was counted for either 5 or 10 minutes using a Beckman LS-8000 liquid scintillation counter. HPLC fractions collected in 7 ml vials were similarly analysed by LSC following addition of 5 ml of BCS cocktail.

Radioactivity in non-liquid samples such as homogenised tissues, gut contents and tissue pellets was determined using a Model OX 300 Biological Material Oxidiser (BMO) (R.J. Harvey Instrument Co., Hillsdale, NJ) followed by LSC. The $^{14}CO_2$ evolved from each sample oxidation was trapped in Carbon 14 Cocktail (R.J. Harvey Instrument Co., Hillsdale, NJ) and counted for 5 minutes using the Beckman LS-8000 LSC. The recovery of radioactivity from sample oxidation was assessed using methyl methacrylate ^{14}C standards (Du Pont Co., Wilmington, DE) and was found to exceed 99%. Tissue homogenates and pellets from untreated crabs were oxidised and counted for use as sample blanks.

4.2.10 Toxicokinetic Analysis

The concentrations of benzo[a]pyrene in the haemolymph obtained following exposure of crabs to benzo[a]pyrene were plotted using Microsoft Excel® or Sigma Plot® Scientific Graph Program Version 1.00 (Jandel Corporation). Curves were fit using PC Nonlin (Statistical Consultants Inc., Lexington, KY). The half-life was calculated by regression of the semi-logarithmic concentration versus time data. The formula used to calculate half-life is presented in Equation 4.1:

$$t_{1/2} = ln(2)/\beta \qquad (4.1)$$

where,

$t_{1/2}$ = half-life

β = elimination rate constant

The elimination rate constant was calculated as the negative slope of the non-weighted least squares curve fit for the logarithmically transformed concentration data versus time data using Equation 4.2.

$$ln\ Ct = ln\ b - t * \beta \tag{4.2}$$

where,

Ct = Concentration at time t

b = Constant

β = elimination rate constant

Apparent bioavailability was calculated using kinetic parameters obtained from PC Nonlin. (Statistical Consultants Inc., Lexington, KY) using the following equations:

$$A\% = (AUC_{oral}/AUC_{oral})(Dose_{iv}/Dose_{iv})(100\%) \tag{4.3}$$

where,

A% = Apparent Bioavailability

AUC_{oral} = Area under the curve for oral dose

AUC_{iv} = Area under the curve for *i.v.* dose

$Dose_{oral}$ = Amount of the oral dose

$Dose_{iv}$ = Amount of the iv dose.

The corrected apparent bioavailability was calculated according to equation 4.5.

$$A\%corr = (AUC_x/AUC_{iv})(Dose_{iv}/Dose_x)(t1/2iv/t1/2x)(100\%) \tag{4.4}$$

Where,

t1/2iv = half-life of the i.v. dose

t1/2x = half-life of the oral dose.

The area under the concentration vs. time curves, AUC, was calculated using the following formula:

$$AUC_{0\rightarrow\infty} = AUC_{0\rightarrow t} + (t_l * C_l / \beta) + (C_l / \beta^2) \quad (4.5)$$

Where,

$AUC_{0\rightarrow\infty}$ = Area under the curve for time 0 to infinity,

$AUC_{0\rightarrow t}$ = Area under the curve for time 0 to t

C_l = the last measurable concentration at time t_l

t_l = the time of the last measurable concentration.

The AUC from 0 to t_l is calculated by means of the linear trapezoid rule, and the AUC from t_l to infinity was estimated using the statistical moment theory. Calculations were performed using the pharmacokinetic functions above (Gibaldi and Perrier, 1982) in Microsoft Excel®.

4.3 Results

4.3.1 Chromatographic Analysis of Benzo[a]pyrene

Table 4.2 shows the extraction recoveries obtained from crab tissues spiked with a known amount of benzo[a]pyrene. The extraction recoveries were generally good for all tissues. The percent recovery was highest for the gill, and the lowest recovery was obtained from bladder tissue.

Table 4.2 Extraction recoveries of benzo[a]pyrene from dungeness crab tissues

Tissue	Recovery (%)
Haemolymph	78.25 ± 2.06
Gill	101.61 ± 7.86
Muscle	88.11 ± 3.29
Testes	81.19 ± 2.53
Gut	76.58 ± 2.48
Heart	71.09 ± 2.77
Bladder	63.38 ± 5.76
Skin	71.67 ± 7.80
Hepatopancreas	75.23 ± 11.99
Water	83.65 ± 5.34

Figure 4.6 shows a typical HPLC chromatogram describing the elution profile of benzanthracene and benzo[a]pyrene. The retention times of benzanthracene and benzo[a]pyrene were approximately 5.8 minutes and 10.3 minutes respectively.

Figure 4.7 A typical HPLC chromatogram of benzo[a]pyrene and benzanthracene (internal standard). Peaks I and II represent benzanthracene and benzo[a]pyrene respectively.

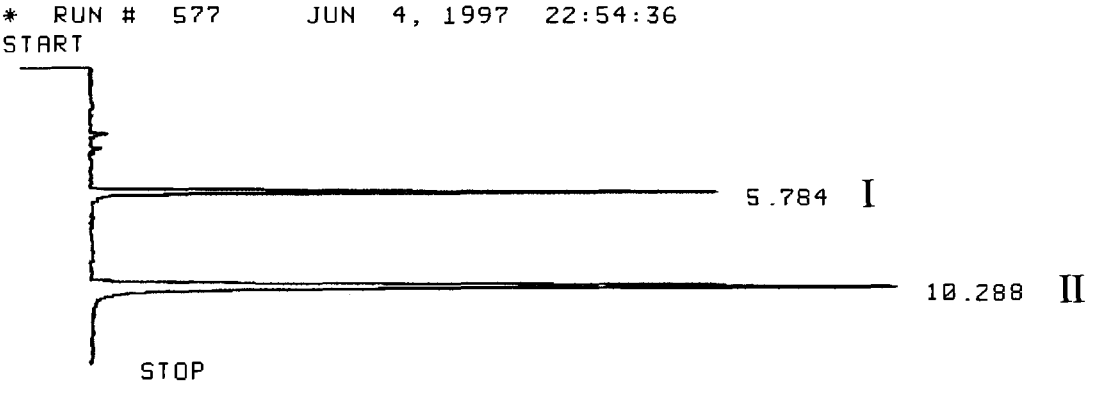

The method detection limit of benzo[a]pyrene ranged from 0.1 – 0.5 ng/ml depending on the HPLC injection volume and the calibration curve.

4.3.2 Toxicokinetics of Benzo[a]pyrene in the Crab Following Intravascular Dose

Figure 4.8 shows the concentration of benzo[a]pyrene determined in the haemolymph of crabs administered with a 2 mg benzo[a]pyrene/kg intravascular dose. Error bars on all graphs represent one standard deviation from the mean of three measurements per time point.

Figure 4.8 Concentrations of benzo[a]pyrene in the haemolymph over time following a 2 mg/kg intravascular dose

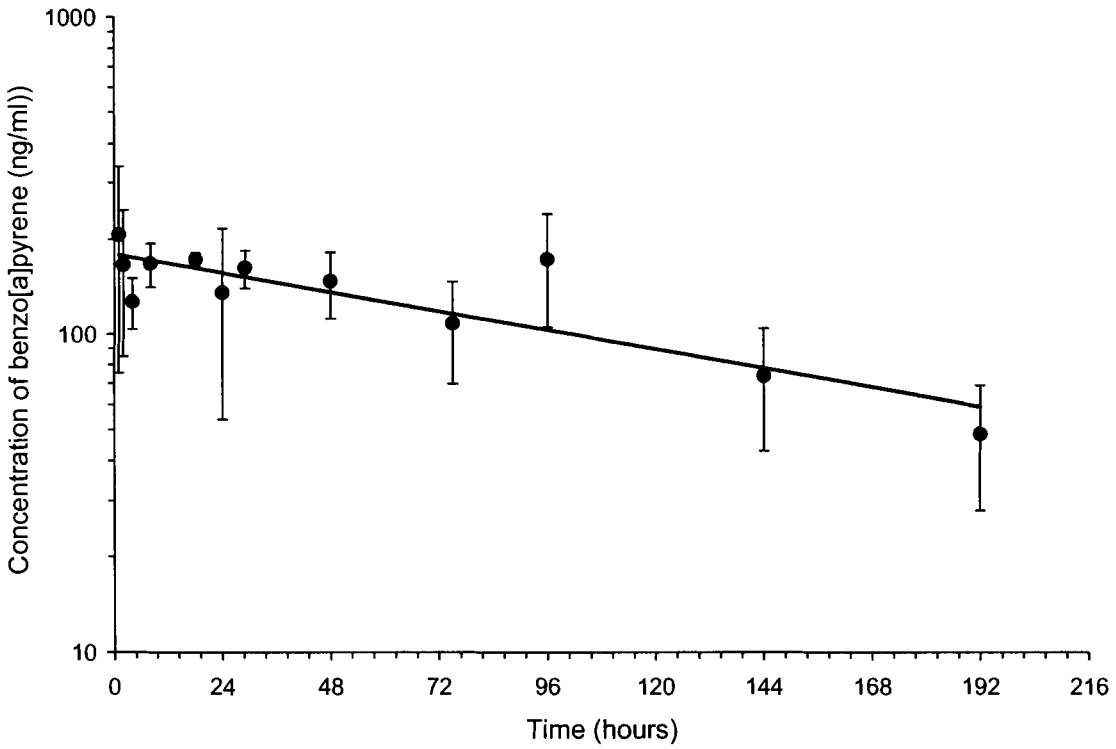

The kinetics of benzo[a]pyrene in the haemolymph suggest that a one compartment classical toxicokinetic model would describe the disposition of

benzo[a]pyrene in the crab following an intravascular dose. The half-life of benzo[a]pyrene in the haemolymph following the intravascular dose was 134 hours.

The mean concentration of benzo[a]pyrene determined in the tissues of crabs is shown in Figure 4.9.

Figure 4.9 Concentrations of benzo[a]pyrene in crab tissues following a 2 mg/kg intravascular dose

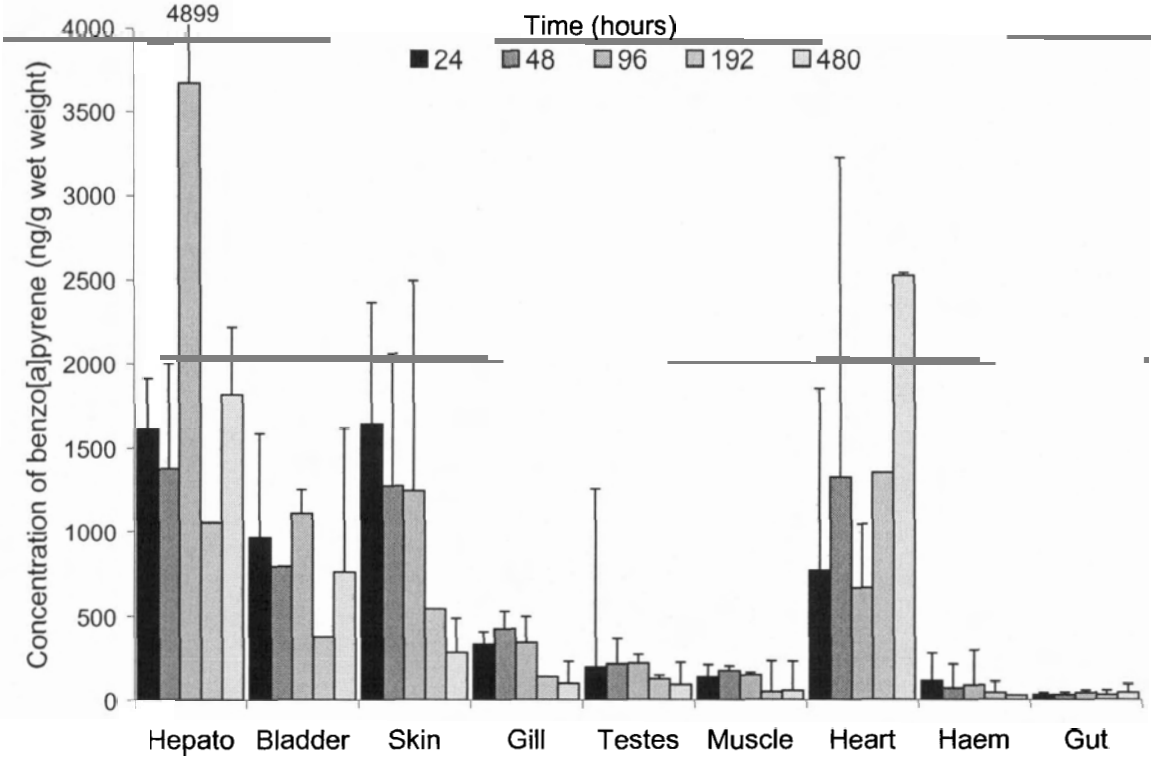

The greatest concentrations of benzo[a]pyrene were determined in the hepatopancreas, bladder, hypodermis, and heart tissues following the intravascular dose. The lowest concentrations were determined in the muscle, haemolymph and gut tissues.

4.3.3 Toxicokinetics of benzo[a]pyrene in the Crab Following Single Oral Bolus Dose

4.3.3.1 Single Oral Bolus Dose 2 mg Benzo[a]pyrene/kg

The concentrations of benzo[a]pyrene determined in the haemolymph of crabs following administration of a 2 mg benzo[a]pyrene/kg single bolus over time is shown in Figure 4.10.

Figure 4.10 Concentration of benzo[a]pyrene in the haemolymph following a 2 mg/kg oral dose

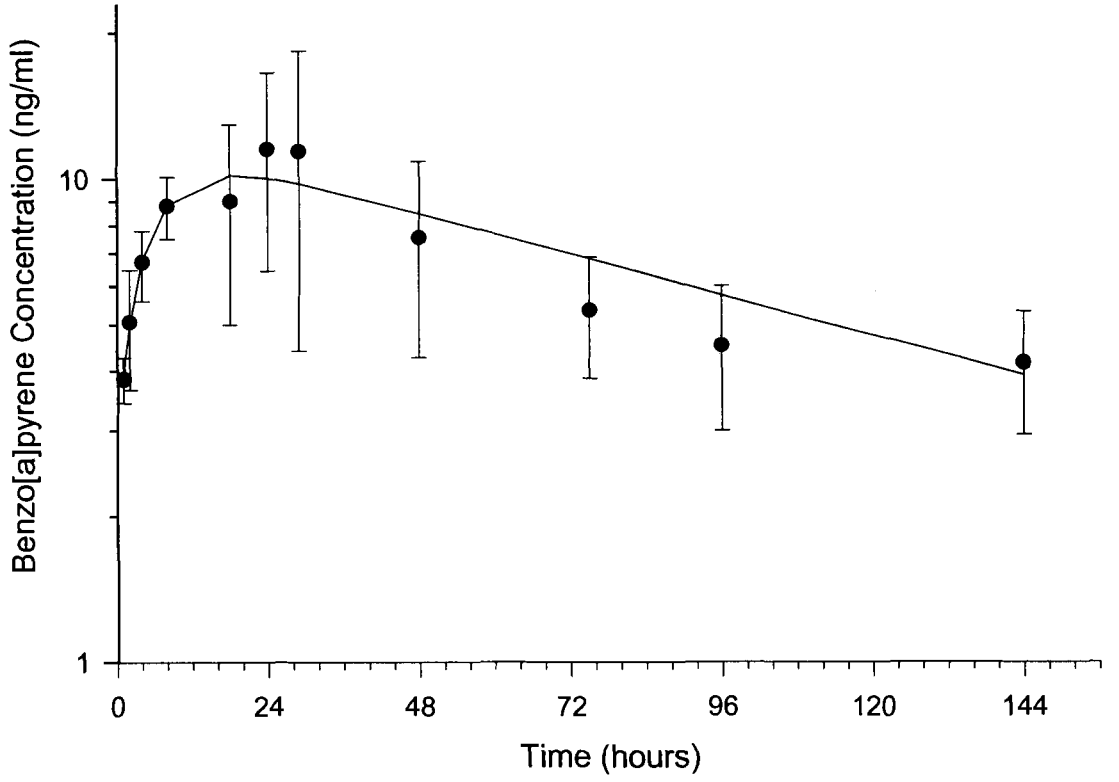

Figure 4.10 shows that there is a fairly rapid uptake of benzo[a]pyrene into the haemolymph from the gastro intestinal tract that peaks at 11.5 ng benzo[a]pyrene/ml, approximately 24 hours after the dose. At this point, there is a fairly rapid linear

elimination of benzo[a]pyrene from the haemolymph as this compound is distributed to the tissues and is excreted from the crab. The half-life of benzo[a]pyrene in the crab following the 2 mg/kg single oral bolus dose was 194 hours.

The mean concentrations of benzo[a]pyrene determined in the tissues of crabs administered with a 2 mg benzo[a]pyrene/kg single bolus oral dose is shown in Figure 4.11. The error bars represent the standard deviation of three measurements per time point.

Figure 4.11 Concentration of benzo[a]pyrene in crab tissues following a 2 mg/kg oral bolus dose

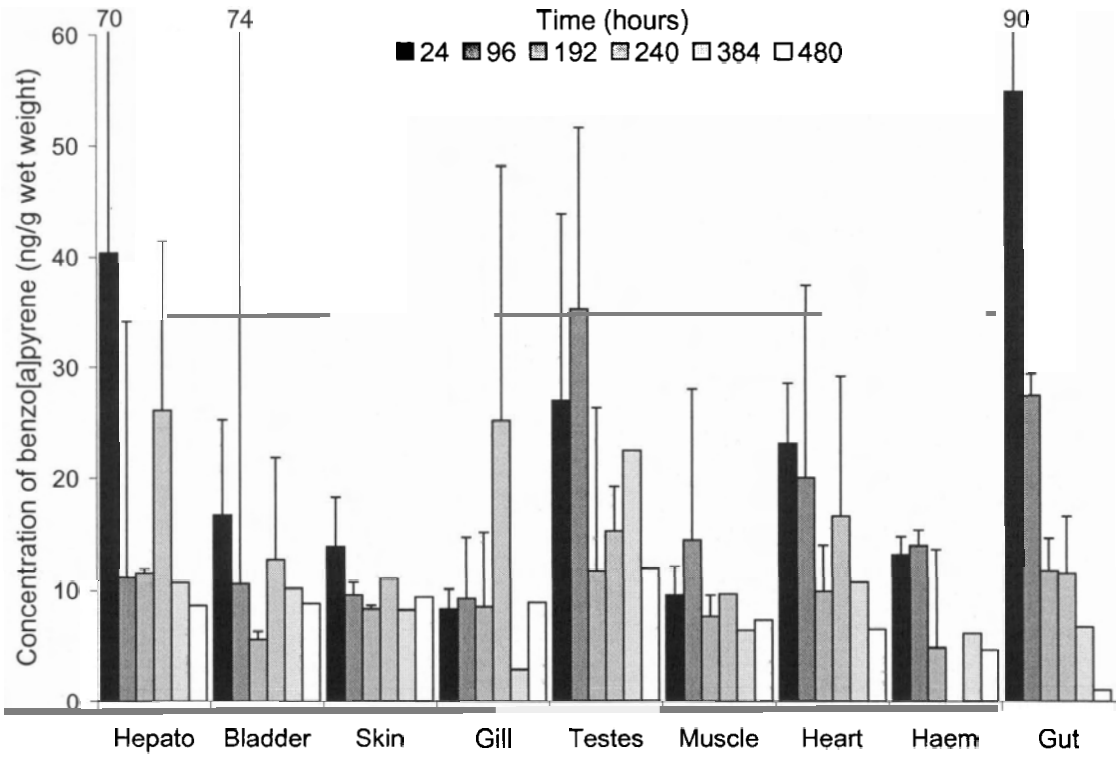

The distribution of benzo[a]pyrene in the various tissues is remarkably similar following a 2 mg/kg oral bolus dose. The highest concentrations were initially associated with the hepatopancreas and gut tissues. After 20 days, the concentrations of

benzo[a]pyrene in most of the tissues were still between 5 – 10 ng/g wet weight indicating that the elimination of benzo[a]pyrene is very slow.

4.3.3.2 Single Oral Bolus Dose 20µg Benzo[a]pyrene/kg

The mean concentrations of benzo[a]pyrene determined in the haemolymph of crabs following administration of a 20 µg benzo[a]pyrene/kg single oral dose is shown in Figure 4.12.

Figure 4.12 Concentration of benzo[a]pyrene in the haemolymph following a 20 µg/kg oral dose

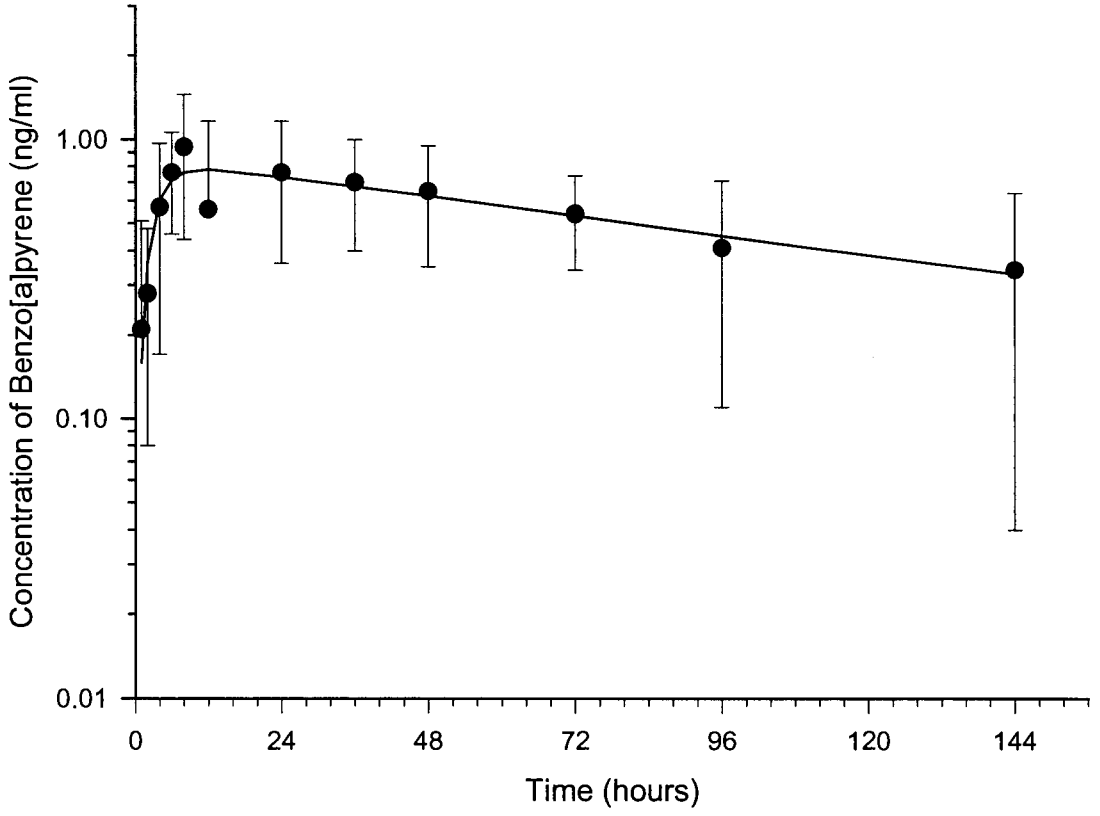

The concentration of benzo[a]pyrene in the haemolymph peaks at 0.94 ng/ml, approximately 8 hours following an oral bolus dose of 20 µg benzo[a]pyrene/kg. The

concentration of benzo[a]pyrene declines slowly at a linear rate following the uptake phase. The half-life of benzo[a]pyrene in the haemolymph following the dose was 354 hours.

The concentrations of benzo[a]pyrene determined in the tissues of crabs following a 20µg benzo[a]pyrene/kg dose is presented in Figure 4.13.

Figure 4.13 Concentration of benzo[a]pyrene in crab tissues following a 20µg/kg oral dose

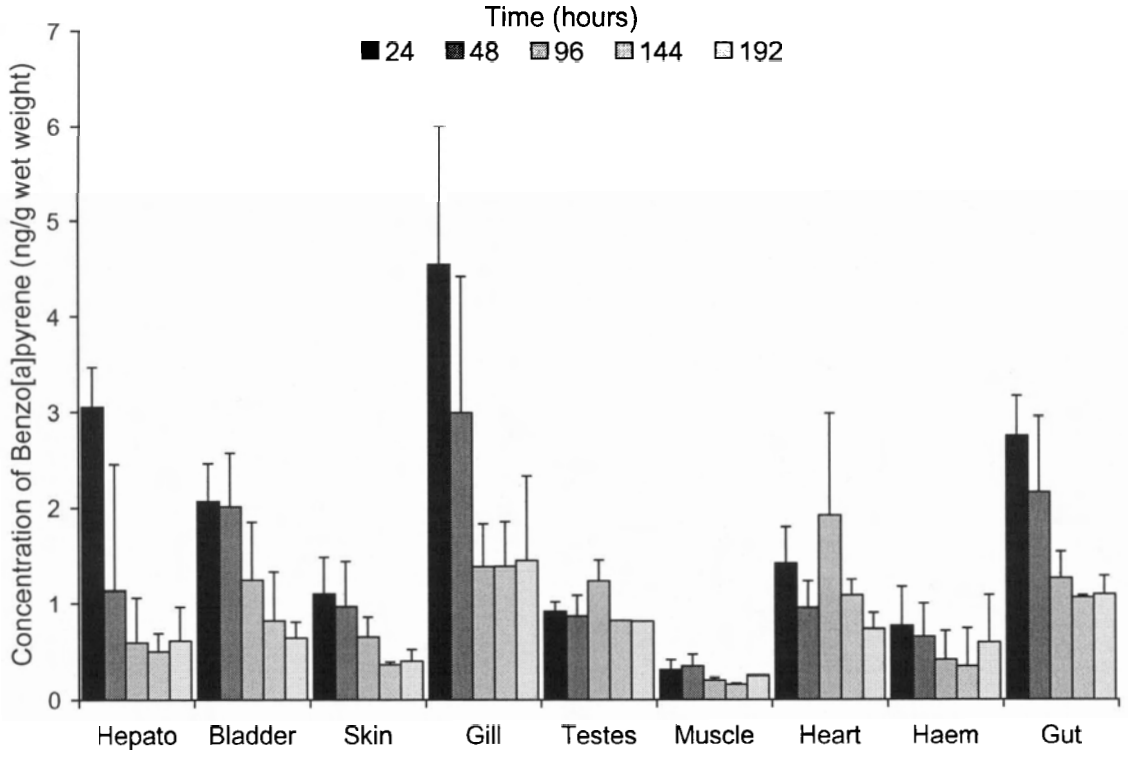

The concentration of benzo[a]pyrene was greatest in the gill, hepatopancreas, gastro-intestinal tract and bladder following the oral dose. The concentration of benzo[a]pyrene was lowest in the haemolymph and muscle tissues. The concentration of benzo[a]pyrene peaked in most tissues at 24 hours following the oral dose, except for in the testes and heart, where the peak concentrations were reached at 96 hours.

4.3.4 Toxicokinetics of Benzo[a]pyrene in the Crab Following Water-borne Exposure

4.3.4.1 Exposure to 20 µg Benzo[a]pyrene/L in Seawater

Crabs were exposed to benzo[a]pyrene in the seawater for a period of 72 hours. Crabs were then placed in fresh seawater to examine chemical elimination. The concentration of benzo[a]pyrene in the water was monitored over time before and during the exposure phase. At the beginning of the exposure phase, the concentration of benzo[a]pyrene in the seawater was 20.5 ± 0.7 ng/L (Figure 4.14). By the end of the exposure phase, the concentration declined to 5 ± 1.7 ng benzo[a]pyrene /L.

Figure 4.14 Mean concentrations of benzo[a]pyrene in seawater over time.

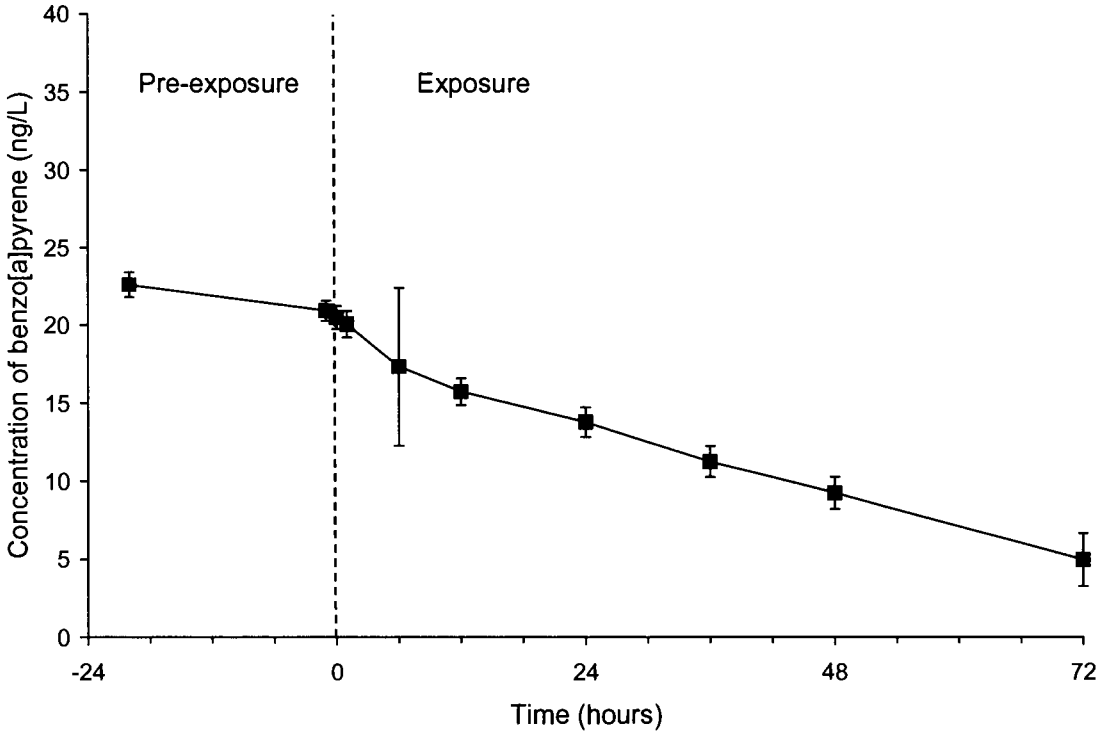

The mean concentrations of benzo[a]pyrene determined in the haemolymph of crabs following exposure to a nominal concentration of 20 μg benzo[a]pyrene/L in 29 ppt seawater is shown in Figure 4.15. The error bars represent one standard deviation from the mean of three samples.

Figure 4.15 Concentration of benzo[a]pyrene in the haemolymph after 72 h exposure to a nominal concentration of 20 μg benzo[a]pyrene/L in seawater

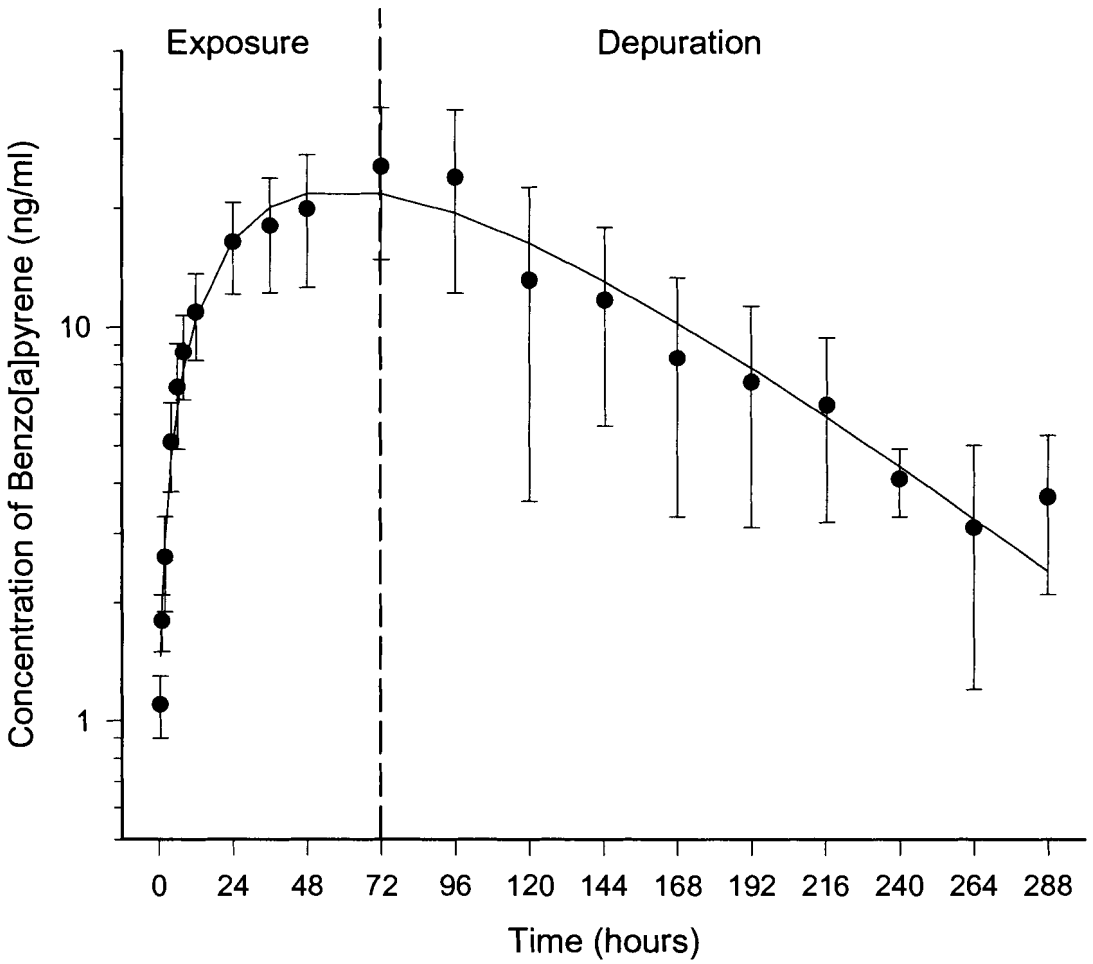

The concentration of benzo[a]pyrene in the haemolymph peaked at 16.9 ng benzo[a]pyrene/ml at 72 hours. The half-life of benzo[a]pyrene in the haemolymph during the depuration phase was 98 hours.

Figure 4.16 shows the concentrations of benzo[a]pyrene determined in the tissues of crabs following 72 hours of exposure to a nominal concentration of 20 µg benzo[a]pyrene/L in seawater.

Figure 4.16 Mean concentrations of benzo[a]pyrene in the tissues of crabs following exposure to a nominal concentration of 20 µg benzo[a]pyrene/L in seawater.

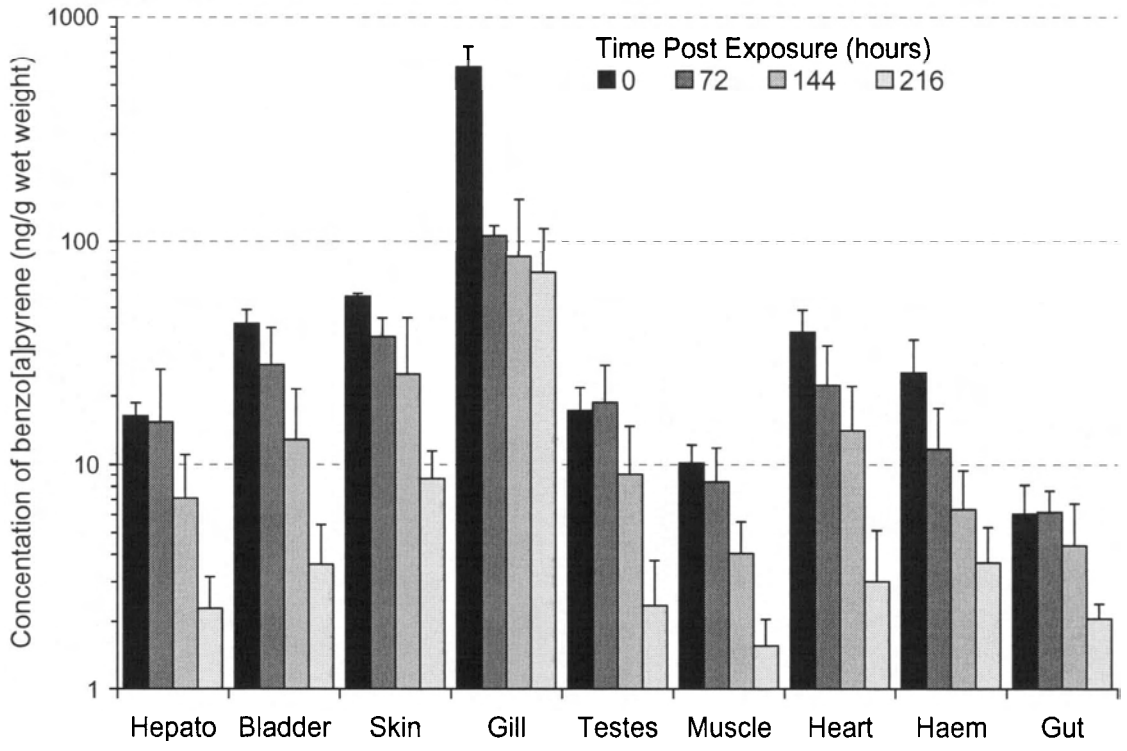

The concentration of benzo[a]pyrene was greatest in the gill following exposure to benzo[a]pyrene in the water. The concentrations of benzo[a]pyrene at time 216 hours in the remaining tissues decreased in the order of hypodermis (skin), bladder, testes, heart, haemolymph, hepatopancreas, gut, and muscle.

4.3.4.2 Exposure to 2 µg Benzo[a]pyrene/L in Seawater

The concentration of benzo[a]pyrene in the seawater was monitored over time before and during the exposure phase. At the beginning of the exposure phase, the mean measured concentration of benzo[a]pyrene in the seawater was 2.5 ± 1.5 ng/L (Figure 4.17). By the end of the 72 hour exposure phase, the mean concentration declined to 0.8 ± 0.6 ng benzo[a]pyrene /L.

Figure 4.17 Mean concentrations of benzo[a]pyrene in the seawater over time

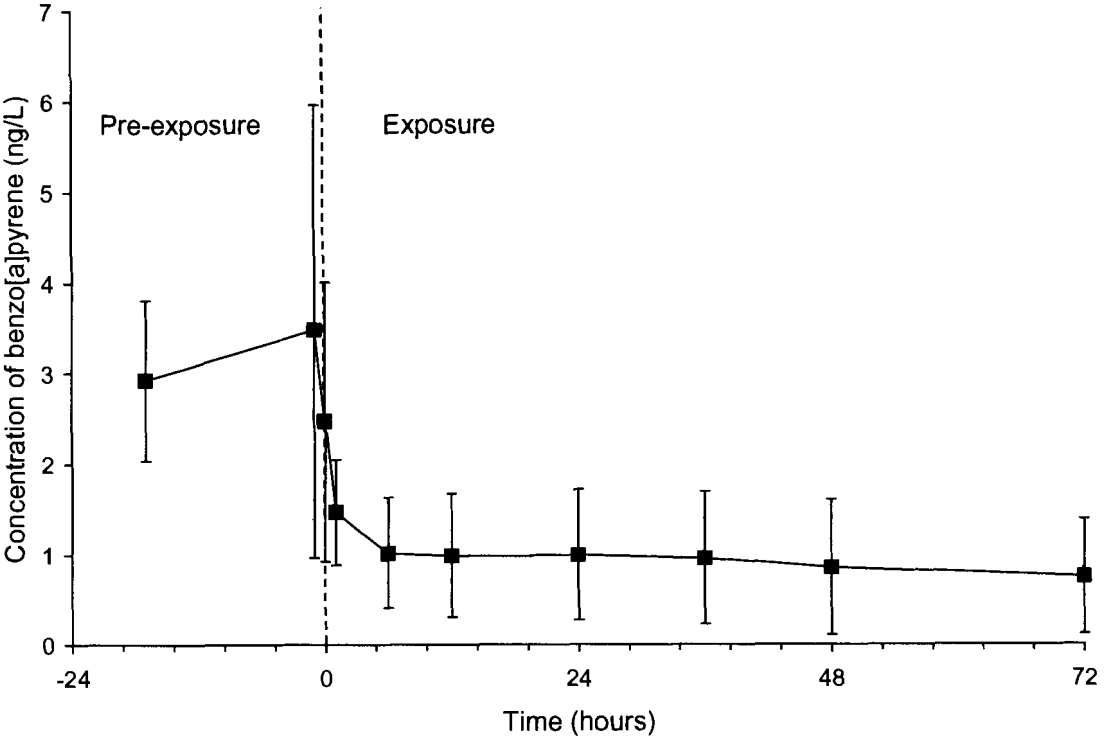

Figure 4.18 shows the mean concentrations of benzo[a]pyrene determined in the haemolymph of crabs following exposure to a nominal concentration of 2 µg benzo[a]pyrene/L in 29 ppt seawater. Crabs were transferred to clean seawater following

72 hours of exposure. The error bars represent one standard deviation from the mean of three samples.

Figure 4.18 Mean concentration of benzo[a]pyrene in the haemolymph of crabs exposed to 2 µg benzo[a]pyrene/L in seawater

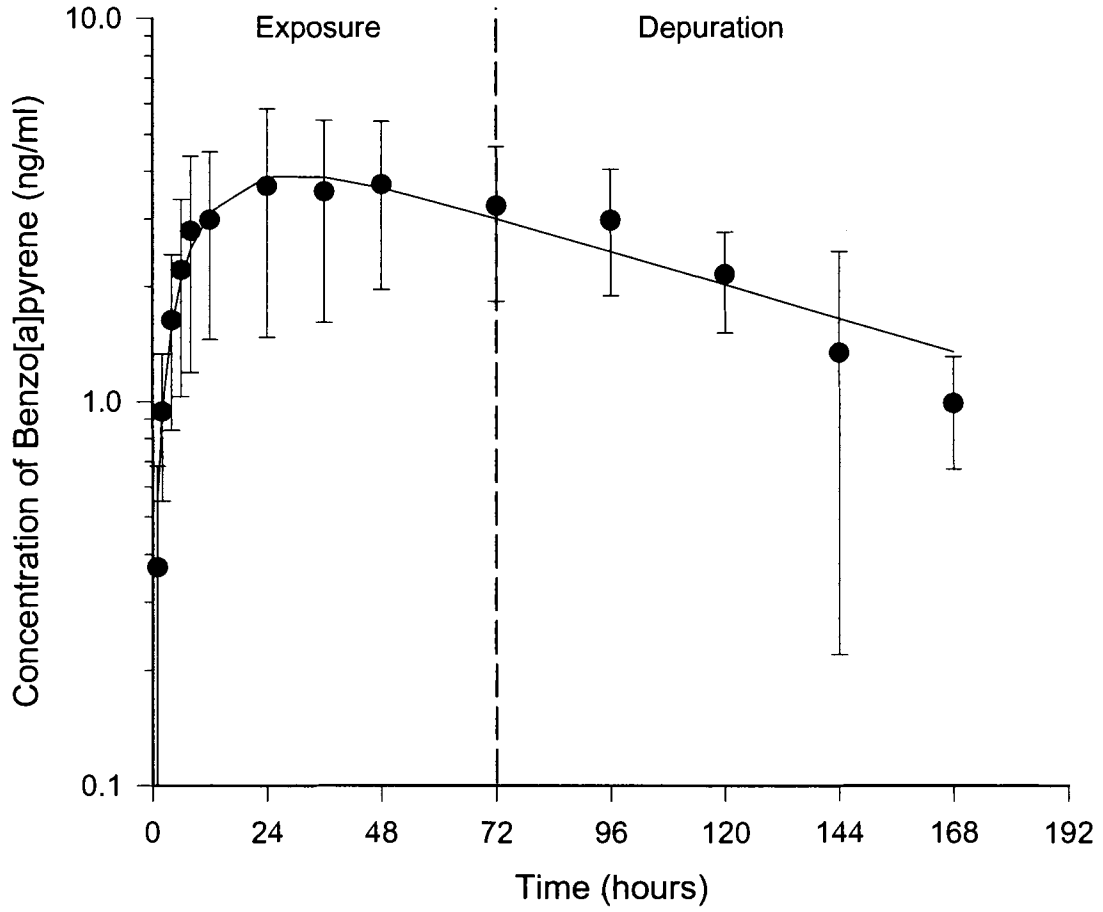

During the exposure phase, the concentration of benzo[a]pyrene in the haemolymph peaked at 5.3 ng benzo[a]pyrene/ml after 24 hours. The half-life of benzo[a]pyrene during the elimination phase was 74 hours.

Figure 4.19 shows the mean concentrations of benzo[a]pyrene determined in the tissues of crabs following water-borne exposure.

Figure 4.19 Mean concentrations of benzo[a]pyrene in the tissues of crabs following exposure to a nominal concentration of 2 µg benzo[a]pyrene/L in seawater.

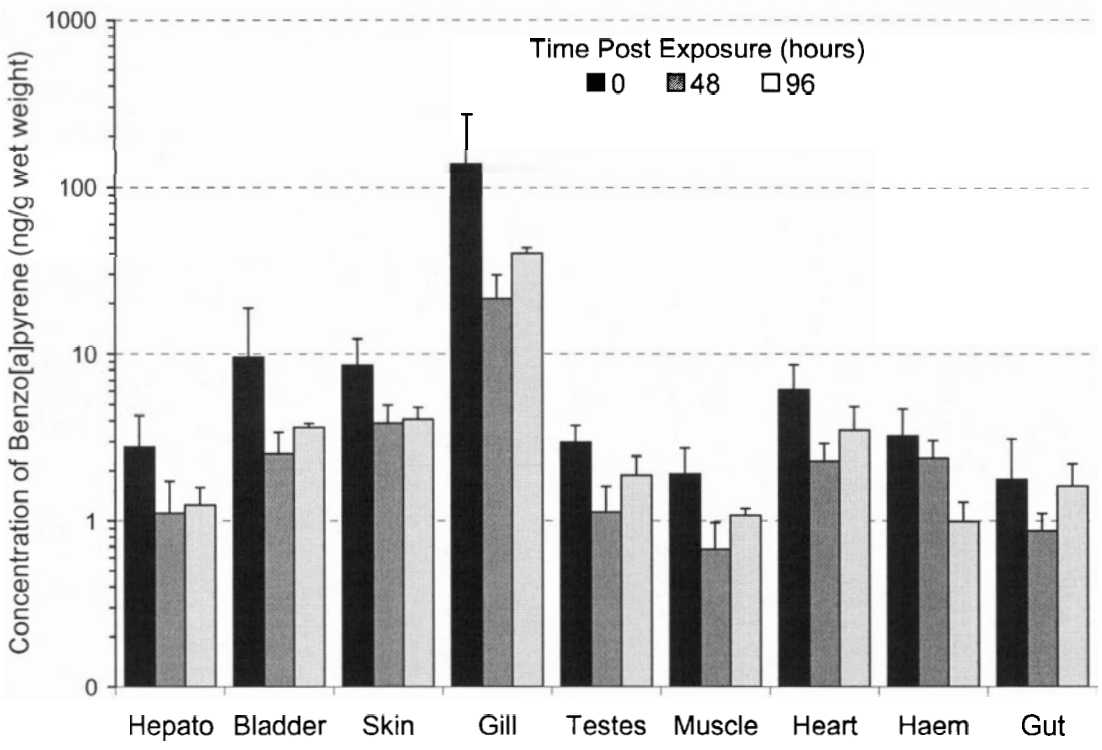

The concentration of benzo[a]pyrene was greatest in the gill following the exposure phase. The concentrations of benzo[a]pyrene in the remaining tissues decreased in the order of hypodermis, bladder, heart, testes, gut, hepatopancreas, muscle and haemolymph.

4.3.5 Apparent Bioavailability of Benzo[a]pyrene

The estimated apparent bioavailability of benzo[a]pyrene was calculated for each route of exposure. A summary of the bioavailability of benzo[a]pyrene in the dungeness crab for each exposure route is presented in Table 4.3.

Table 4.3 Apparent Bioavailability (A%) of benzo[a]pyrene in the crab

Route	iv	oral	oral	branchial	branchial
Dose	2 mg/kg	2 mg/kg	20 µg/kg	320000*	32000*
Dose (ng)	1620000	1696667	13367	209157†	19200†
AUC	47352.6	2546.6	126.88	3672.74	561.93
T1/2	134	194	354	98	74
A%	-	5.1	32	60	100
A% corr	-	3.5	12	82	180

*nominal concentration * volume for branchial route
†average measured concentration * volume for branchial route

These bioavailability values were used as parameters in the PBTK model described in Chapter 5.

4.3.6 Estimation of *in vitro* Partition Coefficients

4.3.6.1 Preliminary Experiment to Determine Tissue Homogenate Volume

Prior to determination of the *in vitro* partition coefficients, a preliminary experiment was conducted to determine the best volume of tissue homogenate to place in the dialysis bags so that tissue concentrations would reach equilibrium over a period of 14 days. The experiment was conducted with two tissues, muscle and hepatopancreas with either 1 or 2 ml of tissue homogenate per bag. A total of 100 ng of benzo[a]pyrene was added to each vial. Two replicates were conducted for each treatment. Figure 4.20 shows that the mean amounts of benzo[a]pyrene in the tissues reached a flatter plateau in the bags containing 2 ml of tissue homogenate for both the muscle and hepatopancreas. Therefore, 2 ml of tissue homogenate per dialysis bag were used for the definitive experiments for determining partition coefficients.

Figure 4.20 Amount of benzo[a]pyrene partitioned into tissues over time

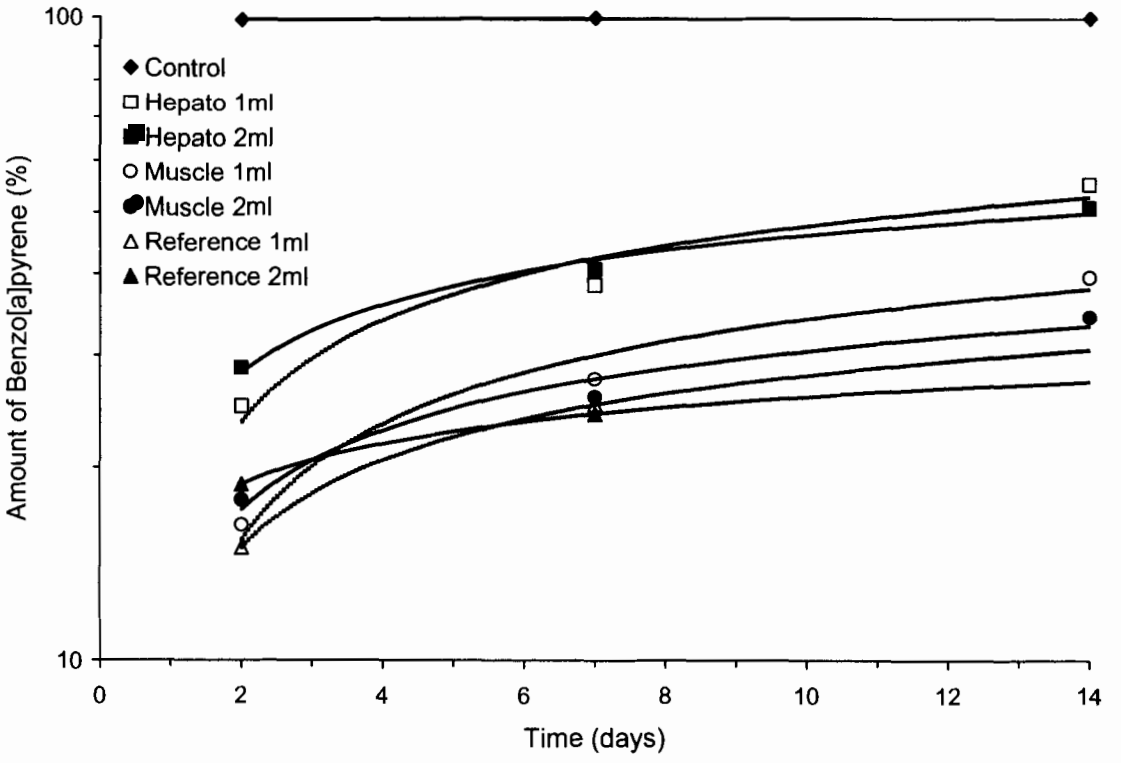

4.3.6.2 Partition Coefficient Determination

Tissue partition coefficient experiments were conducted in the dark at 9°C. The concentration of benzo[a]pyrene was determined in the TBS solutions of each vial by HPLC-fluorescence and scintillation counting techniques. Analysis of reverse phase chromatographs showed that there was one peak present representing benzo[a]pyrene indicating that metabolism of the benzo[a]pyrene did not occur to any measurable extent. Partition coefficients were estimated using either 100 ng or 1000 ng in 20 ml of TBS for each tissue. Partition coefficients for haemolymph were also determined with a seawater medium. The mean calculated percentage of benzo[a]pyrene for each tissue is shown in Figure 4.21.

Figure 4.21 Percentage of total benzo[a]pyrene in 2 ml of homogenised tissues (dialysis bags). Haem SW = haemolymph in seawater, Ref SW = reference seawater.

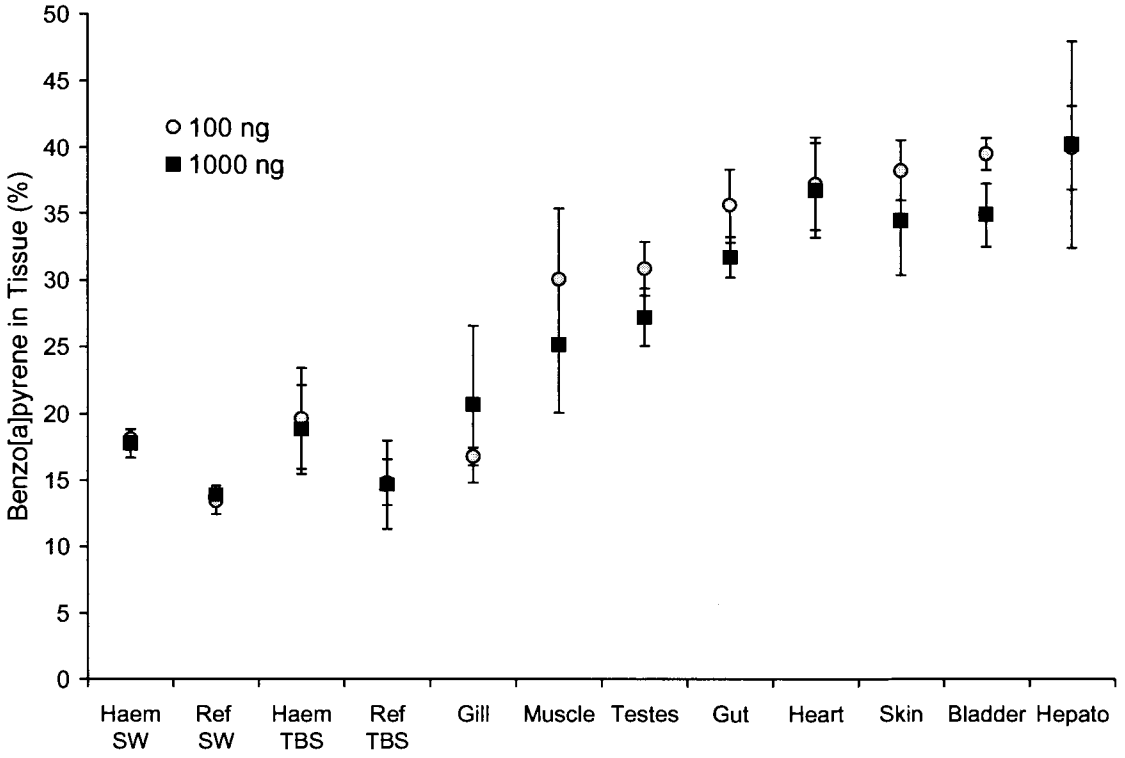

The in vitro partition coefficients estimated for each treatment of benzo[a]pyrene, 100 and 1000 ng, are summarised in Table 4.4. Mean and standard deviations are based on four measurements per treatment.

Table 4.4 Crab tissue:haemolymph partition coefficients for benzo[a]pyrene determined *in vitro*

	100		1000		Overall
Tissue	Mean	SD	Mean	SD	Mean
Gill	0.83	0.17	1.62	0.35	1.22
Muscle	1.76	0.47	2.09	0.36	1.92
Testes	1.83	0.38	2.32	0.29	2.08
Gut	2.26	0.49	2.89	0.34	2.58
Heart	2.43	0.54	3.61	0.48	3.02
Skin (hypodermis)	2.54	0.53	3.27	0.46	2.90
Bladder	2.67	0.54	3.34	0.41	3.00
Hepatopancreas	2.73	0.59	4.18	0.79	3.45

Generally, the partition coefficient obtained using 1000 ng of benzo[a]pyrene in the vials was greater than that obtained when 100 ng was used. The haemolymph:tissue partition coefficients declined in the order of hepatopancreas, heart, bladder, hypodermis, gut, testes, muscle and gill.

4.3.7 Body Composition Analysis

Table 4.5 shows the body composition of the dungeness crab. Mean values and standard deviation for each tissue are presented in terms of tissue mass in grams and percent of total body mass. Nerve tissues and other small organs are represented as "other".

Table 4.5 Body composition of the dungeness crab (n = 57)

Tissue	Mean mass (g)	SD	Mean Percent of Body Weight	SD
Stomach & gut	1.291	0.219	0.19	0.03
Hepatopancreas	25.421	5.783	3.46	0.92
Bladder	2.634	1.201	0.36	0.21
Muscle	161	17	23.2	2.47
Gill	5.864	0.994	0.81	0.12
Heart	1.119	0.191	0.15	0.03
Testes	1.231	0.335	0.18	0.05
Hypodermis	6.317	0.832	0.86	0.15
Haemolymph	248	26	35.7	3.80
Carapace	230	25	33.2	3.54
Other	13.110	-	1.89	-
Total	696	-	100.00	-

The haemolymph, carapace, and muscle tissues have the largest tissue volumes, 35.7%, 33.2% and 23.2% respectively, which together comprise 92.1% of the total body mass of the crab.

4.3.8 Examination of *in vivo* Metabolism and Urinary Excretion

Individual urine samples were collected from three crabs administered with a 2 mg benzo[a]pyrene/kg intravascular dose, and three crabs with a 2 mg benzo[a]pyrene/kg single bolus oral dose. Urine samples were collected daily over a period of ten days. Urine flow rates were calculated based on cumulative urine volumes over time (Figure 4.22). The mean urine flow rate of crabs dosed *per os*, 2.25 ml/kg/hr was greater than that for crabs dosed *i.v.*, 1.51 ml/kg/hr.

Figure 4.22 Mean volume of urine excreted and urinary flow rates measured in crabs following either a 2 mg benzo[a]pyrene/kg intravascular or oral dose

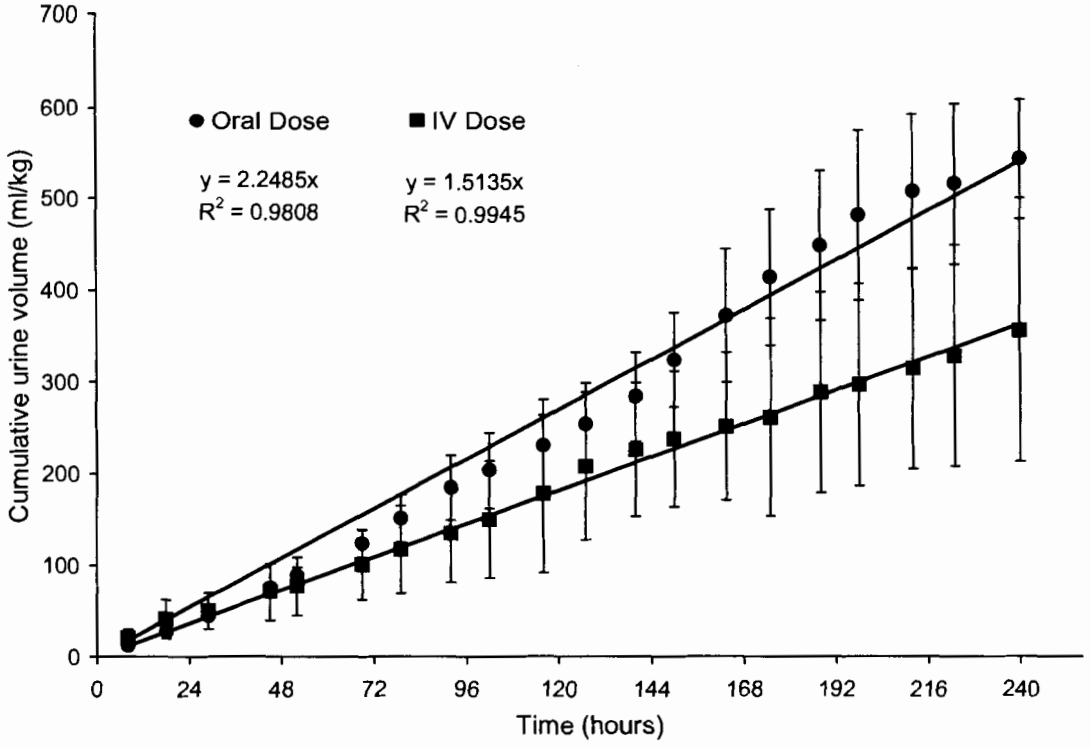

The amount of benzo[a]pyrene equivalents was measured in each urine sample. Figure 4.23 shows the cumulative amount of parent benzo[a]pyrene and metabolites determined in urine samples over time for both sets of crabs.

Figure 4.23 Cumulative amount of benzo[a]pyrene equivalents in urine over time following either a 2 mg benzo[a]pyrene/kg intravascular or oral dose

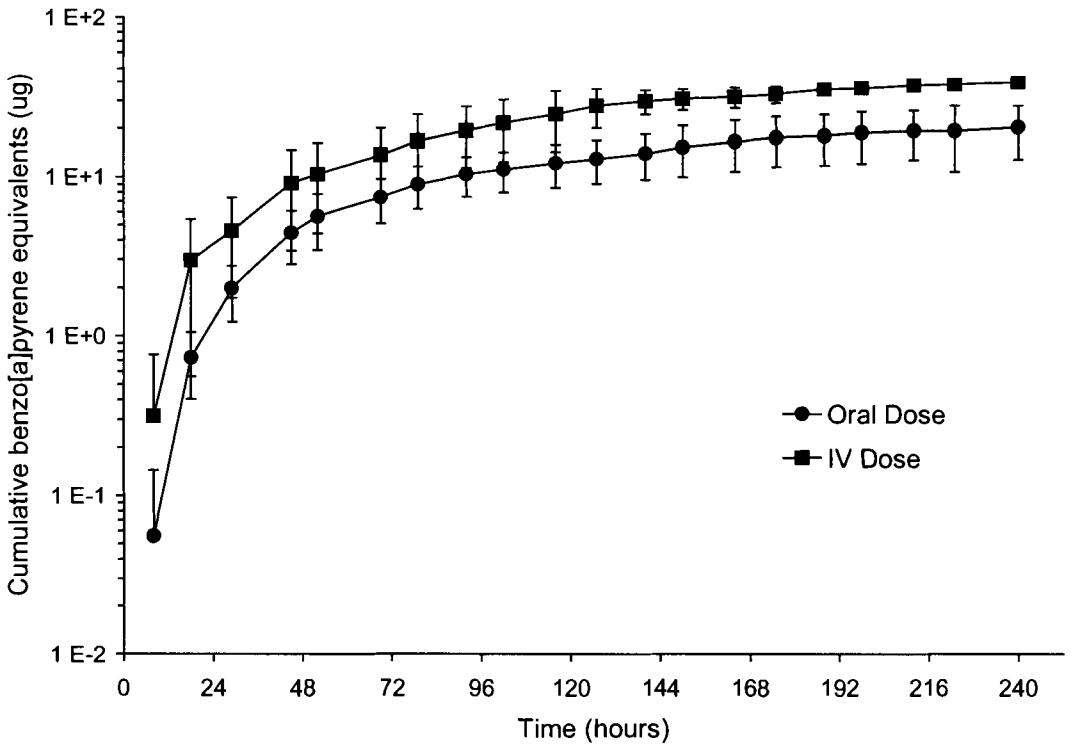

The total amount of benzo[a]pyrene excreted and metabolites in the urine of crabs dosed *per os* represented 1.2% of the total dose, whereas, 2.3% of the total dose was excreted in the urine by crabs administered with an *i.v.* dose.

Urine samples were extracted with ethyl acetate to determine the amount of extractable benzo[a]pyrene and metabolites. Figure 4.24 shows the percentage of radiolabelled benzo[a]pyrene that was associated with either the aqueous fraction (non-extractable) or the solvent extractable fraction.

Figure 4.24 Percentage of benzo[a]pyrene and metabolites excreted in urine associated with aqueous and ethyl acetate extractable fractions from crabs dosed with either a 2 mg benzo[a]pyrene/kg intravascular or oral dose

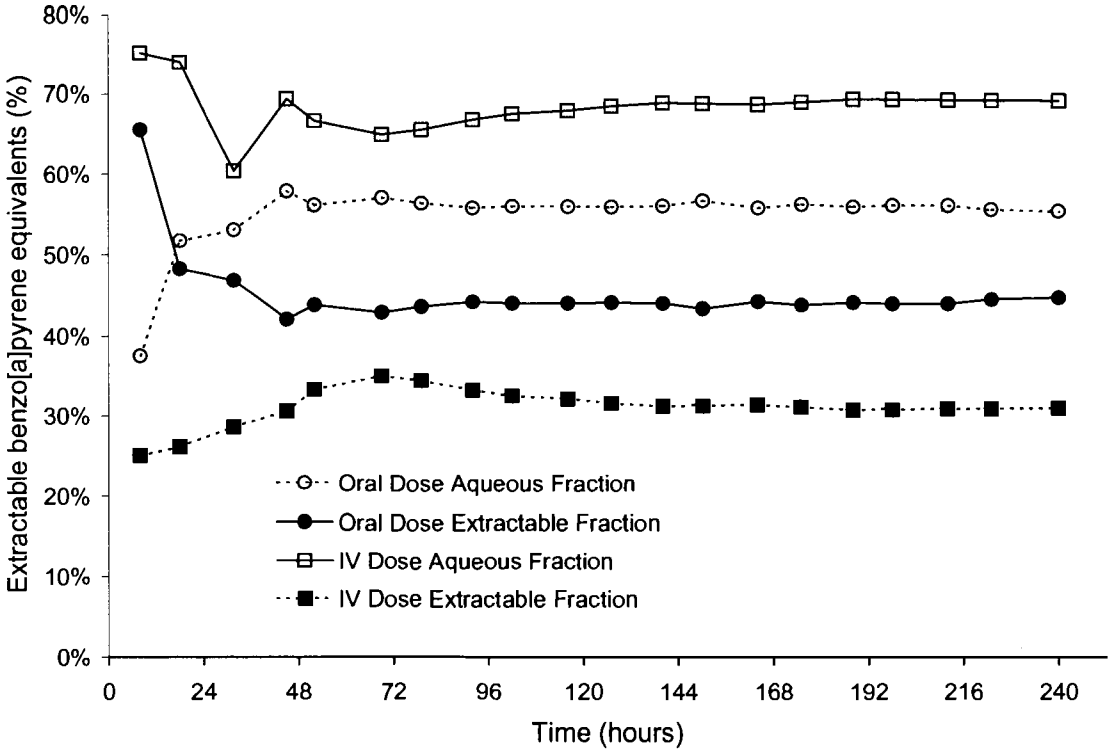

Generally, 45% of the parent benzo[a]pyrene and metabolites were extractable and 55% remained in the aqueous fraction following an oral dose. However, a smaller proportion of benzo[a]pyrene and metabolites was extractable in the urine from crabs administered with an intravascular dose, 31%, while 69% remained in the aqueous fraction.

4.3.9 Identification of Benzo[a]pyrene Metabolites in the Urine

Two benzo[a]pyrene metabolites were identified in the extractable fractions of urine samples. Figure 4.25 shows an overlay of an HPLC-fluorescence chromatogram of

benzo[a]pyrene metabolite standards compared with a histogram showing the radioactivity in fractions collected following injection of an ethyl acetate urine extract.

Figure 4.25 Overlay of HPLC-fluorescence chromatogram and radioactivity of collected fractions for identification of solvent extractable benzo[a]pyrene metabolites in crab urine

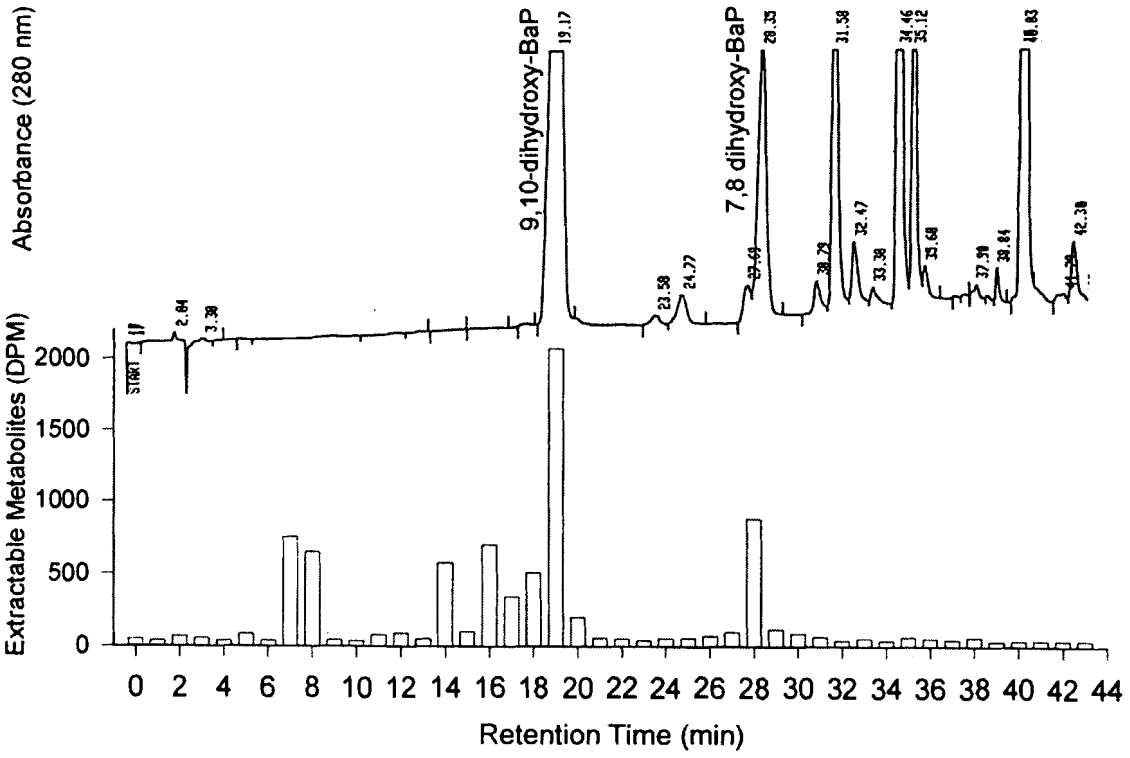

Two of the most prominent peaks matched the metabolite standards for 9,10-dihydroxybenzo[a]pyrene and 7,8-dihydroxybenzo[a]pyrene at retention times of 19 and 28 minutes respectively. Figure 4.26a shows a comparison of the ions determined by GC/MS in the fraction collected at 19 minutes compared with a trans-9,10-dihydroxybenzo[a]pyrene metabolite standard (Figure 4.26b).

Figure 4.26 Comparison of GC/MS ion chromatogram a) benzo[a]pyrene metabolite extracted from crab urine, b) Trans-9,10-dihydroxybenzo[a]pyrene standard.

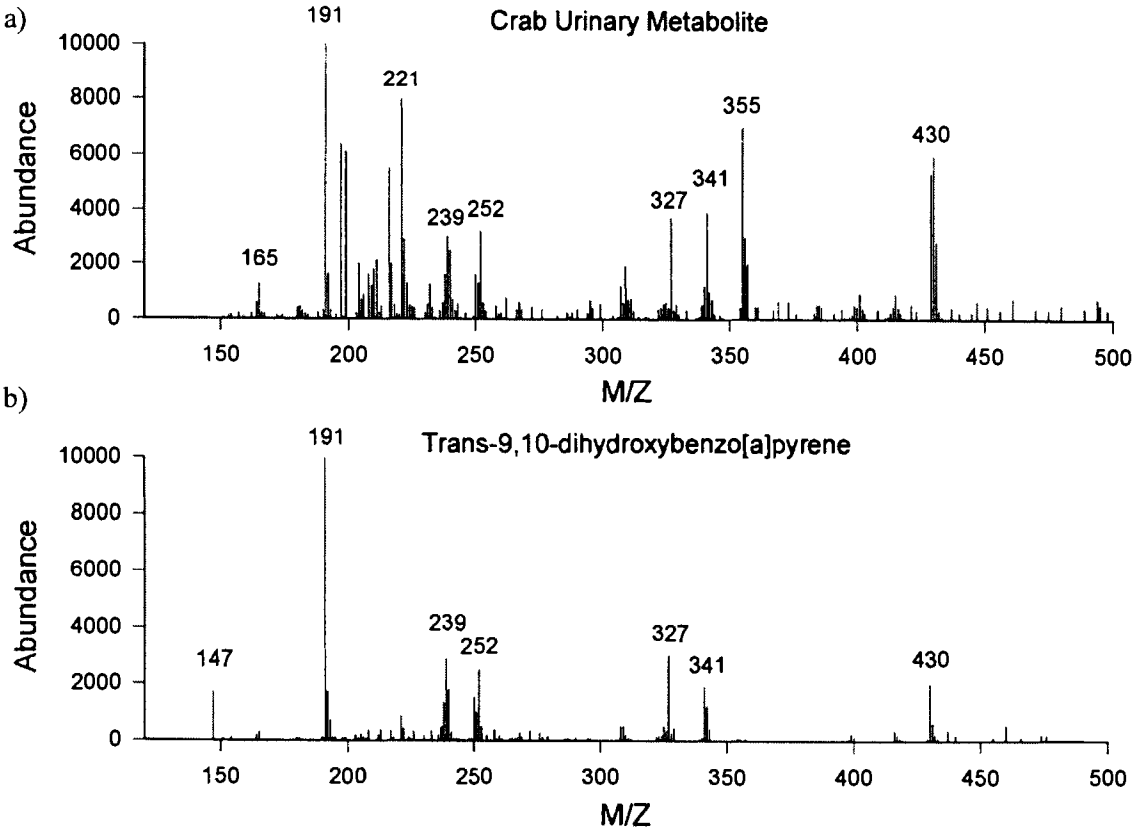

The major ions of the urinary metabolite ion chromatogram match those of the metabolite standard indicating that the metabolite is trans-9,10-dihydroxybenzo[a]pyrene. Figure 4.27 shows a comparison between the prominent ions in the 28 minute HPLC fraction, putatively identified as 7,8-dihydroxybenzo[a]pyrene and the metabolite standard.

Figure 4.27 Comparison of GC/MS chromatograms a) benzo[a]pyrene metabolite extracted from crab urine, b) Trans-7,8-dihydroxybenzo[a]pyrene standard.

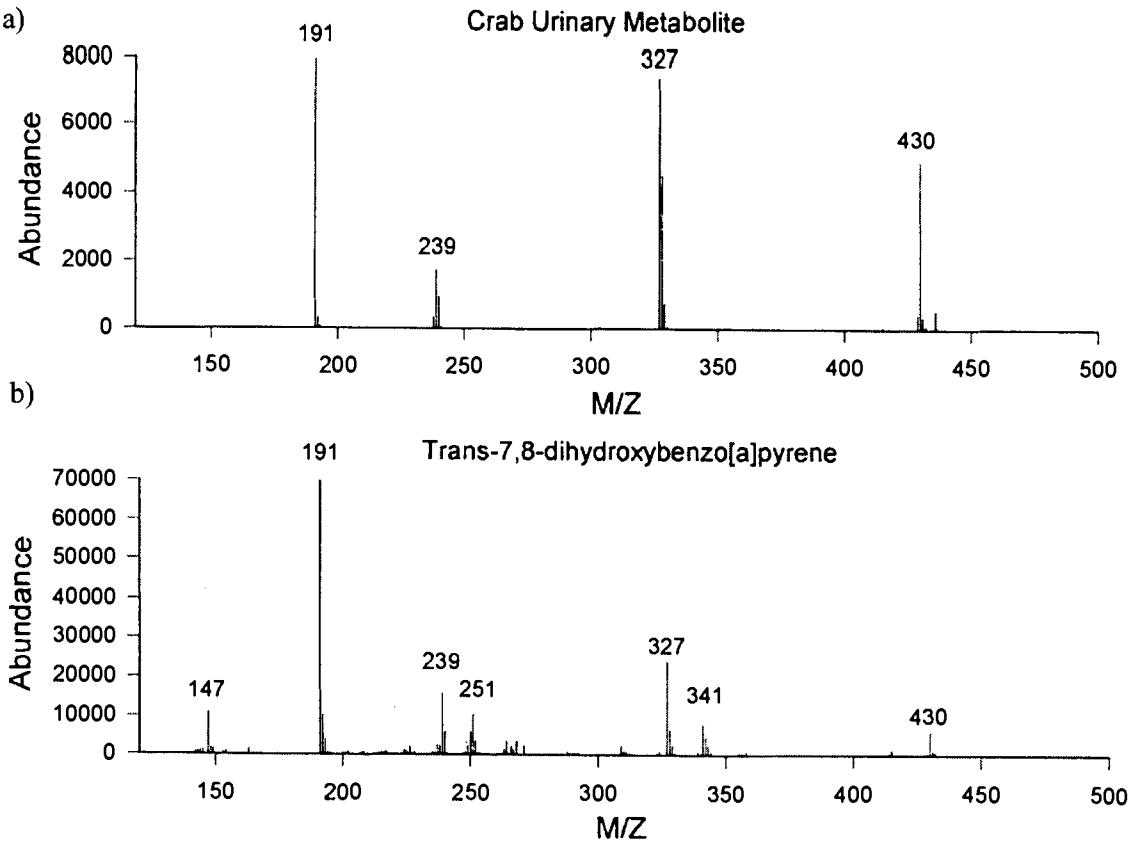

A comparison of the two ion chromatograms indicated that the second metabolite was trans-7,8-dihydroxybenzo[a]pyrene.

4.4 Discussion

4.4.1 Kinetics of Benzo[a]pyrene in the Crab

The uptake of benzo[a]pyrene in the crab following exposure to benzo[a]pyrene in the water or an oral dose was fairly rapid. James *et al.,* (1995) found similar kinetics of benzo[a]pyrene in the haemolymph of the American lobster, *Homarus americanus* following a single oral bolus dose. The uptake and elimination phases following an oral

dose were remarkably similar to those observed in the crab. A rapid uptake in the haemolymph was followed by a slow linear decline (James *et al.,* 1995).

The elimination of benzo[a]pyrene from crabs following exposure was relatively slow. Half-lives of benzo[a]pyrene in the haemolymph ranged from 60 to 354 hours. Analysis of tissues 20 days after administration of a single 2 mg benzo[a]pyrene/kg oral dose showed that tissue concentrations were still relatively high, indicating a very slow rate of elimination from the crabs. However, the half-life of benzo[a]pyrene in lobsters dosed orally with 50 μg benzo[a]pyrene/kg (James *et al.,* 1995) was significantly longer, >672 h, than that observed for the dungeness crab.

The elimination of benzo[a]pyrene in fish is much more rapid in comparison. For example, the whole body half-life of benzo[a]pyrene in fish, such as the bluegill sunfish, is only 2 to 3 days (Dunn and Fee, 1979; Spacie *et al.*, 1983, Shugart *et al.*, 1990). Lamaire *et al.* (1992) estimated that the half-life of benzo[a]pyrene in the liver of the sea bass, (*Dicentrarchus labrax*) following a 20 mg/kg oral dose was 8.18 days. In contrast, the half-life of benzo[a]pyrene in the hepatopancreas of crabs administered with a 10 fold lower oral dose, 2 mg/kg, was 10 days (240 hours).

4.4.2 Tissue Distribution

The distribution of benzo[a]pyrene in the tissues varied depending on the route of administration. For each exposure route, the tissue concentrations of benzo[a]pyrene decreased in the following orders:

Intravascular dose 2mg/kg

Hepatopancreas>bladder>hypodermis>heart>gill>testes>muscle>haemolymph>gut

Oral 2 mg/kg dose:

Testes>hypodermis>gill>bladder>hepatopancreas>muscle>heart>haemolymph>gut

Oral 20 μg/kg dose:

Gill>gut>testes>heart>bladder>hepatopancreas>haemolymph>hypodermis>muscle

Water Exposure 20 μg/L:

Gill>hypodermis>haemolymph>bladder>heart>testes>hepatopancreas>gut>muscle

Water Exposure 2 μg/L:

Gill>hypodermis>bladder>heart>testes>gut>hepatopancreas>muscle>haemolymph

The disposition of benzo[a]pyrene in the spiny lobster was studied by James and Little (1984) following an 1 mg/kg intrapericardal dose of ^{14}C labelled benzo[a]pyrene. The concentration of benzo[a]pyrene equivalents in each tissue decreased according to the following order:

Hepatopancreas>stomach>intestine>green gland>gonad>gill>muscle>haemolymph

This pattern of tissue disposition is somewhat similar to the pattern obtained following the intravascular dose in the crab.

4.4.3 Partition Coefficients

The haemolymph:tissue partition coefficients declined in the order of hepatopancreas, heart, bladder, hypodermis, gut, testes, muscle and gill. The partition coefficients seem to correlate with the lipid content of each tissue. Analysis of *C. magister tissues* by Allen (1971; 1972) showed that the of the seven tissues analysed, the hepatopancreas has the highest concentrations of lipid, followed by the testes, viscera, skeletal muscle, gill, exoskeleton, and haemolymph. This result may be expected because benzo[a]pyrene is a very lipid soluble compound with a relatively high Kow of approximately 6.1 (OME, 1997).

4.4.4 Elimination of Benzo[a]pyrene and Metabolites in the Urine

Analysis of the urine collected from crabs dosed with benzo[a]pyrene showed that crabs are capable of metabolising benzo[a]pyrene. However, the rate of metabolite excretion in the urine appears to be very slow. Crabs were only capable of eliminating 1.2% to 2.3% of the total benzo[a]pyrene dose in the urine over a period of 10 days. It is likely that the urine is not the primary route of benzo[a]pyrene excretion in the crab. For example, the majority of benzo[a]pyrene and metabolites were excreted in the feces of dosed rats, rather than the urine following intraperitoneal or oral administration (van de Wiel *et al.,* 1993). van de Wiel *et al.,* (1993) also found that the amount of benzo[a]pyrene in the urine was greater following an intrapericardial dose compared with an oral dose. This is expected because the whole dose is theoretically bioavailable following intravascular or intrapericardial administration, whereas, only a percentage of an orally administered dose is absorbed.

In fish, the majority of PAH metabolites are eliminated in the bile. Steward *et al.,* (1991) found that 25% of an intraperitoneally administered dose of radio-labelled benzo[a]pyrene was excreted into the bile. Crabs do not possess a gall bladder like structure that is present in fish and other vertebrates. However, the hepatopancreas probably excretes metabolites of PAH such as benzo[a]pyrene directly into the intestine. The total amount of benzo[a]pyrene and metabolites excreted in the feces by crabs was not determined in this study due to difficulties in collecting feces from crabs released into the surrounding medium.

4.4.5 Benzo[a]pyrene Metabolites

Figure 4.25 shows that there were at least two main phase I benzo[a]pyrene metabolites that could be identified in the urine of crabs, trans-9,10-dihydroxybenzo[a]pyrene and trans 7,8-dihydroxybenzo[a]pyrene. These two phase I benzo[a]pyrene metabolites have also been determined in the urine of rats, (van de Weil *et al.,* 1993), in the bile of carp, (Steward *et al.,* 1991), English sole, and starry flounder, (Varanasi *et al.,* 1986), and in the digestive gland and gills of the mussel, *Mytilus galloprovincialis* (Michel *et al.*, 1995). Microsomes isolated from the English sole, Parophrys vetulus, (Nishimoto, *et al.,* 1992), and the sea anemone, (*Bunodosoma cavernata*), (Winston *et al.,* 1998), have also produced trans-9,10-dihydroxybenzo[a]pyrene and trans 7,8-dihydroxybenzo[a]pyrene, metabolites among others.

The presence of trans-7,8-dihydroxybenzo[a]pyrene and trans 9,10-dihydroxybenzo[a]pyrene is significant because these metabolites are the products of

epoxide intermediates catalysed by mixed function oxidases (Gelboin, 1980), and these diol metabolites themselves have also been shown to bind directly to DNA (Borgen *et al.*, 1973). Therefore, the dungeness crab is capable of metabolising benzo[a]pyrene into well characterised carcinogenic compounds. While tumours related to benzo[a]pyrene exposure has been demonstrated in numerous studies of other aquatic species, such as fish, (Varanasi, *et al.*, 1982; Black *et al.*, 1988; Couch and Harshbarger, 1985; Fong *et al.*, 1988; Hawkins *et al.*, 1988; Collier, *et al.*, 1992), to date there are no published studies demonstrating tumours in crabs related to PAH exposure. In addition, it has been shown that American lobsters exposed to PAH do not develop tumours or neoplastic changes, although finfish exposed under the identical conditions do develop cancer (James *et al.*, 1995). There are two factors which may account for a reduced carcinogenic potential of PAH in crabs and other decapod crustaceans, (1) fish metabolise PAH much more rapidly than crabs and therefore, are likely to produce more carcinogenic metabolites that may bind to DNA and cause tumours, (2) crabs may conjugate a large amount of the potentially carcinogenic benzo[a]pyrene metabolites with glutathione.

High levels of glutathione S-transferase activity has been found in the hepatopancreas of the blue crab, *Callinectes sapidus* (Keeran and Lee, 1987). My studies showed that there was a relatively large amount of radiolabelled benzo[a]pyrene metabolites associated with the aqueous fraction of the urine that could not be made soluble in ethyl acetate after hydrolysis treatment with HCl, or treatment with sulfatase or glucosidase enzyme assays (59-69%). It was assumed that most of the metabolites associated with the aqueous fraction were therefore glutathione conjugates. Since glutathione S-transferase has been proposed to protect rats from hepatocarcinogenesis

(Jernström, *et al.,* 1985), this phase II reaction, coupled with a slow rate of phase I metabolism may be the reason that tumours observed in benthic species such as the English sole, have not been similarly observed or reported in crabs. To date there is no literature evidence that PAH cause tumours in crabs.

While protecting the crab from cancer, the relatively slow metabolism and elimination of PAH such as benzo[a]pyrene also makes the crab a better biomonitoring species than the fish. Fish metabolise and eliminate PAH very quickly following exposure, therefore, it is very difficult to determine concentrations of PAH in the tissues of fish caught in the field. Usually PAH exposure in fish is best evaluated by the analysis of metabolites excreted into the bile. However, tissue concentrations of PAH can be determined in the hepatopancreas, muscle, and haemolymph of crabs exposed to PAH as demonstrated in Chapters 2 and 3. Therefore, these slow metabolic and elimination rates make the crab a better sentinel species for monitoring environmental contamination.

4.5 Conclusion

Benzo[a]pyrene is readily absorbed into the haemolymph by dungeness crabs following exposure to contaminated food or water. Once absorbed, this chemical is readily distributed throughout the tissues of the crab. Elimination of benzo[a]pyrene from the crab is very slow compared with fish or mammals. While crabs are capable of metabolising benzo[a]pyrene using very similar enzymatic reactions as vertebrates (James, 1989) the rate of metabolism is relatively slow. However, this slow metabolism may protect the crab from the carcinogenic potential of benzo[a]pyrene and other PAH.

In addition, the slow removal of PAH from the tissues of the crab facilitates the use of the crab as a good biomonitor of PAH in the marine environment.

CHAPTER 5
PBTK MODEL DEVELOPMENT AND VALIDATION

5.1 Introduction

Physiologically based toxicokinetic (PBTK) models have been used extensively to describe the disposition of chemicals in living organisms. One of the strengths of the PBTK modelling approach is the ability to scale a model to different body sizes and species. Most often these models are used to extrapolate the toxicokinetics of a toxicant from rodents to humans (Gerlowski and Jain, 1983). However, many PBTK models have been developed in the aquatic species in recent years. Zaharko, et al. (1972) was the first to report a PBTK model for an aquatic species, the sting ray. Zaharko originally developed a model in the mouse to simulate the disposition of methotrexate in the tissues and then adapted this model to the sting ray. Following this, Bungay et al. (1976) developed a PBTK model to predict the disposition of phenol red in the dogfish shark. Realising the potential of PBTK models to predict the disposition of organic pollutants in fish, Nichols *et al.,* developed a PBTK model to describe the kinetics of chlorinated ethanes in rainbow trout (1991) and then extrapolated this model to the channel catfish (1993). More recently, a PBTK model which predicted pyrene disposition in the rainbow trout (Law *et al.,* 1991) was successfully adapted to marine flatfish species including the starry flounder and flathead sole (Namdari, 1998). This model has also been adapted to predict the elimination of oxytetracycline from the tissues of farmed Atlantic salmon

(Law, 1999). The current study represents the first attempt to extrapolate a PBTK model developed in the vertebrate to an invertebrate, the dungeness crab (*Cancer magister*).

The purpose of this study was to determine if a PBTK model could be developed to describe the disposition of benzo[a]pyrene in the dungeness crab. The PBTK model of pyrene for rainbow trout (Law *et al.*, 1991) was modified to meet this objective. The model design was altered to suit the anatomy and physiology of the crab. Additionally, the anatomical, biochemical and physiological parameters in the rainbow trout model were replaced by those of the crab and the model was then used to predict the time course of benzo[a]pyrene concentrations in the crab tissues. Despite the many differences in the physiology and biochemistry between the trout and the crab, and the physico-chemical differences between pyrene and benzo[a]pyrene, the PBTK model of pyrene for rainbow trout was successfully adapted to predict benzo[a]pyrene distribution in the tissues of the crab.

Many PBTK models have been developed in one animal species using the intravascular route of chemical administration and then used to predict tissue disposition in another animal species after exposure by an environmentally relevant route such as the inhalation, dermal or oral route. For example, Ramsey and Andersen (1984) developed a PBTK model to describe the disposition of styrene in the rat following exposure by inhalation. This model was subsequently adapted to describe the disposition of styrene in humans via inhalation (Ramsey and Andersen, 1984).

The current model was designed to simulate benzo[a]pyrene disposition in the crab following intravascular injection, bolus oral administration with food or exposure

via the water. These exposure routes were chosen in order to develop a model which could be used to predict benzo[a]pyrene concentrations in the tissues of crabs exposed to PAH in the environment. It was my intention to apply the model for this purpose when information on benzo[a]pyrene concentrations in the biota which crabs prey upon, and water of a specific site became available. In addition, we intended to link this model describing the internal toxicokinetics of benzo[a]pyrene in the crab, to a food web model developed by Glenn Harris and Frank Gobas, (Harris, 1999) to describe the fate of PAH such as benzo[a]pyrene in the Kitimat water system. This chapter describes the development and validation of the PBTK model for the crab while Chapter 4 describes the empirical studies used for the development, calibration and validation of the model.

5.2 PBTK Model

5.2.1 Model Conceptualisation

The PBTK model has been conceptualised to simulate the uptake, distribution, metabolism and elimination of benzo[a]pyrene in the dungeness crab following chemical exposure *via* water or food. The model was adapted from a previously reported PBTK model of pyrene for the rainbow trout (Law *et al.,* 1991). The compartmental design of the model was modified to suit the anatomy and physiology of the crab. For example, the membrane-limited muscle compartment in the trout model was replaced with a more suitable flow-limited muscle compartment for the crab. A schematic diagram of the PBTK model of crab is depicted in Figure 5.1. The model is composed of seven compartments which represent the major organs or tissues of the crab; they include the haemolymph, gill, hepatopancreas, gut, urinary bladder, muscle and carcass.

All compartments in the model are connected together *via* the circulatory system represented by the arterial and venous haemolymph. The flux of chemical between the compartments is regulated by flow rates of the haemolymph and haemolymph:tissue partition coefficients of benzo(a)pyrene. The chemical concentration in a compartment is assumed to be homogenous and in equilibrium with the chemical concentration in the haemolymph exiting the compartment.

Figure 5.1 Schematic diagram of the PBTK model for predicting the disposition of benzo[a]pyrene in the dungeness crab.

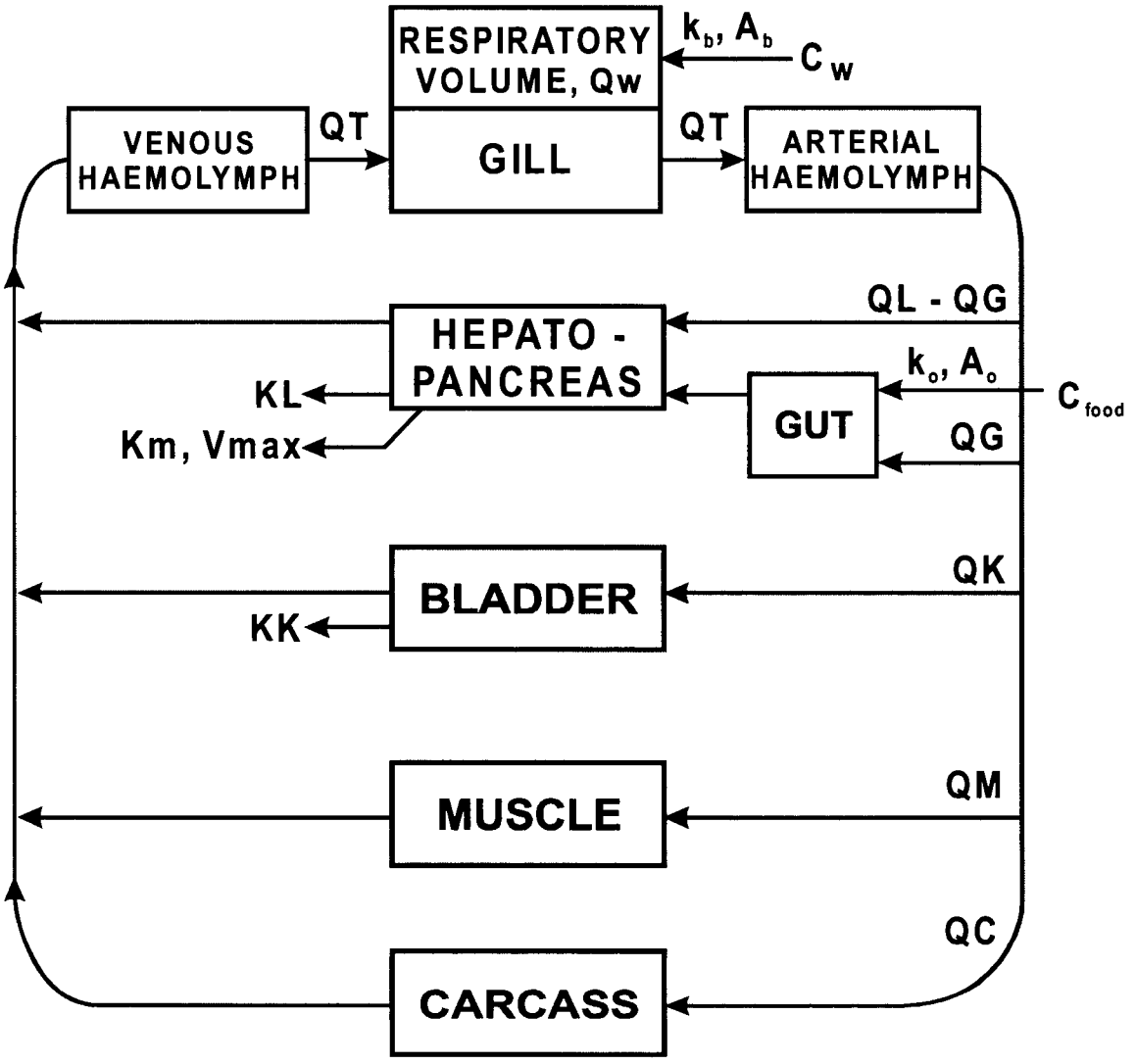

The model is designed to accept benzo(a)pyrene input through the intravascular, oral or branchial route. Thus, the amount of benzo[a]pyrene administered by the *i.v.* or oral dose is used for inputting the chemical into the crab *via* these exposure routes whereas the concentration of benzo(a)pyrene in water is used for inputting waterborne benzo(a)pyrene into the crab *via* the branchial route. In addition, intravascular injection is modelled by direct addition of the chemical into the mixed venous haemolymph. The absorption of benzo[a]pyrene by the gut is represented by a first-order absorption rate constant k_o with bioavailability, A_o. Uptake of chemical from water into the gill compartment and the circulating haemolymph was also modelled by a first-order uptake rate expression which includes gill ventilation (Qw), first-order uptake rate (k_b) and a branchial bioavailability constant (A_b). Elimination of benzo[a]pyrene by metabolism and other processes is assumed to occur in the hepatopancreas and is represented by both linear and Michaelis-Menten saturable clearances.

5.2.2 Mass Balance Differential Equations

The PBTK model is composed of a set of mass-balance differential and algebraic equations which describe the change of benzo[a]pyrene concentration in each tissue compartment over time. The differential equations were simultaneously solved by numerical integration to determine the concentration of chemical in each compartment for any time point. These equations were programmed in Visual Basic® and solved by a spreadsheet program, Microsoft Excel® which stores the input data and model parameters. Model output is stored in Excel and plotted graphically. The basic differential

equation which describes the change of concentration of benzo[a]pyrene per unit of time in a simple compartment is defined by Equation 5.1:

$$dCi/dt = Qi(CA - Ci/Ri)/Vi \qquad (5.1)$$

where Qi represents the haemolymph flow rate constant for the compartment, Vi represents the volume of compartment i, Ri represents the partition coefficient and CA and Ci represent the concentration of chemical in the arterial haemolymph and the tissue compartment respectively. This equation forms the basic unit upon which the entire PBTK model is based. A simple explanation of it's derivation from Fick's First Law can be obtained from O'Flaherty (1987).

Compartment volumes were expressed in units of ml where solid tissues were assumed to have the density of 1.0 g/ml. The concentration of benzo[a]pyrene in each compartment is expressed in units of ng/ml haemolymph or ng/g tissue. The hepatopancreas compartment incorporates elimination through saturable metabolism and linear clearance; the basic compartment equation was modified to accommodate these processes as described by Equation 5.2:

$$dCL/dt = (CBA(QL - QGT) + QGT(CGT/RGT) - QL(CL/RL) - ((V_{max}(VL)(CL/RL))/(K_m + CL/RL)) - KL(CL/RL))/VL \qquad (5.2)$$

where the concentrations of benzo[a]pyrene in the hepatopancreas and arterial haemolymph are represented by CL and CBA, the hepatic partition coefficient is RL and the volume of the compartment is VL. Hepatic clearance is denoted by KL and the Michaelis-Menten rate constants are V_{max} and K_m.

The basic equation was also modified to include direct uptake of benzo[a]pyrene from the gut compartment as shown in Figure 5.1. Thus haemolymph flow and partition coefficient for the gut are represented by QGT and RGT respectively. A complete listing of the mass balance equations that describe the PBTK model are summarised in Appendix C.

5.2.3 Model Parameterisation

Many types of parameters are required to implement the PBTK model. These parameters represent compartment volumes, blood flow, partition coefficients and uptake and clearance rates. The parameters used to simulate the disposition of benzo[a]pyrene in the dungeness crab are displayed in Table 5.1 – Table 5.5. These parameters were determined either empirically in the laboratory or were obtained from the literature. For example, values for some parameters such as tissue blood flow constants were estimated based on information from other researchers. Compartment volumes and partition coefficients were estimated using experimental methods. Other parameters such as uptake and clearance rates were optimised by comparing model simulation results with empirical data.

5.2.3.1 Anatomical Parameters

The PBTK model requires volumes for the tissues represented by the various model compartments. The compartment volumes used for the PBTK model are presented in Table 5.1.

Table 5.1 Compartment volume (% body weight) parameters for the PBTK model of benzo[a]pyrene in the dungeness crab.

Compartment	Abbreviation	Volume (% BW)
Muscle	VM	23.20
Hepatopancreas	VH	3.46
Gut	VGT	0.19
Bladder	VK	0.36
Gill	VGL	0.81
Haemolymph	VB	35.70
Carcass	VC	36.28

Compartment volumes were determined empirically by dissecting the dungeness crabs and weighing the excised organs. It was assumed that all tissues had a density of 1.0 g/ml. The hepatopancreas, gut, bladder, muscle, gill and haemolymph compartments were assigned volumes equal to 3.46, 0.19, 0.36, 23.20, 0.81, and 35.7% of body weight, respectively. The sum of these compartments amounted to 63.72% of the total body volume while the remaining 36.28% was assigned to the carcass.

5.2.3.2 Physiological Parameters

Cardiac output is an important parameter which drives the disposition of chemical throughout the tissue compartments. The circulatory system and cardiac output of the dungeness crab have been extensively studied by researchers at the University of Calgary (Burnett *et al.,* 1981; McMahon and Burnett 1989; McGaw and McMahon 1996; De Wachter and McMahon, 1996; De Wachter and Wilkens, 1996). The parameters that describe haemolymph flow in the PBTK model are presented in Table 5.2. These parameters were calculated for a dungeness crab with a body weight of 750g based on data obtained from the studies of McMahon, *et al.,* 1979; McDonald *et al.*, 1980; Airiess

and McMahon, 1994; McGaw *et al.*, 1994; DeWachter and McMahon, 1996; and McGaw and McMahon 1996.

Table 5.2 Physical parameters and haemolymph flow rates for the PBTK model of benzo[a]pyrene in the dungeness crab based on a 750 g body weight.

Physiological Parameters	Abbreviation	Value
Cardiac output (ml/hr)	QT	5729
Ventilation rate (ml/hr)	Qw	9189
Water temperature (°C)	wtemp	9
Haemolymph flow rates (%QT)	**Abbreviation**	**Value**
Muscle	QM	30
Hepatopancreas	QH	35
Gut	QGT	10, 15*
Bladder	QB	20
Gill	QGL	100
Carcass	QC	15, 10*

A function for the cardiac output of dungeness crabs, based on water temperature, was obtained from a study by B. McMahon *et al.*, (1978). Figure 5.2 shows the regression of cardiac output and temperature data from this study which produced the following linear function described by Equation 5.3:

$$QT = 0.48T + 3.318 \qquad (5.3)$$

where QT and T represent cardiac output (ml g^{-1} h^{-1}) and water temperature (°C). The cardiac output was calculated by multiplying the resulting value of this function by bodyweight, thus the cardiac output of a 750 g crab at 9 °C equals 5729 ml/hr. The line fit had an $r^2 = 0.997$.

Figure 5.2 Plot of Cardiac output (QT) vs Temperature (McMahon *et al.*, 1978)

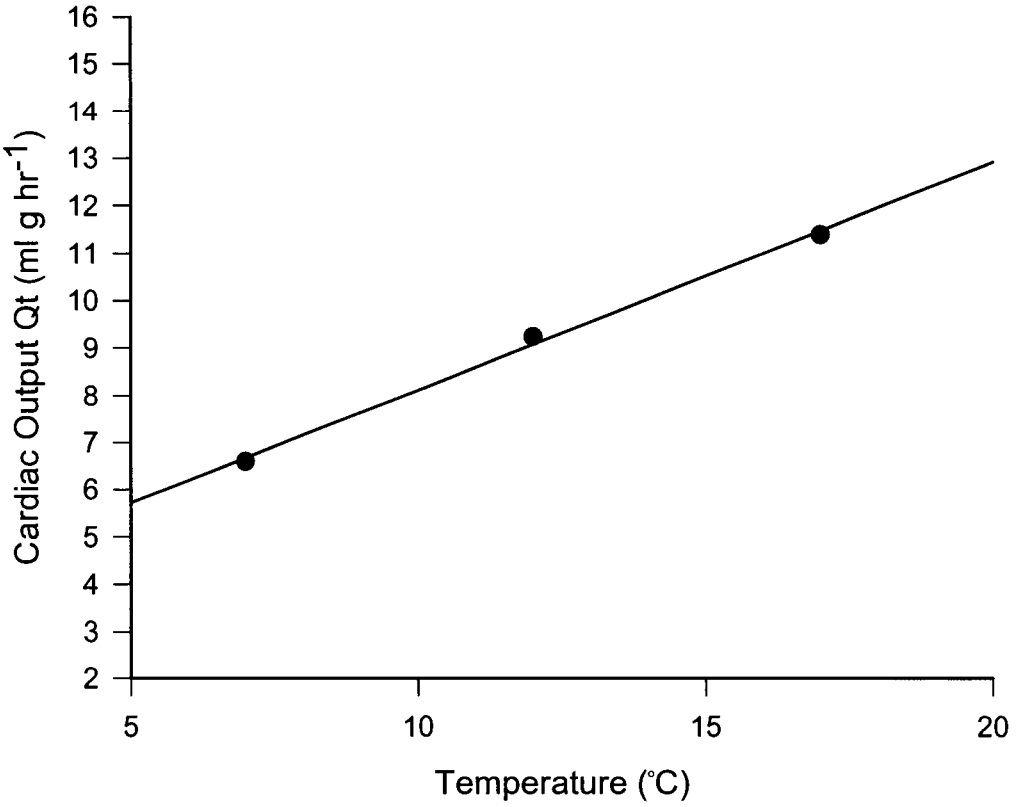

Haemolymph flow rates to the various compartments were initially estimated based on the studies of Airriess and McMahon of the University of Calgary (Airriess and McMahon, 1994 and 1996; McGaw, Airriess and McMahon, 1994) and were defined by model optimisation. Haemolymph flow rates were assigned values of 35, 10, 20, 30 and 15% of QT for hepatopancreas, gut, bladder, muscle and carcass compartments, respectively.

The respiratory volume describes the volume of water which is ventilated across the gills over a period of time. This is an important parameter for calculating the uptake of benzo[a]pyrene through the gills. Gill ventilation rates in *Cancer magister* have also been extensively studied by the aforementioned research group at the University of

Calgary (McMahon, McDonald and Wood, 1979; McDonald, Wood and McMahon, 1980). A function for the gill ventilation rate based on water temperature was obtained from the study by B. McMahon *et al.* (1978). Figure 5.3 shows a regression of gill ventilation rate and temperature data from this study which produced the following linear function described by Equation 5.4:

$$Qw = 2.19T - 7.46 \qquad (5.4)$$

where Qw and T represent ventilation rate (ml g^{-1} hr^{-1}) and water temperature (°C). Qw was calculated by multiplying the resulting value of this function by the bodyweight, thus the Qw of a 750 g crab at 9 °C equals 9189 ml/hr. The line fit had an $r^2 = 0.98$.

Figure 5.3 Plot of gill ventilation rate (QW) vs. temperature (McMahon *et al.*, 1978)

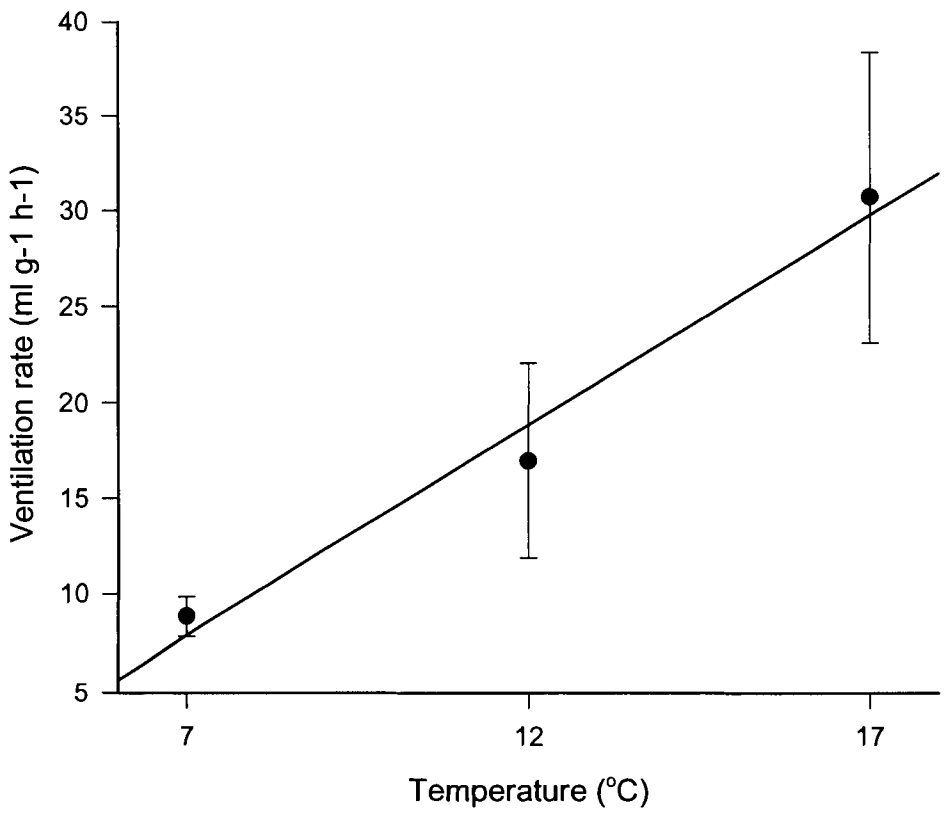

5.2.3.3 Biochemical Parameters

Biochemical parameters in the PBTK model describe the elimination of chemical from the organism through metabolism and excretion. These elimination parameters are presented in Table 5.3.

Table 5.3 Biochemical and Clearance Rate Constants for the PBTK model of benzo[a]pyrene in the dungeness crab based on a 750 g body weight.

Parameter	Abbreviation	Value
V_{max} (ng/hr/g hepatopancreas)	V_{max}	0.53
K_m (ng/ml)	K_m	4.3 E -4
Hepatic clearance (ml/hr)	KL	6.0

It is assumed that all elimination of benzo[a]pyrene occurs in the hepatopancreas compartment by metabolism and other processes represented by Michaelis Menten metabolic rate constants and a linear hepatic clearance rate (KL). Values for the Michaelis Menten rate constants, V_{max} and K_m for benzo[a]pyrene metabolism by dungeness crabs could not be found in the literature. Values for these constants were estimated through model optimisation by matching simulation results with observed data. The linear hepatic clearance, KL was estimated by subtracting Michaelis-Menten and renal clearances from total body clearance. Total body clearance is represented by plasma clearance (Cp) which was determined by pharmacokinetic methods by dividing the amount of an intravenously administered dose by the total area under the chemical concentration-time curve for the haemolymph (AUC). The intravascular dose experiment is described in Chapter 4 from which a $Cp = 42.2 \pm 1.76$ ml kg^{-1} h^{-1} was initially estimated from the data. A value of 5.5 ml kg^{-1} h^{-1} for KL_c was used for model

simulations. Values for V_{max} and KL were scaled using body weight by the following allometric Equations 5.5 and 5.6 previously defined Law *et al,*. (1991):

$$V_{max} = V_{maxc} \, x \, BW^{(0.7)} \tag{5.5}$$

$$KL = KL_c \, x \, BW^{(-0.3)} \tag{5.6}$$

where V_{maxc} and KL_c are the scaling coefficients for the maximum velocity of Michaelis-Menten metabolism and hepatic clearance respectively. The value for K_m was calculated as a simple function of V_{max} using Equation 5.7:

$$K_m = (8 \; E\text{-}4) V_{max} \tag{5.7}$$

5.2.3.4 Physico-biochemical Parameters

The tissue:haemolymph partition coefficients describe the affinity of benzo(a)pyrene for a tissue compartment relative to the haemolymph. The partition coefficients used in the model are summarised in Table 5.4.

Table 5.4 Partition Coefficients for BaP used for the PBTK model of benzo[a]pyrene in the dungeness crab based on a 750 g body weight.

Partition Coefficient Parameter	Abbreviation	Value
Muscle:haemolymph	RM	0.97
Hepatopancreas:haemolymph	RH	3.80
Gut:haemolymph	RGT	2.20
Bladder:haemolymph	RB	3.30
Carcass:haemolymph	RC	2.82
Gill:haemolymph	RGL	1.51

Tissue:haemolymph partition coefficients were determined by both *in vitro* and *in vivo* methods as described in Chapter 4. Other biochemical parameters are presented in Table 5.5.

Table 5.5 Uptake Rate Constants used for the PBTK model of benzo[a]pyrene in the dungeness crab based on a 750 g body weight.

Parameter	Abbreviation	Value
gut first order uptake rate constant (hr^{-1})	k_a	0.25
gill first order uptake rate constant (hr^{-1})	k_b	4.2
oral bioavailability (% dose)	B_a	1.0
branchial bioavailability (% dose)	B_b	17.5

First-order uptake rate constants were used to describe the uptake of benzo(a)pyrene from water or food; they were represented by k_b and k_a respectively. Values for these constants, $k_b = 4.2\ hr^{-1}$ and $k_a = 0.25\ hr^{-1}$, were determined by calibrating the model with experimental data.

The bioavailability of the oral dose (A_o), was estimated to be approximately 3.3%. This was calculated by comparing the area under the curve (AUC) in the haemolymph of an intravascular dose of benzo(a)pyrene (2mg/kg) and the same dose administered orally to the crab. The estimation of bioavailability is described in more detail in Chapter 6. A 1.0 % A_o value was used in the model simulations. An initial estimate of 70.5% for the branchial bioavailability of benzo[a]pyrene (A_b), was similarly obtained from the empirical data. However, $A_b = 17.5\%$ was used for model simulations because this value resulted in a better fit of predicted to observed tissue concentration values.

5.2.4 Model Calibration and Validation

The PBTK model was calibrated by comparing the simulated tissue concentrations with the experimental tissue concentrations of three separate experiments in which the crabs were exposed to benzo(a)pyrene either as a bolus injection (2 mg/kg), an oral dose (2 mg/kg) or *via* the water (20 μg/L). These experiments are described fully in Chapter 4. The values of some of these parameters were adjusted to obtain the best possible fit of the observed data with the model predictions. Model simulations were run to predict tissue concentrations over time for the same duration in which the exposure experiments were conducted. Simulations were performed using a 0.01 minute time increment to represent the change in time, dt. The model was calibrated using a body weight of 750 g; the mean body weight for crabs used in experiments was 694 ± 70 g.

Temperatures in coastal waters are often approximately 9-10°C. Therefore, the exposure and *in vitro* experiments were conducted at 9 ± 1 °C, and this temperature was used to derive the model parameters.

The calibrated model was then validated using a different oral dose or water exposure concentration. Model simulations were compared with data obtained from two additional experiments in which the crabs were exposed either to a 20 μg/kg oral bolus dose or to a 2 μg/L water exposure. The simulation results were then compared with the empirical data to evaluate the validity of the model predictions.

5.3 Uncertainty Analysis

To evaluate model performance, model uncertainty and agreement between predicted and observed results were assessed using the method outlined by Gobas *et al.*, (1998). For each tissue, the ratio of predicted (Cp) vs observed (Co) concentrations i.e., Cp/Co for each time point were calculated. These ratios were then transformed logarithmically to generate a frequency distribution. The mean of this distribution was then expressed in arithmetic form i.e., as Cp/Co and is referred to as model bias (MB). A MB value of <1 indicates systematic under-prediction whereas a MB value of >1 indicates over-prediction of the observed data. Model uncertainty was described by the 95% probability intervals (PI) of the distribution. The PI represents the range of predicted concentrations that includes 95% of the observed concentrations. A large PI indicates a greater uncertainty in model prediction. This uncertainty estimation reflects both errors in measurement and variability of observed data, and errors due to parameterisation or assumptions of the model.

5.4 Results

5.4.1 Intravascular Dose

The PBTK model was initially adapted, parameterised and calibrated by comparing model predictions to observations obtained from exposing crabs to a 2 mg/kg intravascular dose. The model simulates an intravascular injection of 1.5 mg of benzo[a]pyrene into the pericardial chamber of a 750 g crab. Intravascular administration was implemented by inputting 100% of the dose to the venous haemolymph of the model over a 0.06 minute period. This was carried out by placing 14.3% of the dose into the

venous haemolymph at 0.01 minute time increments starting at time 0. Figure 5.4 – Figure 5.8 present the results of the model predictions and the observed data in the crab following intravascular administration of benzo[a]pyrene. Each time point represents the mean of observed concentrations measured in three crabs following exposure. An exception was the time point at 480 minutes which represents the average measurements of only two crabs. Benzo[a]pyrene concentration in the haemolymph was monitored over 192 hours, while tissue concentrations were monitored over 480 hours. In all figures, the symbols represent mean observed concentrations and the solid lines represent model predicted values. Error bars represent one standard deviation from the mean.

Figure 5.4 Observed and predicted concentrations of benzo[a]pyrene in haemolymph following a 2 mg/kg intravascular dose (predicted – line, observed – symbol).

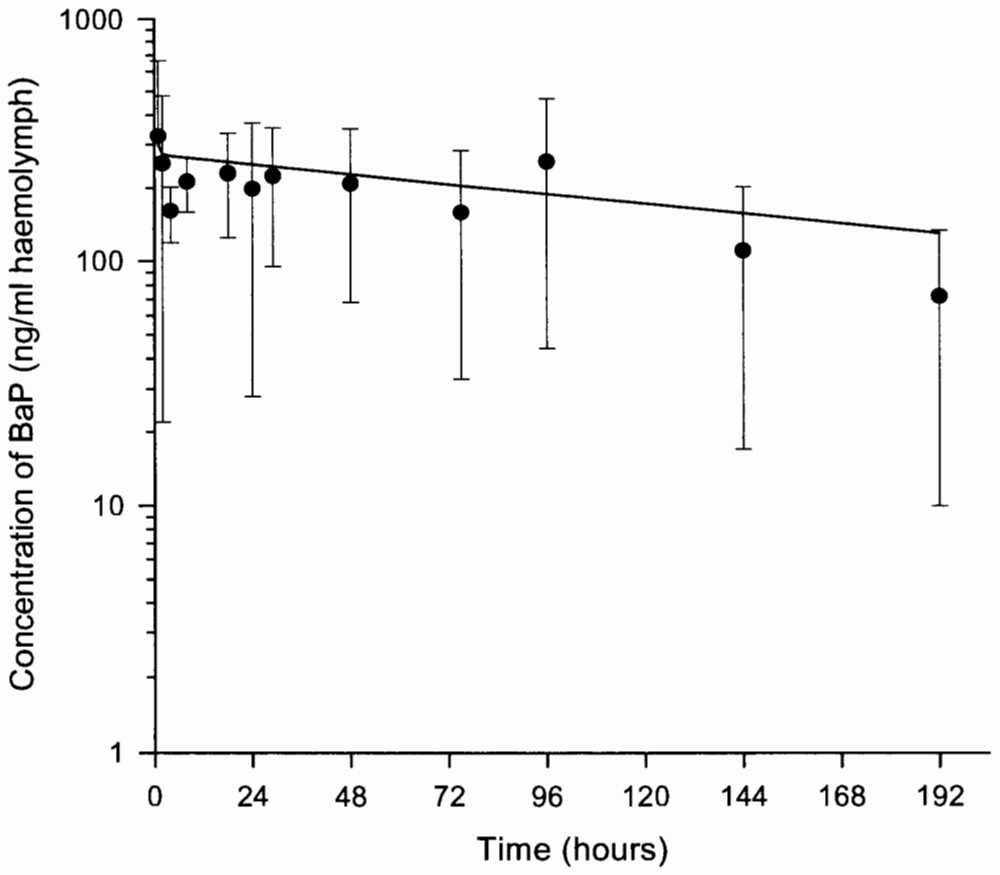

Predicted and observed benzo[a]pyrene concentrations in the hepatopancreas, muscle, bladder, gill and carcass are depicted in Figure 5.5 – Figure 5.8. The predicted concentrations in the carcass were comparable to the mean concentrations of the heart, hypodermis and gonad determined empirically at each time point for all exposure routes.

Figure 5.5 Observed and predicted concentrations of benzo[a]pyrene in hepatopancreas and muscle following a 2 mg/kg intravascular dose (predicted – line, observed – symbol).

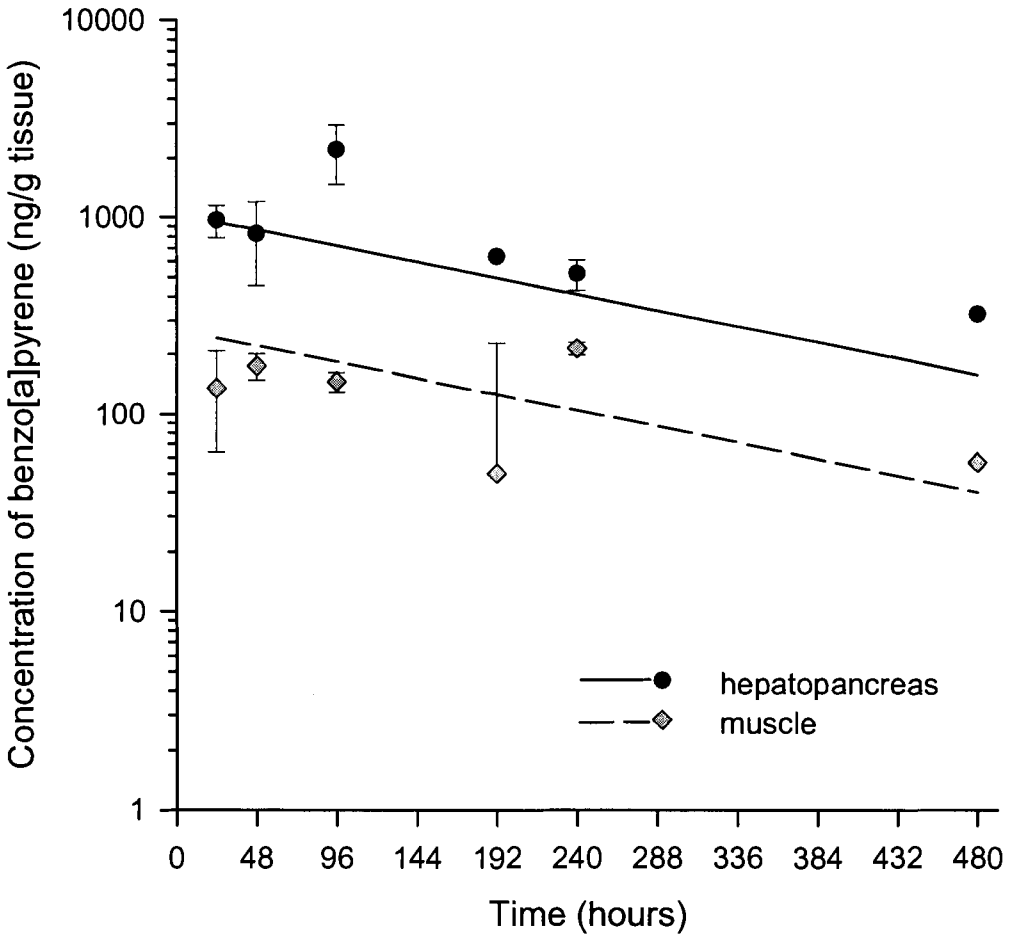

Figure 5.6 Observed and predicted concentrations of benzo[a]pyrene in bladder following a 2 mg/kg intravascular dose (predicted – line, observed – symbol).

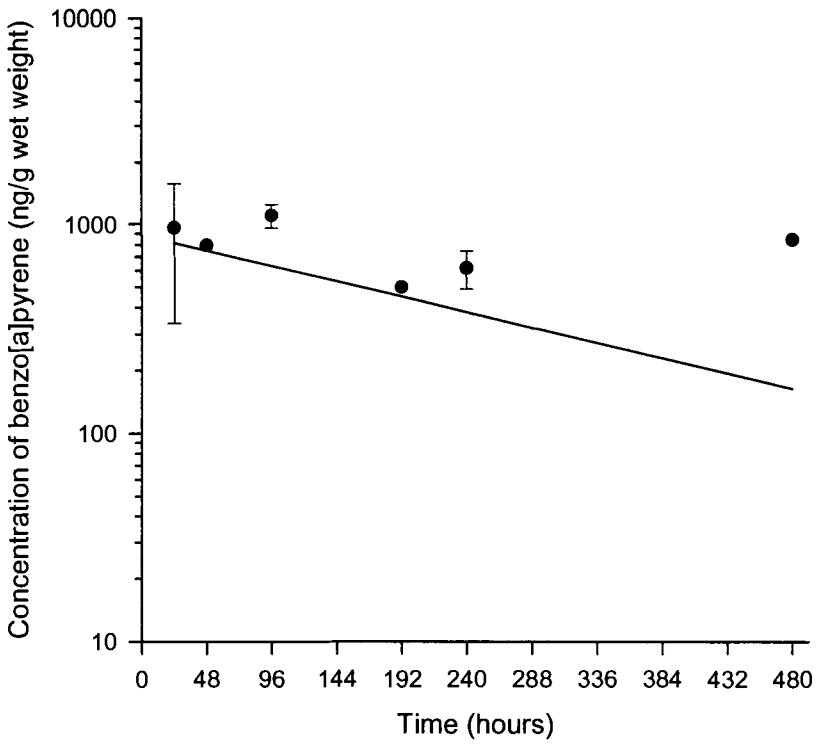

Figure 5.7 Observed and predicted concentrations of benzo[a]pyrene in gill tissue following a 2 mg/kg intravascular dose (predicted – line, observed – symbol).

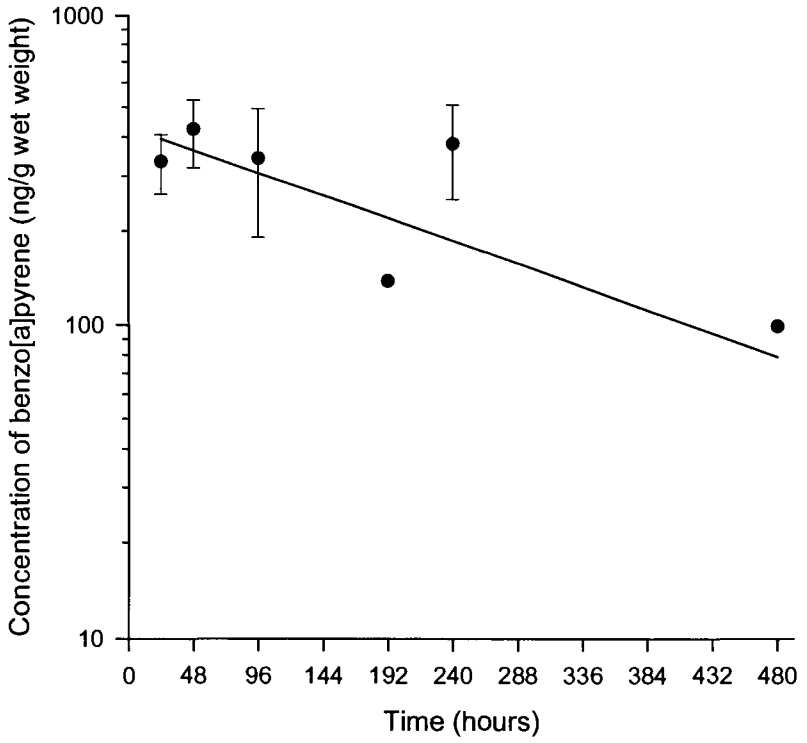

Figure 5.8 Observed and predicted concentrations of benzo[a]pyrene in the carcass following a 2 mg/kg intravascular dose (predicted – line, observed – symbol).

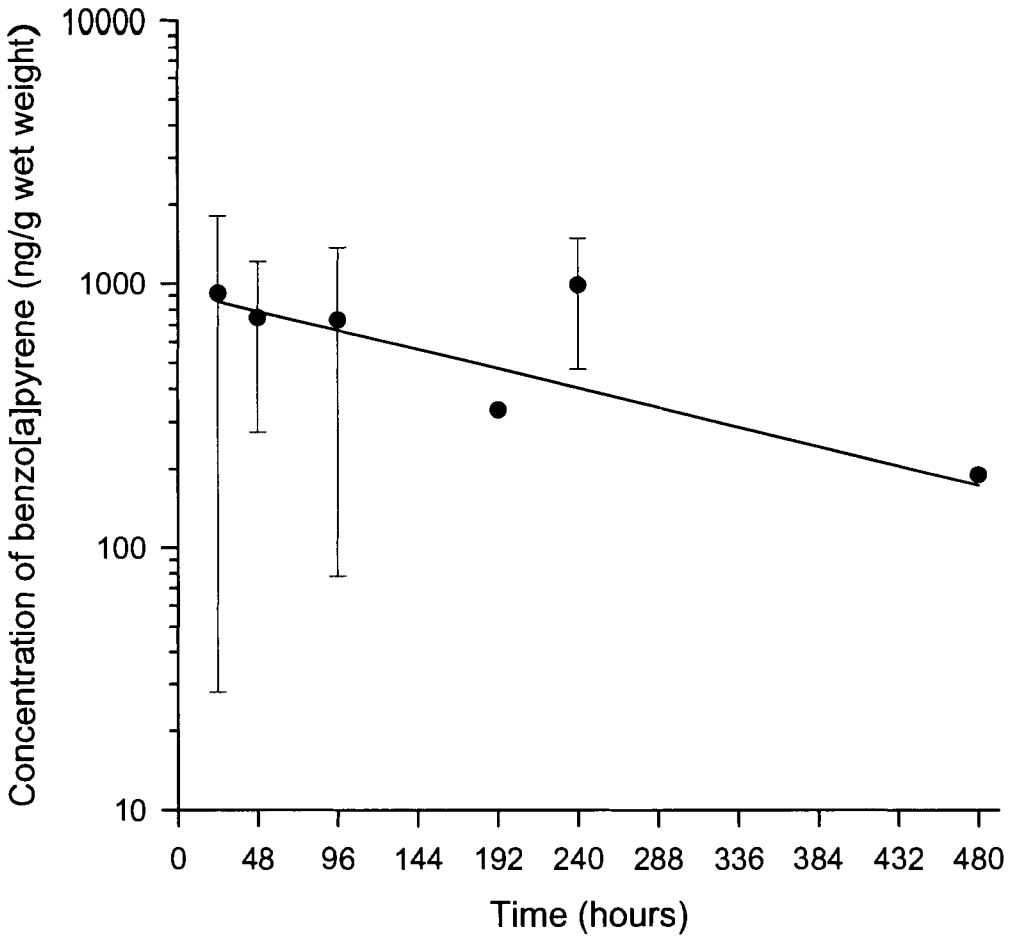

Generally, there is good agreement between predicted and observed results. Figure 5.4 shows that the model slightly over-predicts the concentration of benzo(a)pyrene in the haemolymph over time. However, all but one predicted result are well within one standard deviation of the mean observed tissue concentrations. The model predicts a slow, linear elimination of benzo[a]pyrene from all tissues as seen by fitting the observed data as described in Chapter 4. Visual examination and analysis of model bias show that the model slightly over predicts muscle concentrations (>1) while in some cases marginally under-predicting the other tissues (<1) (Table 5.6).

5.4.2 Oral Dose

5.4.2.1 Model Calibration

The oral bolus dose was simulated such that 100% of a 2 mg/kg dose of benzo[a]pyrene was added to the gut at time zero. The model was calibrated for oral exposure to benzo[a]pyrene by comparing model predictions to observed data as shown in Figure 5.9 – Figure 5.15. Each time point represents the mean of three crabs except at 384 and 480 minutes which are the averages of two crabs. Error bars represent one standard deviation from the mean.

Figure 5.9 Observed and predicted concentrations of benzo[a]pyrene in the haemolymph following a 2 mg/kg oral dose (predicted – line, observed – symbol).

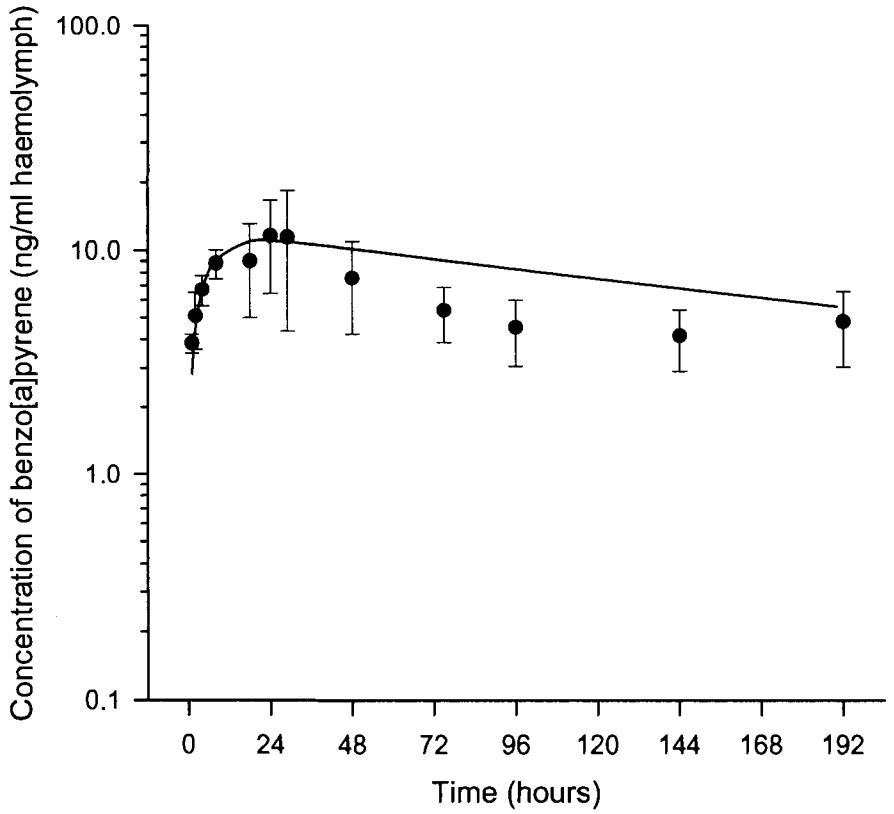

Figure 5.10 Observed and predicted concentrations of benzo[a]pyrene in the hepatopancreas following a 2 mg/kg oral dose (predicted – line, observed – symbol).

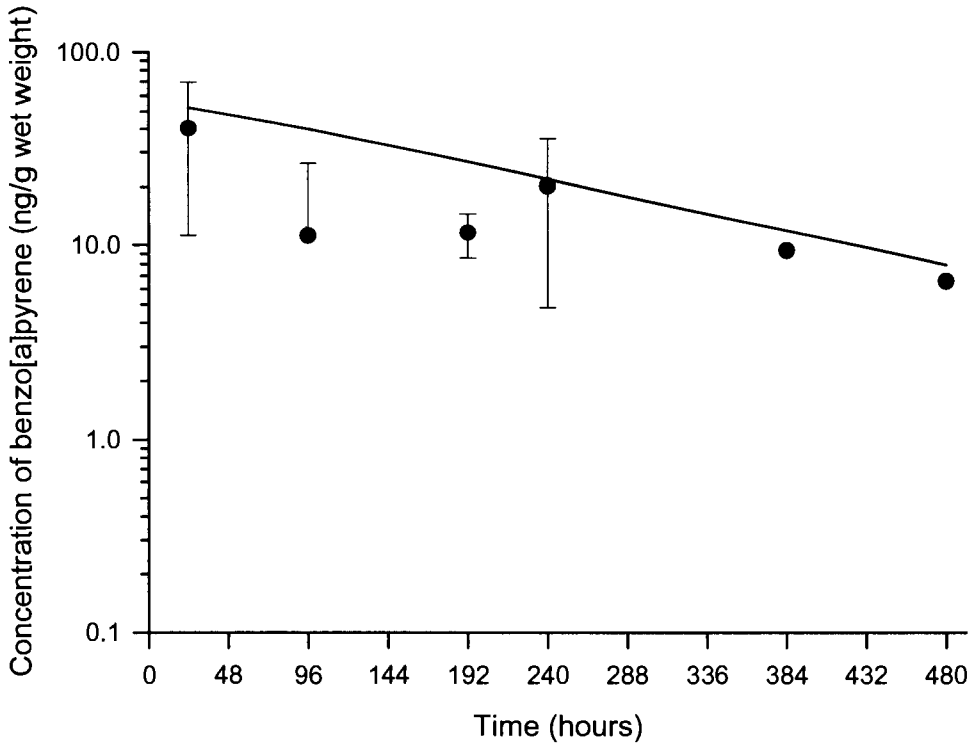

Figure 5.11 Observed and predicted concentrations of benzo[a]pyrene in the muscle following a 2 mg/kg oral dose (predicted – line, observed – symbol).

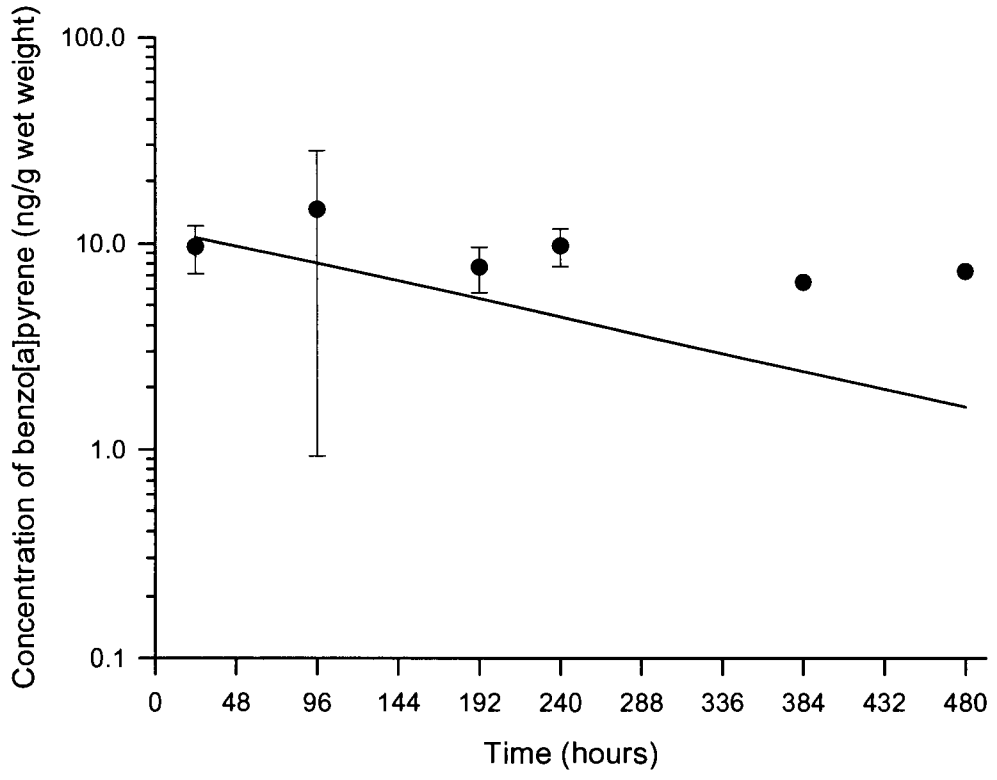

Figure 5.12 **Observed and predicted concentrations of benzo[a]pyrene in the bladder following a 2 mg/kg oral dose (predicted – line, observed – symbol).**

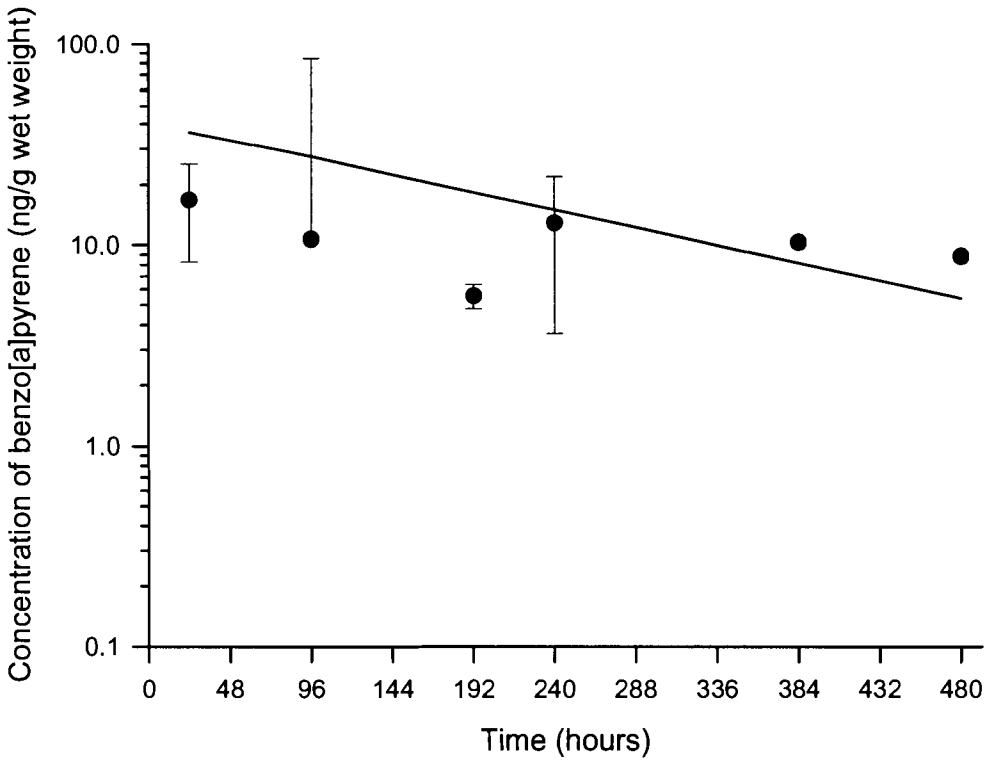

Figure 5.13 **Observed and predicted concentrations of benzo[a]pyrene in the gut following a 2 mg/kg oral dose (predicted – line, observed – symbol).**

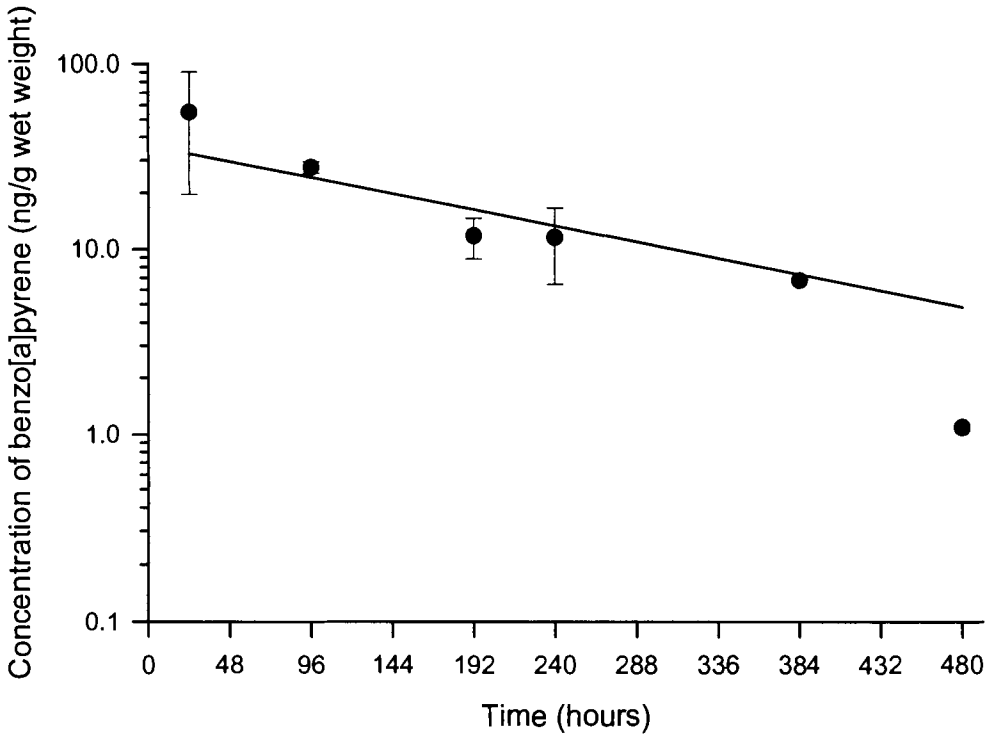

Figure 5.14 **Observed and predicted concentrations of benzo[a]pyrene in the gill following a 2 mg/kg oral dose (predicted – line, observed – symbol).**

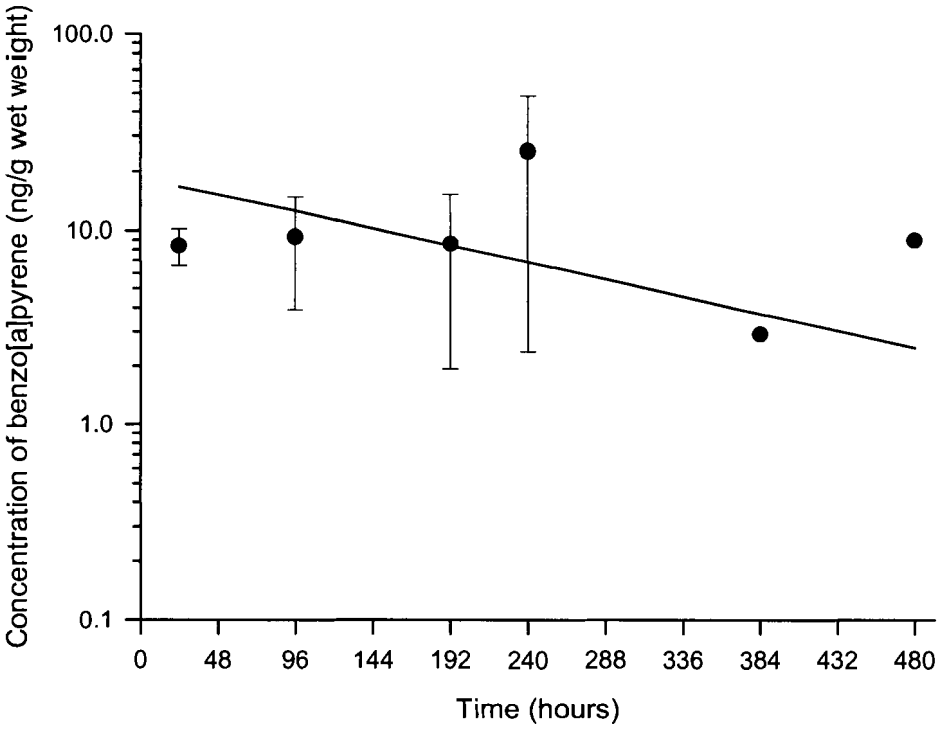

Figure 5.15 **Observed and predicted concentrations of benzo[a]pyrene in the carcass following a 2 mg/kg oral dose (predicted – line, observed – symbol).**

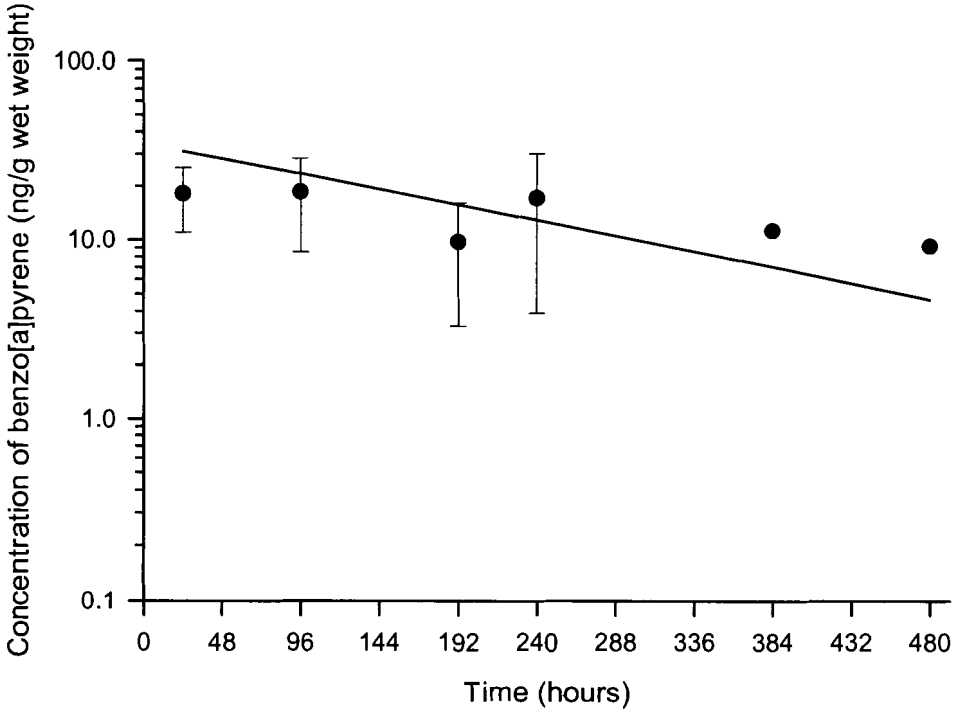

Figure 5.9 shows that the benzo[a]pyrene concentration in the haemolymph is simulated quite well by the model, particularly during the uptake phase or during the 24 hours after the dose was administered. A few of the time points between 72-144 hours post-dosing are slightly over-predicted as indicated by model bias analysis (Table 5.6). This may be due to either model or experimental error. The model also slightly over-predicted concentrations in the hepatopancreas, bladder and gut, Figure 5.10, Figure 5.12, and Figure 5.13) as indicated by model bias analysis.

Benzo(a)pyrene concentrations in the muscle, gill, and carcass, (Figure 5.11, Figure 5.14, and Figure 5.15) were under-predicted but usually within one standard deviation of the mean observed values. The slope of the predicted curve for the muscle seemed to predict a slightly faster elimination of benzo[a]pyrene from this tissue than the observed data although the later observed time points are less accurate than the earlier ones because there is one less data point in the mean, and due to error associated with the analytical method.

5.4.2.2 Model Validation

The PBTK model was validated for predicting tissue concentrations following an oral exposure using a dose of 20 μg/kg, 100 fold lower than the dose used for the model calibration. A more environmentally relevant but lower dose was chosen to determine the importance of the rate-limiting or saturable processes in the disposition of benzo[a]pyrene in the crab. The results of the model predictions and observed data are presented in Figure 5.16 – Figure 5.22.

Figure 5.16 **Observed and predicted concentrations of benzo[a]pyrene in the haemolymph following a 20 μg/kg oral dose (predicted – line, observed – symbol).**

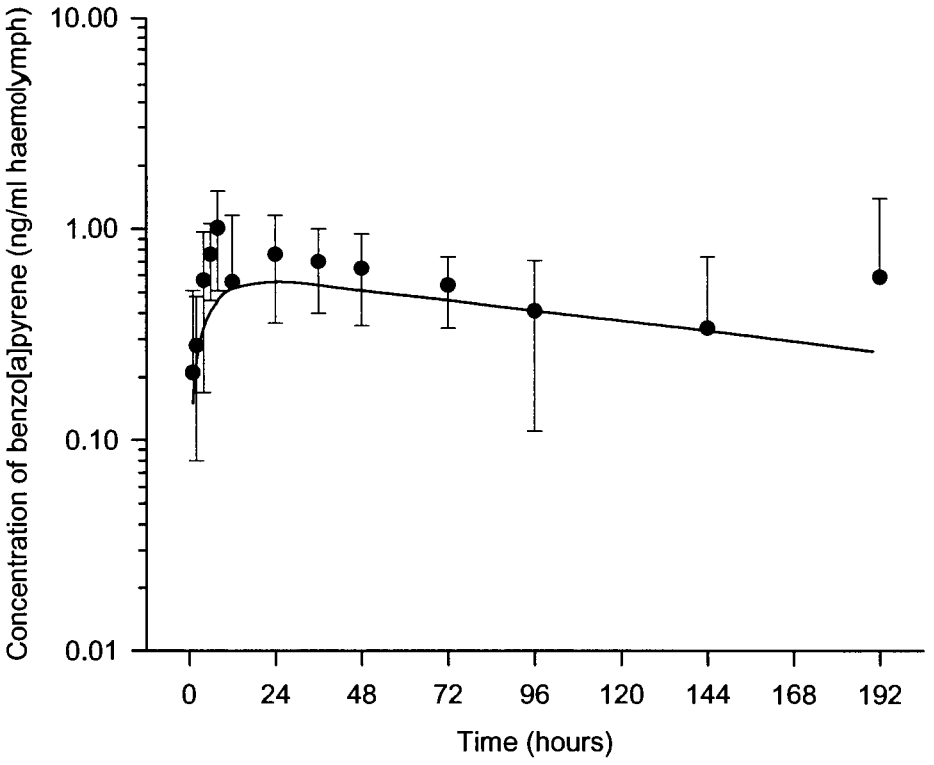

Figure 5.17 **Observed and predicted concentrations of benzo[a]pyrene in the hepatopancreas following a 20 μg/kg oral dose (predicted – line, observed – symbol).**

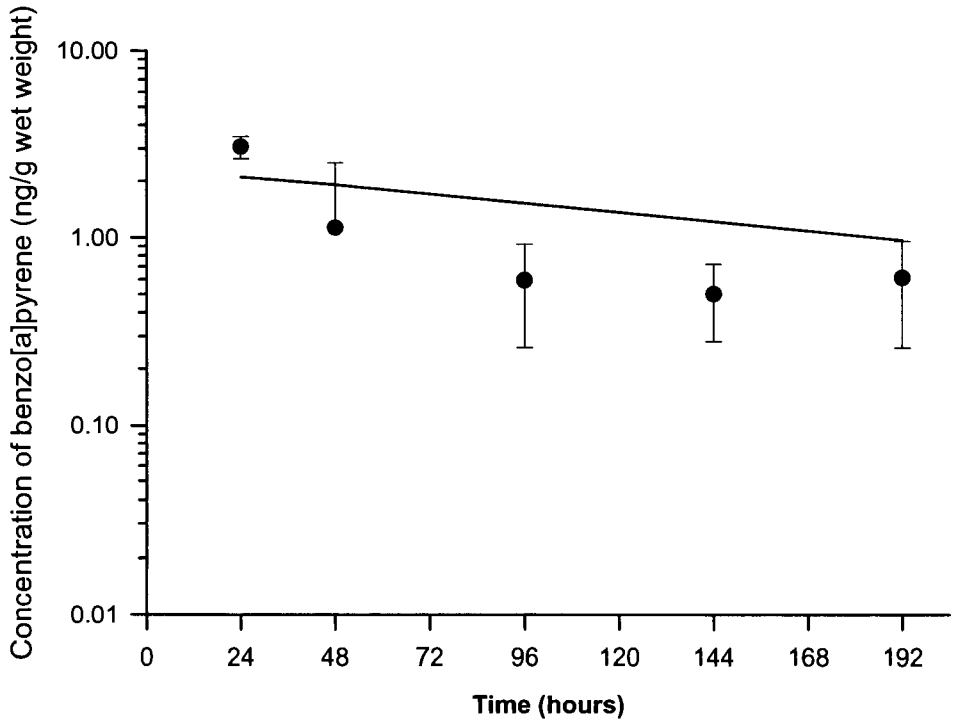

Figure 5.18 **Observed and predicted concentrations of benzo[a]pyrene in the muscle following a 20 µg/kg oral dose (predicted – line, observed – symbol).**

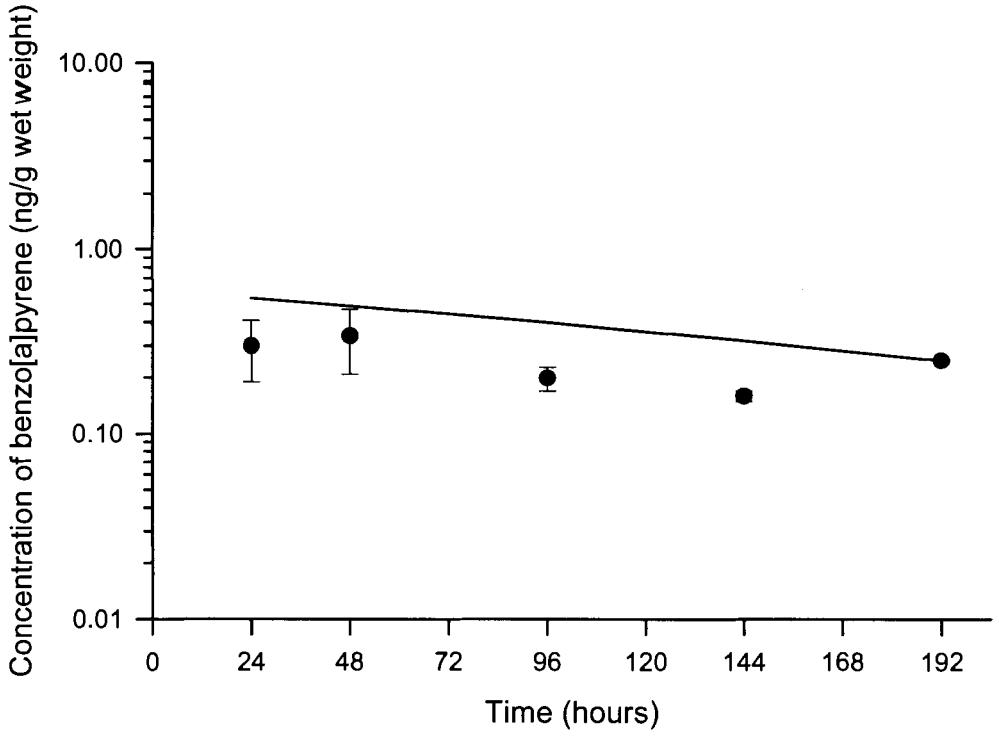

Figure 5.19 **Observed and predicted concentrations of benzo[a]pyrene in the bladder following a 20 µg/kg oral dose (predicted – line, observed – symbol).**

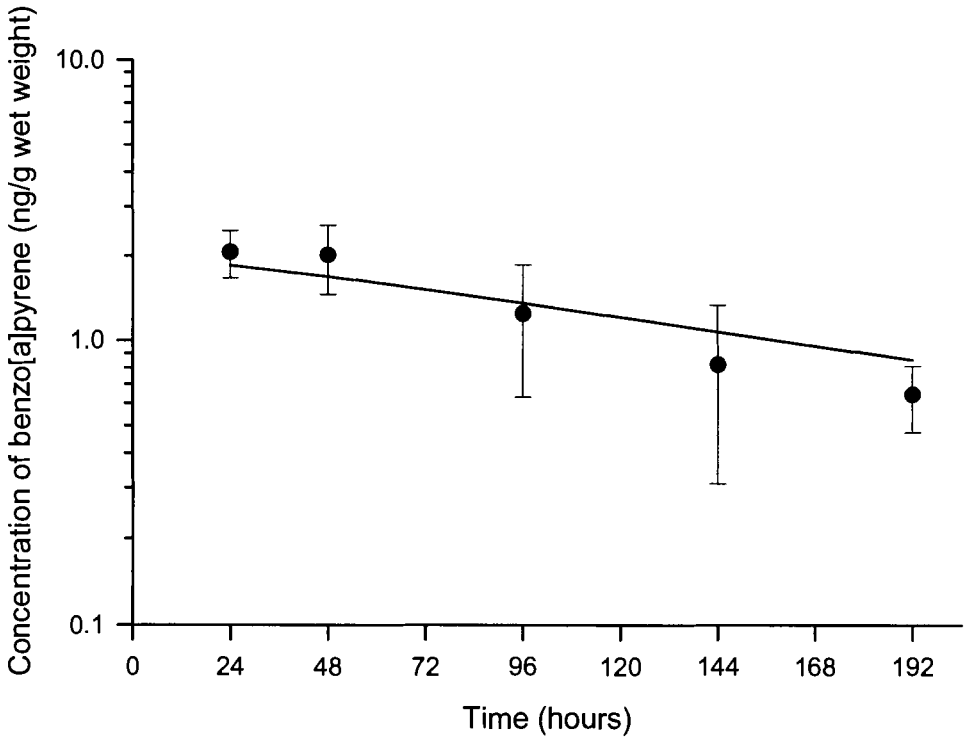

Figure 5.20 **Observed and predicted concentrations of benzo[a]pyrene in the gut following a 20 μg/kg oral dose (predicted – line, observed – symbol).**

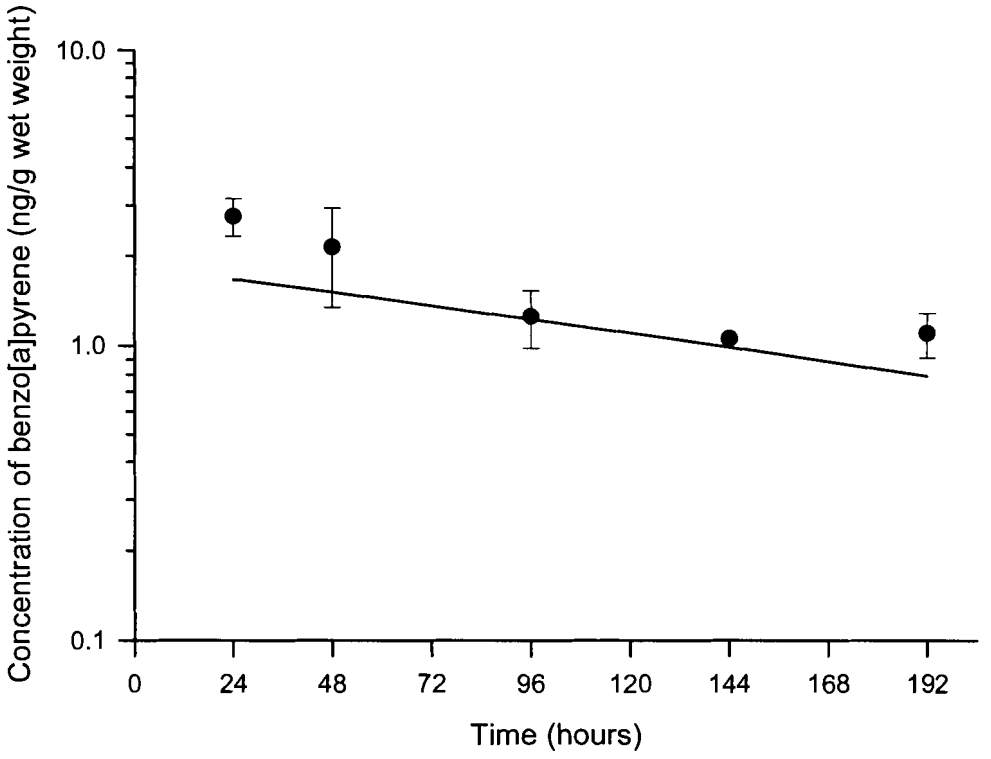

Figure 5.21 **Observed and predicted concentrations of benzo[a]pyrene in the gill following a 20 μg/kg oral dose (predicted – line, observed – symbol).**

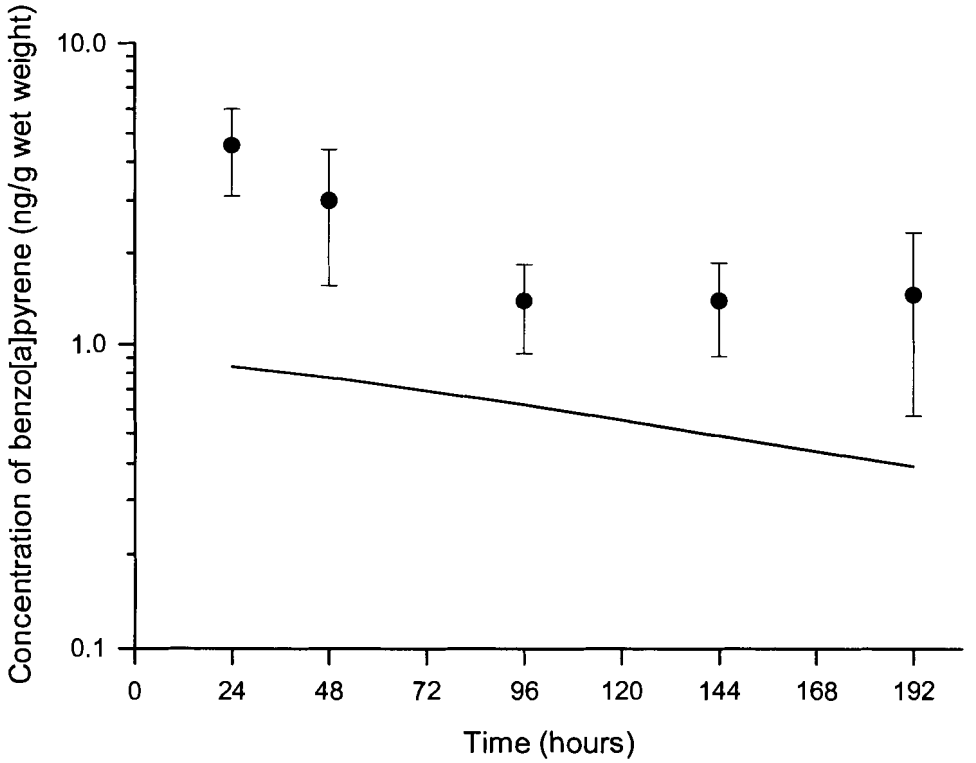

Figure 5.22 Observed and predicted concentrations of benzo[a]pyrene in the carcass following a 20 µg/kg oral dose (predicted – line, observed – symbol).

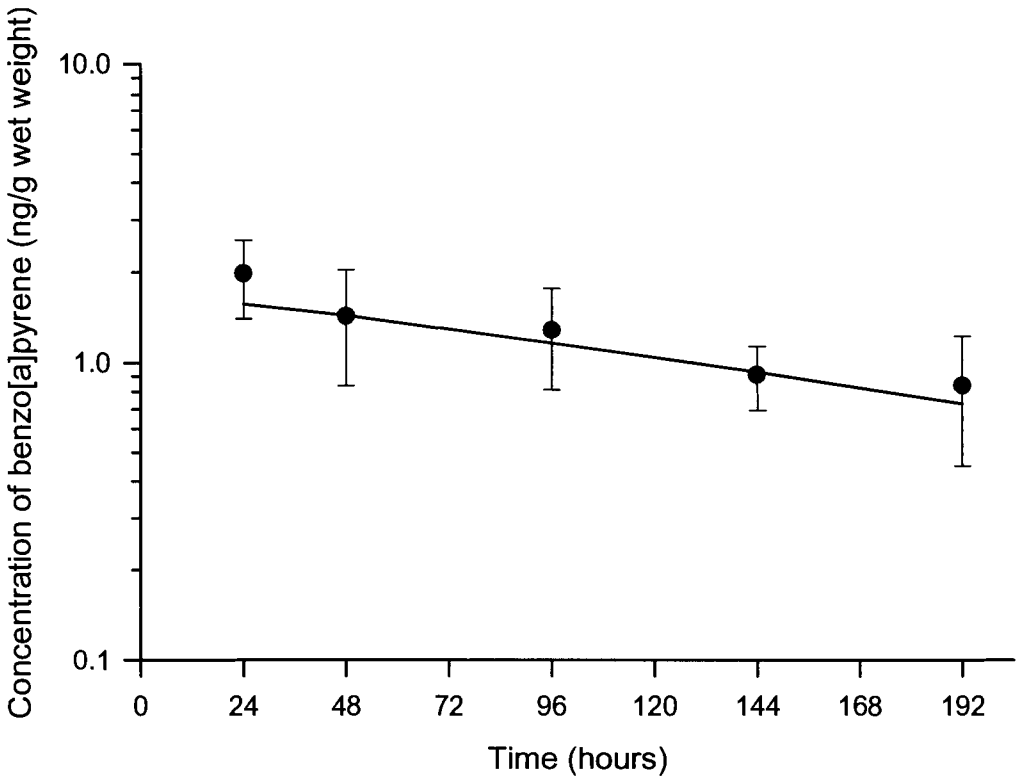

Predicted and observed concentrations are in good agreement and the predicted concentrations are within one standard deviation of the observed values with the exception of the gill. A comparison of predicted and observed concentrations in the haemolymph (Figure 5.16) shows that the model slightly under-predicted haemolymph concentrations especially over the first 48 hours post-exposure. Concentrations of benzo[a]pyrene in the hepatopancreas and muscle were somewhat over-predicted by the model (Figure 5.17 and Figure 5.18) while concentrations in the bladder, gut, and carcass (Figure 5.19, Figure 5.20, and Figure 5.22) were in agreement. Observed concentrations in the gill were significantly under-predicted by the model (Figure 5.21).

5.4.3 Waterborne Exposure

5.4.3.1 Model Calibration

The PBTK model was adapted to predict the disposition of benzo[a]pyrene in the crab following exposure to waterborne chemical. Crabs were exposed to a nominal concentration of 20 μg benzo[a]pyrene/L for 72 hours under static conditions and then were removed to clean seawater for the duration of the experiment to study chemical elimination. The concentration of benzo[a]pyrene in the seawater was analysed over the duration of the exposure period. The measured concentrations were used as the input concentrations of the waterborne exposure experiment. The water exposure experiments are described fully in Chapter 4 and the observed exposure concentrations are summarised in Figure 4.14 and Figure 4.17. The predicted and observed results of the waterborne exposure study are depicted in Figure 5.23 – Figure 5.29.

Figure 5.23 shows that the model predicted the observed concentrations of benzo[a]pyrene in the haemolymph extremely well over the duration of the experiment. Concentrations in the hepatopancreas and gut were significantly over-predicted by the model (Figure 5.24 and Figure 5.27). Predicted concentrations in the hepatopancreas and gut were generally 3.6 and 3.3 fold higher than the observed values respectively. This difference may be related to the problems of route-to-route extrapolation encountered frequently during model development. In contrast, benzo(a)pyrene concentrations in the bladder and carcass tissues were simulated quite well by the model (Figure 5.26 and Figure 5.29). The model generally under-predicted the observed concentrations of benzo[a]pyrene in the gill. The uncertainty analysis showed that there was a relatively large PI value for the gill compartment (Table 5.7).

Figure 5.23 **Observed and predicted concentrations of benzo[a]pyrene in the haemolymph following a 20 µg/L seawater exposure (predicted – line, observed – symbol).**

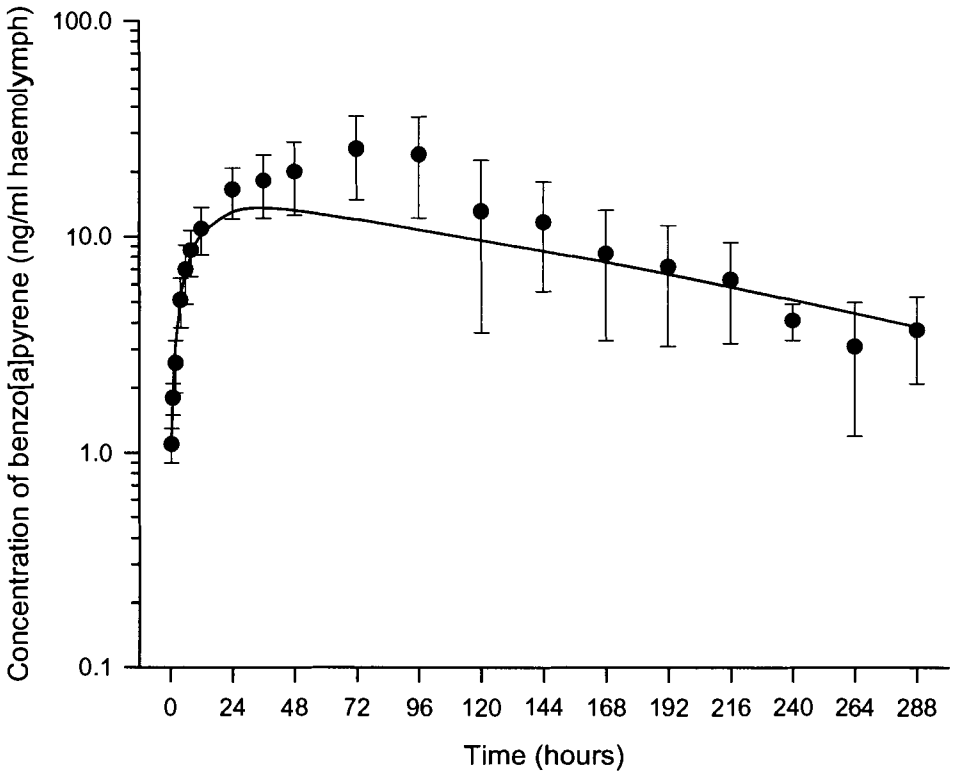

Figure 5.24 **Observed and predicted concentrations of benzo[a]pyrene in the hepatopancreas following a 20 µg/L seawater exposure (predicted – line, observed – symbol).**

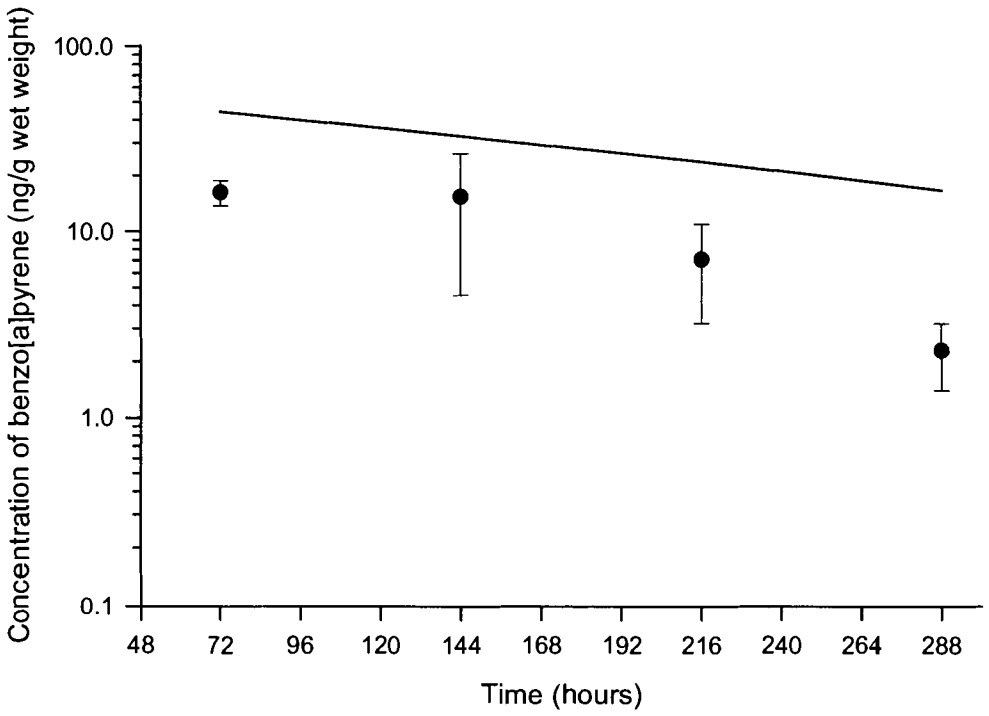

Figure 5.25 **Observed and predicted concentrations of benzo[a]pyrene in the muscle following a 20 µg/L seawater exposure (predicted – line, observed – symbol).**

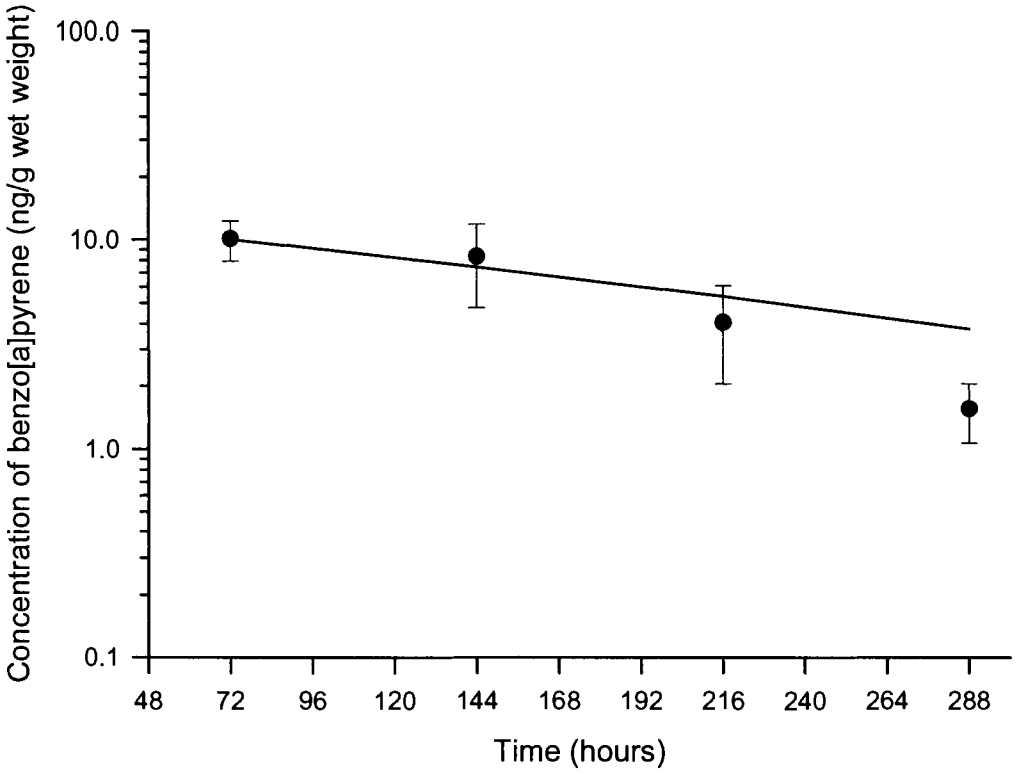

Figure 5.26 **Observed and predicted concentrations of benzo[a]pyrene in the bladder following a 20 µg/L seawater exposure (predicted – line, observed – symbol).**

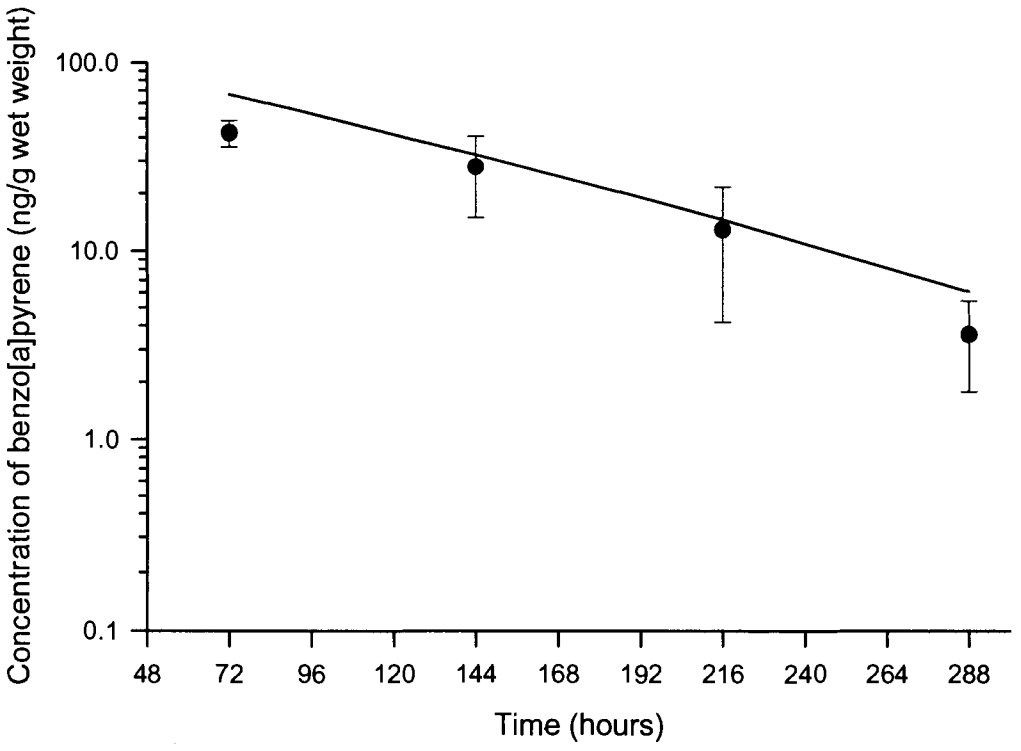

Figure 5.27 Observed and predicted concentrations of benzo[a]pyrene in the gut following a 20 µg/L seawater exposure (predicted – line, observed – symbol).

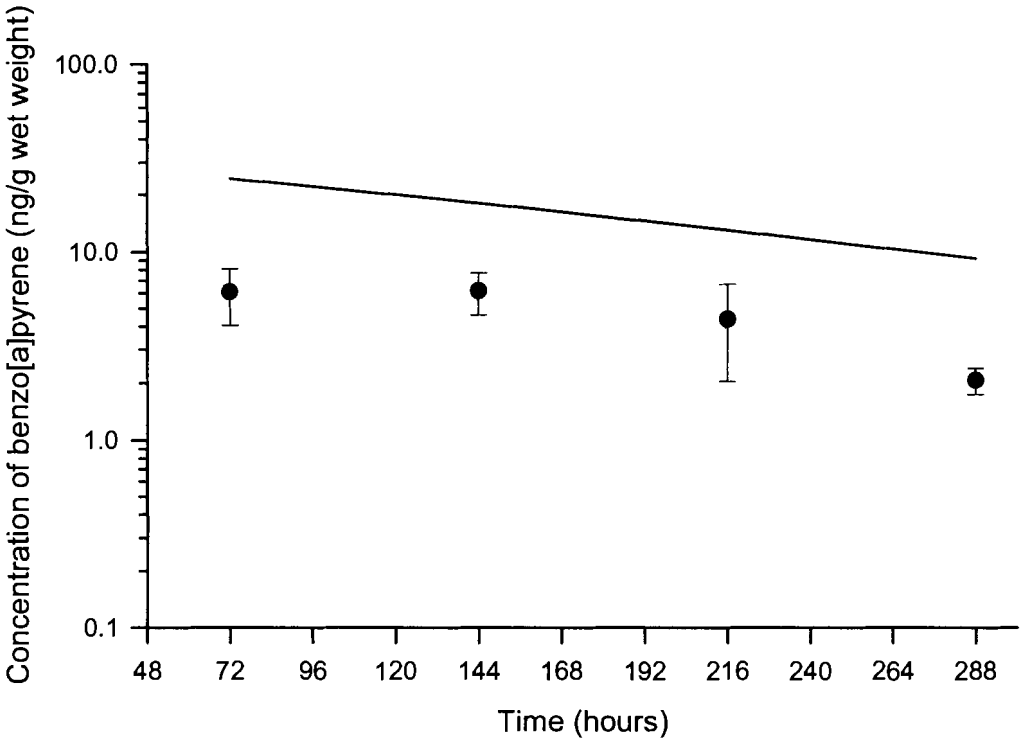

Figure 5.28 Observed and predicted concentrations of benzo[a]pyrene in the gill following a 20 µg/L seawater exposure (predicted – line, observed – symbol).

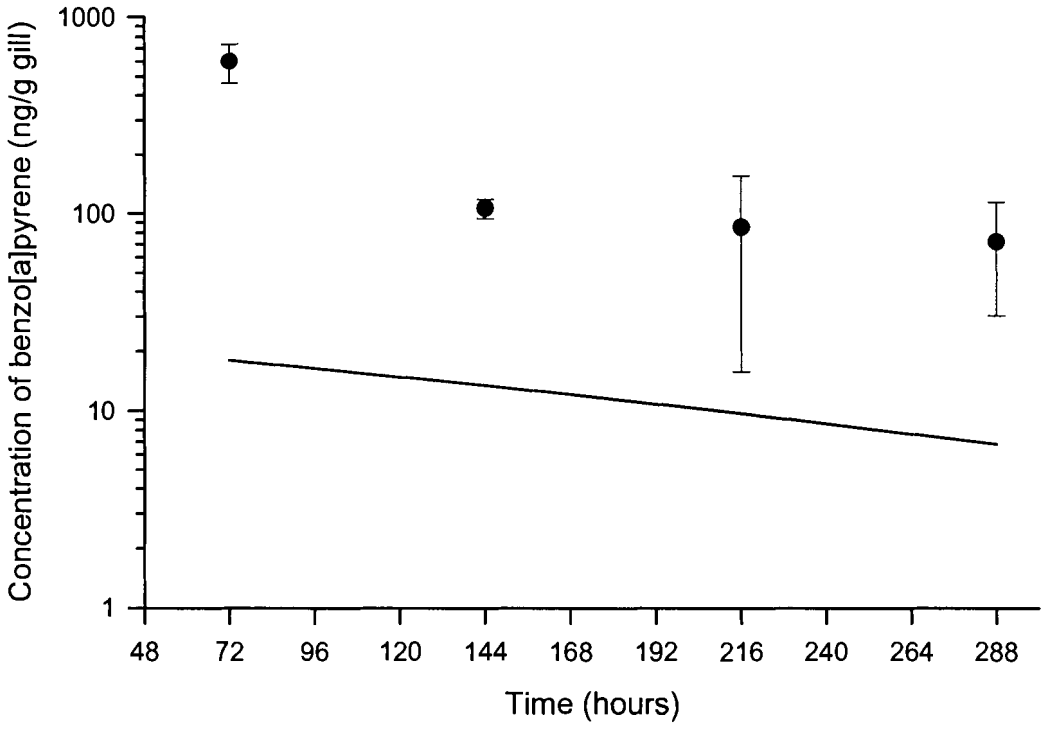

Figure 5.29 Observed and predicted concentrations of benzo[a]pyrene in the carcass following a 20 µg/L seawater exposure (predicted – line, observed – symbol).

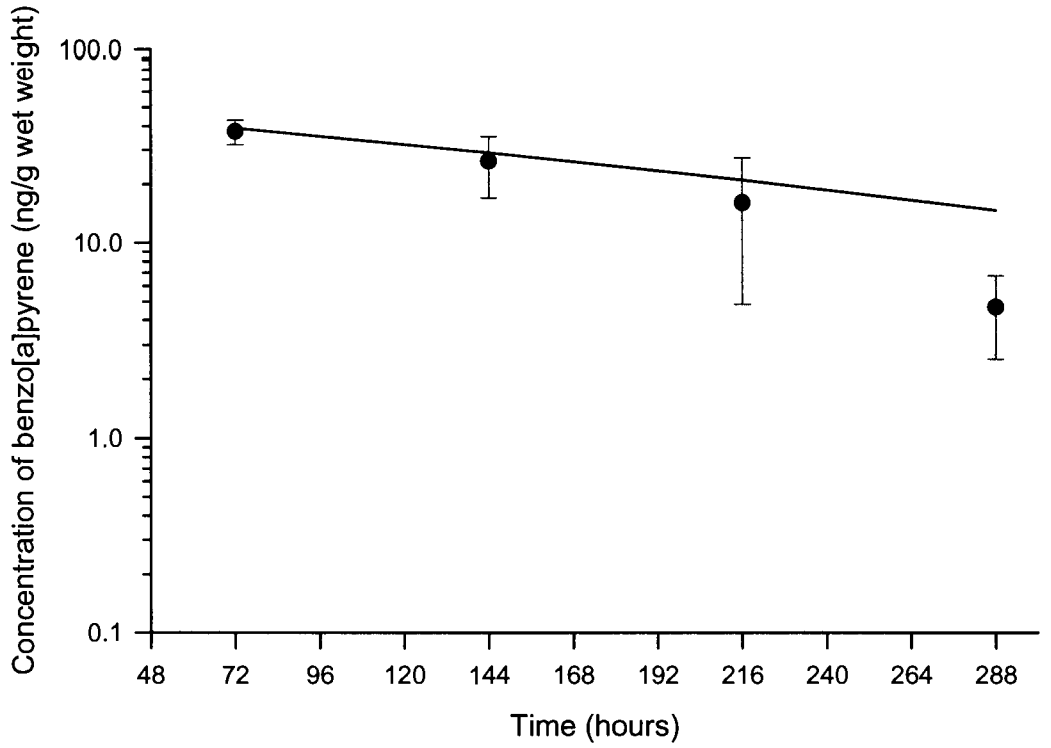

5.4.3.2 Model Validation

The PBTK model was validated for predicting the disposition of benzo[a]pyrene using a seawater exposure concentration of 2 µg/L. This exposure concentration was 10 fold lower than used for model calibration. This concentration is within the range of water solubility values (0.172 – 6.9 µg/L) reported for benzo[a]pyrene (Mackay *et al.*, 1991). Figure 5.30 – Figure 5.36 show the predicted vs. observed tissue concentrations of crabs exposed to a nominal concentration of 2 µg/L waterborne benzo[a]pyrene. Each tissue time point represents the mean of three crabs. Haemolymph time points represent the means of 12 (0.5 – 72 hr), 6 (96 - 120 hr), and 3 crabs (144 – 168 hr). Error bars represent one standard deviation from the mean. The solid line represents the model simulation.

Figure 5.30 **Observed and predicted concentrations of benzo[a]pyrene in the haemolymph following a 2 µg/L seawater exposure (predicted – line, observed – symbol).**

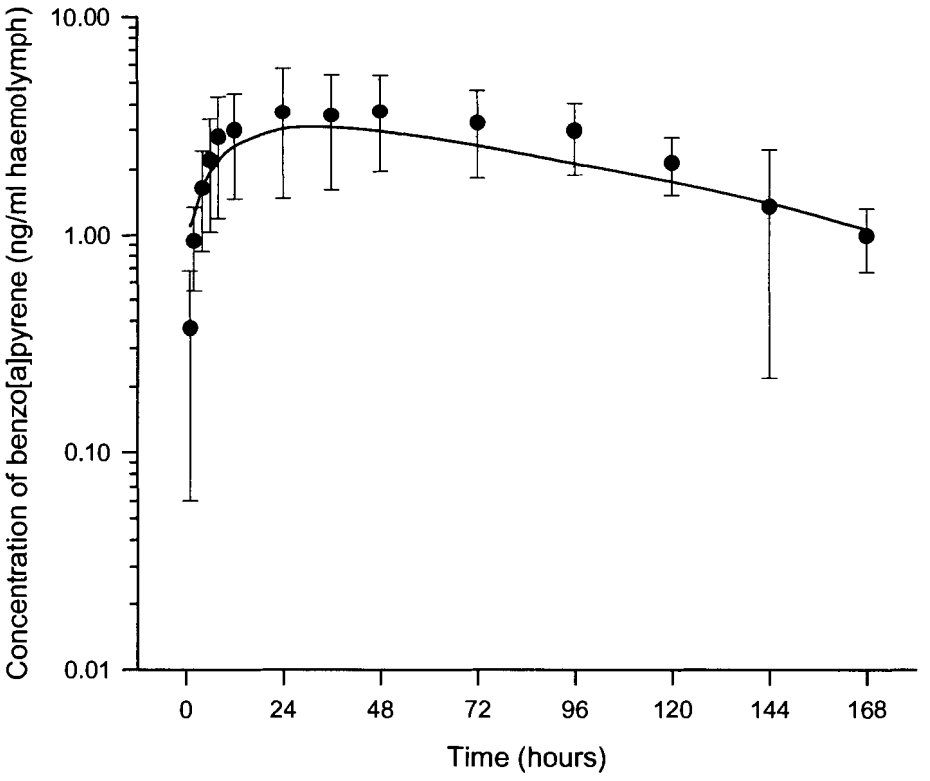

Figure 5.31 **Observed and predicted concentrations of benzo[a]pyrene in the hepatopancreas following a 2 µg/L seawater exposure (predicted – line, observed – symbol).**

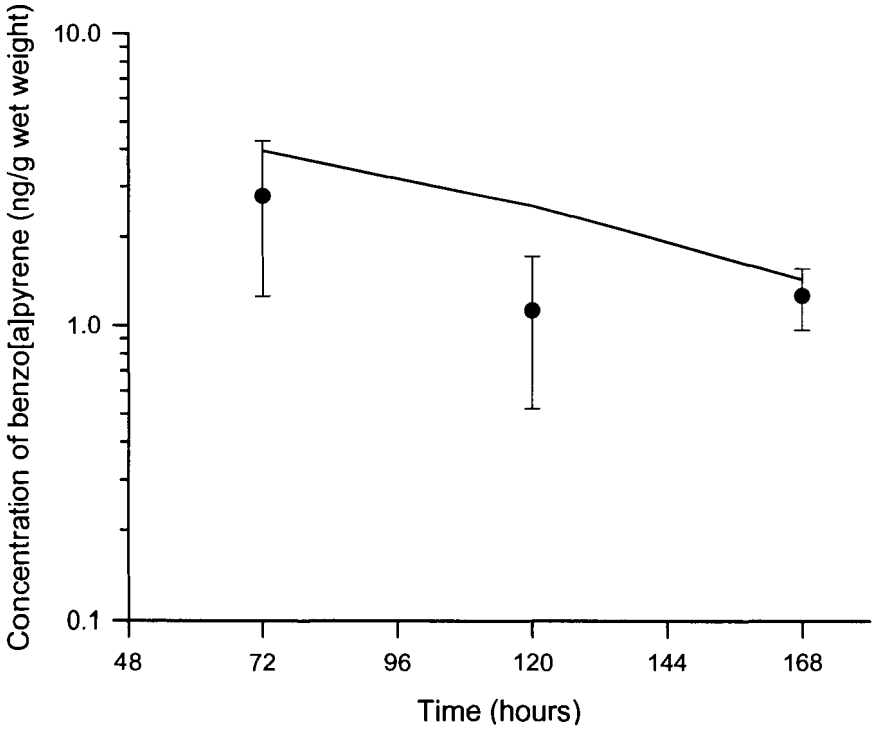

Figure 5.32 **Observed and predicted concentrations of benzo[a]pyrene in the muscle following a 2 µg/L seawater exposure (predicted – line, observed – symbol).**

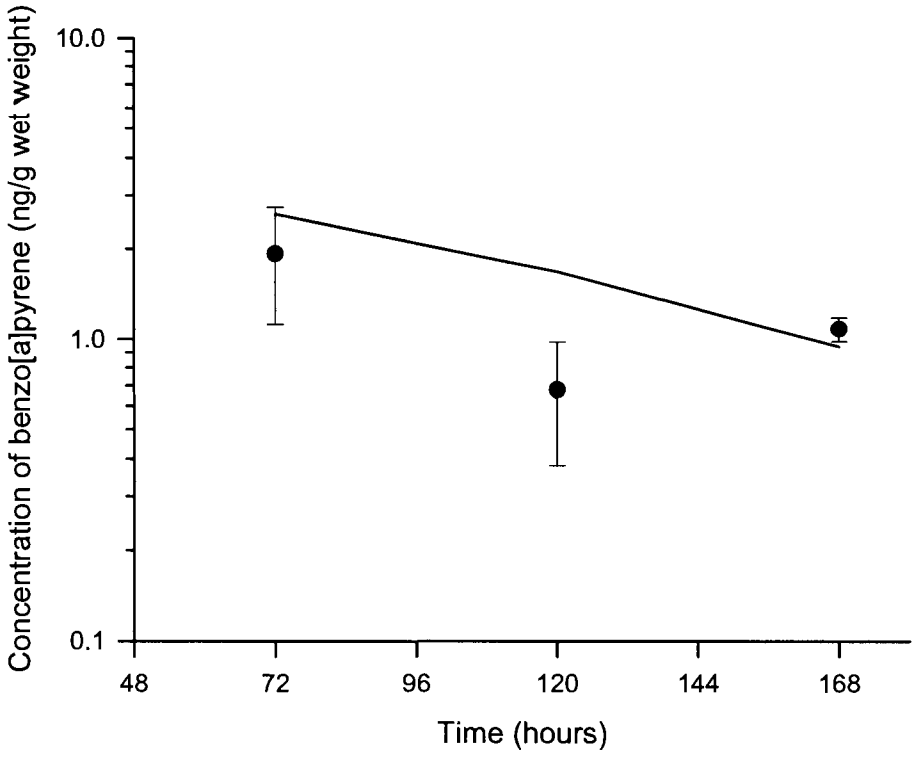

Figure 5.33 **Observed and predicted concentrations of benzo[a]pyrene in the bladder following a 2 µg/L seawater exposure (predicted – line, observed – symbol).**

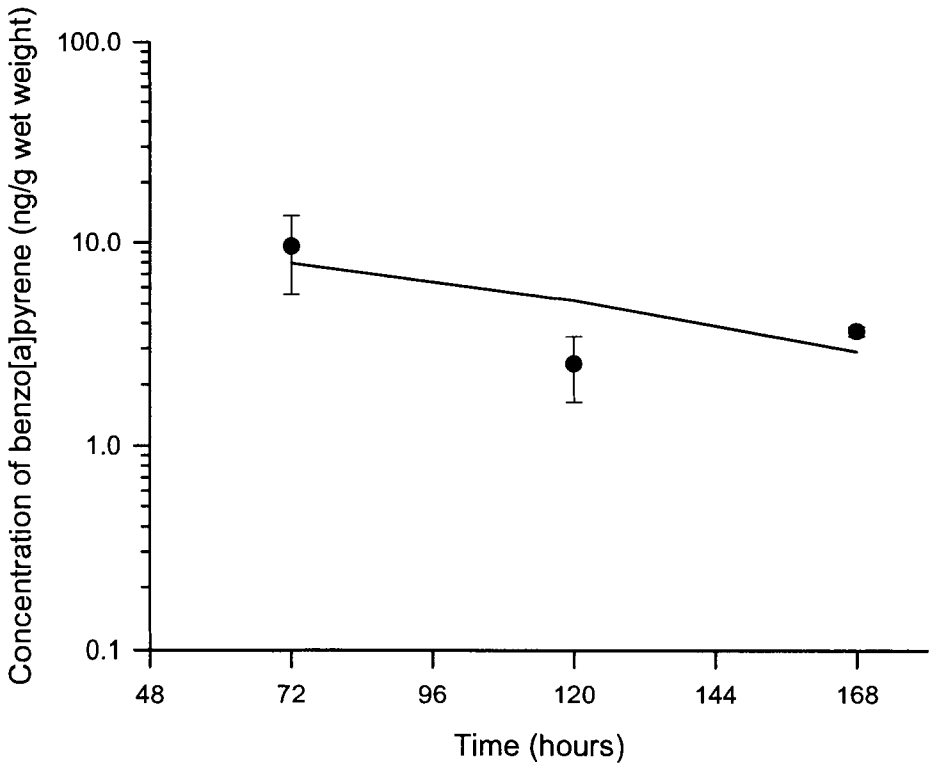

Figure 5.34 **Observed and predicted concentrations of benzo[a]pyrene in the gut following a 2 µg/L seawater exposure(predicted – line, observed – symbol).**

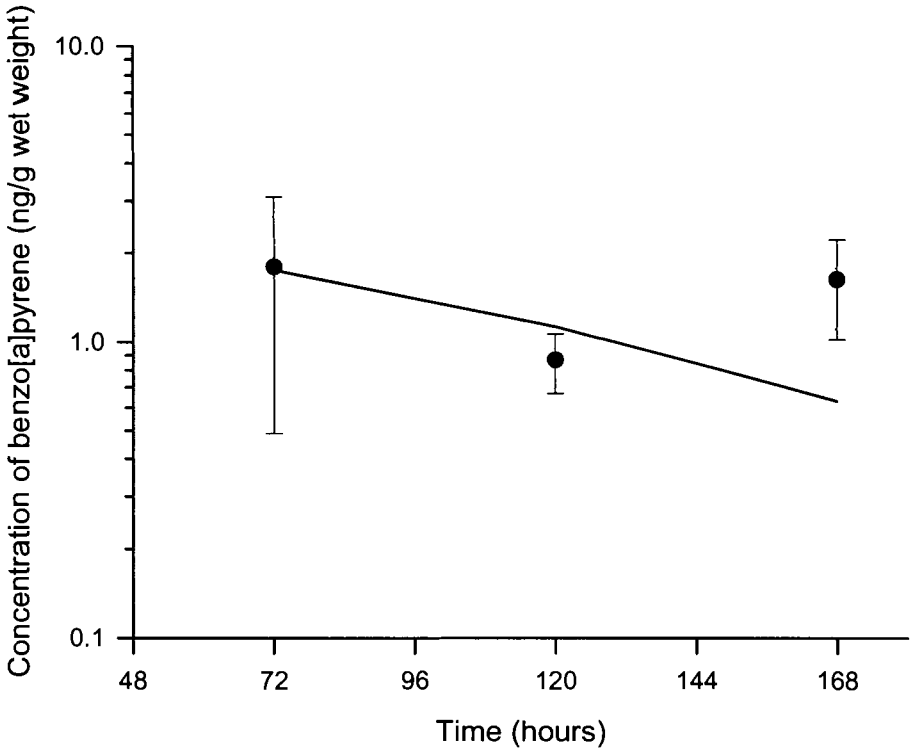

Figure 5.35 **Observed and predicted concentrations of benzo[a]pyrene in the gill following a 2 µg/L seawater exposure (predicted – line, observed – symbol).**

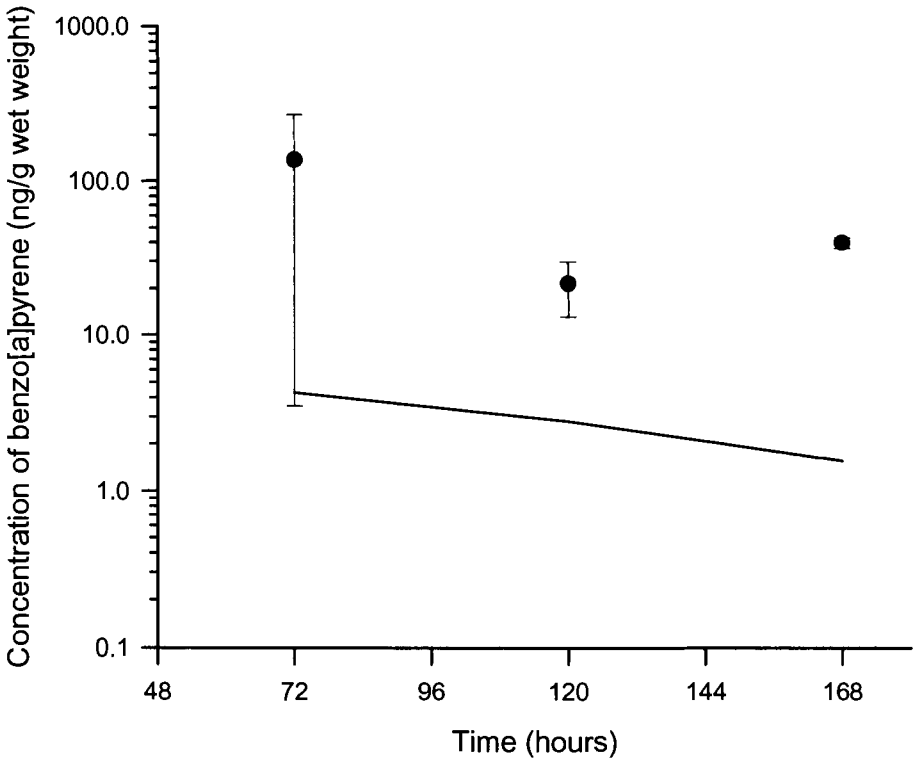

Figure 5.36 Observed and predicted concentrations of benzo[a]pyrene in the carcass following a 2 µg/L seawater exposure (predicted – line, observed – symbol).

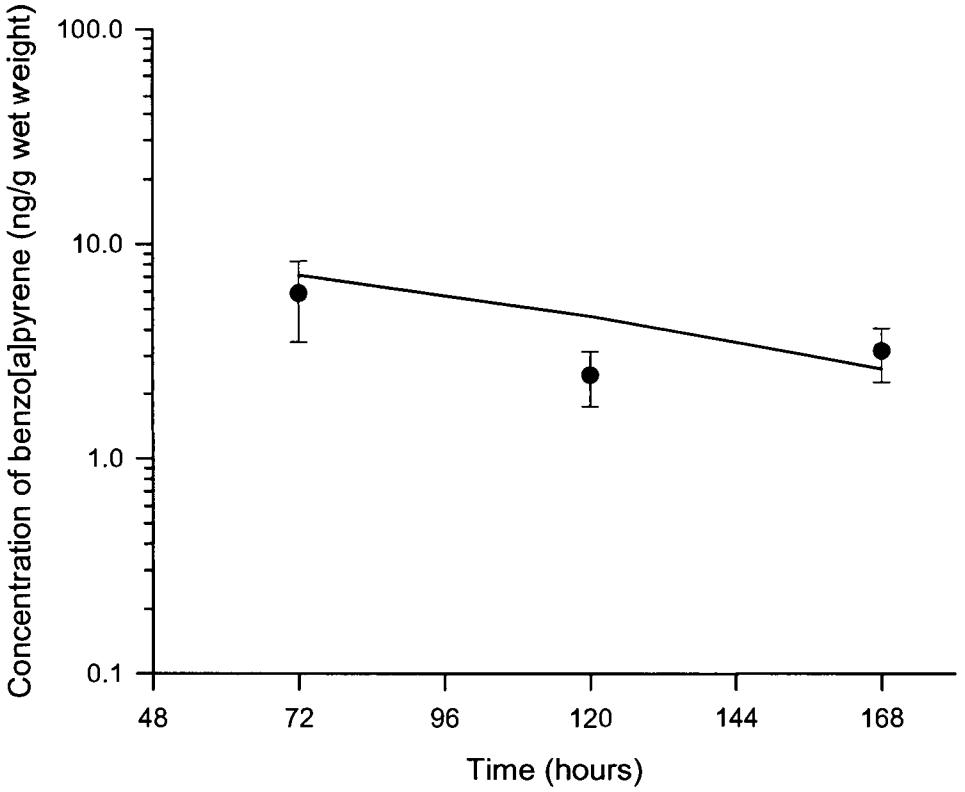

The model predicted concentrations very well in the haemolymph of crabs exposed to 2 µg/L of benzo[a]pyrene in seawater (Figure 5.30). Observed concentrations in the hepatopancreas and gut were again overestimated by the model (Figure 5.31 and Figure 5.34). There was good agreement between predicted and observed concentrations in the muscle, bladder and carcass (Figure 5.32, Figure 5.33, and Figure 5.36). However, gill tissue concentrations were significantly under-predicted. Again, the PI was very high, indicating a great deal of uncertainty in the model simulated values for this compartment (Table 5.7).

5.4.4 Model Bias and Uncertainty

A summary of the model bias analysis is for each set of model predictions and experimental data is presented in Table 5.6.

Table 5.6 Model bias for fit of model predicted benzo[a]pyrene concentrations to empirical benzo[a]pyrene tissue concentrations

Simulation	hepato	muscle	bladder	gut	gill	carcass	haemolymph
iv 2mg/kg	0.68	1.16	0.58	-	0.82	0.69	1.20
Oral 2mg/kg	1.45	0.50	1.37	1.26	0.79	0.97	1.15
Oral 20 μg/kg	1.64	1.60	1.07	0.78	0.29	0.91	0.71
Water 20 μg/L	3.28	1.40	1.50	3.56	0.07	1.19	0.89
Water 2μg/L	4.03	1.46	1.24	2.71	0.05	1.35	0.97

Uncertainty in the model simulated values compared with empirically determined concentrations of benzo[a]pyrene in each tissue compartment is summarised by the 95% probability interval values, presented in Table 5.7.

Table 5.7 Probability Intervals calculated for estimation of uncertainty in model predicted values

Simulation	hepato	muscle	bladder	gut	gill	carcass	haemolymph
iv 2mg/kg	3.4	2.6	4.5	-	2.2	2.2	2.0
Oral 2mg/kg	2.1	4.6	2.4	2.6	4.1	2.8	2.0
Oral 20 μg/kg	2.2	1.9	2.2	2.6	6.2	2.3	2.7
Water 20 μg/L	1.6	2.3	2.7	1.4	37.1	2.7	2.3
Water 2μg/L	1.6	3.3	4.0	2.5	130.6	2.9	2.3

5.4.5 Application of PBTK Model to Predict PAH Concentrations in Muscle Tissue for Human Health Risk Assessment

The PBTK model was used to fill data gaps in the concentrations of PAH determined in muscle tissues of crabs collected in Kitimat Arm. The concentrations of PAH were determined in the hepatopancreas of all of the 187 crabs collected in Kitimat Arm (Chapter 2). However, muscle tissues were only analysed in 15 of the 66 muscle samples from Hospital Beach that had the highest concentrations in the hepatopancreas, and similarly, 4 muscle samples from crabs collected at Kitamaat Village that had high PAH concentrations in the hepatopancreas. No muscle tissue samples were analysed from crabs collected at the other three sites, Wathlsto Creek, Kildala Arm, and Kitkiatka Inlet. The PBTK model was used to predict PAH concentrations in the muscle of crabs collected at all sites based on the concentration of benzo[a]pyrene in each corresponding hepatopancreas sample. The concentration of benzo[a]pyrene was estimated in muscle tissues based on regression analysis of the concentration of benzo[a]pyrene in the hepatopancreas and muscle tissues predicted by the model (Figure 5.37).

Figure 5.37 Regression analysis of PBTK model predicted concentrations of benzo[a]pyrene in hepatopancreas and muscle tissues.

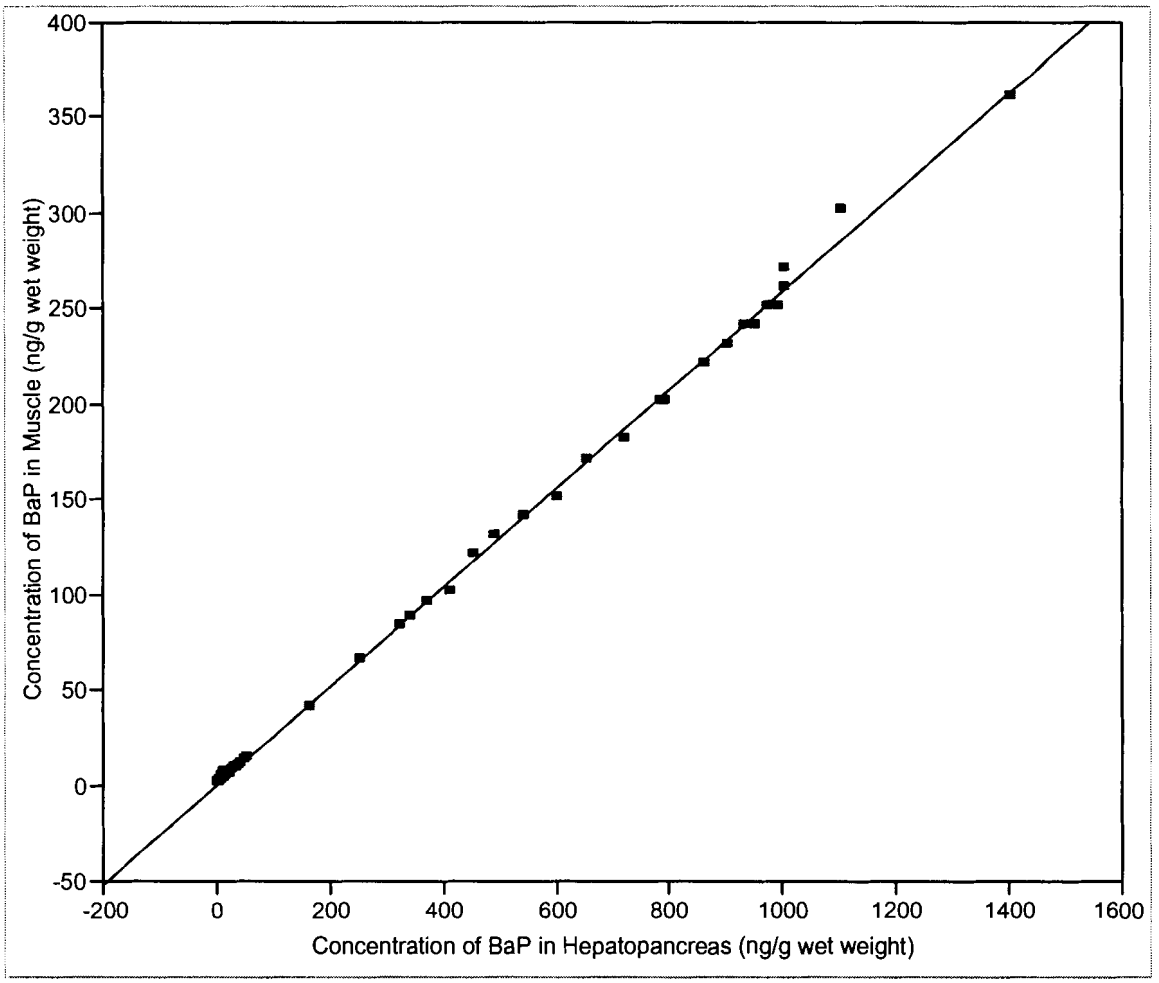

The regression analysis was based on 130 pairs of tissue concentrations predicted by the model. The regression equation is presented in Equation 5.8.

$$CM = 0.2587049 * CL + 0.017887 \tag{5.8}$$

The regression fit statistics are presented in Table 5.8.

Table 5.8 Summary of Regression Analysis Statistics

Statistic				Value
RSquare				0.999275
RSquare Adj				0.999269
Root Mean Square Error				2.242663
Mean of Response				39.70265
Observations (or Sum Wgts)				130
Analysis of Variance				
Source	DF	Sum of Squares	Mean Square	F Ratio
Model	1	887226.09	887226	176403.2
Error	128	643.78	5	Prob > F
C. Total	129	887869.87		<.0001
Parameter Estimates				
Term	Estimate	Std Error	t Ratio	Prob>|t|
Intercept	0.017887	0.218212	0.08	0.9348
CL	0.2587049	0.000616	420.00	<.0001

In order to predict the concentrations of other PAH in the muscle tissues of crabs based on the concentration of benzo[a]pyrene, the relationship of the concentration of each PAH to the concentration of benzo[a]pyrene in 19 muscle tissue samples was examined by regression analysis. The results of the regression analyses are presented in Table 5.9.

Table 5.9 Regression analysis of PAH concentrations vs. the concentration of benzo[a]pyrene determined in muscle tissues

Bivariate Fit of Anthracene By Benzo[a]pyrene

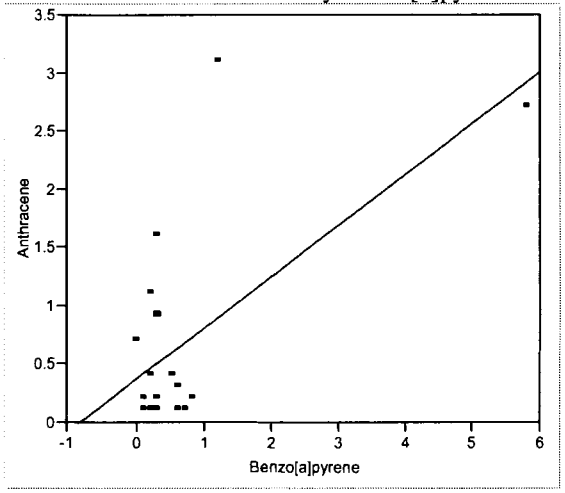

Linear Fit
Anthracene = 0.3649173 + 0.4417914 Benzo[a]pyrene

Summary of Fit

RSquare	0.40004
RSquare Adj	0.364748
Root Mean Square Error	0.711552
Mean of Response	0.657895
Observations (or Sum Wgts)	19

Analysis of Variance

Source	DF	SS	Mean Square	F Ratio
Model	1	5.739102	5.73910	11.3352
Error	17	8.607213	0.50631	Prob > F
C. Total	18	14.346316		0.0037

Parameter Estimates

Term	Estimate	Std Error	t Ratio	Prob>|t|
Intercept	0.3649173	0.184987	1.97	0.0650
BaP	0.4417914	0.131221	3.37	0.0037

Bivariate Fit of Phenanthrene By Benzo[a]pyrene

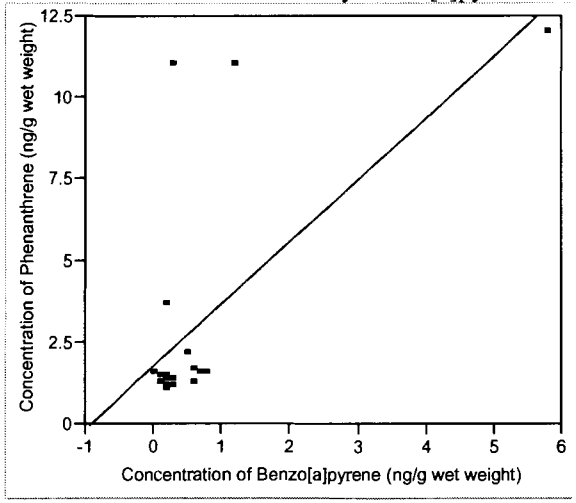

Linear Fit
Phenanthrene = 1.7395299 + 1.9069846 Benzo[a]pyrene

Summary of Fit

RSquare	0.423993
RSquare Adj	0.391993
Root Mean Square Error	2.85069
Mean of Response	2.96
Observations (or Sum Wgts)	19

Analysis of Variance

Source	DF	SS	Mean Square	F Ratio
Model	1	107.67216	107.672	13.2496
Error	18	146.27584	8.126	Prob > F
C. Total	19	253.94800		0.0019

Parameter Estimates

Term	Estimate	Std Error	t Ratio	Prob>|t|
Intercept	1.7395299	0.720239	2.42	0.0266
BaP	1.9069846	0.523897	3.64	0.0019

Bivariate Fit of Fluoranthene By Benzo[a]pyrene

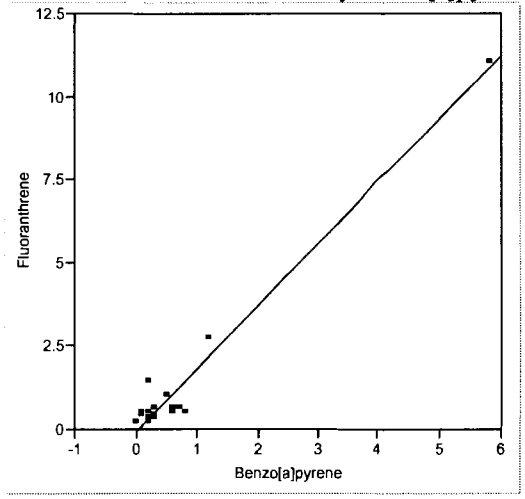

Linear Fit
Fluoranthene = -0.080512 + 1.8836125 Benzo[a]pyrene

Summary of Fit

RSquare	0.965369
RSquare Adj	0.963445
Root Mean Square Error	0.457556
Mean of Response	1.125
Observations (or Sum Wgts)	19

Analysis of Variance

Source	DF	SS	Mean Square	F Ratio
Model	1	105.04907	105.049	501.7697
Error	18	3.76843	0.209	Prob > F
C. Total	19	108.81750		<.0001

Parameter Estimates

Term	Estimate	Std Error	t Ratio	Prob>|t|
Intercept	-0.080512	0.115603	-0.70	0.4950
BaP	1.8836125	0.084089	22.40	<.0001

Table 5.9 Continued - Regression analysis of PAH concentrations vs. the concentration of benzo[a]pyrene determined in muscle tissues

Bivariate Fit of Pyrene By Benzo[a]pyrene

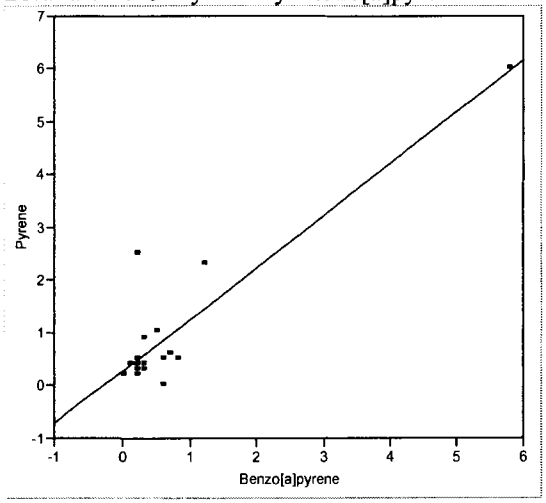

Linear Fit
Pyrene = 0.2699 + 0.9845312 Benzo[a]pyrene

Summary of Fit

RSquare	0.812085
RSquare Adj	0.801645
Root Mean Square Error	0.607404
Mean of Response	0.9
Observations (or Sum Wgts)	19

Analysis of Variance

Source	DF	SS	Mean Square	F Ratio
Model	1	28.699085	28.6991	77.7880
Error	18	6.640915	0.3689	Prob > F
C. Total	19	35.340000		<.0001

Parameter Estimates

Term	Estimate	Std Error	t Ratio	Prob>|t|
Intercept	0.2699	0.153463	1.76	0.0956
BaP	0.9845312	0.111628	8.82	<.0001

Bivariate Fit of Benzanthracene By Benzo[a]pyrene

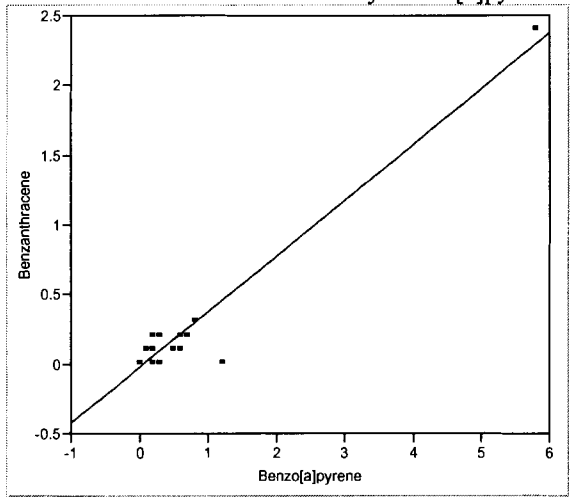

Linear Fit
Benzanthracene = -0.020974 + 0.3999595 Benzo[a]pyrene

Summary of Fit

RSquare	0.931338
RSquare Adj	0.927524
Root Mean Square Error	0.13928
Mean of Response	0.235
Observations (or Sum Wgts)	19

Analysis of Variance

Source	DF	SS	Mean Square	F Ratio
Model	1	4.7363200	4.73632	244.1542
Error	18	0.3491800	0.01940	Prob > F
C. Total	19	5.0855000		<.0001

Parameter Estimates

Term	Estimate	Std Error	t Ratio	Prob>|t|
Intercept	-0.020974	0.03519	-0.60	0.5586
BaP	0.3999595	0.025597	15.63	<.0001

Bivariate Fit of Chrysene By Benzo[a]pyrene

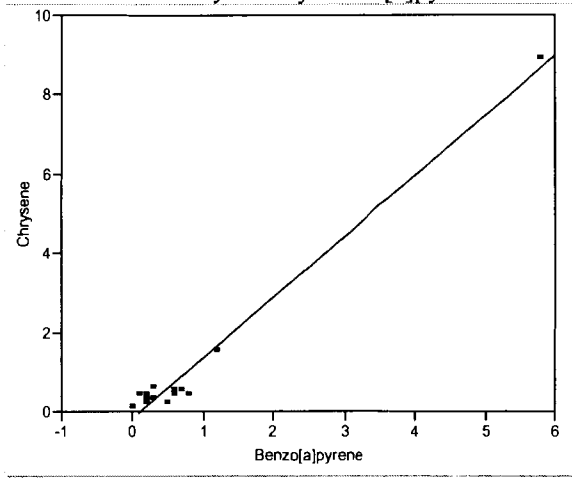

Linear Fit
Chrysene = -0.154526 + 1.5226966 Benzo[a]pyrene

Summary of Fit

RSquare	0.97663
RSquare Adj	0.975331
Root Mean Square Error	0.302099
Mean of Response	0.82
Observations (or Sum Wgts)	19

Analysis of Variance

Source	DF	SS	Mean Square	F Ratio
Model	1	68.649252	68.6493	752.2070
Error	18	1.642748	0.0913	Prob > F
C. Total	19	70.292000		<.0001

Parameter Estimates

Term	Estimate	Std Error	t Ratio	Prob>|t|
Intercept	-0.154526	0.076327	-2.02	0.0580
BaP	1.5226966	0.055519	27.43	<.0001

Table 5.9 Continued - Regression analysis of PAH concentrations vs. the concentration of benzo[a]pyrene determined in muscle tissues

Bivariate Fit of Benzofluoranthenes By Benzo[a]pyrene

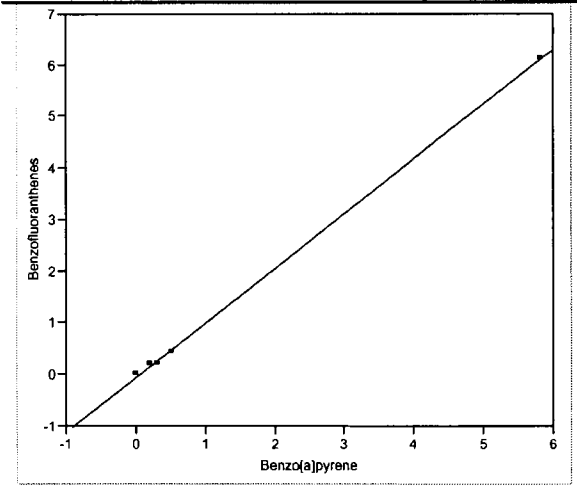

Linear Fit

Benzofluoranthenes = -0.052871 + 1.0596035 Benzo[a]pyrene

Summary of Fit

RSquare	0.999438
RSquare Adj	0.999298
Root Mean Square Error	0.063924
Mean of Response	1.183333
Observations (or Sum Wgts)	6

Analysis of Variance

Source	DF	SS	Mean Square	F Ratio
Model	1	29.071988	29.0720	7114.474
Error	4	0.016345	0.0041	Prob > F
C. Total	5	29.088333		<.0001

Parameter Estimates

Term	Estimate	Std Error	t Ratio	Prob>|t|
Intercept	-0.052871	0.029931	-1.77	0.1521
BaP	1.0596035	0.012562	84.35	<.0001

The concentration of each PAH, anthracene, phenanthrene, fluoranthene, pyrene, chrysene, benz[a]anthracene, and benzofluoranthenes in the muscle was calculated for each of the 187 crabs based on the calculated concentration of benzo[a]pyrene estimated using the PBTK model. The concentration of BaP-TEF in the muscle for each crab was then calculated using the method of Nisbet and LaGoy, (1992). Figure 5.38 shows a comparison of the measured and predicted concentrations of BaP-TEF in the muscle tissues of crabs. The mean measured concentration of BaP-TEF was 0.69 ng/g wet weight, while the mean predicted muscle tissue concentration was 0.23 ng/g wet weight. However, a student t test of the means indicated that there was no significant difference between the mean values. A visual inspection of Figure 5.38 shows that the BaP-TEF concentrations were most often under predicted by the PBTK model. The mean difference between measured and predicted values was – 0.46 ng BaP-TEF/g wet weight.

Figure 5.38 Measured and predicted concentrations of BaP-TEF in muscle samples

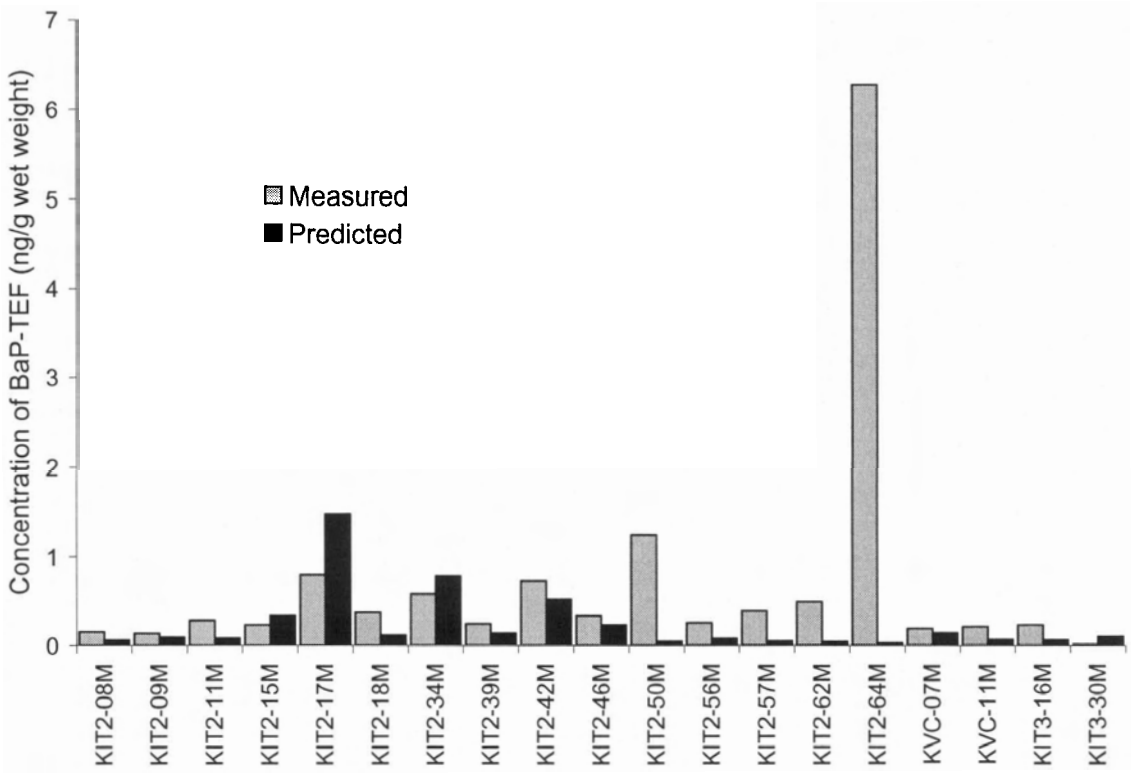

The standard deviation, mean, minimum, and maximum concentration of the PBTK model predicted BaP-TEF are presented in Table 7.1 in Chapter 7.

5.5 Discussion

5.5.1 PBTK Model Parameters

The PBTK model has been adapted for predicting the concentrations of benzo[a]pyrene in seven tissue compartments of the crab following exposure through a single intravascular bolus dose, a single oral bolus dose or waterborne chemical. Parameter values estimated empirically were used without adjustment except the values of several partition coefficients, metabolic constants (V_{max} and K_m) and the blood flow to

the gut (QGT) and carcass (QC). Partition coefficients (R) were found to be the most sensitive model parameters and adjustment of these parameters was necessary to obtain one set of values which could be used to predict the tissue concentration of all three exposure routes. The adjusted partition coefficients did not deviate more than 1.5 times of the mean values determined experimentally and were within one standard deviation of the observed mean determined by the *in vitro* method.

The metabolic constants, V_{max} and K_m, were modified from those determined for pyrene metabolism in the trout. The value of V_{max} for the crab is 50 fold lower than that used for the fish. This is in agreement with the general consensus that aquatic invertebrates have a capacity for PAH metabolism an order of magnitude lower than that of vertebrates such as fish (Dunn and Fee, 1979). Indeed comparisons to other studies in our laboratory showed that the rainbow trout (Kennedy, 1990; Namdari, 1994) and starry flounder (Namdari, 1998) metabolised PAH more rapidly than crabs.

It was found that adjustment of QGT and QC was needed to simulate closely the time course of benzo(a)pyrene in the crab following oral exposure. Table 5.1 – Table 5.5 show the two different sets of values used for model simulation. The first set are used for intravascular and water exposure simulation, while the second set denoted by an asterisk is used for oral exposure predictions. The difference in blood flow between these two sets of data is 5% of QT which represent the volume of blood shunted from the carcass to the gut compartment. This blood flow shunt is related to the physiological changes in the crab following food ingestion. Airriess and McMahon (1992) have shown that haemolymph redistribution is subject to neurohormonal control and may be necessary to supply the increased metabolic requirements of digestion.

5.5.2 Differences between PBTK Model Developed for Fish and Crab

5.5.2.1 Physiological and Biochemical Differences

There are many differences in the physiology and biochemistry between a vertebrate such as the trout, and an invertebrate such as the dungeness crab. These differences were considered in the design of the PBTK model. The trout has a closed circulatory system which is characteristic of all vertebrates, a small blood volume, (4.11 % of body weight) and a cardiac output of approximately 1184 ml kg^{-1} hr^{-1}. In contrast, the dungeness crab has a comparatively much larger blood volume (35.7% BW) and a higher cardiac output, 7638 ml kg^{-1} hr^{-1}. Despite the common perception of an open circulatory system, the crab has a complex, highly efficient, and tightly regulated circulatory system which rivals the closed vertebrate system in terms of tissue perfusion (McMahon and Burnett 1990).

5.5.2.2 Model Conceptualisation

Since the physiology and function of the crab differ significantly to the fish and other vertebrate, they require further explanation. For example, the haemolymph compartment of the crab is analogous to the blood compartment of vertebrates. The hepatopancreas is a digestive and metabolic organ which combines the functions of the small intestine, liver and pancreas of the vertebrates (Gibson, 1979). On the other hand, the urinary bladder or antennal gland of the crab functions very similarly to the kidney of fish.

Due to these fundamental differences in physiology and biochemistry, the PBTK model for the crab was conceptualised differently than the fish model. The model developed for the fish consisted of nine compartments representing major organs such as the liver, kidney, muscle, gill, gut, skin, blood and carcass (Namdari, 1998). In contrast, the PBTK model for the crab was simplified to seven main compartments representing the hepatopancreas, urinary bladder, muscle, gill, gut, haemolymph, and carcass.

Some of the tissues and organs in the PBTK model of the crab were grouped together differently to that of the trout model. For example, the gut compartment of the crab model consists of the oesophagus, cardiac stomach, midgut and hindgut whereas the carcass compartment consists of all other tissues such as the gill, hypodermis, carapace, nervous tissues, heart and gonad.

5.5.2.3 Skin Compartment

The skin compartment for the fish represented a barrier between the external environment and the internal organs. This compartment included a function for uptake of chemical from the water as well as from the blood compartment (Namdari, 1998). The crab however, has a hard chitinous exoskeleton known as the carapace which was assumed to be relatively impervious to chemical uptake, and not a route of chemical excretion. In addition, experiments involving the exposure of crabs to ^{14}C labelled benzo[a]pyrene in the water demonstrated that very little chemical was associated with the carapace as determined by biological oxidation. Finally, the hypodermis, or skin below the surface of the carapace represents a small portion of the total mass of the crab,

0.86% based on dissections of crabs used in laboratory experiments. Therefore, the skin compartment was not included in the crab PBTK model.

5.5.2.4 Muscle Compartment

A membrane-limited muscle compartment was used for the fish model since a flow-limited compartment resulted in the over-prediction of pyrene concentrations in the trout muscle (Law *et al.,* 1991). However, a flow-limited muscle compartment was found to be more appropriate for the crab since the use of a membrane-limited compartment under-predicted benzo[a]pyrene concentrations in the crab muscle The membrane-limited approach was deemed to be appropriate for the trout due to poor vascularisation of white muscle tissue. In contrast to the low blood supply to the fish muscle, crab locomotory muscle seems to be well perfused with a large centrally located artery which supplies haemolymph flow to each appendage (McMahon and Burnett, 1990).

5.5.2.5 Gill Compartment

The PBTK model for the dungeness crab uses a simple first order uptake equation to represent the uptake of benzo[a]pyrene from the water, through the gill and into the haemolymph compartment.

$$dCGL/dt = ((Qt\ (CBV - CGL/RGL) + (Cw(Qw)(A_b)UR))/VGL \quad (5.9)$$

where the first order uptake function is described by:

$$UR = k_b * e^{(-k_b t)} \quad (5.10)$$

This differs from the fish model from which it was adapted (Namdari, 1998). The fish model uses a more complicated flow and diffusion limited equation to describe the flux of chemical across the gills as follows:

$$K_G=(e^{-KD/KB}-e^{-KD/QW})/((e^{-KD/KB}/QW)-(e^{-KD/QW}/KB) \quad (5.11)$$

Where: K_G = chemical uptake
QW = water flow across gills
KB = blood flow
KD = diffusion rate

This model for the exchange of organic chemicals at fish gills is described in detail by Erickson and McKim (1990b). Although this more complicated equation, (5.11), describes the uptake of chemical using physiological parameters in the fish, the simple, first order uptake equation, (5.9) was found to be more effective for predicting uptake of benzo[a]pyrene through the gills from the water for the crab. As Figure 5.23 and Figure 5.30 show, the first order uptake equation was able to adequately simulate the uptake of benzo[a]pyrene from the water, through the gill compartment and into the haemolymph. Equation 5.11, used for the fish model, describes a much more rapid uptake of chemical from the water. Repeated attempts to parameterise the model with this equation were fruitless.

The fish model was calibrated for use with a wide range of polar and non-polar molecules (Erickson, 1990b; Namdari, 1998; Law, 1999). The fish model developed by Namdari, (1998) was calibrated for waterborne exposure to pyrene. While pyrene is a neutral PAH similar to benzo[a]pyrene, the log Kow for pyrene ranges from 4.38 – 5.32 (Mackay, 1991). The log Kow for benzo[a]pyrene is estimated to be an order of magnitude greater. Benzo[a]pyrene log Kow measurements range from 4.05 – 6.57

(Mackay, 1991). As stated by Hayton and Barron, (1990), chemicals with different properties may have different rate limiting barriers that control uptake through the gill. The uptake of more polar compounds like pyrene may be governed more by flow and diffusion limitations and less by a first order process such as passive diffusion. Erickson and McKim (1990a) have found that for high log Kow compounds, the uptake rate is approximately constant and approaches Qw, the rate at which water can transport chemical to and from the gill. Therefore, the simple first order equation may be adequate to describe the uptake of high log Kow compounds such as benzo[a]pyrene. When modelling, it is often the best practice to use the simplest expression that can be used adequately perform simulations. However, it is probable that the uptake equations developed by Erickson and McKim (1990a, 1990b) may be more effective with the crab PBTK model for describing the uptake of less water soluble compounds than benzo[a]pyrene through the gills.

While the uptake equations used to simulate uptake of benzo[a]pyrene into the haemolymph from the gill seemed to work fairly well to simulate concentrations of benzo[a]pyrene in the haemolymph and some other tissues, such as the muscle, bladder, and carcass, the fit was often not as good for the hepatopancreas, gut, gill tissues. This lead to the adjustment of some partition coefficients in an attempt to improve model fit for these compartments. These problems may in fact be due to the equations used to model benzo[a]pyrene uptake and excretion by the gill compartment. In the future, it would be wise to revisit this part of the PBTK model to improve the ability of the model to accurately predict the concentration of benzo[a]pyrene in all tissues following waterborne or oral exposure. It would be best to re-examine the applicability of either the

simple, flow limited gill model developed by Erickson and McKim (1990a) or the more complicated flow and diffusion limited gill model developed by Erickson and McKim (1990b) used by Namdari (1988) and Law (1999) for PBTK modelling in fish.

5.5.3 Adaptability of PBTK Model to Environmental Conditions

The PBTK model for predicting the disposition of benzo[a]pyrene in the dungeness crab was designed to be adaptable to the external environment. Environmental factors such as temperature and salinity are known to cause changes in the physiology of aquatic organisms. Cardiac output, Qt is affected by external ambient temperature as described by Equation 5.3 based on water temperature effects on cardiac output of observed by B. McMahon *et al.*, (1978). Observed effects on the ventilation rate of the gills, Qw, is also controlled by temperature as shown in Equation 5.4 (McMahon *et al.*, 1978).

Salinity has also been shown to affect cardiac output and haemolymph flow patterns (McGaw and McMahon, 1996, 2003). Salinity is an important factor because crabs often venture into estuaries where salinities below 11 ppt are present (Cleaver, 1957; Stevens *et al.*, 1984; Pauley *et al.*, 1986; McGaw and McMahon, 2003). Studies have shown that crabs exposed to reductions in salinity from 100% seawater to 35% seawater (12 ppt) increased heart rates immediately after salinity was reduced (McGaw and McMahon, 2003). Crabs also will burrow into sediments and become quiescent in response to low salinity (McGaw *et al.*, 1999). This behaviour is associated with a drop in cardiac output and haemolymph flow through the gills (McGaw and McMahon, 2003). Because cardiac output and haemolymph flow rates are important physiological factors

for controlling the disposition of chemicals in the PBTK model, the model could be made to be more responsive to external conditions by incorporating equations that vary cardiac output and haemolymph flow patterns based on water salinity. Other external factors such as hypoxia, and dissolved oxygen content in the water have also been shown to affect cardiac output, haemolymph flow, and gill ventilation rates (Airriess and McMahon, 1994; McGaw and McMahon, 2003).

5.5.4 Applications of PBTK Model

The PBTK model is a useful tool to study the toxicokinetics of chemicals in the crab. The model can point to areas that require more study to understand properly, such as uptake and excretion of chemicals by the gill. The model can be used as a framework to study the parameters that are most important for describing the disposition of chemical in the various compartments or tissues.

The model can also be used as a tool to predict the concentration of chemical in one compartment, based on known amounts of chemical in another. For example, the PBTK model for the dungeness crab has been used to predict concentrations of benzo[a]pyrene in the muscle of crabs based on hepatopancreas concentrations. This data was then used to estimate the concentration of BaP-TEF for the stochastic risk assessment (Chapter 7). This is a very useful application of the model for risk assessment purposes to fill data gaps.

5.5.5 Further Studies

Future studies of the PBTK model should be focused on improving the chemical uptake equations for the gill compartment. This would help to resolve any problems in simulating uptake of benzo[a]pyrene from the water, and disposition into the tissue compartments.

An exciting extension of the model would be to incorporate Monté Carlo simulation techniques. The model is currently parameterised using mean values for most input parameters. Many input parameters such as blood flow to various compartments could be described by frequency distributions, rather than by a single mean value. In this way, the model could incorporate more variability in the measurement of input parameters, and this variability and the effect on model output could be studied further. For example, there is frequency distribution data available describing the heart rate and flow rates of haemolymph through the arteries of the dungeness crab (McGaw *et al.*, 1994). Most of the haemolymph flow rates are described as lognormal distributions, while heart rate appears to be normally distributed crab (McGaw *et al.*, 1994). It would be very interesting to incorporate these frequency distributions into the parameters describing haemolymph flow to the various compartments. This would allow for a better estimation of the flow parameters, and would make the PBTK model more powerful in predicting the disposition of benzo[a]pyrene in the crab.

Another extension of the of the PBTK model for the dungeness crab would be to calibrate the model for predicting the disposition of other PAH on the EPA priority list of 16 PAH. This could be done by adjusting important parameters such as partition

coefficients for the different PAH. Table 5.9 shows that there is a stronger relationship between the concentrations of some PAH in the muscle tissue compared with benzo[a]pyrene than others. Generally, there was a strong linear relationship between the concentrations of larger molecular weight PAH such as chrysene, benzanthracene, fluoranthene and benzofluoranthenes and the concentration of benzo[a]pyrene. The model might only require some small adjustments in partition coefficients to simulate the disposition of these compounds in the crab. Other lower molecular weight PAH such as anthracene, phenanthrene and pyrene did not fit a linear relationship with benzo[a]pyrene concentrations as well. A greater adjustment in partition coefficients and perhaps metabolic parameters might be necessary to predict the disposition of these PAH with the PBTK model. However, this illustrates the power and flexibility of the PBTK model in that it could be used with minor adjustments to predict the disposition of other PAH in the crab.

Finally, this PBTK model which describes the internal toxicokinetics of benzo[a]pyrene could be linked to the food web model of Harris and Gobas, (Harris, 1999) as an extension of their model for predicting concentrations of benzo[a]pyrene and other PAH in the tissues of crabs. Currently, the model employs a non-equilibrium steady-state model developed by Morrison et al. (1996), and parameterised by Harris (1999) to calculate steady-state biota sediment accumulation factors (BSAF) in adult crabs. This comparatively simplified approach has been found to work reasonably well to predict the tissue concentration of non-metabolisable environmental contaminants such as dioxins, however, it lacks the ability to deal with metabolisable compounds such as PAH. Therefore, this type of model usually over predicts the BSAF of PAH such as

benzo[a]pyrene in the tissues of crabs (Harris 1999). The PBTK model therefore, can be used to enhance the power of the food web model to more accurately predict BSAF values for crabs.

5.6 Conclusion

A PBTK model has been adapted to describe the disposition of benzo[a]pyrene in the tissues of the dungeness crab. This represents the first time that a PBTK model has been applied to describe toxicokinetics in crabs. The model has been calibrated and validated with empirical data to predict concentrations of benzo[a]pyrene in seven tissue compartments following intravascular injection, oral dose, and water-borne exposure.

CHAPTER 6
DETERMINISTIC ESTIMATION OF HUMAN HEALTH RISK DUE TO CONSUMPTION OF PAH-CONTAMINATED DUNGENESS CRABS CAUGHT IN KITIMAT ARM, B.C

6.1 Introduction:

An aluminium smelter has emitted polycyclic aromatic hydrocarbons (PAH) into the receiving waters since 1954. The determination of PAH levels in the sediments and biota of Kitimat Arm has been the subject of previous studies (Cretney *et al.,* 1983; EVS, 1995 1998; Paine *et al.*, 1996; Simpson, 1996; Simpson, 1997). In general, these studies have demonstrated elevated levels of PAH in the sediments. However, inconsistent results have been reported on the extent of PAH contamination in the biota.

Significant levels of high molecular weight PAH were determined in the tissues of dungeness crabs collected at sites close to the aluminium smelter as described in Chapter 2 (Eickhoff, 1999; Eickhoff, 2000, Eickhoff 2003a). Moreover, PAH concentrations in the crab tissues were found to decrease significantly with increasing distance from the alleged source of pollution. HPAH such as benzo[a]pyrene and benz[a]anthracene are of particular concern because of their carcinogenic potentials. Therefore, these results suggest that Kitimat Arm has been contaminated by PAH and that ingestion of crabs may be a significant pathway of human exposure to these carcinogens.

The dungeness crab *(Cancer magister)* is a significant food source and recreational fishery for the local residents. Concerns of health safety due to consumption of crabs and shellfish exposed to dioxins and furans have led to closure of commercial fishing activity in 1989 (DFO, 1989). Health and Welfare Canada also has established a consumption advisory for the hepatopancreas of crabs at 30 g/week for the aboriginal and recreational harvesters. Although the consumption advisory for the hepatopancreas of crabs was lifted in 1996, the area is still closed to the commercial fishing of crabs (DFO, 1996).

The objective of this study was to determine if PAH contaminated crabs are a significant health risk to local consumers of crabs. For this purpose, a deterministic human health risk assessment (HHRA) was conducted. The risk assessment was based on the concentrations of PAH determined in the crabs, and information from a dietary survey conducted by the Kitamaat Village Council of the Haisla Nation who live in Kitamaat Village on the east shore of Kitimat Arm (Figure 1.2).

6.2 Risk Assessment

6.2.1 Hazard Identification and Dose-response Assessment

The hazard identification and dose-response assessment paradigm promulgated by the U.S. Environmental Protection Agency (USEPA, 1989) and the Ontario Ministry of Environment (OME, 1997) were used for the risk assessment. PAH such as BaP and BA are classified as B2 or probable human carcinogens (USEPA-IRIS, 1998). The toxic endpoints are the probability of developing stomach cancer (USEPA, year) or stomach

and lung cancer (OME, 1997) in humans due to consumption of the PAH-contaminated crabs. The mechanism of cancer development is assumed to be a non-threshold process.

6.2.2 Exposure Assessment

6.2.2.1 Field Data Collection and Analysis

PAH concentrations in crab tissues were taken from the field study on dungeness crabs (Chapter 2). Concentrations below the estimated sample specific detection limit (EDL) were represented as ½ of the EDL according to the U.S. EPA Risk Assessment Guidance Manual (US EPA, 1991). The arithmetic mean values and standard deviation for concentrations of PAH determined in the crabs used in the risk assessment are presented in Table 6.1.

Table 6.1 Mean concentrations of PAH in crab tissues (ng/g wet weight).

Tissue	Hepatopancreas				Muscle	
Site	Hospital Beach	Kitamaat Village	Wathlsto Creek	Kildala Arm	Hospital Beach	Kitamaat Village
Analyte	Mean ± SD	Mean ± SD	Mean ± SD	Mean ± SD	Mean ± SD	Mean ± SD
PHN	12.9 ± 32.4	2.5 ± 3.4	0.28 ± 0.63	1.3 ± 0.6	2.9 ± 3.6	1.2 ± 0.25
ANT	3.5 ± 6.2	2.7 ± 6.3	0.19 ± 0.17	0.11 ± 0.28	0.57 ± 0.74	0.22 ± 0.30
FLR	11.9 ± 53.8	0.94 ± 0.84	0.40 ± 0.23	0.35 ± 0.31	1.3 ± 2.7	0.28 ± 0.13
PYR	5.7 ± 26.4	0.73 ± 0.49	0.50 ± 0.28	0.47 ± 0.26	0.97 ± 1.5	0.30 ± 0.13
BA	2.3 ± 7.2	0.20 ± 0.41	0.14 ± 0.09	0.16 ± 0.14	0.28 ± 0.58	0.11 ± 0.07
CRY	7.9 ± 41.8	0.73 ± 0.83	0.37 ± 0.18	0.36 ± 0.21	0.95 ± 2.2	0.22 ± 0.12
BF	1.8 ± 1.9	0.48 ± 0.14	0.34 ± 0.16	0.40 ± 0.16	1.4 ± 2.6	0.01
BaP	0.81 ± 1.3	0.23 ± 0.14	0.14 ± 0.13	0.18 ± 0.47	0.74 ± 1.4	0.14 ± 0.09

6.2.2.2 PAH Toxic Equivalents

Benzo[a]pyrene toxic equivalents (BaP-TEQ) were calculated from the PAH concentrations in crab tissues according to the methods recommended by the EPA (1989) and OME (1997). The IPM TEQ calculation is based on the assumption that the risk from individual PAH in a mixture are additive. By comparison, the OME WMM approach is based on the assumption that the potency of a PAH mixture is proportional to the BaP content. These TEQ approaches are summarised as follows:

(a) The BaP-TEF of Nisbet and LaGoy (1992) were used to calculate the TEQ for the U.S. EPA model.

(b) The OME IPM model uses a formula to determine BaP-TEF, based on relative potency of each individual PAH to benzo[a]pyrene (OME, 1997).

(c) The OME WMM model includes a statistical comparison of the concentrations of carcinogenic PAH relative to benzo[a]pyrene with a Mixture of Standard Composition, (MSC) (OME, 1997).

Toxic equivalents were calculated for hepatopancreas, muscle, and hepatopancreas and muscle tissues combined as in a typical meal of crab. The amount of hepatopancreas for a typical crab was estimated at 13% of the edible portion while the muscle constituted the remaining 87%. This estimate was based upon dissections of crabs to determine the proportion of each tissue to the total mass. The hepatopancreas constitutes 3.46% of total body weight, while the muscle makes up 23.2% (Chapter 6). It

was assumed that the hepatopancreas and muscle tissues together represented the total edible mass of the dungeness crab.

6.2.2.3 Calculation of Lifetime Average Daily Dose

Lifetime average daily dose (LADD) values were calculated for the following consumption scenarios: hepatopancreas alone (worst case), muscle alone (best case), and a combination of muscle and hepatopancreas (most likely). It should be noted that while many North Americans do not consume the hepatopancreas of crabs, it is a delicacy for the aboriginal and Asian consumers. We assume that aboriginal consumers eat all edible portions of the crab in a typical meal based on personal conversations with members of the Haisla Nation of Kitamaat Village.

LADD values based on the consumption of PAH-contaminated crab tissues over a period of 75 years were calculated for the EPA and OME exposure assessment models using the following equations:

EPA model: $LADD = Cc/Cv \times IR \times EF \times ED / BW \times AT$ (6.1)

OME model: $LADD = Cc/Cv \times IR \times EF \times ED / AT$ (6.2)

where:

LADD = lifetime average daily dose (ng/kg-day)

Cc = concentration of BaP-TEF in edible portion of crab (ng/g wet weight)

IR = crab intake rate (g/meal)

EF = exposure frequency (meals/year)

ED = exposure duration; 75 years

Cv = volume reduction of crab meat due to cooking; 0.57

BW = body weight

AT = averaging time or lifetime in days; 27375 days

The concentration of PAH-TEF in the edible portion of the crab, Cc can be further characterised as follows:

$$Cc = Ch * Hp + Cm * Mp \quad (6.3)$$

Where:

Ch = concentration of BaP-TEF in the hepatopancreas (ng/g wet weight)

Cm = concentration of BaP-TEF in the muscle (ng/g wet weight)

Hp = proportion of hepatopancreas to total crab mass; 3.46%

Hm = proportion of muscle to total crab mass; 23.2%

The major difference between the EPA and OME LADD calculations is the absence of body weight in the OME exposure model. Mean exposure estimates for intake rate (IR) and exposure frequency (EF) were obtained from the Haisla Diet Survey (1994); and are summarised in Table 6.2. The number of respondents who participated in the survey upon which the mean IR and EF estimates are based upon is also reported. The IR varied significantly with the season, gender and age of respondents. Crab consumption is generally the highest in adult males during the summer months (Table 6.2).

Table 6.2 Mean intake rate of crab of aboriginal population by gender, age group, and season*

Age	1-11				12-17				18-49				50+			
Season	winter		summer		winter		summer		winter		summer		winter		summer	
Gender	F	M	F	M	F	M	F	M	F	M	F	M	F	M	F	M
# Resp.	9	7	7	6	4	5	5	5	24	34	16	29	13	12	11	9
IR, (g/meal)	118	237	118	237	118	237	118	237	327	473	237	473	237	473	327	710
EF (meals/yr)	6	12	12	12	6	6	12	9	12	12	18	12	6	6	12	18

*Data from Haisla Diet Survey, Kitimat Village Council 1994.

The exposure frequency, or the number of meals per year also varied with the gender, age and season. For the risk assessment, each year was equally divided into two six month seasons, winter and summer based on the northern location of Kitimat Arm and the available consumption behaviour data for the population. The calculated exposures were summed for both seasons over each year as follows:

$$\text{Yearly Exposure} = IR_{s,a,g} \times EF_{s,a,g} + IR_{w,a,g} \times EF_{w,a,g} \quad (6.4)$$

Where, s = summer, w = winter, a = age, g = gender.

PAH concentration as TEQ in the crab tissues (Cc) was divided by Cv to correct for the reduction in tissue volume due to cooking (Winquist, 1998). The net effect is an increase in TEQ concentrations in the cooked meat of crabs.

Mean body weights (BW) of the Haisla were used to estimate the LADD in the EPA model; they were obtained from the same dietary survey (Table 6.3). Mean weights of typical North American populations were included for comparison. It is believed that

aboriginal populations generally have a greater average weight than that of North American communities (Winquist, 1998).

Table 6.3 Body weight data used for risk assessment

Age Group	North American body weight† (kg)	Aboriginal body weight* (kg)
1-11	18	30
12-17	49	56
18-49	70	84
50+	70	87

†Law and Gudaitis (1994); *Kitamaat Village Council (1994)

6.2.3 Risk Characterisation

Human health risks associated with the exposure to PAH through the consumption of contaminated crabs were estimated by 3 different approaches: the standard EPA approach and the approaches using the Whole Mixture Model (WMM) and Individual PAH Model (IPM) of the OME. The risks are estimated using the following equations:

EPA model: $$\text{Risk} = \text{LADD} \times \text{CPF} \times \text{CF} \quad (6.5)$$

where:

LADD = Lifetime average daily dose (ng/kg-day)

CPF* = Cancer potency factor for stomach cancer (risk mg^{-1} kg^{-1} day^{-1})

CF = Conversion factor (10^{-6} mg/ng)

OME model: $$\text{Risk} = \text{LADD} \times (\text{CPF}_{stm} + \text{CPF}_{lng}) \quad (6.6)$$

where:

LADD = Lifetime average daily dose (ng/day)

$CPF_{stm}^{\dagger}$ = Cancer potency factor for stomach cancer (risk ng^{-1} day^{-1})

$CPF_{lng}^{\dagger}$ = Cancer potency factor for lung cancer (risk ng^{-1} day^{-1})

*EPA CPF 7.3 (risk mg^{-1} kg^{-1} day^{-1}) (Oral in diet) (IRIS, 1998)

†OME IPM CPF_{stm} 2.6 E-9 (risk ng^{-1} day^{-1}) (Oral in diet) (OME, 1997)

†OME IPM CPF_{lng} 2.1 E-10 (risk ng^{-1} day^{-1}) (Oral in diet) (OME, 1997)

†OME WMM CPF_{stm} 4.2 E-8 (risk ng^{-1} day^{-1}) (Oral in diet) (OME, 1997)

†OME WMM CPF_{lng} 3.4 E-9 (risk ng^{-1} day^{-1}) (Oral in diet) (OME, 1997)

The cancer slope factors (risk per ng/kg d^{-1}, EPA; risk per ng/d, OME) are derived from a low-dose extrapolation model. The conversion factor, CF is used in the EPA model to convert units from ng to mg.

6.3 Results

The arithmetic mean of tissue PAH concentration in crabs as BaP TEQ used for the US EPA risk assessment model are presented in Table 6.4. Unless specifically noted, the concentration refers to that determined in the hepatopancreas of crabs.

Table 6.4 Summary Statistics for BaP-TEQs used for EPA Model.

Statistic	Hospital Beach	Kitamaat Village	Wathlsto Creek	Kildala Arm	HB Muscle	Village-Muscle
Mean	1.36	0.34	0.20	0.24	0.83	0.16
Minimum	0.08	0.07	0.06	0.05	0.13	0.01
Maximum	9.91	0.78	0.48	2.78	6.28	0.23
SD	1.79	0.16	0.13	0.51	1.53	0.10

The mean concentrations of BaP-TEQ calculated as a measure of relative potency for the OME IPM model are presented in Table 6.5.

Table 6.5 Summary Statistics for BaP Relative Potency used for IPM.

Statistic	Hospital Beach	Kitamaat Village	Wathlsto Creek	Kildala Arm	HB Muscle	Village Muscle
Mean	1.18	0.29	0.18	0.22	0.84	0.13
Minimum	0.05	0.05	0.03	0.03	0.12	0.00
Maximum	9.73	0.55	0.46	2.69	6.55	0.21
SD	1.74	0.14	0.13	0.48	1.61	0.11

The mean concentrations of BaP surrogates (BaPS) calculated using the OME WMM approach are presented in Table 6.6.

Table 6.6 Summary Statistics for Concentration of BaP in Crab Tissues used for WMM.

Statistic	Hospital Beach	Kitamaat Village	Wathlsto Creek	Kildala Arm	HB Muscle	Village Muscle
Mean	0.81	0.23	0.14	0.18	0.78	0.19
Minimum	0.00	0.00	0.00	0.00	0.11	0.02
Maximum	6.30	0.47	0.41	2.58	5.83	0.16
SD	1.31	0.14	0.13	0.47	1.43	0.21

The WMM expresses PAH mixtures that are statistically similar to the MSC as benzo[a]pyrene surrogates, BaPS. Of the two OME methods, IPM and WMM, the WMM method was found to be most applicable to the data set because the total risk estimated for the crab tissue PAH concentrations (CC) was similar to that of the MSC. The criteria of applying the OME WMM for a given PAH mixture is that the ratio of "total risks" of the two PAH mixtures CC and MSC must be between 0.1 and 10 (OME, 1997). A summary of the values calculated to determine the application of the OME IPM or WMM method is displayed in Table 6.7.

Table 6.7 Stomach tumour risk attributable to PAH mixtures due to oral exposure for comparison of MSC and Kitimat PAH crab hepatopancreas concentrations, (HC) relative to benzo[a]pyrene.

Mixture	PHEN $Risk_{PAH}$ (/ng BaP/m^3)	BA $Risk_{PAH}$ (/ng BaP/m^3)	CRY $Risk_{PAH}$ (/ng BaP/m^3)	BF $Risk_{PAH}$ (/ng BaP/m^3)	TOTAL $Risk_{PAH}$ (/ng BaP/m^3)	MSC/HC Ratio	Use IPM or WMM
Hospital Beach	9.4 E-12	5.8 E-11	4.4 E-10	9.3 E-10	1.4 E-09	0.47	WMM
Kitamaat Village	8.3 E-12	4.3 E-11	2.7 E-10	6.0 E-10	9.2 E-10	0.73	WMM
Wathlsto Creek	6.2 E-13	1.3 E-10	6.7 E-10	1.8 E-09	2.6 E-09	0.26	WMM
Kildala Arm	7.8 E-11	1.9 E-10	9.1 E-10	3.6 E-09	4.7 E-09	0.14	WMM
Kitimat Arm Ave.	1.1 E-11	6.9 E-11	3.7 E-10	9.4 E-10	1.4 E-09	0.48	WMM
MSC	7.3 E-12	4.4 E-11	1.4 E-10	4.9 E-10	6.8 E-10	1.00	WMM

Figure 6.1 shows the mean concentrations of PAH in crab tissues collected from the four sites expressed as benzo[a]pyrene toxic equivalents, BaP-TEQ (EPA, year; OME IPM, year) or benzo[a]pyrene surrogates (BaPS), (OME WMM, year). The data are

grouped under the following consumption scenarios: hepatopancreas alone, muscle alone and a combination of hepatopancreas and muscle (H&M). The hepatopancreas and muscle tissues together are assumed to represent the total edible mass of the dungeness crabs. Also, the hepatopancreas and muscle represent about 13% and 87%, respectively of the edible tissue in crabs (unpublished observations). Therefore, the H&M concentrations were calculated as a ratio of the concentrations determined in the hepatopancreas and muscle tissues.

Figure 6.1 Calculated PAH toxic equivalent or surrogate concentrations in crab tissues from different sites in Kitimat Arm.

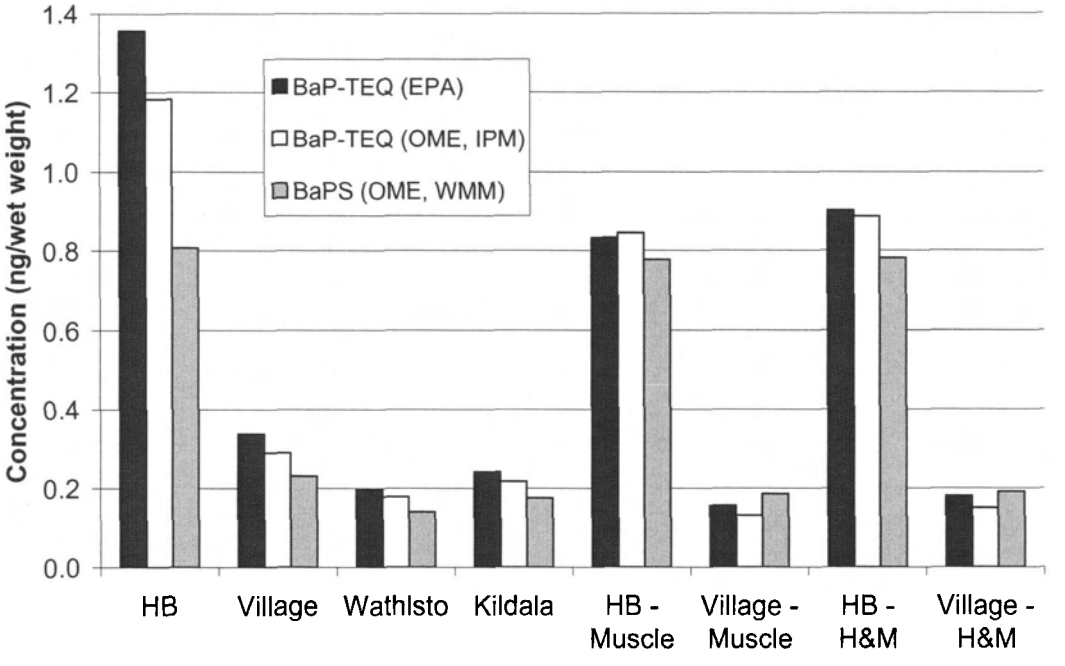

TEQ levels were the highest in crabs collected in at Hospital Beach close to the aluminium smelter and decreased with distance from the smelter. Moreover, TEQ concentrations in crabs were slightly higher in Kitamaat Village than those collected

downstream at Wathlsto Creek and Kildala Arm. In general, TEQ and BaPS levels were higher in the hepatopancreas than the muscle. The TEQ and BaPS of combined H&M are only slightly higher than the muscle, due to the fact that a large proportion of the edible tissue is comprised of the muscle tissue and that muscle/hepatopancreas weight ratio is approximately 6.7 in crabs.

Figure 6.2 shows the LADD in the different age groups of both genders due to consumption of the hepatopancreas only as the entire amount of crab tissues consumed.

Figure 6.2 Chronic daily intake (LADD) of BaP-TEQs based on consumption of PAH contaminated crab hepatopancreas estimated by following models; a) EPA, b) OME-IPM, c) OME-WMM.

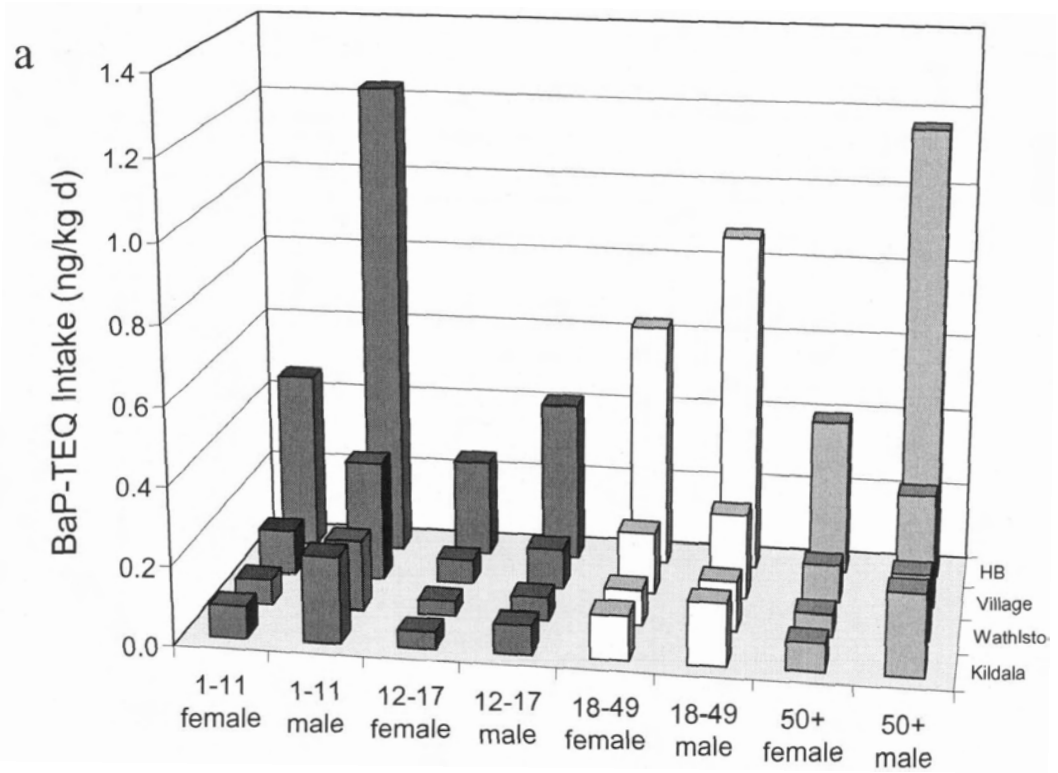

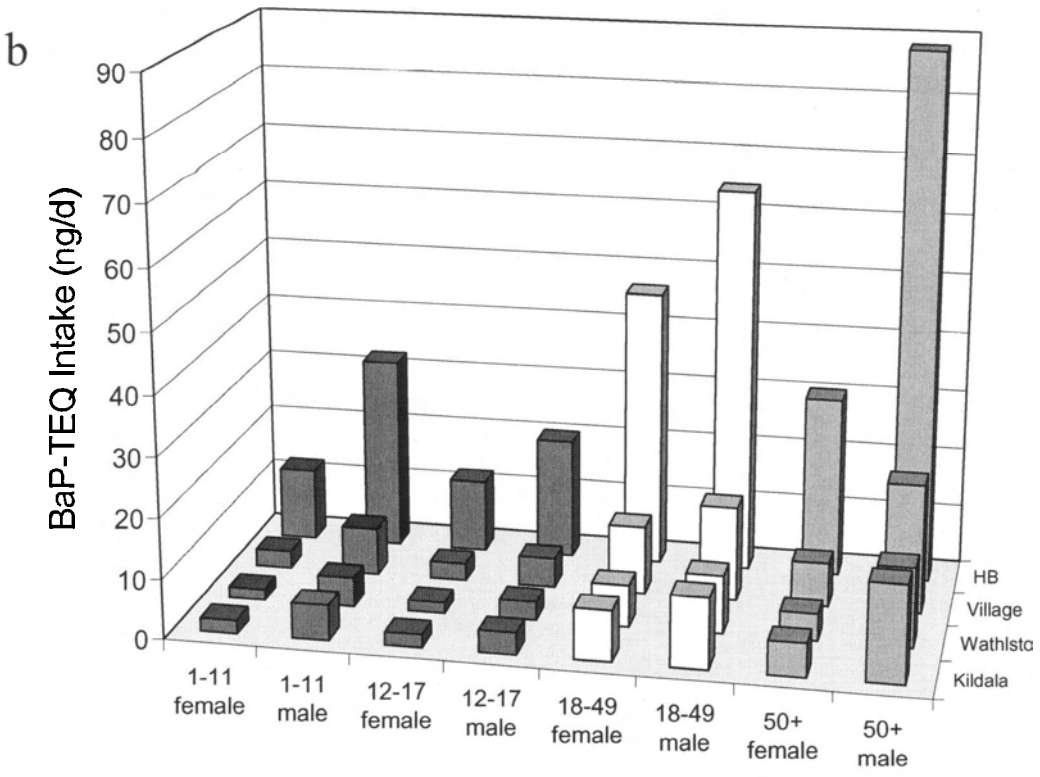
b
BaP-TEQ Intake (ng/d)
90
80
70
60
50
40
30
20
10
0
1-11 female
1-11 male
12-17 female
12-17 male
18-49 female
18-49 male
50+ female
50+ male
HB
Village
Wathlsto
Kildala

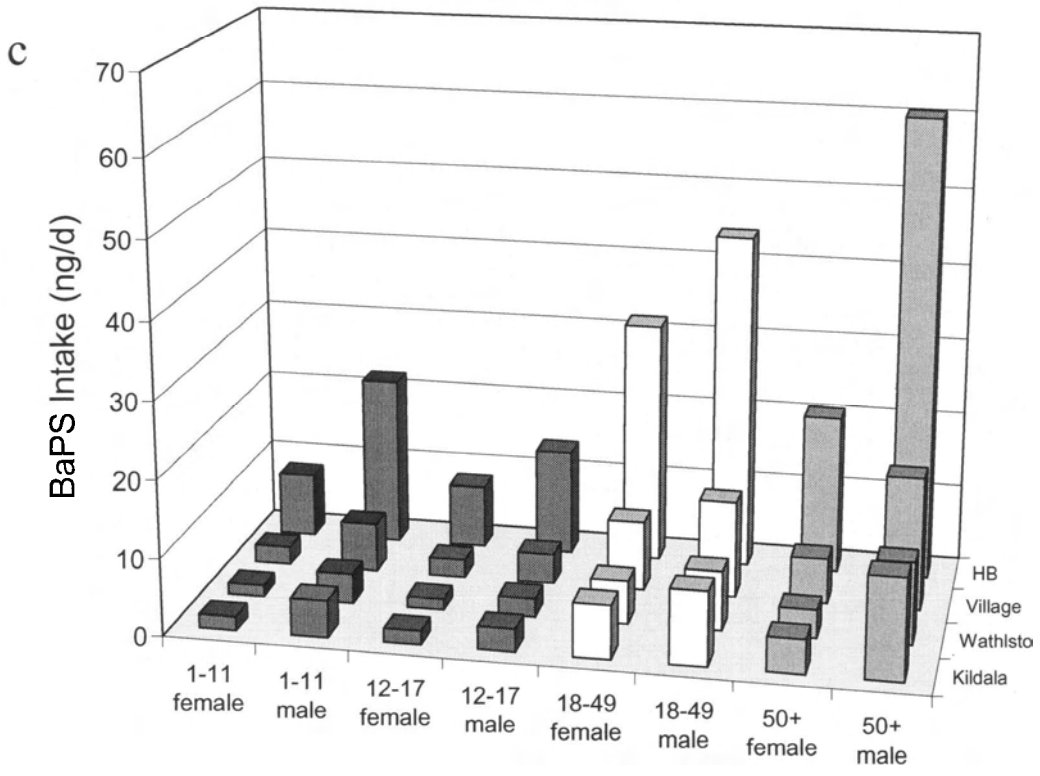
c
BaPS Intake (ng/d)
70
60
50
40
30
20
10
0
1-11 female
1-11 male
12-17 female
12-17 male
18-49 female
18-49 male
50+ female
50+ male
HB
Village
Wathlsto
Kildala

The LADD predicted by the EPA model range from 0.03 – 1.23 ng BP equivalents/kg-d (Figure 6.2a). Male children (1-11) and senior males (50+) are exposed to more PAH than the other age groups. Females are exposed to lower TEQ than males in all age groups due to smaller meal sizes and less frequency of crab consumption (Table 6.3). By comparison, both OME models predict a very different age-related exposure scenario; both adult groups are exposed to greater LADD than children or youth (Figure 6.2 b and c).

The OME models predict that children and youth are exposed to roughly half of the LADD in the adult groups, and senior adults are exposed to even higher levels than adults (18-49). The LADD calculated using the IPM BaP-TEF range from 1.33 – 88.6 ng BP equivalents /d (Figure 6.2b) while the WMM BaPS range is slightly lower at 1.44 – 60.52 ng BP /d (Figure 6.2c). The LADD calculated by the OME methods are much higher than those obtained from the EPA approach due to absence of body weight in the OME exposure assessment equation.

Figure 6.3 shows the LADD in the different age groups of both genders due to consumption of muscle only or a combination of muscle and hepatopancreas. PAH exposure is much greater after consuming muscle or whole crab (combined H&M) caught at Hospital Beach. PAH exposure due to the consumption of muscle or combined H&M is lower than the worst case scenario of eating hepatopancreas alone. The LADD due to consumption of muscle alone is only slightly lower than that of H&M because the muscle makes up 87% of the edible crab tissue. The PAH exposure patterns in different age and gender groups due to consumption of crabs caught near Kitamaat Village are not found to be very different to one another.

Figure 6.3 Life-time average daily dose due to consumption of the muscle tissue or hepatopancreas and muscle (H&M) calculated by; a) EPA, b) IPM, c) WMM, model.

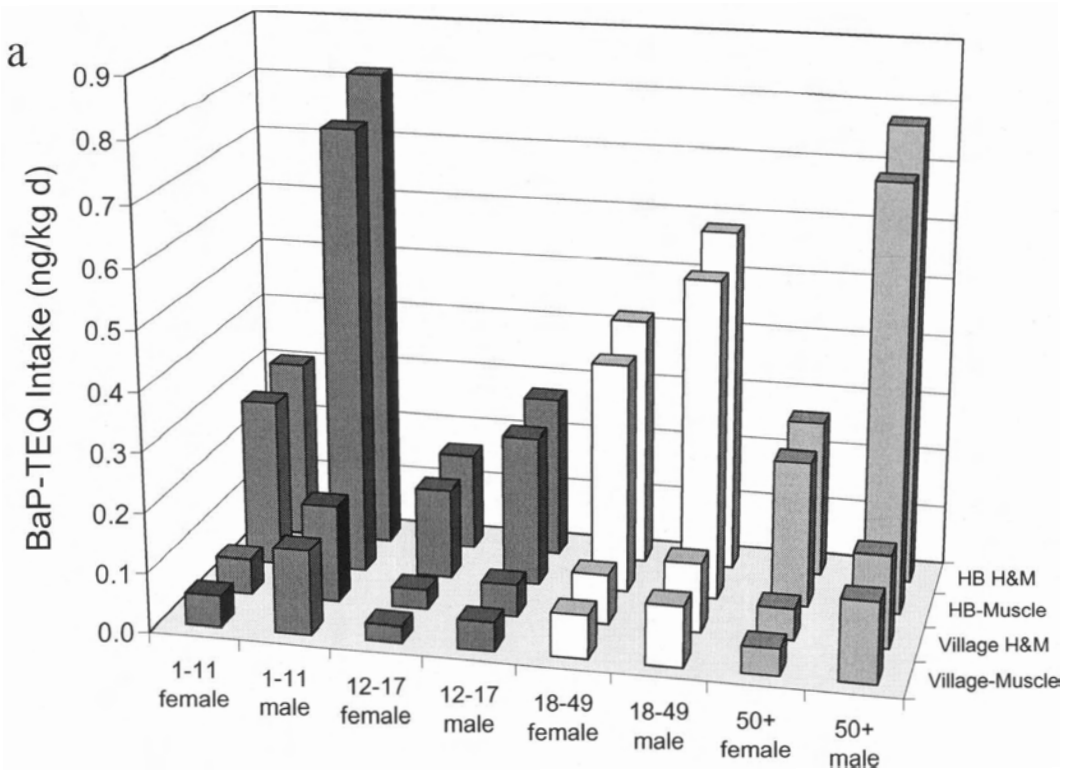

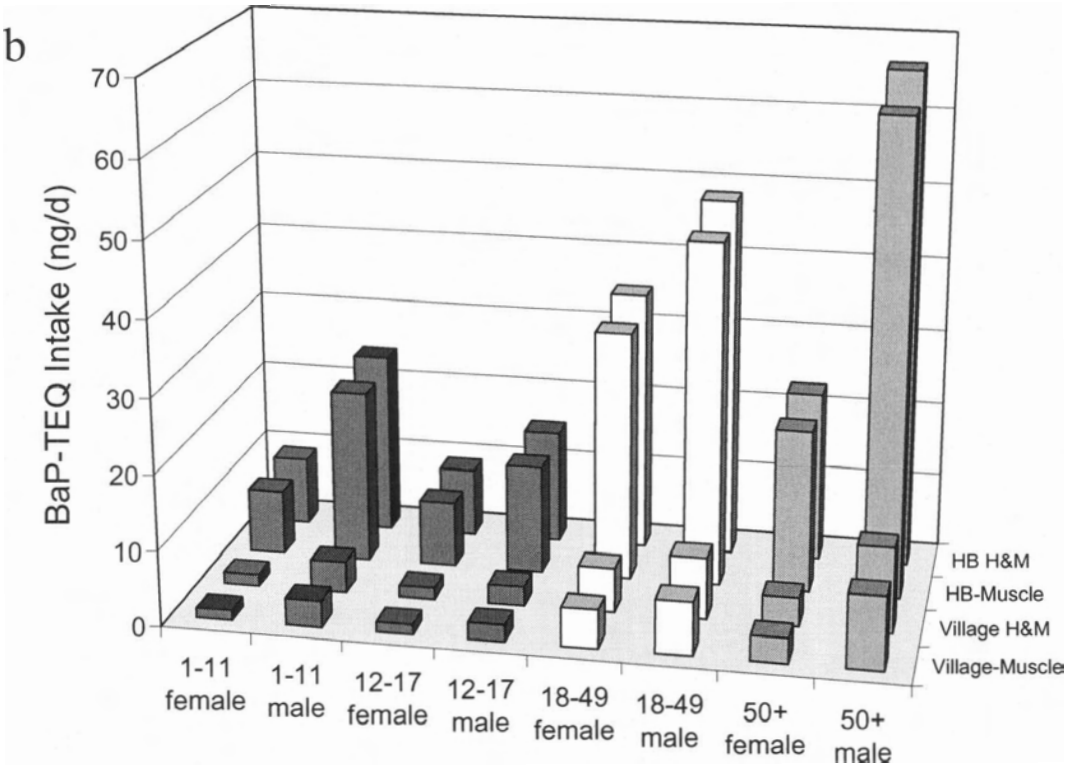

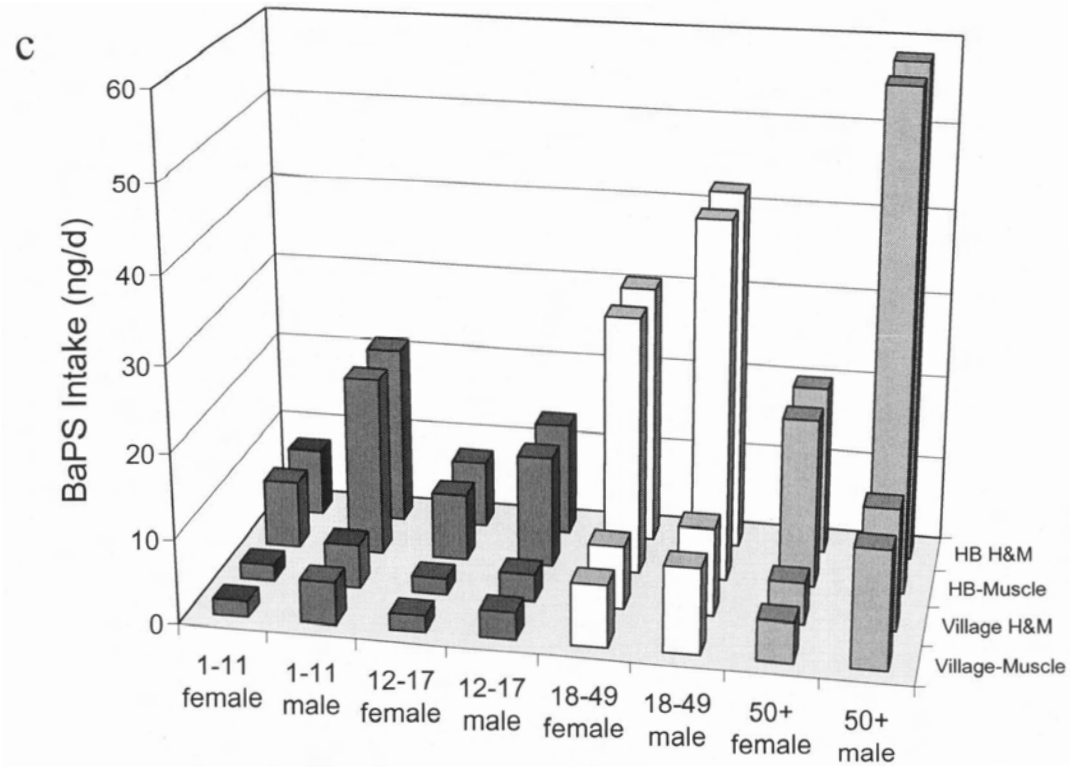

Figure 6.4 shows the number of excess cancer incidences predicted from eating only the hepatopancreas of crabs as the entire meal using the EPA and OME approaches. The risk estimates generally reflect the corresponding LADD values in Figure 6.2. The EPA model predicts the greatest risk of cancer in the 1-11 age group whereas the OME models predict the greatest risk to adults and mature adults. Consumption of the hepatopancreas from crabs caught at Hospital Beach near the source of PAH contamination poses the greatest cancer risk, which exceeds the virtual safe risk level (1 E-6) in all age groups. The maximum risk for male children is 9.0 E-6 and the risk to senior adult males is 8.5 E-6 (Figure 6.4a).

Figure 6.4 Probability of developing stomach cancer (EPA) or stomach and lung cancer (OME) due to the consumption of the hepatopancreas of crabs; a) EPA, b) IPM, c) WMM.

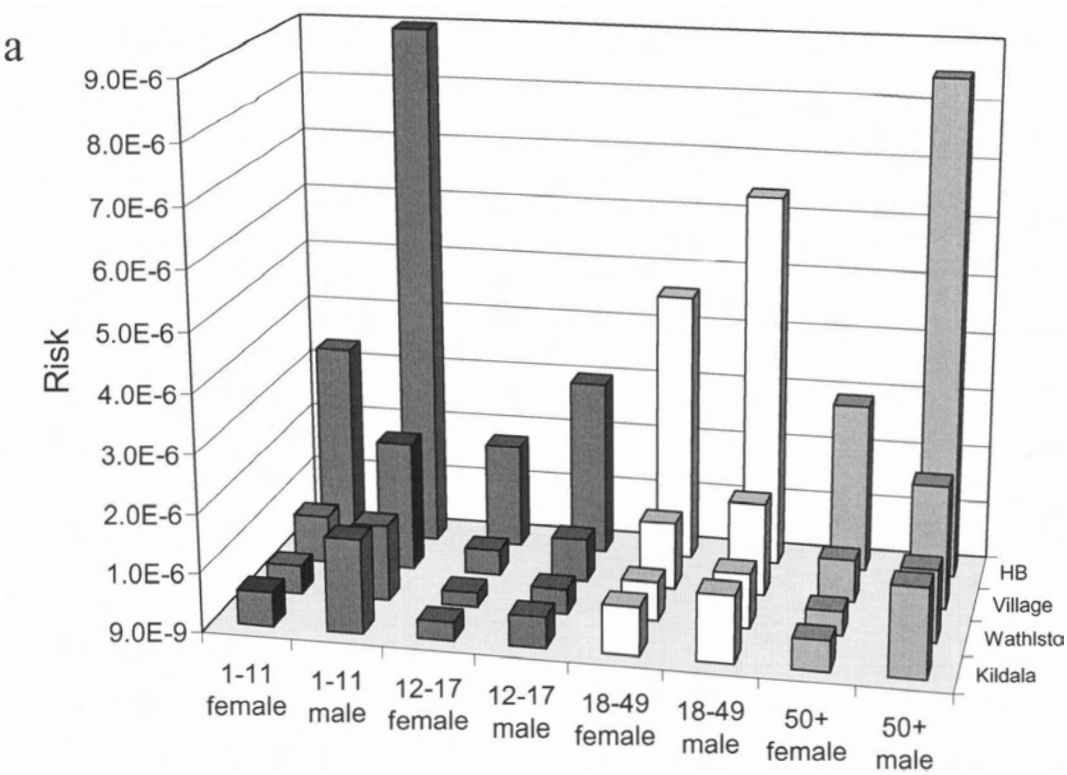

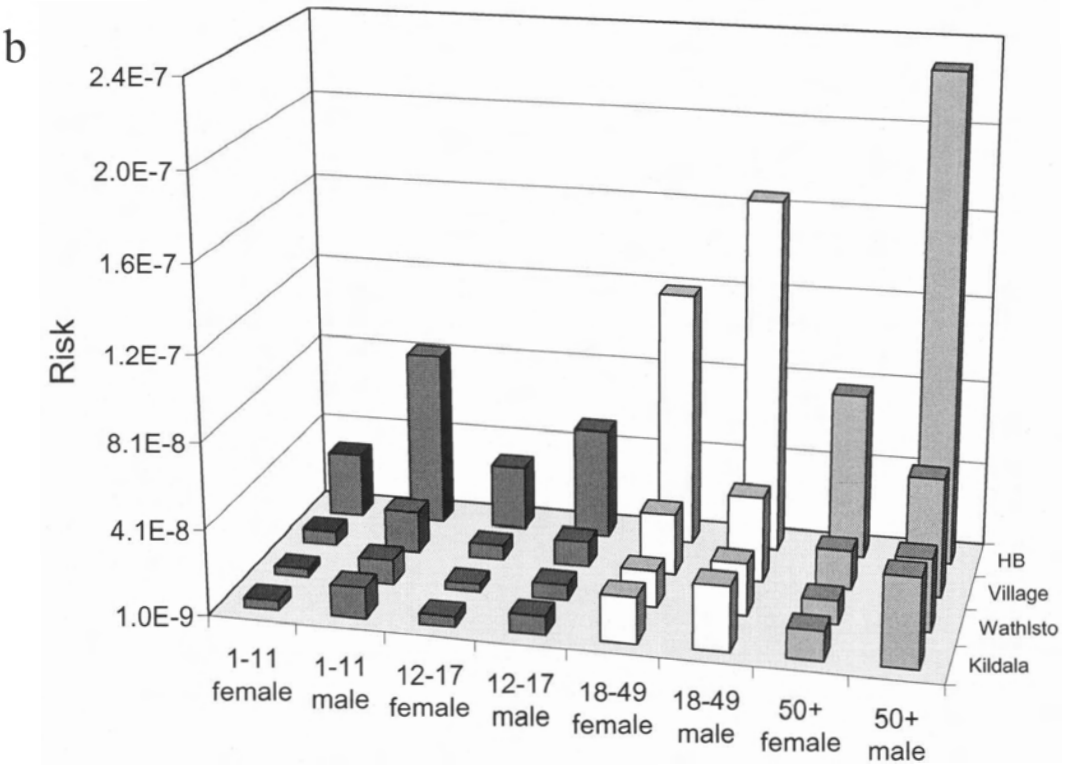

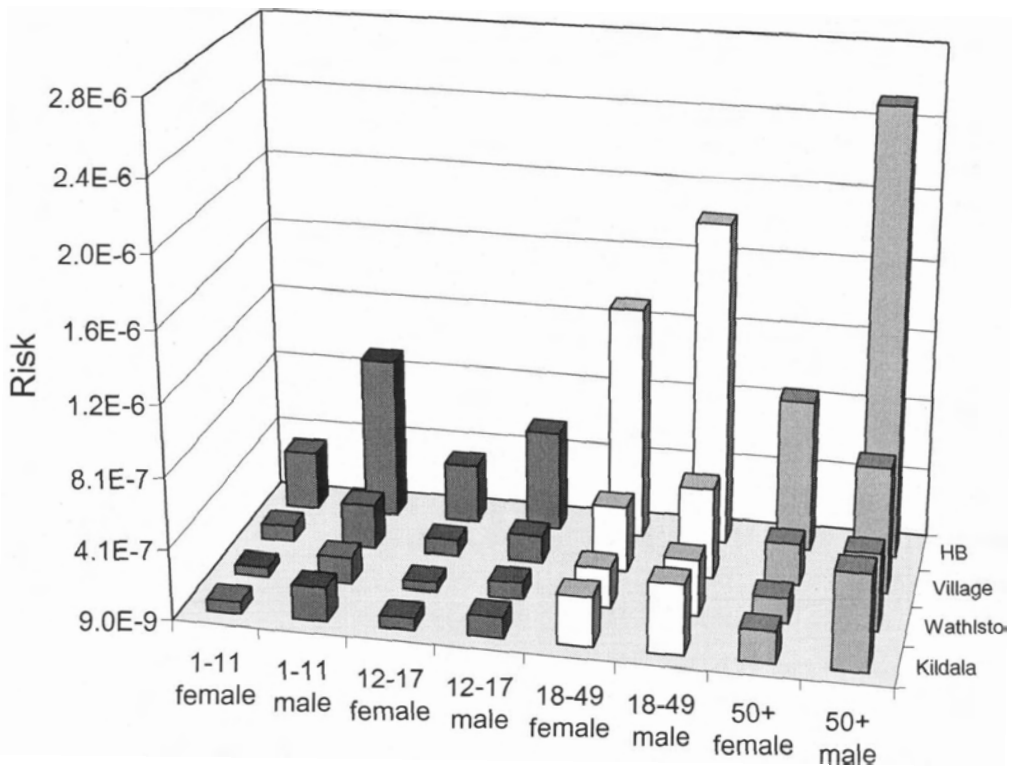

The risk estimates determined according to the OME-IPM model are an order of magnitude lower than the EPA estimates; the maximum risk for senior males is 2.3 E-7 (Figure 6.4b). The WMM model predicts a risk estimate, which is closer to, but lower than the EPA estimate; the maximum risk of stomach tumours for senior males consuming crabs from Hospital Beach is 2.5 E-6 (Figure 6.4c), while the risk for stomach and lung tumours is 2.7 E-6. As expected from the LADD values (Figure 6.2), the risk to females of all age groups is much lower than that for males. However, the risk estimates of the EPA and WMM models also exceed 10^{-6} for adult females (ages 18-49) eating crab caught near the smelter. The risk of consuming crabs from the other sites in Kitimat Arm is below the risk criterion of 1 E-6.

Figure 6.5 shows the probability of developing cancer from eating muscle alone or the whole crab (H&M) collected from the Hospital Beach and the village sites.

Figure 6.5 Probability of developing stomach cancer (EPA) or stomach and lung cancer incidence (OME) due to the consumption of muscle or hepatopancreas and muscle; a) EPA, b) IPM, c) WMM.

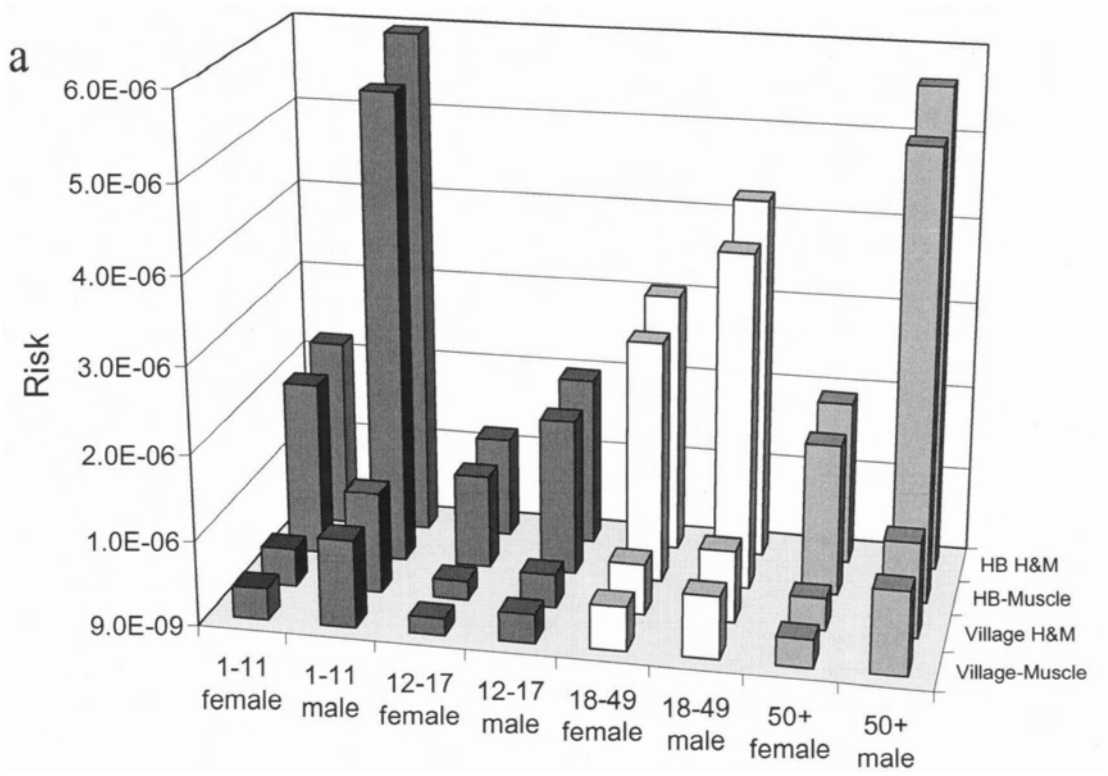

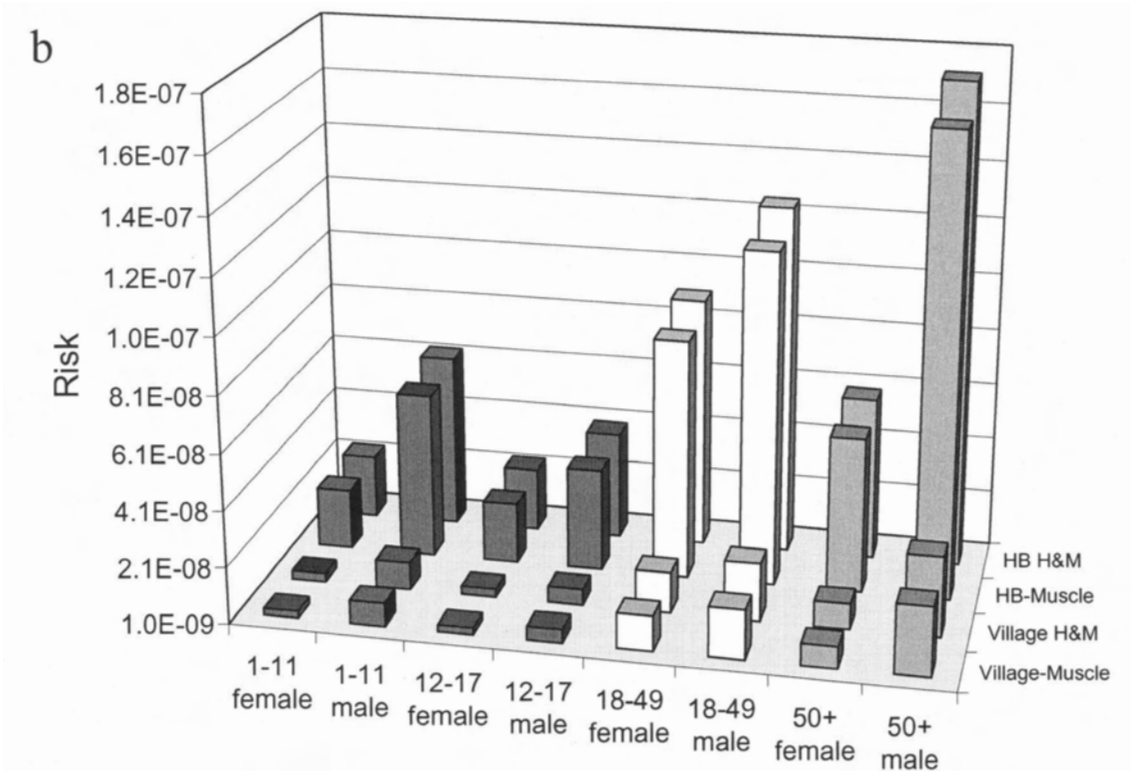

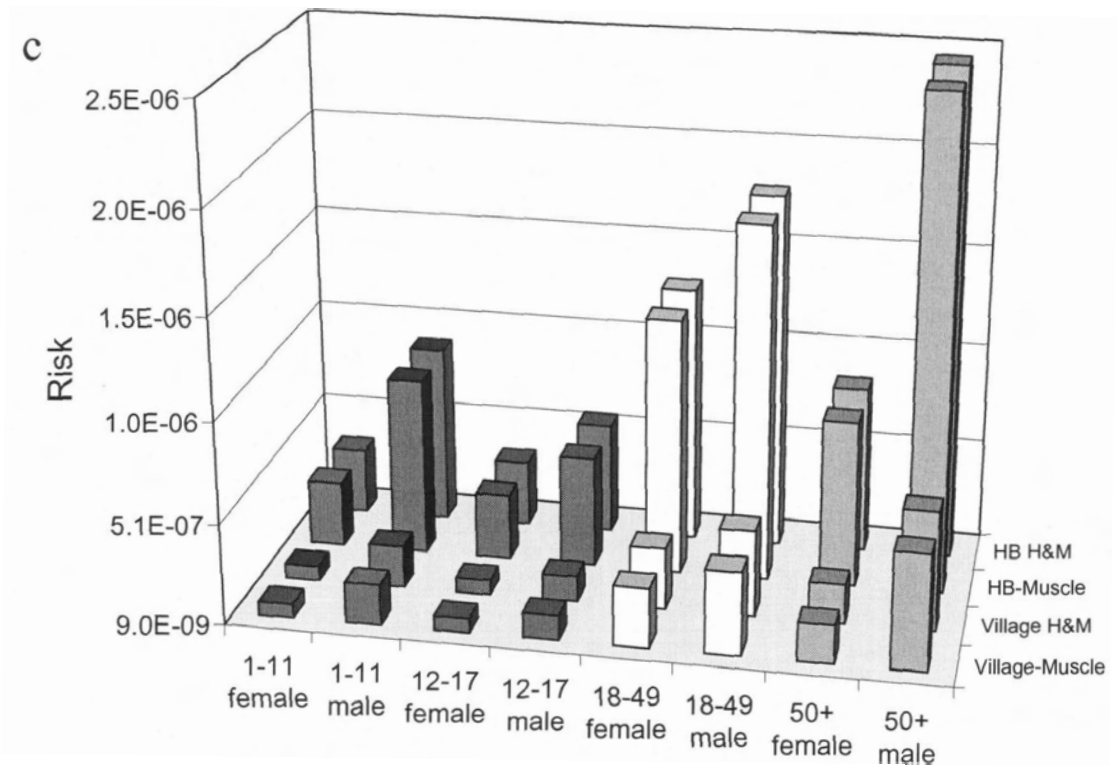

The cancer risk of consuming the whole crab (H&M) is just slightly higher than that of eating muscle alone. The EPA approach-predicted cancer risk exceeds the virtual safety criterion of 1 E-6 in both genders for all age groups. The highest risk is for male children consuming the whole crab (6.0 E-6) while the lowest risk is for female youths (1.2 E-6) (Figure 6.5a). The IPM approach predicts that the risk of consuming the whole crab or muscle alone from either Hospital Beach or the village site is below 1 E-6 for all gender and age groups. These risk estimates are several orders of magnitude lower than the EPA estimates and range from a minimum of 3.5 E-9 for female youth and children eating crab muscle to a maximum of 1.7 E-7 for senior males consuming the whole crab (H&M). The WMM risk estimates are lower than those predicted by the EPA model but are an order of magnitude greater than the IPM estimates. The WMM shows that adults

of both genders and senior males consuming the muscle or the whole crab have a risk of stomach tumours or stomach and lung tumours higher than the 1 E-6 criterion.

A summary of the minimum and the maximum cancer risks for the Haisla is displayed in Figure 6.6. The risk estimates calculated by the three approaches decrease in the order of EPA > WMM > IPM.

Figure 6.6 A summary of the mean, minimum and maximum risk estimates obtained using the EPA and OME models.

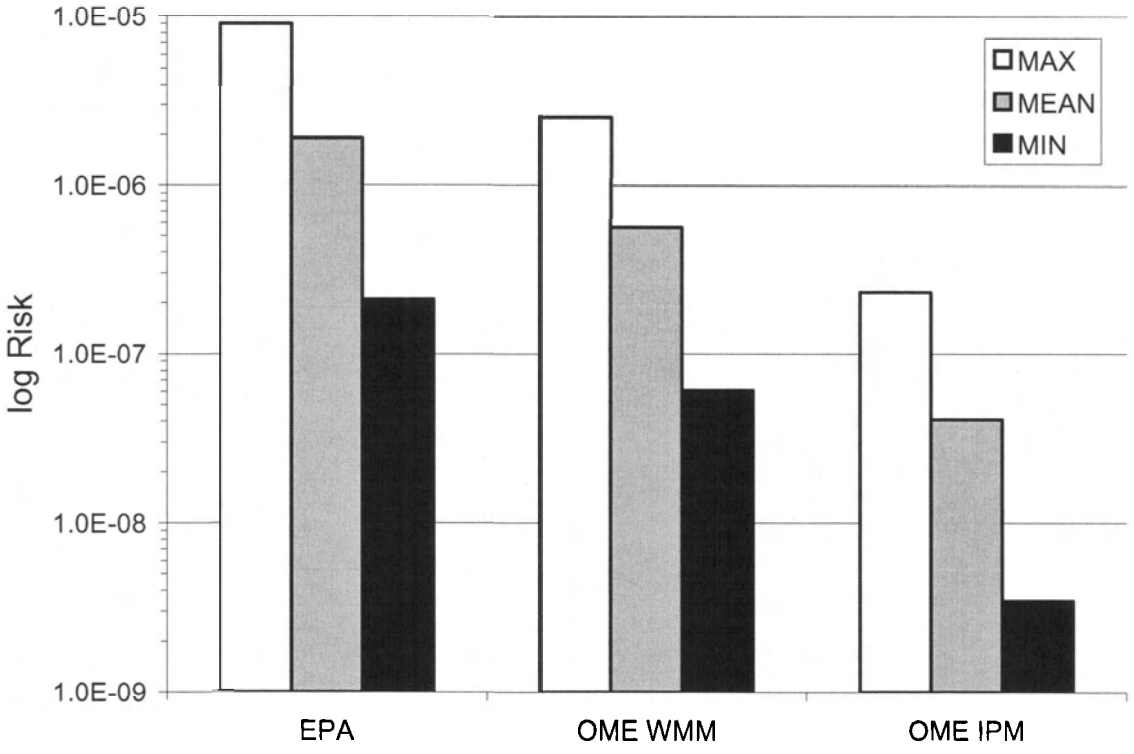

The crab consumption rates reported in the aboriginal dietary survey (Kitamaat Village Council, 1994) are similar to those reported in a diet survey conducted among different Asian groups living in Greater Vancouver, BC (Marion, 1996). The hepatopancreas consumption rate of the Haisla was estimated by multiplying the consumption rate of the whole crab by the proportion of hepatopancreas in the edible

tissues (13%) and is found to lie between the mean and the maximum hepatopancreas consumption rates of the Asian population in Vancouver, BC, Canada. (Table 6.8).

Table 6.8 Aboriginal and Asian hepatopancreas consumption (g/year)

Age	Aboriginal*		Asian‡	
Group	Female	Male	Max	Mean
0-11	184	738	2137	185
12-17	276	461	2137	185
18-49	1063	1473	4274	397
50+	694	2027	4274	293

*Kitamaat Village Council (1994); ‡Marion (1996)

Figure 6.7a shows a comparison of risk estimates calculated for the Aboriginal and Asian communities consuming crab hepatopancreas alone using the U.S. EPA model. This contrasts with the previous risk estimates where the worst case scenario was assumed that the entire meal or LADD consisted of hepatopancreas tissue. Generally, the aboriginal consumers are at a greater risk from consuming crab hepatopancreas than the Asian consumers based on mean consumption rates. The risk for both consumer groups for consuming a relatively small portion of hepatopancreas alone per meal was less than the acceptable risk criteria of 1 E-6. As shown in Table 6.8, there was a large difference, >10 fold, between maximum and mean consumers of hepatopancreas among the Asian community. Figure 6.7b shows a comparison of risks calculated for the maximum and mean consumers of hepatopancreas among the Asian survey respondents. The estimated risk for the heaviest consumers in the Asian community ranged from 2.1 E-6 to 5.6 E-6, which is greater than the acceptable risk criteria of 1 E-6.

Figure 6.7 Comparison of Risk values calculated a) for Aboriginal (Native) and Asian consumers of hepatopancreas alone; b) for maximum and mean consumers of crab hepatopancreas among the Asian community using the USEPA model.

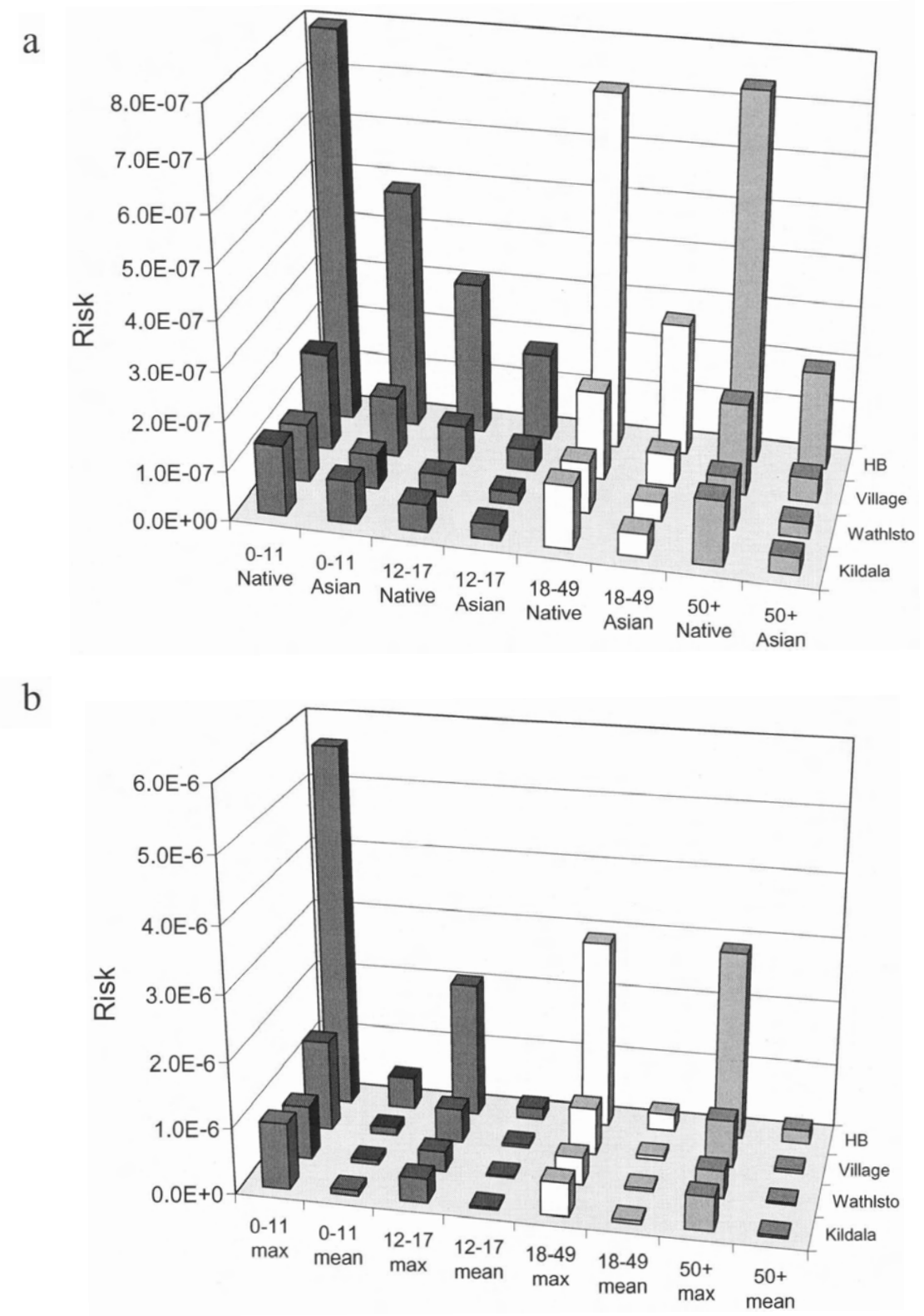

6.4 Discussion

6.4.1 Use of Arithmetic means for Input Data

The arithmetic means of PAH concentrations in the hepatopancreas and muscle (Table 6.1) are used in the exposure assessment because the arithmetic means introduce less bias than the geometric means in a data set (Crump, 1998).

6.4.2 Comparison of Calculated BaP-TEQ with Water Quality Criteria

As shown in Figure 6.1, the mean TEQ of hepatopancreas and muscle are about 1.0 ng BaP equivalents/g and 0.8 ng BaP equivalents/g wet weight, respectively in crabs collected near the smelter. These are very close to the maximum BaP concentration allowed in fish and shellfish (1 ng/g wet weight) for a heavy seafood consumer (about 200 g/week) (BCMELP, 1995). Therefore, consumption of crab tissues at a rate of 200 g/week may pose a serious health risk to the human consumers. It should be pointed out that the mean BaP concentration is calculated from 16 muscle samples whereas the hepatopancreas data is composed of 147 samples (Table 6.1). Therefore, the mean BaP concentration in the hepatopancreas is much more reliable than that of the muscle.

6.4.3 Comparison of Dietary Survey Results with Consumption Criteria

The Haisla's dietary survey (Kitamaat Village Council, 1994) shows that the consumption rate of crabs varies significantly among the different age groups and genders. According to the BCMELP consumption criteria (BCMELP, 1995), the Haisla may be categorised into the following consumption groups: (a) less than low consumer group (2,600 g/yr). This group includes female children (1,416 g/yr) and juveniles (2,124

g/yr); (b) low to moderate consumer group. (2,600-5,200 g/yr). This includes male juveniles (3,555 g/yr), (c) moderate consumer group (5,200g/yr). This includes male children (5,688 g/yr) and senior females (5,346g), and (d) heavy consumer group (10,400g/yr). This includes male adults (11,352 g/yr) and seniors (15,618 g/yr).

6.4.4 Comparison of Haisla and Canadian-Asian Dietary Survey Data

The comparison of the aboriginal (Kitamaat Village Council, 1994) and Asian dietary survey (Marion, 1996) (Table 6.5) corroborates the intake rates and exposure frequencies obtained from the aboriginal dietary survey.

6.4.5 Difference in LADD Among Age Groups

The LADD of the youth is the lowest among the four age groups (Table 6.3) for the U.S. EPA model. Perhaps, this is a result of the different body weights of the age groups and the low IR of this age category. In general, juveniles consume a less varied and healthy diet than adults and children. Therefore, the IR for juvenile males (12-17) is lower than that of male children (1-11) (Table 6.2). This is similar to the results of the Asian diet survey where the consumption rate for juveniles is reported to be the same as that of the children (Table 6.8).

6.4.6 Effect of Cooking Crab Tissues on PAH Bioavailability

It is assumed that the PAH in crab tissues are completely bioavailable and absorbed by the human consumer. Moreover, the PAH in the crab tissues are not destroyed by cooking; although some lower molecular weight PAH may volatilise

through heating but the less volatile high molecular weight, and carcinogenic PAH are probably unaffected. Indeed, cooking of crab tissue may result in an increase rather than a decrease in PAH concentration because the volume of tissue is reduced while the amount of PAH remains unchanged.

6.4.7 Differences in EPA and OME Risk Assessment Models

There are a number of differences in risk assessment approaches taken by the EPA and the OME. These differences have resulted in markedly different cancer risk predictions. The differences in approach are listed as follows:

(a) The OME characterises the health risks of PAH exposure by cancer development in the stomach (as the primary organ) and the lung (as the secondary organ) (OME, 1997) while the EPA characterises risk from stomach cancer development only.

(b) The methods of determining the TEF of PAH differ in the two agencies. Although a number of TEF estimation methods has been proposed (Thomas Petry *et al.*, 1996), the method of Nisbet and LaGoy (1992), which reflects the relative potency of individual PAH, is commonly used to estimate cancer risk in the EPA approach. In contrast, the OME has devised it's own methods of TEF calculation (OME, 1997); the OME IPM and the OME WMM methods. The OME IPM method estimates the risks of a PAH mixture by summing the risks attributable to individual PAH present in the mixture. It is very similar to the Nisbet and LaGoy approach (1992) but differs in the manner by which the relative potency of individual PAH is ascribed to BaP. In contrast the OME WMM method assesses the risk of a PAH mixture as a whole and assumes that the potency is proportional only to the BaP content of the mixture. This model assumes that both the

profile and the potency of a PAH mixture are similar to those of a mixture of standard composition (MSC). The assumption is based on the fact that the differences between the PAH profiles are too small to have a significant effect on the potency of the mixtures (OME, 1997). The different TEF calculation methods do not seem to affect the results significantly since all three methods produce similar TEQ in the crab tissues (Figure 6.1).

(c) Results of the present study show that the EPA model generally predicts the greatest cancer risk in children whereas the OME model predicts the greatest risk in adults. The difference in results may be explainable by the absence of body weight in the OME exposure assessment equation. In the EPA model, a child's body weight is less than that of an adult. Therefore, the LADD of children is divided by a smaller number, which results in a higher risk estimate. In the OME approach, the weight bias on risk calculation is removed from the equation so that the LADD estimate is influenced mainly by intake rate and exposure frequency.

6.4.8 Comparison of Risk Estimates Produced from EPA and OME Models

In general, the EPA approach yields a more conservative risk estimate than the OME models (Figure 6.4-Figure 6.6). The EPA model predicts a risk of >1 E-6 in all age groups and genders when consuming crabs caught near the smelter. The WMM model also predicts a risk of >1 E-6 for adults and mature adults consuming crabs collected near the smelter. But children, youth and adults do not exceed the 1 E-6 risk level when consuming the muscle or a combination of muscle and hepatopancreas in crabs from the other sites (Figure 6.5). The IPM model produces the lowest risk estimates (Figure 6.4-

Figure 6.6); this model does not predict a <1 E-6 risk for any age group consuming crabs from any of the four study sites in Kitimat Arm.

According to the OME (1997), the "actual risk" of cancer due to PAH exposure lies somewhere between the WMM and IPM estimates although it is likely to be closer to the WMM estimate. The WMM model generally predicts a higher risk estimate than the IPM model although the IPM model predicts slightly higher exposure levels (Figure 6.2-Figure 6.3). The WMM employs a slope factor in the risk calculation, which is more than an order of magnitude greater than that used by the IPM model for risk characterisation. The WMM is recommended by the OME as the primary model in most circumstances. The IPM is indicated only when the PAH mixture deviates from the mixture of standard composition (MSC). Table 6.2 shows that the PAH mixture in the crab tissue samples conformed to the MSC and so the WMM model is the most appropriate approach to conduct the risk assessment.

6.4.9 Features of the OME-WMM Approach

The WMM method can be used to reduce analysis time and costs once a preliminary study has been performed to determine if the PAH mixture in the sample is conformed to the MSC since the WMM method requires only the analysis of BaP in environmental samples. This also serves to reduce the uncertainty inherent in assessing the potency of individual PAH relative to BaP and in determining the concentrations of all the individual PAH in the environmental samples. It may also be useful in comparing the cancer risks of different PAH mixtures as long as these mixtures contain BaP.

6.4.10 Comparison of Risk Estimates Based on Haisla and Asian Diet Surveys

The risks estimated for the aboriginal community consuming hepatopancreas tissues as a portion of a larger meal of crab was compared to that for a Canadian-Asian community based on published hepatopancreas consumption rates (Marion, 1996). While the risk estimates for the mean consumers of crab hepatopancreas among the Asian community were lower than those for the aboriginal community and the acceptable risk limit, the risk estimates for the maximum Asian consumers was much greater than the aboriginal consumers and exceeded 1 E-6 (Figure 6.7).

6.4.11 Future Directions for Assessment of Risk to PAH Exposure in Kitimat Arm

This study has focused on quantifying the risk of cancer due to PAH exposure through one route, the consumption of PAH contaminated dungeness crabs. A natural extension of this work would be to expand this risk assessment to estimate the risk of cancer through consumption of a variety of other traditional foods which may be contaminated with PAH including a variety of fish species, seaweed, seals, game species, and other shellfish such as clams and mussels as well as traditionally processed foods such as eulachon grease and smoked fish.

6.5 Summary

This quantitative human health risk assessment has shown that heavy consumers of crab caught near the aluminium smelter are at risk (>1 E-6) based on an exposure assessment and risk characterisation using the EPA and OME models. The most conservative risk estimates were obtained using the EPA model, while the OME IPM

model yielded the lowest risk estimates. In addition, the EPA model predicts the greatest risk for children, while the OME models predict greater risk for adult consumers of PAH contaminated crabs. Further studies are required to examine the cancer risk of consuming crabs in combination with other traditional foods.

CHAPTER 7
HUMAN HEALTH RISK ASSESSMENT FOR THE CONSUMPTION OF PAH-CONTAMINATED CRABS USING A MONTÉ CARLO MICRO-EXPOSURE EVENT APPROACH.

7.1 Introduction

The deterministic risk assessment described in Chapter 6 examined the risk of cancer due to the consumption of PAH contaminated crabs. This risk assessment was based on the hazard identification and dose response assessments promulgated by the U.S. Environmental Protection Agency, (EPA 1989) and the Ontario Ministry of Environment, (OME 1997). It was determined that heavy consumers of crabs from an area contaminated with PAH, particularly adult males, were at an unacceptable risk for developing cancer. This risk assessment also determined that the risk estimates obtained using the EPA exposure assessment and risk characterisation were more conservative than those obtained using the OME approach.

The deterministic risk assessment involved an exposure assessment based on mean values for PAH concentrations in crab tissues, and mean intake rates, exposure frequencies, and body weight, data obtained from a dietary survey study performed for a local aboriginal population (Kitamaat Village Council, 1996). This risk assessment used a simple algebraic equation to estimate mean exposure and risk estimates (Equation 5.1). This approach is often used to make conservative estimates of the LADD and cancer risk.

In order to examine inter-individual variability and uncertainty in the parameters used for the deterministic risk assessment, a probability based, stochastic risk assessment was performed using probability distributions for the input data used in the exposure assessment. The stochastic risk assessment model was implemented with the micro-exposure event approach (Price *et al.* 1996) using the Microsoft Excel® spreadsheet, Visual Basic® language, and Monté Carlo analysis. The exposure assessment and risk characterisation was based on the method promulgated by the U.S. EPA.

Monté Carlo analysis can be used to characterise the uncertainty and inter-individual variability inherent in each parameter involved in the exposure estimate equation. Variability represents the true heterogeneity in a population, whereas uncertainty represents a lack of perfect knowledge of each input parameter. In order to introduce individual and exposure concentration variability, probability distributions can be used instead of a single mean value. In addition, a micro-exposure event approach can be used to incorporate different dose or exposure rates over the lifetime of many individuals. This is important because a number of the parameters that are used to calculate the LADD, such as intake rate, exposure frequency, and body weight vary over the lifetime of each individual. There is also a great deal in variability in these parameters within a given population. Gender is also an important determinant of these parameters, and seasonal changes in food consumption patterns can also influence the estimation of exposure.

The Monté Carlo micro-exposure event approach is used to incorporate uncertainties and variability in input parameters that the deterministic approach cannot easily accommodate. Therefore, it is expected that the stochastic approach will produce a

more "realistic" estimate of exposure to PAH over the lifetime of a population, and will provide a more detailed estimate of the risk of cancer from consuming PAH contaminated crabs over the duration of a lifetime.

We are fortunate to have very detailed and specific dietary information in the Haisla diet survey (Kitamaat Village Council, 1996) that can be used to estimate exposure. Therefore, this data was used to incorporate the individual and gender specific variability into the risk assessment examine the effects of inter-individual, and gender differences on exposure and cancer risk in this population.

The objective of this study was to further investigate the lifetime cancer risk due to consumption of PAH contaminated crabs in Kitimat Arm, and to incorporate the individual variability inherent in the Haisla diet survey to examine dietary PAH exposure for aboriginal individuals who consume crabs from specific sites in Kitimat arm for which we have crab tissue concentration data (Chapter 2).

7.2 Approach Description

The Monté Carlo micro-exposure event model was adapted from the micro exposure event model described by Price *et al.*, 1996. The model was designed to characterise variability in the following input parameters: gender, body weight, intake rate, exposure frequency, crab mass, and concentration of benzo[a]pyrene toxic equivalents (BaP-TEF) in the hepatopancreas and muscle of the crabs consumed from different locations in Kitimat Arm. The model simulates the consumption of crab caught at specific sites by individuals of a local aboriginal population over a lifetime in order to obtain distribution estimates for the LADD and lifetime cancer risk.

7.3 Model Description

A flowchart for the Monté Carlo, micro-exposure event model is presented in Figure 7.1.

Figure 7.1 Flow diagram of micro-exposure event Monté Carlo model

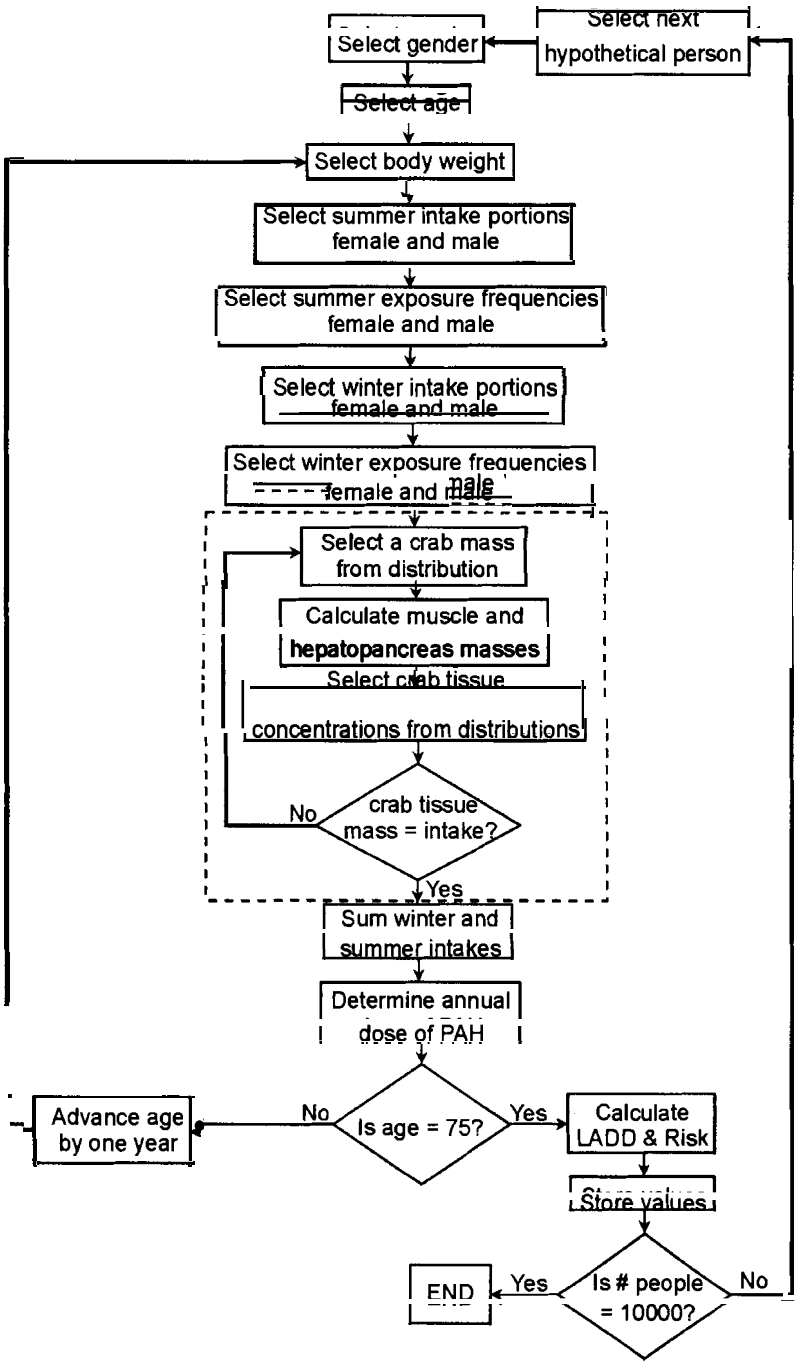

Before running the model, the site from which crabs are consumed is selected. The model starts by selecting the gender of an individual. The gender is randomly selected based on a probability of 0.551 that the individual is female.

The body weight of the individual was randomly selected from lognormal distributions specific to the age and gender of the individual and based on body weight statistics obtained from the Haisla Dietary Survey (Kitamaat Village Council 1996). The model evaluates each meal of crab as a separate exposure event. The size of the meal portion was randomly selected from the distribution appropriate for the age and gender of the individual and the season.

The mass of the crabs ingested during the meal was randomly selected from the input distribution of crab weights. A nested loop is included to ensure that the mass of the crab equals the meal portion size (intake) for each meal.

The number of exposure events (meals of crab) in a given month of an individual's life was determined from the exposure frequencies for the winter and summer seasons. It was assumed that each year in this northern community was equally divided into 6 winter and 6 summer months, and each year is divided into 12 months or exposure periods. Annual exposure is the sum of the exposures simulated over the winter and summer months.

At the end of each year, the model determined if the individual had reached the maximal age of 75 years, thus, the model assumes that exposures occurred over the duration of a lifetime. The LADD and lifetime cancer risk for the individual were calculated by summing the annual doses and dividing by the average human life span of

75 years. The model continues to calculate individual LADD and risk estimates until it has completed estimates for 10,000 individuals.

The LADD for each individual was calculated based on the model shown in Figure 5.1 which is summarised by Equation 7.1:

$$\text{LADD} = \frac{1}{75\ \text{yrs.}} \sum_{j=1}^{75} \frac{1}{\text{BW}_j} \sum_{i=1}^{\text{crab consumed}_j} (\text{Ch}_{ij} * \text{Hp} + \text{Cm}_{ij} * \text{Mp}) * \text{Crab mass}_{ij} / \text{CV} \qquad (7.1)$$

where crab consumed$_j$ is the amount of crab consumed in the jth year of the individual's exposure; BW$_j$ is the body weight in the jth year; Ch$_{ij}$ is the concentration of BaP-TEF in the hepatopancreas; Hp is the proportion of hepatopancreas tissue of the Crabmass$_{ij}$; Cm$_{ij}$ is the concentration of BaP-TEF in the muscle, Mp is the proportion of muscle tissue of the Crab mass$_{ij}$; Crab mass$_{ij}$ is the mass of each crab consumed as a meal portion for the ith meal in the jth year.

The risk for each individual was calculated based on the U.S. EPA risk characterisation presented in Equation 7.2:

$$Risk = LADD \times CPF \times CF \qquad (7.2)$$

where:

LADD = Lifetime average daily dose (ng/kg-day)

CPF* = Cancer potency factor for stomach cancer (risk mg^{-1} kg^{-1} day^{-1})

CF = Conversion factor (10^{-6} mg/ng).

7.4 Model Input Parameters

The model input parameters and distributions describing the tissue concentration distributions, tissue masses and volumes, and carcinogenic potential of BaP-TEF are presented in Table 7.1.

Table 7.1 Model input parameters and distributions

Parameter	Mean	SD	Max	Min	Distribution Type
Measured Tissue Concentrations (ng BaP-TEF/g wet weight)					
Ch_{HB}	1.356	1.794	9.907	0.081	Lognormal
$Ch_{village}$	0.337	0.158	0.779	0.068	Lognormal
$Ch_{wathlsto}$	0.197	0.130	0.479	0.056	Lognormal
$Ch_{kildala}$	0.242	0.514	2.782	0.050	Lognormal
Cm_{HB}	0.833	1.534	6.278	0.134	Lognormal
$Cm_{village}$	0.157	0.098	0.226	0.012	Lognormal
Predicted Tissue Concentrations (ng BaP-TEF/g wet weight)					
Cm_{HB} – P	0.264	0.395	1.926	0.026	Lognormal
Cm_{HB} – M&P	0.380	0.780	5.834	0.026	Lognormal
$Cm_{village}$ – P	0.089	0.039	0.159	0.026	Lognormal
$Cm_{village}$ - M&P	0.093	0.046	0.206	0.026	Lognormal
$Ch_{wathlsto}$ – P	0.064	0.037	0.141	0.026	Lognormal
$Ch_{kildala}$ – P	0.076	0.141	0.800	0.026	Lognormal
Crab mass (g)	740	131	1120	378	lognormal
Hp (%)	3.1				-
Mp (%)	23.2				-
Fp (%)	55.1				-
CV*	0.571				-
CPF† (risk mg^{-1} kg^{-1} day^{-1})	7.3				-
CF† (mg/ng)	1.0E-6				-

*(Winquist, 1998), †(EPA CPF 7.3 risk mg^{-1} kg^{-1} day^{-1}, Oral in diet, IRIS, 1998)

Table 7.2 shows the input parameters used to generate lognormal distributions for individual bodyweights.

Table 7.2 Descriptive statistics for individual body weights* (kg)

Age	1-11		12-17		18-49		50+		All	
Gender	F	M	F	M	F	M	F	M	F	M
Mean	32	29	51	61	75	90	82	93	68	80
SD	12	10	10	32	12	16	11	10	21	25
Min	21	18	39	43	55	64	64	76	21	18
Max	52	45	60	118	100	126	102	108	102	126

*Kitamaat Village Council (1996)

The probabilities used to generate exposure frequency distributions for crab consumption during summer, (a) and winter, (b) months are shown in Figure 7.2.

Figure 7.2 Exposure frequency, number of meals per month in a) summer. b) winter.

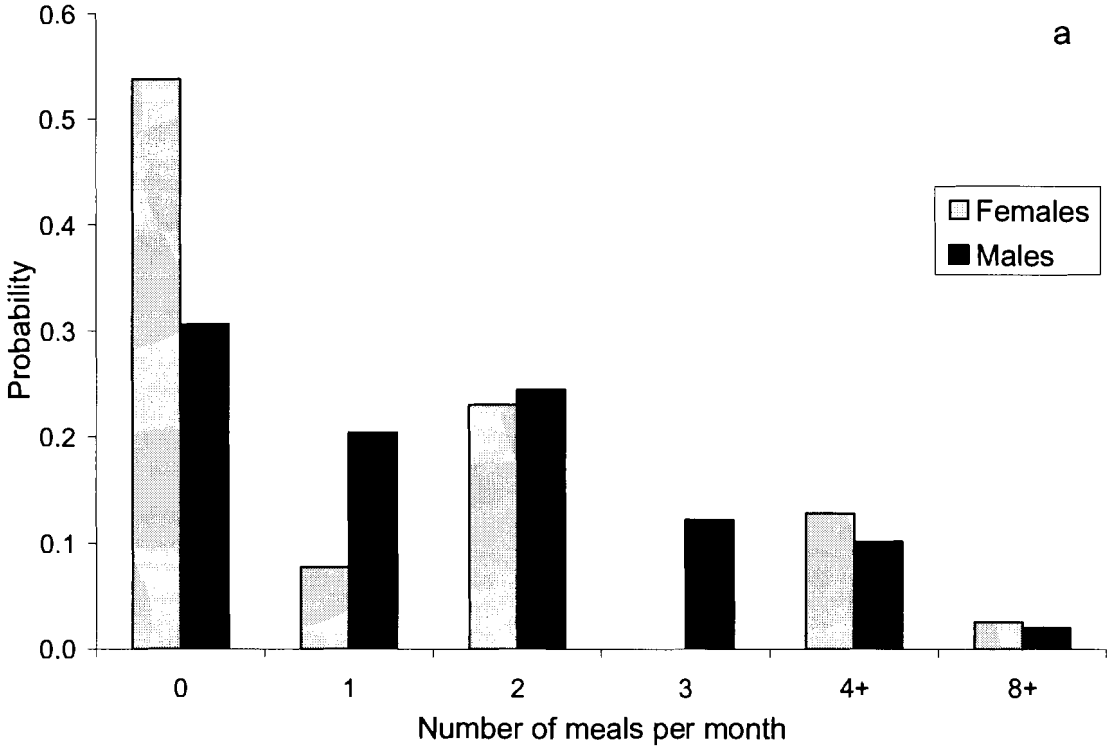

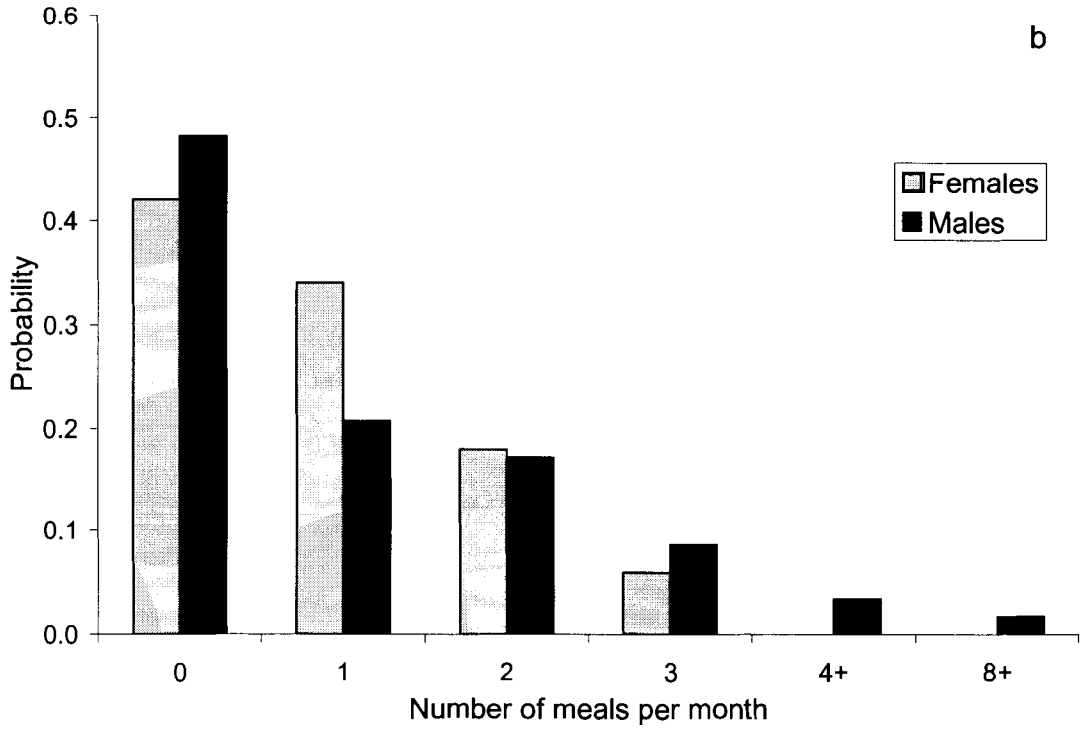

Figure 7.3 displays the probability distribution for the amount of crab consumed per meal during summer, (a) and winter, (b) months.

Figure 7.3 Amount of crab consumed per meal in: a) summer, b) winter.

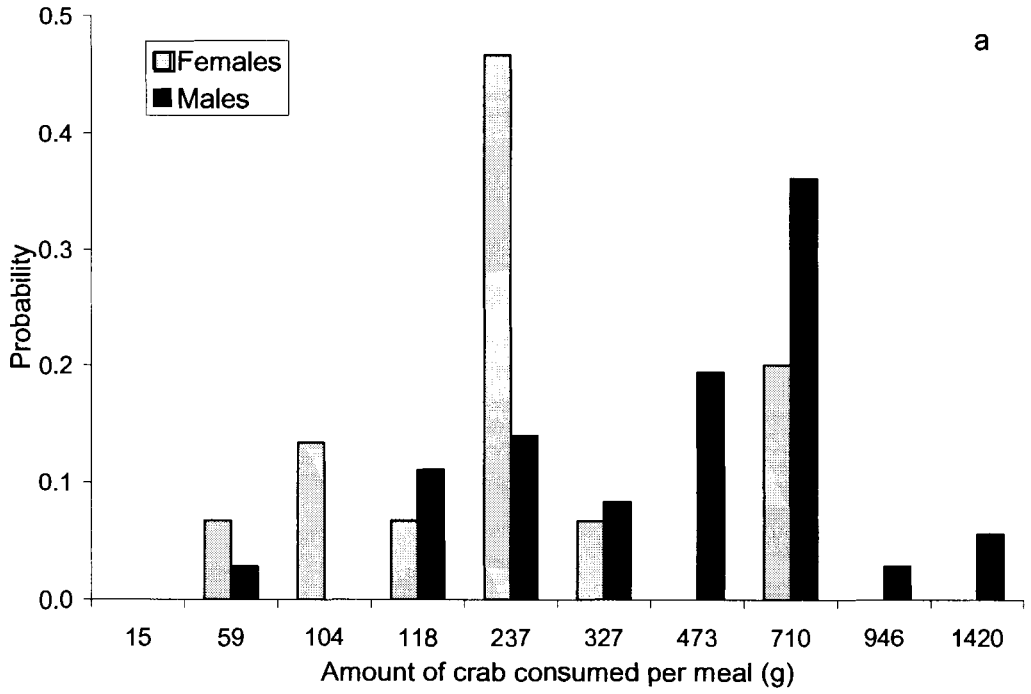

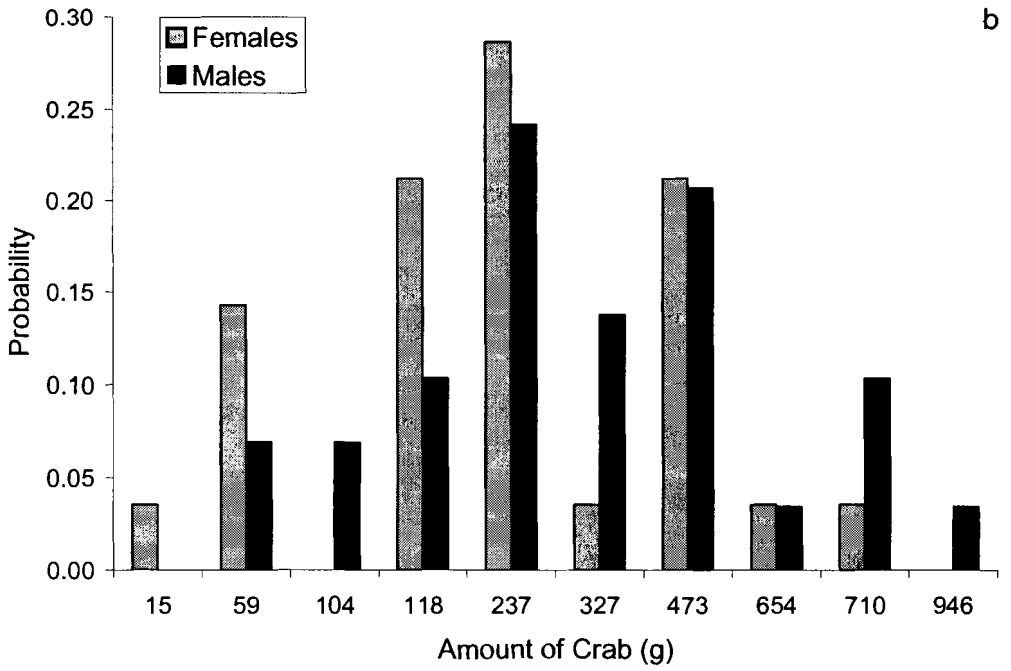

The data used to develop the probability distributions was obtained from the dietary survey study performed for a local aboriginal population (Kitamaat Village Council, 1996). These custom frequency distributions were used directly to characterise exposure and were not fitted to standard distribution patterns.

The input data used to characterise the variability in the concentration of benzo[a]pyrene toxic equivalent factors (BaP-TEF) in crab tissues were obtained from the concentrations of PAH determined in dungeness crab tissues as described in Chapter 2.

Muscle tissue concentrations were predicted for samples that were not analysed using the PBTK model and measured muscle tissue concentration data. The muscle tissue concentrations were estimated based on the concentration of BaP in the hepatopancreas of each crab. These calculations are presented and described in Chapter 5.

BaP-TEF were calculated from parent PAH concentrations following the method of Nisbet and LaGoy (1992). The parent PAH concentrations below the estimated sample specific detection limit, ESSDL were represented as ½ ESSDL. The mean and standard deviation for whole crab and tissue wet weights were determined by weighing crabs and tissues that were collected for analysis of PAH.

7.5 Model Specifications

The model was written in Microsoft Visual Basic® using the Microsoft Excel® 97 SR-2 spreadsheet for storing input variables used to generate distributions. Random numbers were generated for normal and lognormal parameter distributions using functions coded in Visual Basic® and Excel®. The model also allows for the use of a random number generator (RNG) based on a normal distribution function derived from source code written by Dr. Michael P. McLaughlin from his Urandom library (McLaughlin 1998). This code was translated into Visual Basic by Thomas Achenbach based on a Macintosh implementation of the Ultra pseudo-random number generator, Urandom, developed by: Dr. George Marsaglia *et al.* (1991). These functions are presented in Appendix D. The model was run various computers including a Pentium II based PC with 400 MHz clock speed, Pentium 4 PCs with 1 GHz clock speed, and an AMD Athalon XP based PC with 1700 MHz clock speed.

Each Monté Carlo model run simulated the consumption of crab for 10,000 individuals. Several model runs were conducted which demonstrated that 10,000 individuals provided stable estimates for the minimum, 5^{th} percentile, mean, median, 95^{th} percentile and maximum of the LADD and risk output values (Table 7.3 - Table 7.5).

The Pentium II computer took approximately 5 hours of computing time to estimate the LADD and risk for 10,000 individuals. The Pentium 4 and AMD Athalon XP based PCs were much faster and required approximately 15 – 19 minutes per run.

The model output generated for each individual was stored in an Excel® spreadsheet which held the values for LADD, risk, amount of crab consumed per year, and concentrations of BaP-TEF in crab hepatopancreas and muscle tissues. Statistical analysis of model output was performed using Microsoft Excel. Crystal Ball 4.0, Decisioneering Inc. 1996, was used to evaluate the output of the Excel® RNG, the Urandom RNG, and the visual basic lognormal distribution function.

7.6 Results

7.6.1 Random Number Generator Validity

Monté Carlo simulation requires a pseudo-random number generator with good statistical properties (Barry, 1996). The random number generator (RNG), in Microsoft Excel was used in the Monté Carlo simulations to obtain numbers for the input parameter distributions. A number of authors have questioned the numerical accuracy of some statistical functions in Microsoft Excel® 5.0, (Barry 1996) and the Excel® version in Microsoft Office 97 for Windows® (Knüsel, 1998; McCullough and Wilson, 1999). The output of the RNG of was assessed by McCullough and Wilson (1999) using statistical tests for randomness. McCollough and Wilson (1999) concluded that the random number generator was inadequate for statistical calculations. Therefore, the performance of the excel random number generator, RAND, was evaluated to ensure that the Monté Carlo

simulations were performed using a random number generator with good statistical properties. Figure 7.4 displays the output obtained running the RAND with a simple lognormal function coded in Visual Basic® to generate 50,000 lognormally distributed random numbers.

Figure 7.4 Random numbers generated using RAND and simple lognormal function

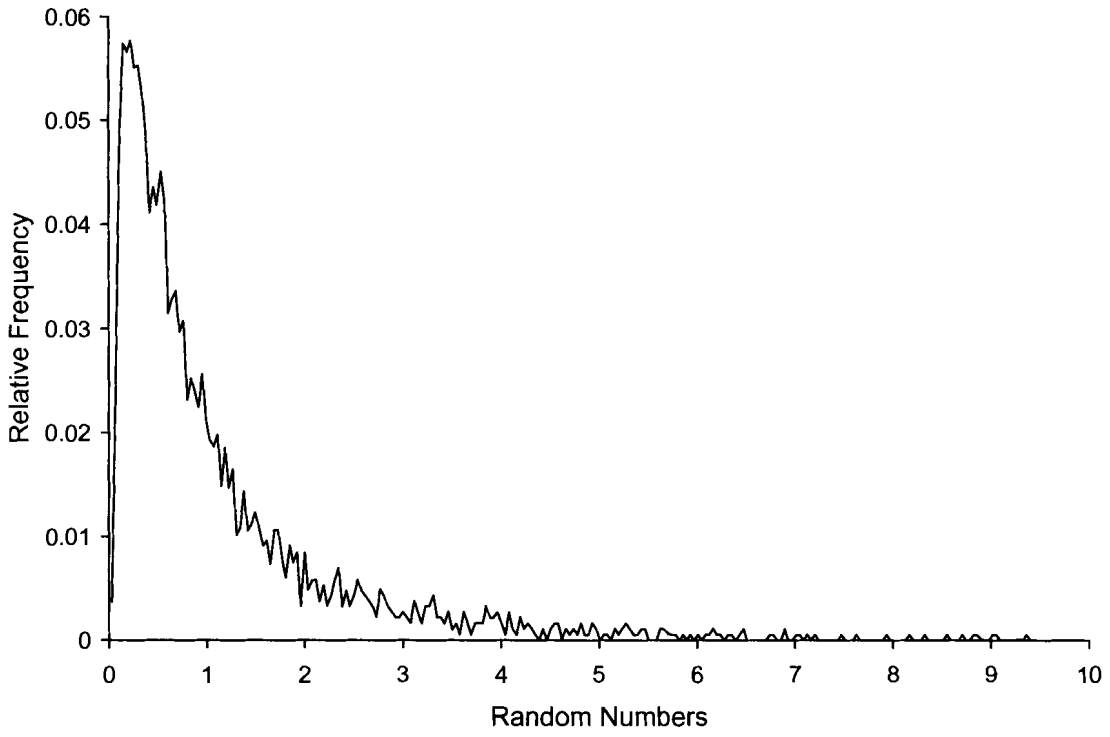

An improved lognormal distribution function, Lognormalcalc, was introduced into the Visual Basic® risk assessment model and was used to produce lognormally distributed random numbers from RAND. The output is presented in Figure 7.5.

Figure 7.5 Random numbers generated using RAND and Lognormalcalc function

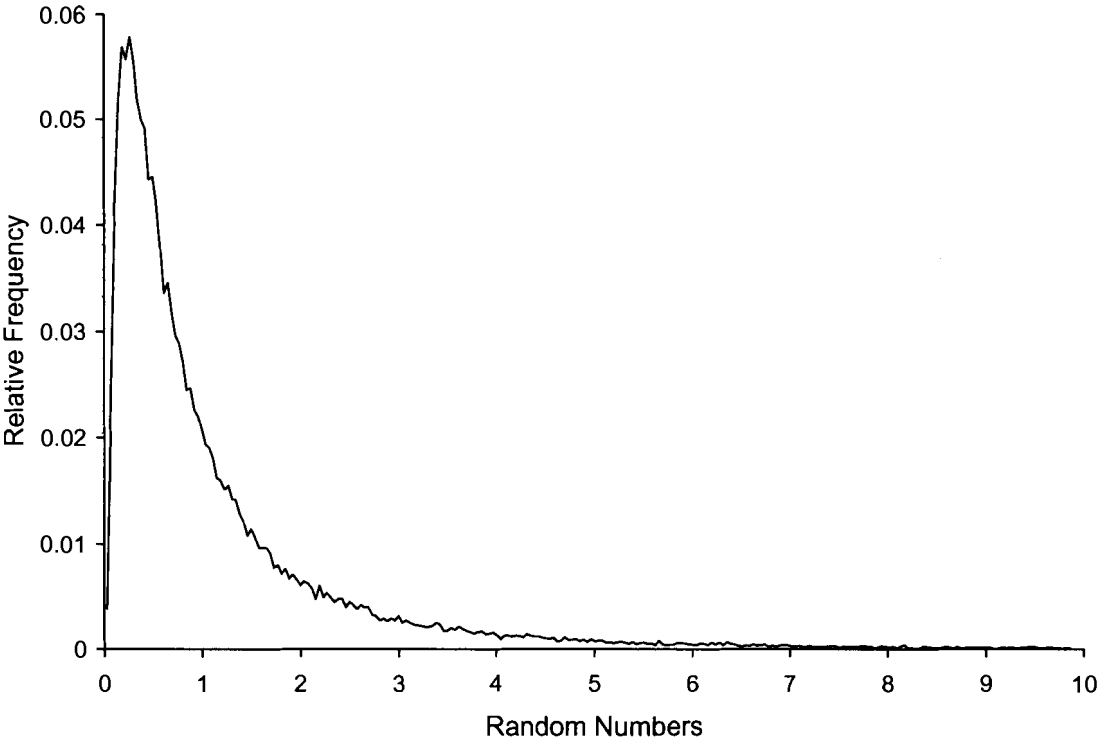

The random numbers produced by RAND and the simple lognormal function produced a very irregular distribution of random numbers (Figure 7.4). There were a number of values in the tail of the distribution with an often recurring frequency of 27 and 0. The random numbers produced with RAND and Lognormalcalc produced a much smoother frequency distribution of random numbers. Also, the numbers in the tail were distributed much more evenly (Figure 7.5). This is very important because the numbers in the upper tail of the BaP-TEQ tissue concentration distributions represent the maximum concentrations and contribute most significantly to the maximum LADD and risk.

The Excel® RAND with the simple lognormal function, and improved Lognormalcalc were evaluated by comparison with random numbers generated by Crystal Ball 4.0®, and the ultra pseudo random number generator, Urandom coupled with

Lognormalcalc. The four random number generation methods were each implemented three times to produce lognormal distributions of BaP-TEQ based on 10,000 iterations. Each run was implemented with the following input values: mean = 1.191, SD = 1.773, minimum = 0, maximum = 9.91. The standard deviation, minimum, 5th percentile, median, mean, 95th percentile, and maximum values were determined for each of the three runs using Excel® functions. The mean results of this statistical analysis are presented in Figure 7.6.

Figure 7.6 Comparison of output distributions from four random number generators, Crystal Ball 4.0, RAND-Lognormalcalc, Urandom-Lognormalcalc, and RAND with a simple lognormal function.

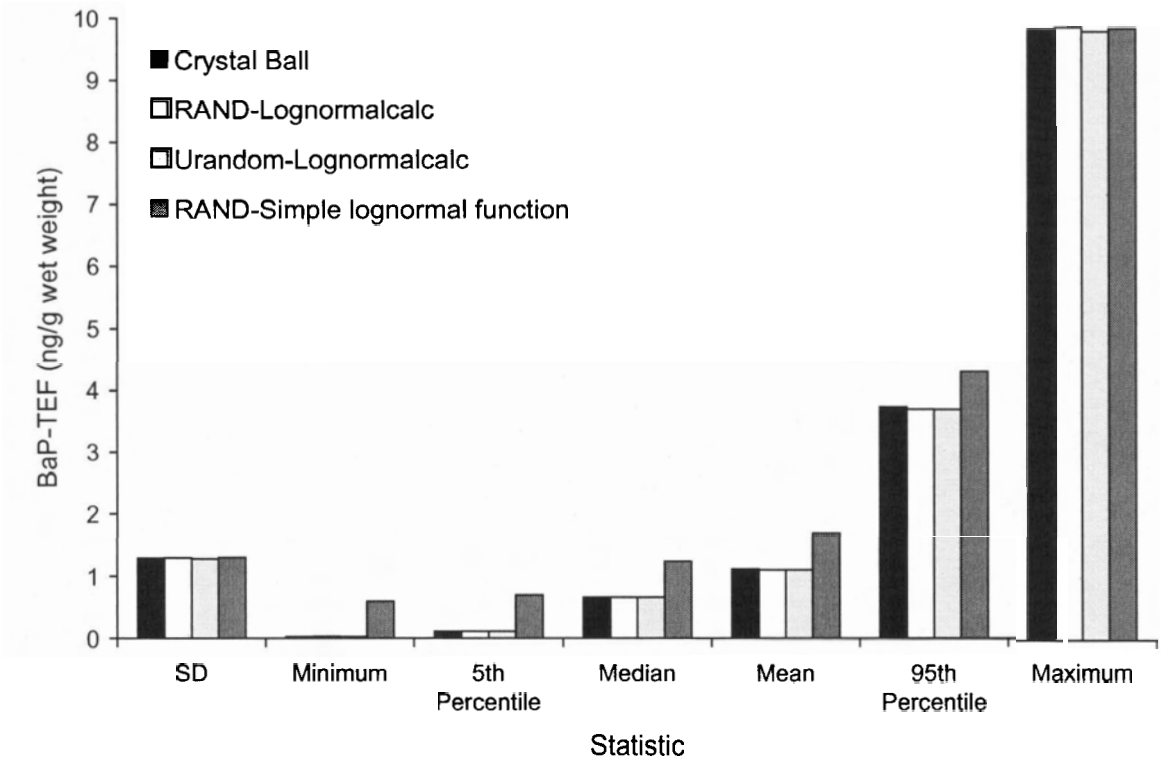

Figure 7.6 shows that the distributions generated by Crystal Ball 4.0®, RAND-Lognormalcalc, and Urandom-Lognormalcalc were statistically very similar. However, the Excel® RAND coupled with the simple lognormal function produced an unacceptable frequency distribution of randomly generated BaP-TEF tissue concentrations. The minimum, 5th percentile, median, mean, and 95th percentile values were much greater than those obtained from the other three random number generators.

7.6.2 Simulation Results

The micro-exposure event model was implemented using the statistically acceptable RAND-lognormalcalc random number generator for generating lognormal input distributions. The minimum BaP-TEF tissue concentrations in the hepatopancreas and muscle were set to 0 to avoid left censoring the input distributions (Porter *et al.*, 1988; Newman *et al.*, 1989).

The mean, 5th percentile, median, and 95th percentile, and maximum (if one exists) values are shown in graphs and tables according to principles of good practice for the use of Monté Carlo techniques in human health risk assessment (Burmaster and Anderson, 1993).

Table 7.3 and Table 7.4 display summary statistics of the LADD and risk estimates calculated by two model runs of 10,000 individuals, male and female, who consumed crabs collected from Hospital Beach in Kitimat Arm.

Table 7.3 Output value stability of Lifetime Cancer Risk from two separate model runs of 10,000 individuals consuming crabs caught at Hospital Beach near Smelter

Statistic	Run 1	Run 2	Mean	Relative Precision
SD	6.35E-7	6.36E-7	6.36E-7	0.04%
Minimum	8.03E-7	7.85E-7	7.94E-7	1.14%
5th Percentile	1.20E-6	1.20E-6	1.20E-6	0.18%
Median	1.72E-6	1.72E-6	1.72E-6	0.05%
Mean	1.98E-6	1.97E-6	1.97E-6	0.10%
95th Percentile	3.03E-6	3.04E-6	3.04E-6	0.10%
Maximum	3.97E-6	4.16E-6	4.06E-6	2.35%

Table 7.4 Output value stability of Lifetime Cancer Risk from two separate model runs of 10,000 and 20,000 individuals consuming crabs caught at Hospital Beach near Smelter

Statistic	Run 1 10,000	Run 2 20,000	Mean	Relative Precision
SD	6.36E-7	6.44E-7	6.40E-7	0.65%
Minimum	7.85E-7	7.44E-7	7.65E-7	2.63%
5th Percentile	1.20E-6	1.16E-6	1.18E-6	1.79%
Median	1.72E-6	1.73E-6	1.73E-6	0.42%
Mean	1.97E-6	1.96E-6	1.97E-6	0.20%
95th Percentile	3.04E-6	3.05E-6	3.04E-6	0.21%
Maximum	4.16E-6	4.05E-6	4.11E-6	1.28%

If the Monté Carlo risk assessment is run with minimum concentration values for BaP-TEF in the hepatopancreas and muscle tissues, the LADD and resultant risk estimates are slightly greater. Table 7.5 shows the results of two simulations where minimum concentration values were set at 0.081 and 0.134 ng BaP-TEF/g wet weight for the hepatopancreas and muscle respectively.

Table 7.5 Output value stability of Lifetime Cancer Risk from two simulations of 10,000 individuals consuming crabs caught at Hospital Beach near Smelter using minimum concentration values

Statistic	Run 1	Run 2	Mean	Relative Precision
SD	7.50E-7	7.50E-7	7.50E-7	0.01%
Minimum	7.83E-7	8.17E-7	8.00E-7	2.11%
5th Percentile	1.38E-6	1.37E-6	1.38E-6	0.07%
Median	1.99E-6	2.02E-6	2.00E-6	0.67%
Mean	2.29E-6	2.30E-6	2.29E-6	0.24%
95th Percentile	3.55E-6	3.54E-6	3.54E-6	0.08%
Maximum	4.68E-6	4.58E-6	4.63E-6	1.07%

The maximum risk increased from 4.16E-6 to 4.68E-6, approximately a 12.5% increase when the model was run with the minimal values for tissue BaP-TEF concentrations. The mean relative precision of the statistical parameters shows that there is little difference in variability in the risk estimates when minimum tissue concentration values are used in the model simulation. However, it is more realistic to assume that crabs with tissue concentrations lower than those measured in my limited sample number may be encountered. Also, the minimum concentration is influenced by the analytical detection limits. Therefore, the risk assessment was performed using no fixed minimum BaP-TEF tissue concentrations.

Figure 7.7 and Figure 7.8 display frequency distributions of PAH-TEF residues in the hepatopancreas and muscle tissues of crabs collected from Hospital Beach produced by a model exposure simulation.

Figure 7.7 Frequency distribution for the concentration of BaP-TEF in hepatopancreas tissues of crabs consumed from Inner Harbour.

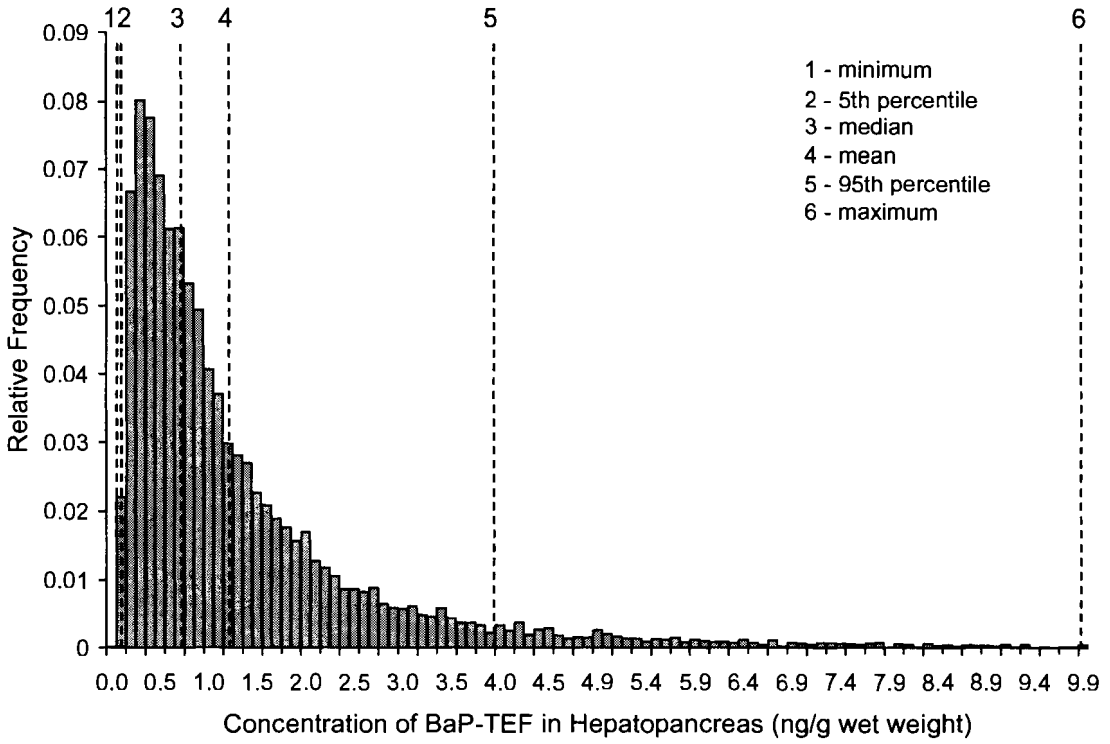

Figure 7.8 Frequency distribution for the concentration of BaP-TEF in muscle tissues of crabs consumed from Inner Harbour

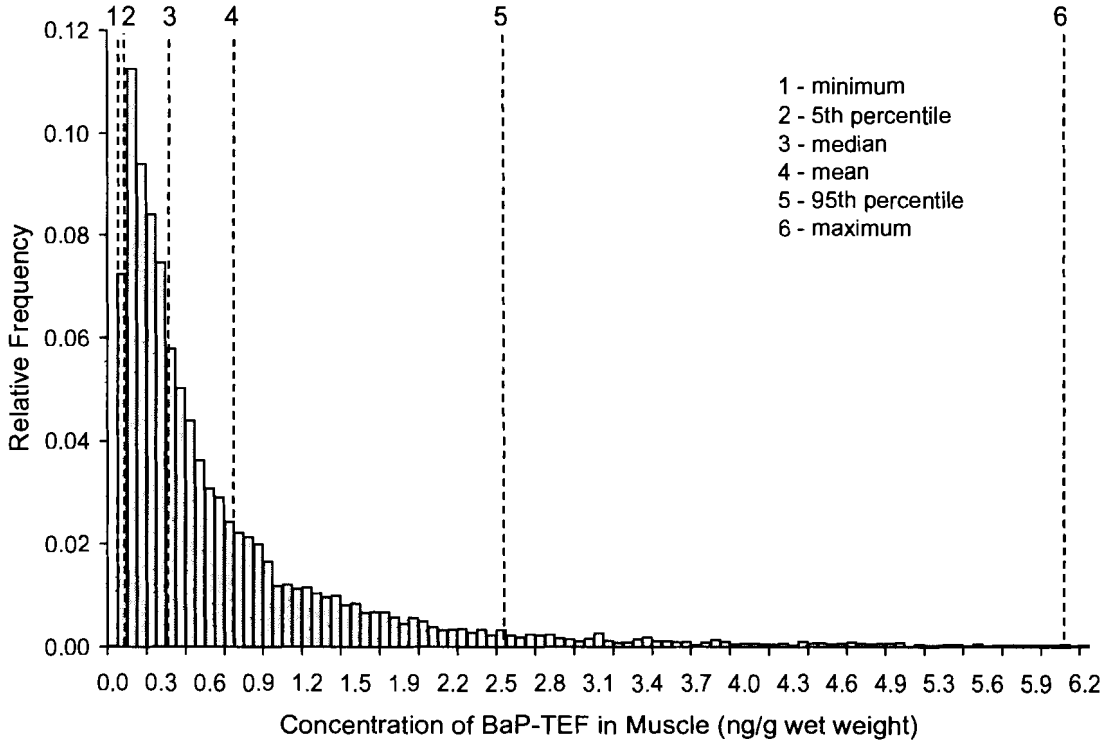

Figure 7.7 and Figure 7.8 show that the PAH-TEF tissue concentrations generated by the model were lognormally distributed similar to the measured tissue concentrations. Table 7.6 shows a statistical comparison of lognormal distributions predicted by the stochastic model for BaP-TEF in the hepatopancreas of crabs and concentrations of BaP-TEF determined in the hepatopancreas of crabs obtained from Hospital Beach.

Table 7.6 Comparison of BaP-TEF determined in crab hepatopancreas tissues from Hospital Beach, and PBTK and Stochastic Risk Assessment model predicted values.

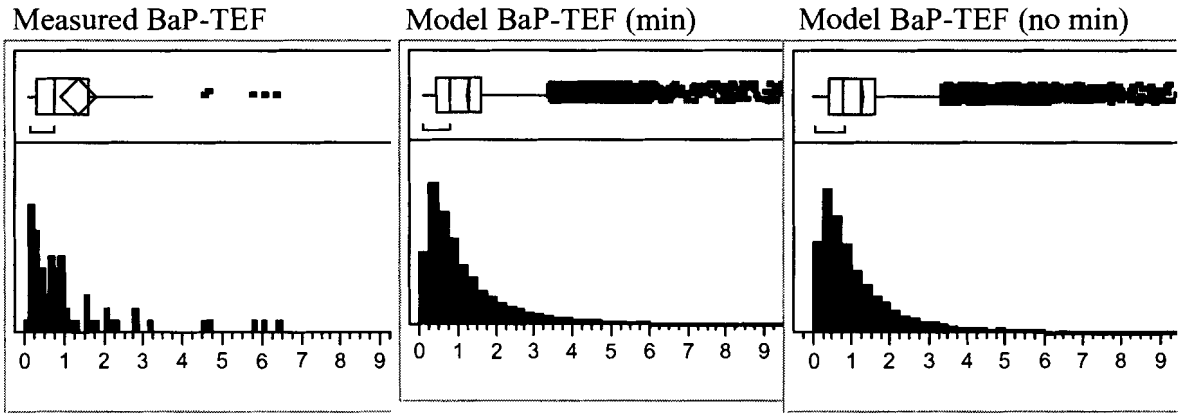

Quantiles			Quantiles			Quantiles		
100.0%	maximum	9.9070	100.0%	maximum	9.9000	100.0%	maximum	9.8800
99.5%		9.9070	99.5%		8.1899	99.5%		7.9400
97.5%		7.5317	97.5%		5.3895	97.5%		5.3398
90.0%		3.6438	90.0%		2.9700	90.0%		2.9000
75.0%	quartile	1.5933	75.0%	quartile	1.6200	75.0%	quartile	1.6100
50.0%	median	0.7365	50.0%	median	0.8300	50.0%	median	0.8100
25.0%	quartile	0.3273	25.0%	quartile	0.4300	25.0%	quartile	0.4100
10.0%		0.1516	10.0%		0.2400	10.0%		0.2200
2.5%		0.1121	2.5%		0.1300	2.5%		0.1100
0.0%	minimum	0.0810	0.0%	minimum	0.0800	0.0%	minimum	0.0100
Moments			Moments			Moments		
Mean		1.356258	Mean		1.307036	Mean		1.275167
Std Dev		1.794509	Std Dev		1.390984	Std Dev		1.364467
Std Err Mean		0.220889	Std Err Mean		0.013910	Std Err Mean		0.013645
upper 95% Mean		1.797403	upper 95% Mean		1.334303	upper 95% Mean		1.301914
lower 95% Mean		0.915112	lower 95% Mean		1.279769	lower 95% Mean		1.248420
N		66.	N		10000	N		10000

Table 7.7 shows a statistical comparison of lognormal distributions predicted by the stochastic model for BaP-TEF in the muscle of crabs with measured and PBTK model predicted concentrations of BaP-TEF in the muscle of crabs from Hospital Beach.

Table 7.7 Comparison of BaP-TEF determined in crab muscle tissues from Hospital Beach, and PBTK and Stochastic RA model predicted values.

Measured BaP-TEF			PBTK Pred. BaP-TEF			M&P BaP-TEF			Stochastic BaP-TEF (no min)			Stochastic BaP-TEF (min)		
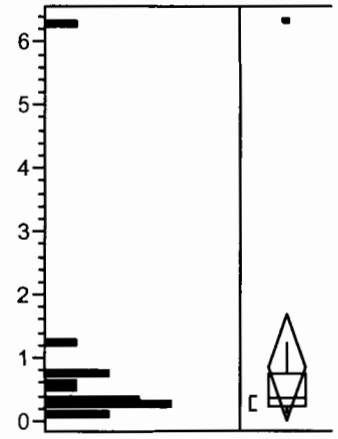			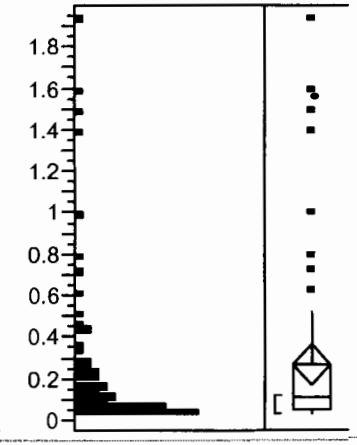			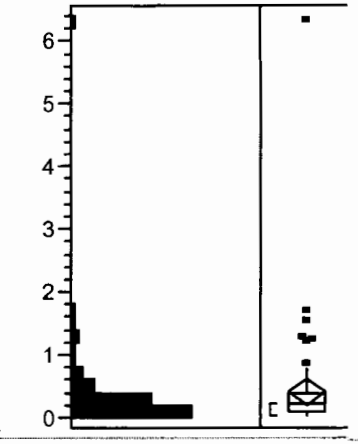			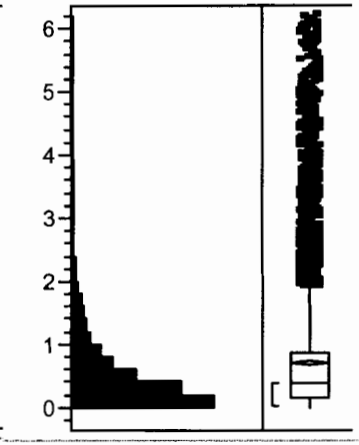			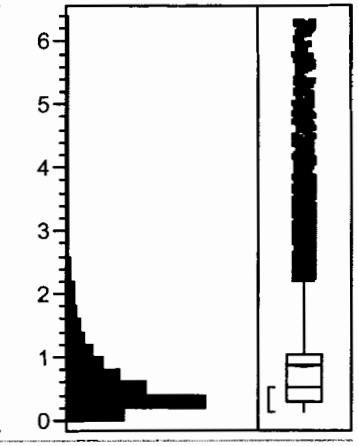		
Quantiles			Quantiles			Quantiles			Quantiles			Quantiles		
100.0%	maximum	6.2800	100.0%	maximum	1.9300	100.0%	maximum	6.2800	100.0%	maximum	6.1800	100.0%	maximum	6.2600
99.5%		6.2800	99.5%		1.9300	99.5%		6.2800	99.5%		5.2300	99.5%		5.5100
97.5%		6.2800	97.5%		1.6938	97.5%		3.1554	97.5%		3.4298	97.5%		3.6800
90.0%		3.2560	90.0%		0.7310	90.0%		0.9413	90.0%		1.7290	90.0%		2.0100
75.0%	quartile	0.7300	75.0%	quartile	0.2675	75.0%	quartile	0.3853	75.0%	quartile	0.8600	75.0%	quartile	1.0400
50.0%	median	0.3700	50.0%	median	0.1100	50.0%	median	0.2120	50.0%	median	0.3800	50.0%	median	0.5200
25.0%	quartile	0.2400	25.0%	quartile	0.0500	25.0%	quartile	0.0998	25.0%	quartile	0.1700	25.0%	quartile	0.2800
10.0%		0.1420	10.0%		0.0300	10.0%		0.0395	10.0%		0.0800	10.0%		0.1900
2.5%		0.1300	2.5%		0.0300	2.5%		0.0291	2.5%		0.0400	2.5%		0.1500
0.0%	minimum	0.1300	0.0%	minimum	0.0300	0.0%	minimum	0.0210	0.0%	minimum	0.0000	0.0%	minimum	0.1300
Moments			Moments			Moments			Moments			Moments		
Mean		0.8326667	Mean		0.2650000	Mean		0.4093788	Mean		0.7060930	Mean		0.8636090
Std Dev		1.5352686	Std Dev		0.3951524	Std Dev		0.8151265	Std Dev		0.8926774	Std Dev		0.9406976
Std Err Mean		0.3964046	Std Err Mean		0.0486399	Std Err Mean		0.1003351	Std Err Mean		0.0089268	Std Err Mean		0.0094070
upper 95% Mean		1.6828680	upper 95% Mean		0.3621407	upper 95% Mean		0.6097621	upper 95% Mean		0.7235916	upper 95% Mean		0.8820489
lower 95% Mean		-0.017535	lower 95% Mean		0.1678593	lower 95% Mean		0.2089954	lower 95% Mean		0.6885944	lower 95% Mean		0.8451691
N		15	N		66	N		66	N		10000	N		10000

The amount of crab consumed per person is shown in Figure 7.9. It is readily apparent that males typically consumed significantly larger amounts of crab per meal than females in the model simulations.

Figure 7.9 Frequency distribution of the amount of crab consumed from Hospital Beach.

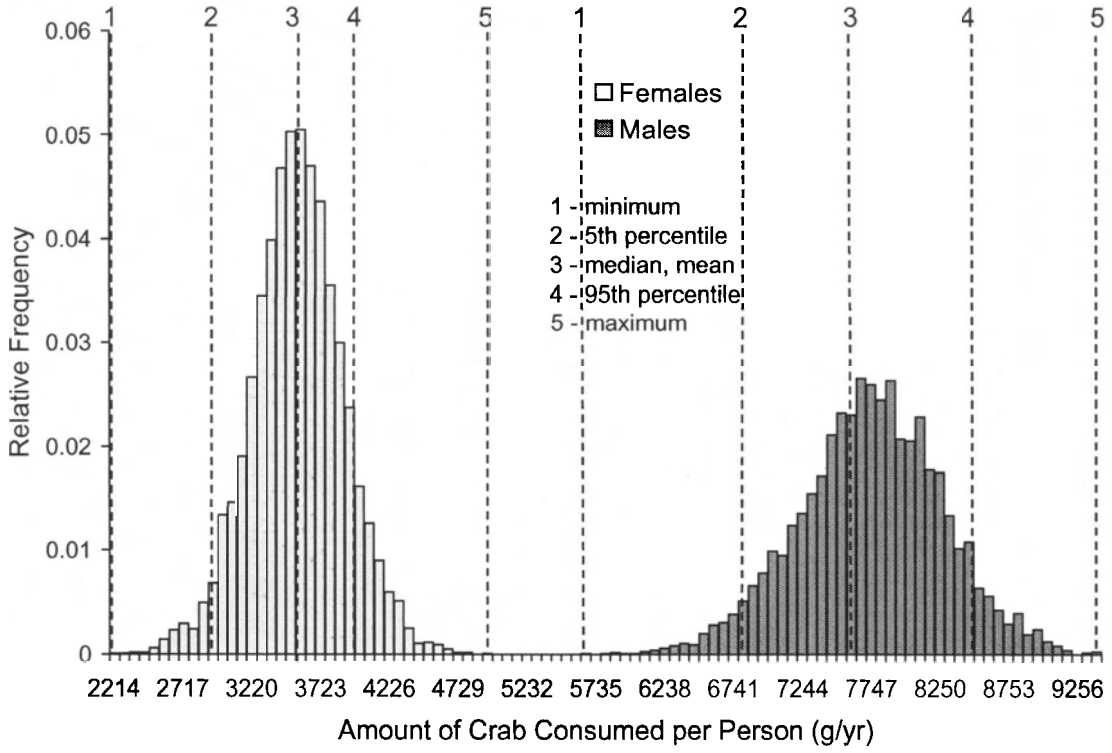

The predicted LADD from the model simulation is shown for all persons, (Figure 7.10a) and for each gender (Figure 7.10b). The probability distributions for the lifetime cancer risk associated with the consumption of crabs from Hospital Beach are shown in Figure 7.11. The predicted lifetime cancer risk from consumption of contaminated crabs is shown for all persons, (Figure 7.11a) and for each gender (Figure 7.11b). The mean lifetime cancer risks estimated in Chapter 6 using the deterministic US EPA risk model for each age group are shown on Figure 7.11a for comparison.

Figure 7.10 Relative Frequency distributions of lifetime average daily dose estimated for the consumption of crabs from the Inner Harbour: a) all persons, b) genders identified.

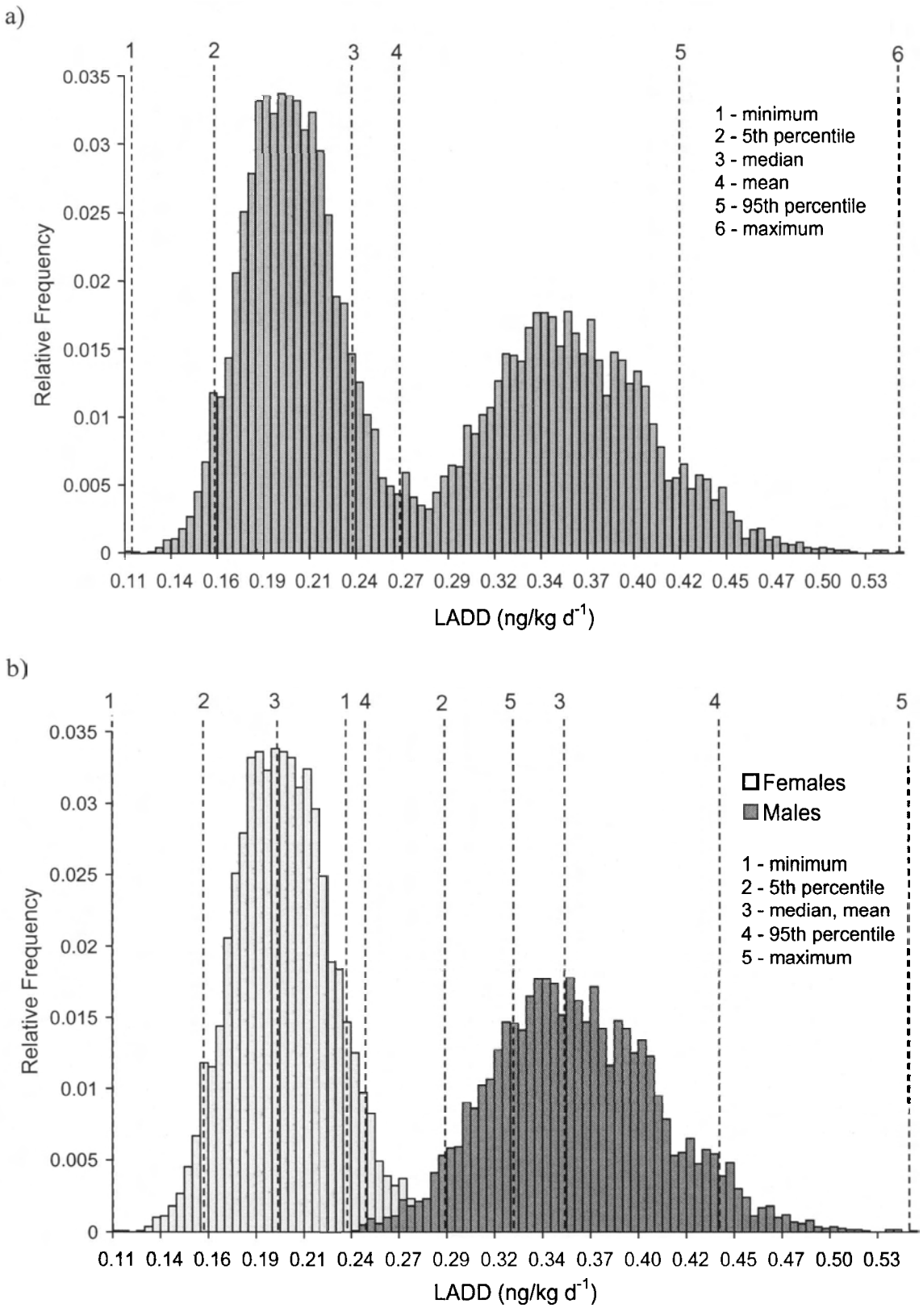

Figure 7.11 Probability distributions for lifetime cancer risk from the consumption of crabs collected from Hospital Beach: a) both genders, b) genders separated.

a)

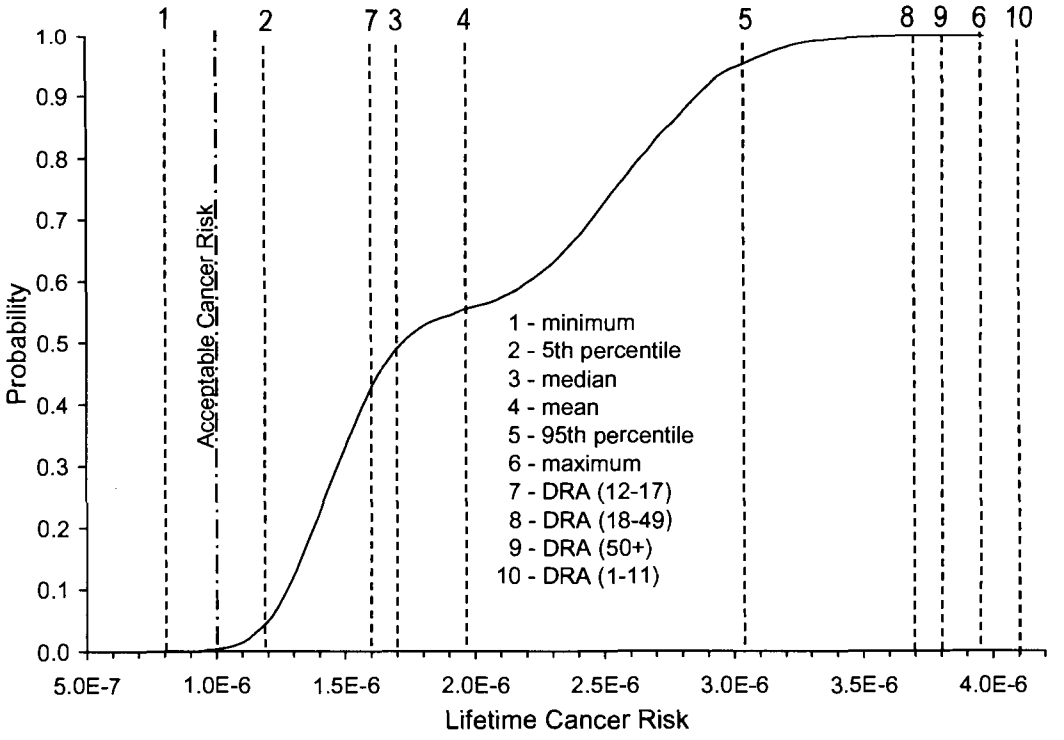

b)

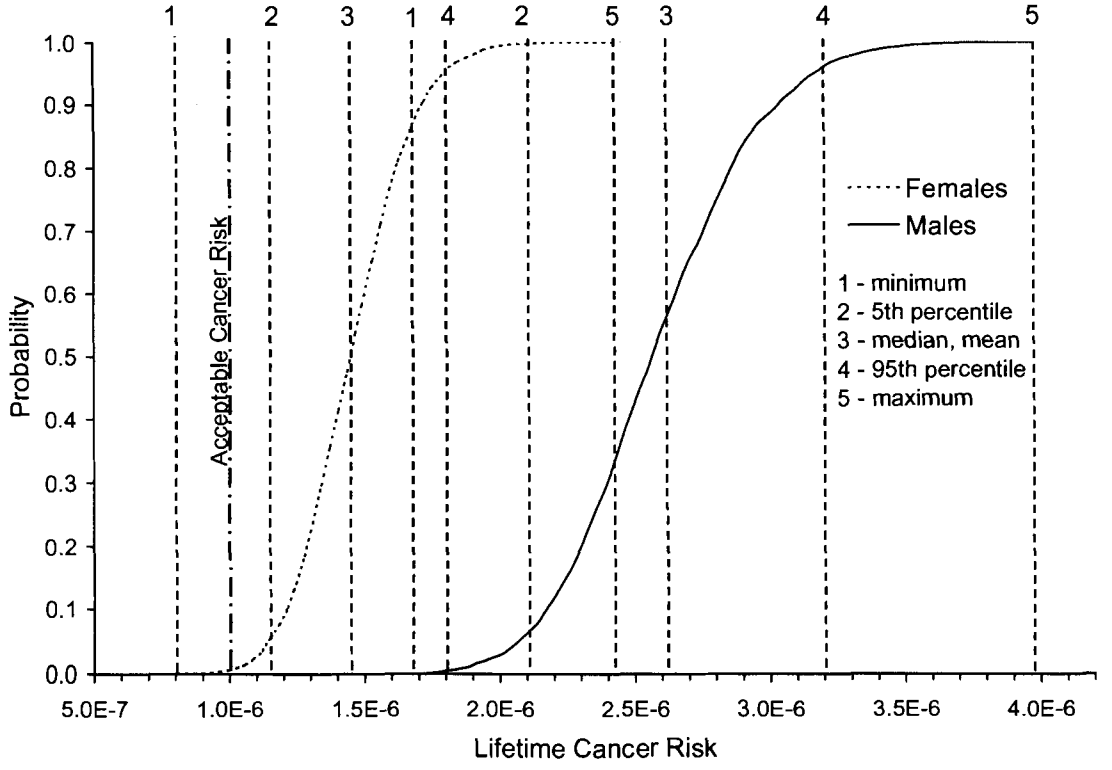

The mean lifetime cancer risks estimated for different age groups in the deterministic risk assessment (Chapter 6) are indicated on Figure 7.11a for comparison. The mean lifetime cancer risk estimated by the stochastic model, 1.97E-6, is between the mean estimated risk of 1.6E-6 for 12-17 year olds and 3.7E-6 estimated for adults aged 18-49 obtained from the deterministic risk model. The maximum risk estimated by the Monté Carlo approach, 4.0E-6, was between the mean risks estimated for adults over 50 years old, 3.8E-6, and the most conservative risk level for children aged 1-11, 4.1E-6.

Figure 7.11b shows that the estimated lifetime cancer risk distribution for males is significantly greater than that for females. This reflects the difference in consumption of crab tissue (Figure 7.9) and lifetime average daily dose Figure 7.10b between males and females.

Table 7.8 and Table 7.9 present the model output estimates for exposure and risk associated with consuming dungeness crabs from Hospital Beach and Kitamaat Village respectively. These risk estimates were performed using parameters based on the measured concentrations of PAH in the hepatopancreas and muscle tissues. The LADD and risk estimates are generally an order of magnitude greater for consuming crabs from Hospital Beach. The lifetime cancer risk associated with consuming crabs from Hospital Beach near the smelter lagoon discharge exceeds the acceptable cancer risk of 10^{-6}. The mean risk is 1.98 E-6, while the maximum risk is 3.97 E-6. Generally, it is safer to consume crabs further away from the source of PAH contamination, the maximum risk of excess cancer from consuming crabs collected near the village, 7.57 E-7, is lower than the acceptable cancer risk of 10^{-6}.

Table 7.8 Descriptive statistics of model output for consumption of crabs caught at Hospital Beach near smelter

Statistic	Ch_{HB} (ng/g)	Cm_{HB} (ng/g)	Ac/yr (g)	LADD (ng/kg d^{-1})	Risk
SD	1.36	0.89	2128	0.09	6.35 E-7
Minimum	0.01	0.004	2214	0.11	8.03 E-7
5^{th} percentile	0.15	0.05	3077	0.16	1.20 E-6
Median	0.81	0.38	3947	0.24	1.72 E-6
Mean	1.28	0.71	5396	0.27	1.98 E-6
95^{th} percentile	4.09	2.52	8327	0.42	3.03 E-6
Maximum	9.88	6.18	9400	0.54	3.97 E-6

Table 7.9 Descriptive statistics of model output for consumption of crabs caught near Kitamaat Village

Statistic	$Ch_{village}$ (ng/g)	$Cm_{village}$ (ng/g)	Ac/yr (g)	LADD (ng/kg day)	Risk
SD	0.14	0.05	2155	0.016	1.20 E-7
Minimum	0.05	0.02	2066	0.019	1.40 E-7
5^{th} percentile	0.15	0.05	2975	0.030	2.18 E-7
Median	0.30	0.12	3971	0.044	3.21 E-7
Mean	0.33	0.12	5378	0.050	3.66 E-7
95^{th} percentile	0.60	0.21	8376	0.078	5.67 E-7
Maximum	0.78	0.23	9541	0.104	7.57 E-7

The Monté Carlo, micro-exposure event model was run in two different modes: 1) with an exposure frequency defined by the minimum exposure level of 0 meals per month (Figure 7.2) obtained from the Haisla dietary survey (Kitamaat Village Council, 1996), and 2) with a minimum exposure of 1 meal per month. The differences in LADD and risk estimates from these two simulation modes are shown in Figure 7.12. The LADD and risk estimates from the deterministic risk assessment (Chapter 6) are indicated for comparison.

Figure 7.12 Comparison of model estimates calculated with min EF = 0, and min EF = 1 meal per month a) Lifetime Average Daily Dose, and b) Lifetime Cancer Risk

a)

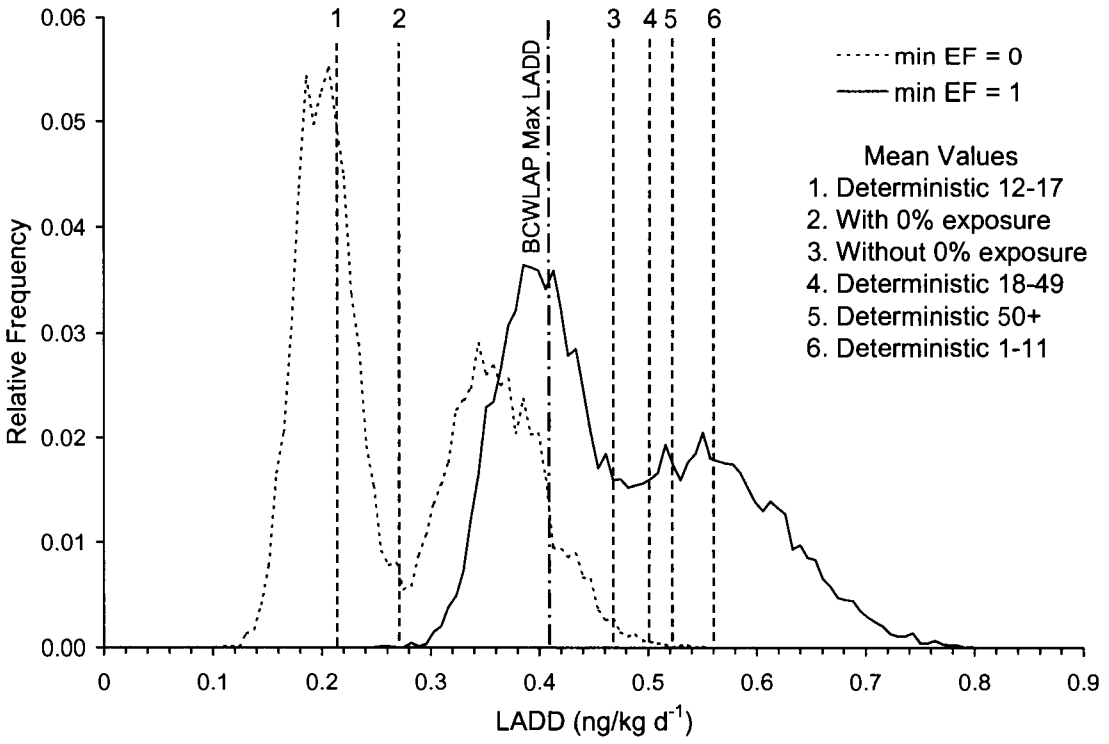

b)

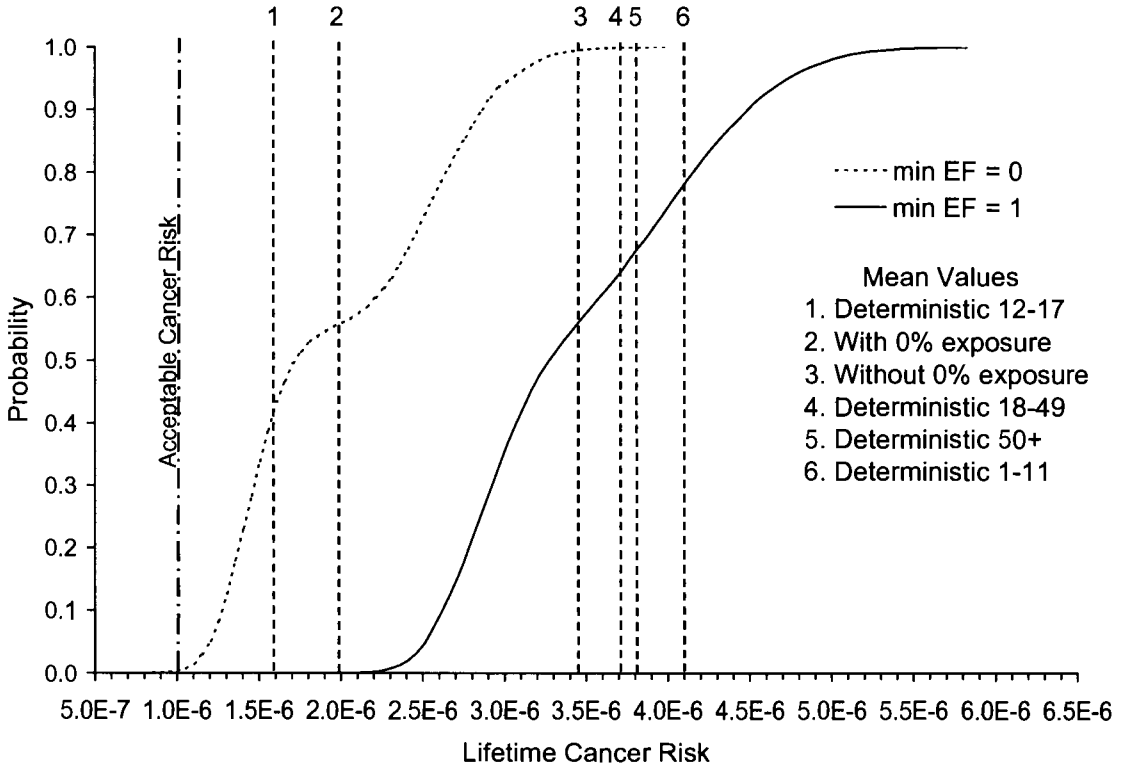

Table 7.10 shows the descriptive statistics for the LADD and risk when the model is run with a minimum EF of 0 meals per month, and a minimum EF of 1 meal per month for consumption of crabs obtained from Hospital Beach.

Table 7.10 Descriptive statistics of model output for consumption of crabs from Hospital Beach with a minimum EF = 0 and a minimum EF = 1 meal per month.

	Min EF = 0			Min EF = 1		
Statistic	Ac/yr (g)	LADD (ng/kg d^{-1})	Risk	Ac/yr (g)	LADD (ng/kg d^{-1})	Risk
SD	2128	0.09	6.35E-7	2539	0.10	7.19E-7
Minimum	2214	0.11	8.03E-7	5616	0.25	1.85E-6
5^{th} Percentile	3077	0.16	1.20E-6	6727	0.34	2.51E-6
Median	3947	0.24	1.72E-6	7562	0.45	3.27E-6
Mean	5396	0.27	1.98E-6	9396	0.47	3.45E-6
95^{th} Percentile	8327	0.42	3.03E-6	12744	0.65	4.72E-6
Maximum	9400	0.54	3.97E-6	13977	0.80	5.83E-6

The maximum risk estimated when a minimum exposure frequency of 1 meal per month, (5.83E-6) was significantly greater than that obtained with a minimum exposure frequency of 0 meals per month (3.97E-6). However, it is expected that the minimum EF = 0 is a more realistic scenario for most consumers of crab. Figure 7.12 shows that the mean lifetime cancer risk when the minimum EF=1 is similar to the mean lifetime cancer risk estimates obtained from the deterministic risk assessment.

The stochastic risk assessment was also performed using parameters based on measured hepatopancreas concentrations for all four sites, and predicted, or combined measured and predicted concentrations of PAH in the muscle tissues of crabs collected at four sites, Hospital Beach, Kitamaat Village, Wathlsto Creek, and Kildala Arm. Table

7.11 - Table 7.14 summarise the output estimates from simulations run for consumption of crabs from each site. The risk assessment model was run using either predicted, or combined measured and predicted muscle BaP-TEF concentrations for the Hospital Beach (HB) and Kitamaat Village (KV) sites. The combined predicted and measured (M&P) muscle BaP-TEF tissue concentrations were obtained by filling the existing data set of measured concentrations with those predicted by the PBTK model. Measured concentrations of PAH in muscle were not available for the Wathlsto Creek and Kildala Arm sites, therefore, PBTK model predicted values were used. Table 7.11 displays the descriptive statistics for the concentration of BaP-TEF in the muscle generated by the model simulations for each site.

Table 7.11 Descriptive statistics for the concentrations of BaP-TEF in muscle tissue generated by model simulation based on either predicted, or combined measured and predicted (M&P) muscle tissue concentrations, (ng/g wet weight).

Statistic	Wathlsto Predicted	Kildala Predicted	KV Predicted	KV M&P	HB Predicted	HB M&P
SD	0.03	0.10	0.03	0.04	0.28	0.58
Minimum	0.0063	0.0003	0.0170	0.0129	0.0017	0.0012
5th Percentile	0.022	0.005	0.039	0.038	0.025	0.020
Median	0.05	0.03	0.08	0.08	0.15	0.17
Mean	0.06	0.07	0.08	0.09	0.24	0.36
95th Percentile	0.11	0.26	0.14	0.16	0.81	1.37
Maximum	0.14	0.80	0.16	0.21	1.90	5.83

The descriptive statistics for the concentrations of BaP-TEF in the hepatopancreas of consumed crabs simulated for each site are presented in Table 7.12.

Table 7.12 Descriptive statistics for the concentrations of BaP-TEF in hepatopancreas tissue generated by model simulation with either predicted, or combined measured and predicted (M&P) muscle tissue concentrations, (ng/g wet weight).

Statistic	Wathlsto Predicted	Kildala Predicted	KV Predicted	KV M&P	HB Predicted	HB M&P
SD	0.02	0.083	0.14	0.14	1.40	1.35
Minimum	0.004	0.0002	0.05	0.07	0.02	0.02
5th Percentile	0.02	0.003	0.15	0.15	0.15	0.16
Median	0.04	0.026	0.30	0.31	0.81	0.79
Mean	0.05	0.056	0.33	0.33	1.29	1.25
95th Percentile	0.10	0.212	0.60	0.60	4.12	3.98
Maximum	0.12	0.712	0.78	0.78	9.90	9.83

There were no significant differences in the amount of crab consumed at each site in the model simulations. The lifetime average daily dose distributions estimated for the consumption of crabs from each site based on measured and/or predicted tissue concentrations are presented in Table 7.13.

Table 7.13 Descriptive statistics for the estimated LADD (ng/kg d^{-1}) based on either predicted, or combined measured and predicted (M&P) muscle tissue concentrations.

Statistic	Wathlsto Predicted	Kildala Predicted	KV Predicted	KV M&P	HB Predicted	HB M&P
SD	0.01	0.01	0.01	0.01	0.04	0.05
Minimum	0.01	0.01	0.01	0.02	0.05	0.07
5th Percentile	0.012	0.014	0.024	0.025	0.076	0.097
Median	0.02	0.02	0.03	0.03	0.11	0.14
Mean	0.02	0.02	0.04	0.04	0.13	0.16
95th Percentile	0.03	0.04	0.06	0.06	0.19	0.25
Maximum	0.04	0.05	0.08	0.08	0.26	0.32

The estimated lifetime cancer risk distributions based on combined measured and predicted muscle tissue concentrations are described in Table 7.14.

Table 7.14 Descriptive statistics for the estimated lifetime cancer risk based on either predicted, or combined measured and predicted (M&P) muscle tissue concentrations.

Statistic	Wathlsto Predicted	Kildala Predicted	KV Predicted	KV M&P	HB Predicted	HB M&P
SD	4.67E-8	5.45E-8	9.10E-8	9.45E-8	2.95E-7	3.77E-7
Minimum	6.23E-8	6.40E-8	9.46E-8	1.31E-7	3.58E-7	4.77E-7
5th Percentile	8.86E-8	1.03E-7	1.72E-7	1.80E-7	5.55E-7	7.08E-7
Median	1.24E-7	1.48E-7	2.44E-7	2.52E-7	8.00E-7	1.01E-6
Mean	1.44E-7	1.70E-7	2.81E-7	2.93E-7	9.14E-7	1.17E-6
95th Percentile	2.23E-7	2.60E-7	4.32E-7	4.53E-7	1.41E-6	1.79E-6
Maximum	2.91E-7	3.38E-7	5.62E-7	6.11E-7	1.93E-6	2.36E-6

The lifetime cancer risk estimates for all four sites based on both measured and predicted tissue concentrations are presented for comparison in Figure 7.1. Mean values and the acceptable lifetime cancer risk are indicated.

Figure 7.13 Lifetime cancer risk estimates based on measured hepatopancreas and measured and predicted muscle BaP-TEF concentrations for consumption of crabs from each site.

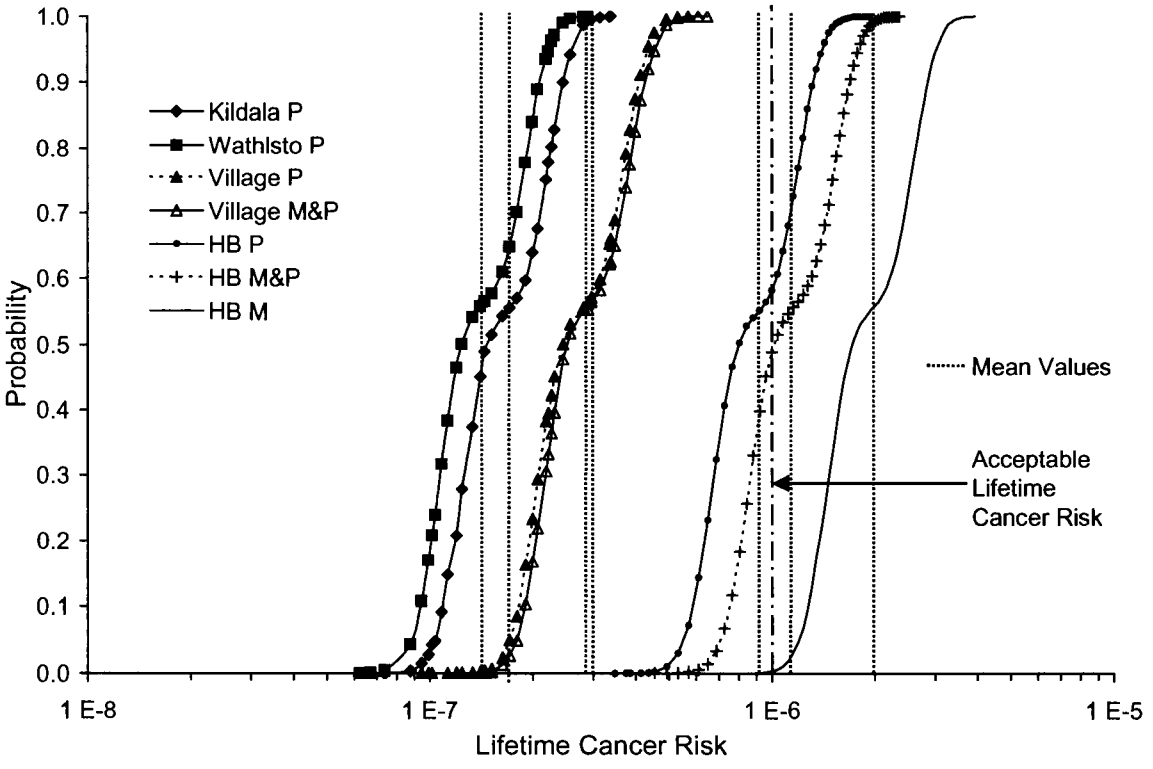

Figure 7.14 shows a plot of lifetime cancer risk model output obtained for sensitivity analysis of input parameters.

Figure 7.14 Plot of lifetime cancer risk descriptive statistics for sensitivity analysis

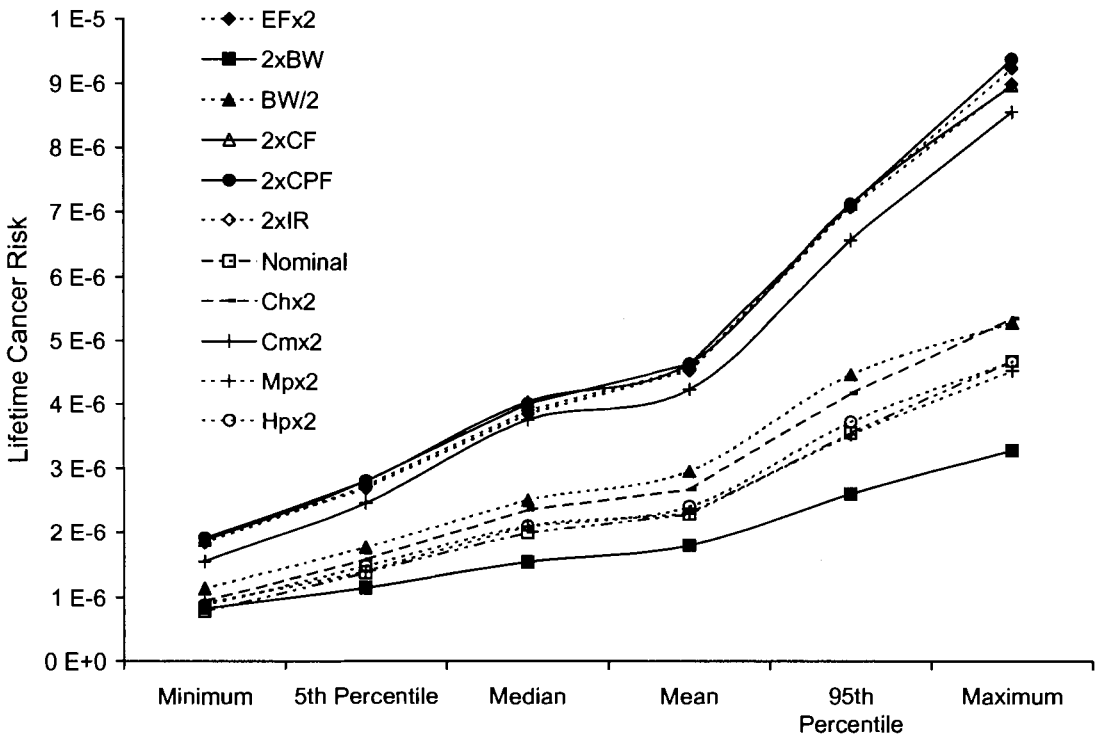

Parameter values for Ch, Cm, EF, IR, Hp, Mp, CF, and CSF were individually multiplied by a factor of 2 prior to model runs to examine the effect on model output. Body weight (BW), which is in the denominator of Equation 7.1, was also divided by a factor of 2 for comparison.

7.7 Discussion

7.7.1 Adaptations of the Price Micro-Exposure Event Model

There are a number of adaptations or changes that were made in the micro-event exposure (MEE) model developed by Price *et al.* (1996) for this risk assessment. First, the Price MEE model is designed to simulate the exposure of fishermen to toxic compounds in fish, thus has provision for fishermen moving away and it is also designed to look at exposure over a relatively short period of time in a lifetime, 7 years (Price, 1996). The current risk assessment is designed to examine the potential health effects for an aboriginal population that does not move or change location over the course of an individual's lifetime. Therefore, no provision for individuals moving has been incorporated into the MEE, and exposure is simulated over the duration of a lifetime.

The Price MEE used an annual consumption rate to simulate exposure over the course of each year (Price, 1996). The current MEE incorporates monthly changes in exposure frequency and intake rates over the course of each year. This adaptation has been made to accommodate seasonal differences in EF and IR that were observed in the Haisla Diet Survey (Kitamaat Village Council, 1996). This adaptation allows for greater temporal variability in crab consumption rates for each simulation.

The current MEE model is designed to incorporate concentrations of potentially toxic compounds such as BaP-TEF in both the hepatopancreas and muscle tissue of crabs. This adaptation was made because the Price model was designed to use a concentration of toxic compound in only the muscle tissue. It is expected that most consumers of fish

eat only the meat portion of the fish. However, consumers of crab may eat both the muscle and hepatopancreas, and the concentrations of BaP-TEF in each tissue are quite different (Table 7.1, Figure 7.7 and Figure 7.8).

7.7.2 Advantages of the Stochastic, Micro-Exposure Model Approach

The stochastic risk assessment approach is more powerful than the deterministic approach because the ability to incorporate variability in input parameters provides a more realistic assessment of risk for a population. For example, the exposure frequency that describes the number of meals per month allows for a number of possible scenarios over time, including 0 meals per month. This is important because the frequency distributions that describe exposure frequency (Figure 7.2) in the population show that respondents in the dietary survey indicated that the ate 0 meals of crab per month more often than they ate one or more meals. The standard equation for the deterministic exposure model is not able to accommodate monthly changes in exposure or an exposure frequency of 0 meals per month. As a result, the LADD and risk estimates can be considered to be much more "realistic" than those estimated using the deterministic approach.

Another advantage of the micro-exposure event model approach is the ability to accommodate temporal changes in the input variables, such as seasonal changes in consumption rates, and age related changes in body weight, exposure frequency and intake rates. This allows for a better assessment of the range of exposure and lifetime cancer risk that might be for a given population.

The stochastic, micro-exposure event stochastic risk assessment approach has enabled the incorporation of detailed information on the consumption behaviour and physical characteristics of the aboriginal population situated along the shore of Kitimat Arm. Thus, the greatest advantage of stochastic model is the ability to represent variability in the input parameters that describe exposure, such as intake rate, exposure frequency, tissue concentration data, and human body weight over the lifetime of a population of individuals for a given population The result of this incorporation of human variability can be seen in Figure 7.11. Variability in consumption rates related to gender can be observed in the probability distributions estimated by the stochastic model for lifetime cancer risk. Figure 7.11b shows that probability curve for female risk is steeper than that for males. This reflects the gender related differences in the consumption of crabs observed in Figure 7.9, and the LADD (Figure 7.10). Therefore, the ability to estimate risk for a "population of individuals" rather than for a mean characteristics of a population allows the risk assessor to examine variability within a population and pick out trends related to differences in gender or other influences on human behaviour.

7.7.3 Model Parameterisation

The model input distributions were based on statistical analysis of the population and tissue concentration data. Lognormal distributions were chosen for human body weight because this parameter is known to be lognormally distributed (Burmaster, 1997). Body weight statistics were obtained from the Haisla Diet Survey (Kitamaat Village Council, 1996). Concentrations of PAH in hepatopancreas and muscle tissues of dungeness crabs collected in Kitimat Arm were also found to be lognormally distributed

(Chapter 2), as shown in Figure 7.7 and Figure 7.8. The probability distributions for exposure frequency, the number of meals consumed per month in winter or summer, appear to be lognormal (Figure 7.2). However, the probability distributions for the amount of crab consumed per meal appear to be normally distributed (Figure 7.3).

7.7.4 Input Parameter Uncertainty

There are a number of sources of uncertainty in the current risk assessment which should be recognised. This uncertainty is inherent in the input parameters used for simulating exposure to PAH through the consumption of PAH contaminated crabs. These input parameters include those that describe human factors affecting dietary uptake, and the characteristics of the food that is consumed.

7.7.4.1 Parameters Describing Dietary Exposure

The parameters that describe exposure based on human factors are intake rate, exposure frequency, and body weight. The population statistics used to characterise these parameters are based on a subset of an aboriginal population that responded to questionnaires used to obtain information about age, gender, body weight, and consumption rates and frequencies. It is assumed that this information adequately reflects the overall population. There is also error and uncertainty in the recollections of individual estimates of exposure frequency and meal portion sizes. Respondents were asked to remember how often they consumed various fish and shell fish species over both winter and summer months. Respondents used different sized mounds or bowls to indicate meal portion size (Kitamaat Village Council, 1996). There is additional error

inherent in the body weights; most individuals self reported these without use of a scale at the time this information was recorded. Finally, probability distributions for gender, body weight, exposure frequency, and meal portion sizes were developed from the available data. These probability distributions were not fit to generic probability distributions. As such, there may be gaps in the distributions which may have been filled if a larger number of respondents were involved in the dietary survey.

7.7.4.2 Crab Tissue Concentration Data

There is a relatively large sample size of BaP-TEF concentrations determined in crab hepatopancreas tissues for each of the four sites (Chapter 2). However, very few muscle tissue samples were tested for analysis. The model generated muscle tissue concentrations for Hospital Beach are based on only 15 samples, and only 4 for the village sites in contrast to 66 and 53 BaP-TEF hepatopancreas tissue concentrations for the Hospital Beach and Kitamaat Village sites respectively. Therefore, there is much less certainty in the muscle tissue concentrations used for the risk assessment. In order to fill this data gap, the PBTK model was used to predict BaP-TEF concentrations in the muscle tissues, based on the concentration of benzo[a]pyrene in the hepatopancreas, and the relationships between other individual PAH in the muscle with benzo[a]pyrene. This approach is described in detail in Chapter 5.

The same concentration distribution of BaP-TEF in crab tissues was used over the lifetime of the individual. In actual circumstances, the concentrations of PAH in crabs collected from Kitimat Arm may decline or increase depending on the rate of input from industry over time.

7.7.5 Random Number Generator

In this study, the Excel® random number generator, RAND, coupled with a simple lognormal distribution function in Visual Basic®, was also found to be inadequate for generating lognormal distributions (Figure 7.4). RAND was found to produce a very rough frequency distribution, and repeatedly picked similar values in the tail of the lognormal distribution. This problem was also reported by Barry (1996). Therefore, alternative methods were sought to generate lognormal distributions. An improved lognormal number generator function was coded into Visual Basic®. This function, Lognormalcalc, presented in Appendix D, uses two random numbers generated from RAND for each lognormal number generated. Lognormalcalc calls a function, Randshuffle, that stores 100 random numbers and then randomly picks a new number and replaces that random number from the stored numbers. This prevents the newly generated number from having dependencies on the previously generated number. In this manner, Lognormalcalc solves the problem of dependency on previously generated random numbers that is known to occur in RAND. In this manner, the random number generator was significantly improved as shown in Figure 7.5

Lognormal distributions obtained using the RAND-Lognormalcalc combination were compared to those obtained from RAND and the simple lognormal function, from Crystal Ball 4.0, an accepted program used commonly as a Microsoft Excel add-in for Monté Carlo risk assessments, and Urandom, an ultra random number generator developed by Marsaglia and Zaman (1991). It should be noted that Crystal Ball does not use RAND (Decisioneering 1996). Lognormal distributions (10,000 iterations) for the concentration of PAH TEF in the hepatopancreas of crabs were obtained using each

program. These lognormal distributions were compared statistically. There appeared to be no differences between the lognormal distributions obtained from RAND-lognormalcalc, Urandom-lognormalcalc and Crystal Ball 4.0 (Figure 7.6). Therefore, the RAND-lognormalcalc random number generator was considered to be acceptable for generating lognormal input distributions for the Monté Carlo simulations. However, the output from RAND with a simple function for deriving lognormal output was quite different, and was therefore no longer used in the model.

7.7.6 Model Stability and Convergence

The results from three independent simulations with 10,000 iterations were compared to test the convergence and stability of the model (Table 7.3 - Table 7.5). Thompson (1992) stated that for two independent runs of 10,000 each, the estimated means, standard deviations, variances, and the 90^{th} and 95^{th} percentiles should agree within 1%. Also, for two independent runs of 10,000 and 20,000 iterations, all of the summary statistics except the sensitive 95^{th} percentile and maximum should agree within 1% (Thompson 1992). For two runs where no minimum tissue concentration was used, the estimated, standard deviation, 5^{th} percentile, median, mean, and 95^{th} values all agreed within 1%. Only the mean relative precision of the minimum, 1.14%, and maximum, 2.35%, values varied slightly over 1% (Table 7.3). The same trend was found when the descriptive statistics were compared between a run of 10,000 and a separate run of 20,000 iterations (Table 7.4).

The variability in the minimum, and maximum values, was very similar when minimum tissue concentrations were used in the model simulation (Table 7.5). The mean

relative precision was 2.11%, and 1.07% for minimum and maximum values respectively. From these results, it was concluded that 10,000 iterations were sufficient to ensure convergence and stability of the output distributions according to the criteria of Thompson *et al.* (1992).

7.7.7 Sensitivity Analysis

A sensitivity analysis was performed to examine the sensitivity of the stochastic model to important input parameters. The deterministic, one at a time analysis of each factor was performed, holding all others constant at nominal values according to the method of Morgan and Henrion (1990). Each parameter was multiplied by a factor of 2 to examine the resulting effect on lifetime cancer risk output estimates.

The results showed that the model was equally sensitive to changes in intake rate, IR, exposure frequency, EF, cancer potency factor, CPF, and conversion factor, CSF (Figure 7.14). Changes in these parameters resulted in a similar increase in the resultant lifetime cancer risk. The concentration of BaP-TEF in muscle, Cm, was also very sensitive, and a two fold increase in both Ch and Cm, resulted in a two fold increase in risk. The concentration of BaP-TEF in the hepatopancreas, Ch, was less sensitive than Cm. This shows that it is important to have adequate data describing the concentration of PAH in muscle tissues, and underlines the usefulness of the PBTK for predicting concentrations when sufficient data is unavailable. The model was less sensitive to changes in body weight, BW, than most of the other model parameters. Body weight is in the denominator of Equation 7.1, therefore it was also divided by a factor of 2 The least

sensitive parameters of the model were those for the percent composition of muscle, Mp and hepatopancreas, Hp in the crab.

7.7.8 Discussion of Monté Carlo Simulation Results

7.7.8.1 Comparison of Simulated and Measured Tissue Concentrations

The model simulated BaP-TEF tissue concentration distributions are presented in Figure 7.7and Figure 7.8. The model predicted concentrations of BaP-TEF in the hepatopancreas were very similar to those determined in the tissues of crabs collected from Hospital Beach. A statistical comparison of simulated and measured BaP-TEF in the hepatopancreas of crabs caught at Hospital Beach is shown in Table 7.6. The simulated hepatopancreas tissue concentrations had lognormal distributions similar to that observed for the measured concentrations determined in the tissues by GC/MS. Table 7.7 compares the model simulated BaP-TEF concentrations in the muscle with measured, and those predicted by the PBTK model. The Monté Carlo simulated BaP-TEF concentrations in the muscle were statistically very similar to the limited number of measured, or combined measured and predicted tissue concentrations, although the PBTK model predicts concentrations that are somewhat lower than measured concentrations (Chapter 5).

The simulated values generated when a minimum value was specified for characterising the lognormal distribution had minimum and maximum values that were closer to the combined measured and predicted tissue concentration values than the simulations where no min was specified. However, as stated previously, it is more

realistic to assume that crabs with lower tissue concentrations than those measured may be encountered, and the minimum concentration is influenced by the analytical detection limits.

For both simulated hepatopancreas and muscle tissues, the Monté Carlo simulations generated lognormal distributions of numbers that were statistically quite similar to the combined measured and predicted BaP-TEF tissue concentration distributions in the hepatopancreas and muscle. This shows that the model was effective for predicting BaP-TEF tissue concentrations in the Monté Carlo simulations.

7.7.8.2 Annual Consumption of Crab

The Monté Carlo simulation produced a bimodal frequency distribution that describes the amount of crab consumed per person (Figure 7.9). The frequency distribution shows that males are predicted to consume greater amounts of crab per year than females. Each mode of the frequency distribution is normally distributed and represents a fusion of the custom distributions for exposure frequency and intake rate. The variability in consumption by males is a little greater than that for females. The mode describing the amount consumed by males is shorter and wider, while the distribution representing female consumption is narrower and higher around the mean.

The maximum amount of crab consumed by females, 4918 g/yr, is less than the minimum amount of crab consumed by males, 5627 g/yr. The mean amount of crab consumed by males, 7711 g/yr, is 2.2 fold greater than the mean amount consumed by

females, 3521 g/yr over a year. The maximum amount of crabs consumed by males, 9400 g/yr is almost twice (1.9) the maximum amount consumed by females.

7.7.8.3 Lifetime Average Daily Dose Associated with Hospital Beach Crab Consumption

The frequency distribution that describes the LADD is bimodal as may be expected based on the frequency distribution for the amount of crab consumed per year (Figure 7.10a). Again, the greater LADD values in the distribution represent predicted values for males, and the lower values represent the daily dose expected for females (Figure 7.10b). However the frequency distributions, for each gender, overlap. The minimum LADD for males, 0.24 ng/kg d^{-1}, is lower than the maximum for females, 0.33 ng/kg d^{-1}. This is due to the fact that the LADD frequency distribution represents a synthesis of the distributions for BaP-TEF concentrations in the muscle and hepatopancreas, and the frequency distributions representing intake rate, exposure frequency, and body weight.

The mean LADD for males, 0.36 ng/kg d^{-1} was 1.8 fold greater than the mean LADD for females, 0.20 ng/kg d^{-1}. However, the maximum male LADD, 0.54 ng/kg d^{-1}, was only 1.6 fold greater than the maximum LADD for females due to the difference in shape for each mode of the frequency distribution.

7.7.8.4 Lifetime Cancer Risk Associated with Consumption of Crabs from Hospital Beach

The lifetime cancer risk for consuming crabs from the most PAH contaminated area of Kitimat Arm is summarised in Figure 7.11a. The minimum cancer risk is 8.0E-7, while the maximum risk is 4.0E-6. This maximum risk is 4 times the acceptable cancer

risk level (1.0E-6). The mean cancer risk is 2.0E-6 for the entire population, double the acceptable level. The shape of the probability plot suggests that it is bimodal in nature. This might be expected from the bimodal nature of the frequency distributions for the amount of crab consumed and LADD.

7.7.8.5 Gender Differences in Lifetime Cancer Risk

Gender differences in the annual consumption of crab meals and LADD result in similar differences in the lifetime cancer risk estimated for both males and females. The differences in risk estimates are shown in Figure 7.11b. It is readily apparent that females have a significantly lower lifetime cancer risk than males, mainly due to lower consumption rates. The mean cancer risk for females associated with the consumption of crabs from Hospital Beach, 1.5 E-6, is 1.8 fold lower than the mean risk for males, 2.6 E-6. While the mean risk for females is lower than that for males, it exceeds the acceptable cancer risk level. In fact, the 1st percentile risk value for females is 1.04 E-6. This means that 99% of women consuming crabs from Hospital Beach will have an excess lifetime cancer risk. All risk estimates for males were in excess of the acceptable cancer risk level. The model predicts that 95% of males will have a cancer risk greater than twice the acceptable cancer level, and 5% of males will have a risk greater than 3 times the acceptable cancer level.

7.7.8.6 Comparison of Cancer Risk Calculated by Deterministic and Stochastic Risk Assessment Models

The mean risk predicted by the stochastic model for crabs consumed from Hospital Beach is between the mean risk estimated for youth (12-17 yrs) and adults (19-

49 yrs) using the deterministic model. The maximum risk is between the mean risk calculated for mature adults (50+ yrs) and children (1-10 yrs), (Figure 7.11a).

These risk estimates were obtained by running the stochastic model with an exposure frequency of 0 meals per month. Figure 7.2 shows that the highest probability for the number of meals consumed per month for both males and females in summer and winter months is 0. This is very significant because the deterministic risk model has no provision for including probabilities of different exposure levels, only the mean exposure values. As a result, the LADD and risk levels estimated by the deterministic method are expected to be more conservative than those obtained using the stochastic model. In order to examine this further, the Monté Carlo simulations were performed after removing the probabilities for 0 meals per month, so that consumers always consumed crab between 1 to 8 times per month (Figure 7.2).

Figure 7.12a shows that the LADD and risk estimates are shifted to the right when the minimum exposure frequency of 0 meals per month is removed. The mean LADD, is increased from 0.27 ng/kg d^{-1} to 0.47 ng/kg d^{-1}, a 1.7 fold increase. Without the minimal exposure level, the LADD now exceeds the BC Ministry of Land Air Water and Parks acceptable limit of 0.41 ng/kg d^{-1} for benzo[a]pyrene equivalents. In addition, the mean LADD is much closer to the most conservative deterministic LADD estimates for mature adults and children (Figure 7.12a).

The risk estimates are similarly increased from a mean of 2 E-6 to 3.5 E-6 (Figure 7.12b) when the minimal exposure level of 0 meals of crab per month was removed. The mean risk was now much closer to the estimates obtained using the deterministic risk

model. The maximum risk level was increased to 5.8 E-6, almost 6 times the acceptable risk level. Therefore, presence or absence of the minimum EF of 0 meals per month illustrates the main difference between the LADD and risk estimates obtained by the two risk assessment approaches.

7.7.8.7 Lifetime Cancer Risk Associated with Consumption of Crabs from Four Sites in Kitimat Arm

The concentrations of PAH determined in crab tissues were highest in crabs obtained from Hospital Beach. The other sites that were examined had much lower PAH concentrations in the hepatopancreas. The risk estimates obtained from the stochastic model for all four sites are summarised in Figure 7.13. The risk estimates based on either measured or PBTK model predicted BaP-TEF muscle tissue concentrations show that consumers are only at an excess cancer risk when consuming crab tissues from Hospital Beach.

Crabs consumed from Kitamaat Village posed a greater health risk than those obtained from either Kildala Arm or Wathlsto Creek. The mean cancer risk estimates for the consumption of crabs collected near Kitamaat Village 2.8 – 2.9E-7, are approximately 3.5 fold lower than the acceptable cancer limit while the mean risks estimated for consuming Kildala Arm or Wathlsto Creek crabs are 6 and 7 fold lower respectively (Figure 7.13).

7.7.8.8 Uncertainty in Lifetime Cancer Risk Estimates

There is some uncertainty in the lifetime cancer risk estimates that is linked to the uncertainty in the concentration of PAH in the muscle tissues. This uncertainty is

represented in Figure 7.13. The greatest amount of uncertainty is related to the risk estimates for crabs consumed from Hospital Beach. The risk estimates are strongly related to the use of measured and PBTK model predicted BaP-TEF for the input distribution. If measured concentrations are used for the risk assessment, the mean estimated risk, 2.0 E-6, is 1.7 fold greater than the mean for combined measured and predicted values, 1.17E-6, and 2.2 fold greater than the mean for PBTK model predicted concentrations, 9.14E-7. As shown in Figure 7.13, the mean estimated risk is either above the acceptable cancer risk level, when measured, or combined measured and predicted concentrations are used, or below the acceptable risk, when only predicted concentrations are used. Analysis of the PBTK model predicted muscle concentrations indicated that they were under predicted in most cases (Chapter 5). Therefore, the "true" risk is probably closest to the risk estimated using measured BaP-TEF concentrations in the muscle tissue.

Figure 7.13 indicates that there is less uncertainty in the risk estimates for Kitamaat Village based on the combined measured and predicted muscle tissue concentrations. This is mainly because there were fewer, namely 4, measured muscle tissue concentrations that might influence the predicted muscle concentrations in the input distributions. Also, there was a smaller difference between the combined measured and predicted BaP-TEF concentrations compared to those observed for Hospital Beach.

Because the concentration of BaP-TEF in muscle tissues been shown to be a very sensitive parameter, it is important that a sufficient number of muscle tissue concentrations are available for the risk assessment to reduce uncertainty in the risk estimates.

7.7.8.9 Implications of Stochastic Risk Assessment for the Local Aboriginal Population

The results of the stochastic risk assessment have shown that consumption of crabs from sites in Kitimat Arm other than areas with high PAH concentrations such as Hospital Beach is reasonably safe. The maximum lifetime cancer risk estimates associated with males who consume crabs most regularly from the Kitamaat Village site were between 5.6 E-7 and 6.1 E-7, which is below the acceptable risk level. Similarly, the risk of cancer for the heaviest consumers of crabs from either Kildala Arm or Wathlsto Creek is below acceptable levels. Therefore, the consumption of crabs from areas that are not close to the source of PAH near the head of Kitimat Arm on the west side near the aluminium refinery can be considered to be safe in terms of PAH exposure. All consumers should avoid the regular consumption of crabs collected at Hospital Beach or other sites near the industrial area that are contaminated with PAH. The stochastic risk assessment has shown that the regular consumption of crabs collected from the Hospital Beach area poses an unacceptable lifetime cancer risk.

7.7.9 Further Studies

This risk assessment has focused on estimating the risk associated with the consumption of crab tissues by an aboriginal population, collected from an area known to be contaminated with PAH. Aboriginal populations in Canada are known to subsist to a great extent on wildlife obtained from their local environments. Therefore, a logical extension of this risk assessment would be to examine the risks associated with the consumption of other food organism collected from this region such as fish, shellfish, seals, deer, and other wildlife that are common dietary items. The Haisla Dietary Survey

(Kitamaat Village Council, 1996) has information related to the consumption of other types of foods other than crabs. If data could be obtained for the concentrations of PAH or other potentially toxic compounds in other species, the scope of the risk assessment could be expanded to encompass the consumption of all fish and wildlife species.

The uncertainty and sensitivity analyses have shown that it is important to have as much certainty in the input parameters as possible. Therefore, this risk assessment could be improved if more information was available for the most important input parameters such as exposure frequency, intake rate, and the concentrations of BaP-TEF in the muscle tissues of crabs collected from sites that are commonly used for crab fishing. The Haisla Dietary Survey has provided fairly detailed information on consumption of crab tissues that has been used in the model. However, more information on the concentration of PAH in the muscle of crabs could be obtained to reduce uncertainty in the risk assessment.

The concentrations of PAH in crab tissues may change over time depending on in the flux of PAH into or out of the aquatic environment. PAH levels may increase over time through increased industrial activities, or they may decrease due to reductions in sediment concentrations caused by biological metabolism or sediment burial. The risk assessment is based on concentrations determined or estimated in crab tissues collected from Kitimat Arm over a finite period of four years. Therefore, this risk assessment could be updated periodically with new information regarding concentrations of PAH in crab tissues and local population statistics that influence exposure.

The stochastic MEE model was implemented in Microsoft Excel® and Visual Basic® because this framework allowed us to program loops in the model and the

generation of randomly generated input distributions for each parameter. Crystal Ball is a software platform that is commonly used for stochastic risk assessment. However, at the time that the model was originally developed, Crystal Ball could not easily accommodate program loops. Since this time, Crystal Ball has been improved to incorporate this feature. Crystal Ball also has more tools that makes sensitivity and uncertainty analysis easier to perform. Therefore, if the current model was to be adapted for future risk assessments, it could be rewritten into the newest version of Crystal Ball. This would be beneficial if the model was expanded to incorporate all possible dietary sources of PAH.

7.8 Conclusions

A stochastic, micro-exposure event risk assessment model was implemented to examine the potential adverse health effects associated with the consumption of PAH contaminated crabs collected in Kitimat Arm. The stochastic model was used successfully to examine uncertainties in the deterministic risk assessment, and to incorporate inter-individual variability associated with a local aboriginal population situated in Kitamaat Village. The stochastic risk assessment showed that the deterministic risk approach (Chapter 6) yielded lifetime cancer risks that were a little more conservative than might be expected if inter-individual variation was incorporated into the risk assessment process. The stochastic risk assessment also corroborated the general level of risk (within an order of magnitude) that might be expected from the consumption of contaminated crab tissues collected from Kitimat Arm.

This stochastic risk assessment has indicated that members of the local aboriginal population or other local residents in the Kitimat region should avoid consuming crabs

from areas near the source of the PAH contamination such as Hospital Beach. The consumption of crabs from other sites in Kitimat Arm further away from the source of PAH contamination that are relatively "clean" such as Kildala Arm and Wathlsto Creek can be considered to be safe in terms of the lifetime risk of cancer due to the consumption of crab tissues.

REFERENCES

Airriess, C.N. and McMahon, B.R. (1992) Aminergic modulation of circulatory performance in the crab, *Cancer magister*. Comp. Phys. 11, 123-131.

Airriess, C.N. and McMahon, B.R. (1994) Cardiovascular adaptations enhance tolerance of environmental hypoxia in the crab *Cancer magister*. J. Exp. Biol. 190, 23-41.

Airriess, C.N. and McMahon, B.R. (1996) Short-term emersion affects cardiac function and regional haemolymph distribution in the crab *Cancer magister*. J. Exp. Biol. 199, 569-578.

Aldridge J.B. and Cameron, J.N. (1979) CO_2 Exchange in the blue crab, *Callinectes sapidus* (Rathbun). J. Exp. Zool. 207, 321-328.

Allen, W.V. (1971) Amino acid and fatty acid composition of tissues of the dungeness crab (*Cancer magister*). J. Fish. Res. Bd. Can. 28, 1191-1195.

Allen, W.V. (1972) Lipid transport in the dungeness crab, *Cancer magister* Dana. Comp. Biochem. Physiol. 43B, 193-207.

Anon. (1990) That crab meat might be toxic. US Water News September 1990 7(3), 13.

Andersen, M.E., Gargas, M.L., and Ramsey. J.C. (1984) Inhalation pharmacokinetics: Evaluating systemic extraction, total in vivo metabolism, and the time course of enzyme induction for inhaled styrene in rats based on arterial blood:inhaled air concentration ratios. Toxicol. Appl. Pharmacol. 73, 176-187.

Ariese F, Kok S.J., Verkaik, M., Gooijer, C., Velthorst, N.H., and Hofstaat, J.W. (1993) Synchronous fluorescence spectrometry of fish bile: A rapid screening method for the biomonitoring of PAH exposure. Aquat. Toxicol. 26, 273-286.

Autrup, H. (1979) Separation of water-soluble metabolites of benzo[*a*]pyrene from a cultured human colon. Biochem. Pharmacol. 28, 1727-1730.

Axys Group. (1995) Determination of polyaromatic hydrocarbons (PAH) including alkylated PAH in tissues. SOP # PH-T-01\ver.2. Axys Group, Sidney, BC, Canada.

Barra, J., Pequeux, A., and Humbert, W. (1983) A morphological study on gills of a crab acclimated to fresh water. Tissue and Cell 15 (4), 583-596.

Barron, M.G., Stehly, G.R. and Hayton, W.L. (1990) Review: Pharmacokinetic modeling in aquatic animals I. Models and concepts. Aquat. Toxicol. 18, 61-86.

Barry, T.M. (1996). Recommendations on the Testing and Use of Pseudo-Random Number Generators Used in Monte Carlo Analysis for Risk Assessment. Risk Analysis 16 (1), 93-105.

Baumard, P., Budzinski, H., Garrigues, P., Sorbe, J.C., Burgeot, T., and Bellocq, J. (1998) Concentrations of PAHs (Polycyclic Aromatic Hydrocarbons) in various marine organisms in relation to those in sediments and to trophic level. Mar. Pollut. Bull. 36, 951-960.

BCMELP (B.C. Ministry of Environment, Lands and Parks). (1995) Approved and working criteria for water quality – 1995. Water Quality Branch, Environmental Protection Department, B.C. Ministry of Environment, Lands and Parks.

Bjorseth, A., and Becher, G. (1986) PAH in work atmospheres: Occurence and determination. CRC Press, Boca Raton, Fla.

Black, J.J., Maccubbin, A.E., Johnston, C.J. (1988) Carcinogenicity of benzo-a-pyrene in rainbow trout resulting from embryo microinjection. Aquat. Toxicol. 13, 297-308.

Bliss, D.E. (1982) The biology of crustacean. Academic Press, New York, NY.

Bone, Q., Marshall, N.B., and Blaxter, J.H.S. (1995) Biology of fishes. Blackie, London.

Borgen, A., Davey, H. Castognoli, N., Crocker, T.T., Rasmussen, R.E., and Wang, I.Y. (1973) Metabolic conversion of benzo[a]pyrene by Syrian hamster liver microsomes and binding of metabolites to deoxyribonucleic acid. J. Med. Chem. 16, 502-506.

Bright, D.A., Cretney, W.J., Macdonald, R.W., Ikonomou, M.G. and S.L. Grundy. (1999) Differentiation of polychlorinated dibenzo-p-dioxin and dibenzofuran sources in coastal British Columbia, Canada. Environ. Toxicol. Chem. 18 (6), 1097-1108.

Bungay, P.M., Dedrick R.L., and Guarino, A.M. (1976) Pharmacokinetic modeling of the dogfish shark (*Squalus acanthias*): distribution and urinary and biliary excretion of phenol red and its glucuronide. Journal of Pharmacokinetics and Biopharmaceutics, 4 (5), 377-388.

Burmaster, D. E., and Crouch, E. A. C. (1997) Lognormal Distributions for Body Weight as a Function of Age for Males and Females in the United States, 1976-1980. Risk Analysis, 17 (4), 499-505.

Burmaster, D. E., and Anderson, P. D. (1994) Principles of Good Practice for the Use of Monte Carlo Techniques in Human Health and Ecological Risk Assessments. Risk Analysis, 14 (4), 477-481.

Burnett, L.E., De Fur, P.L., and Jorgensen, D. D. (1981) Application of the thermodilution technique for measuring cardiac output and assessing cardiac stroke volume in crabs. J. Exp. Zool. 218, 165-173.

Cleaver, F.C. (1957) Preliminary results of the coastal (*Cancer magister*) investigation. Department of Fisheries Washington State Biology Report 57A:47-82.

Collier, T.K., Singh, S.V., Awasthi, Y.C., and Varanasi, U. (1992) Hepatic xenobiotic metabolising enzymes in two species of benthic fish showing different prevalences of contaminant-associated liver neoplasms. Toxicol. Appl. Pharmacol. 113, 319-324.

Couch J.A., and Harshbarger J.C. (1985) Effects of carcinogenic agents on aquatic animals: an environmental and experimental overview. J Environ Sci Health, Part C, Environ. Carcinog. Rev. 3, 63-105.

Cretney W.J., Wong C.S., MacDonald R.W., Erickson P.E., and Fowler B.R. (1983) Polycyclic aromatic hydrocarbons in surface sediments and age-dated cores from Kitimat Arm, Douglas Channel and adjoining water-ways. In: RW MacDonald, ed, Proceedings of a Workshop on the Kitimat Marine Environment. Can Tech Rep of Hydrogr. Ocean Sci. 18, 162-195.

Crump, K.S. (1998) On summarizing group exposures in risk assessment: Is an arithmetic mean or a geometric mean more appropriate? Risk Analysis, 18 (3), 293-297.

Decisioneering, Inc. (1996) Crystal Ball Version 4.0 User Manual. Denver, Co..

De Wachter, B., and McMahon, B.R. (1996). Haemolymph flow distribution, cardiac performance and ventillation during moderate walking activity in *Cancer magister* (Dana) (Decapoda, Crustacea). J. Exp. Biol. 199, 627-633.

De Wachter, B. and Wilkens, J. L. (1996). Comparison of temperature effects on heart performance of the dungeness crab, *Cancer magister*, in vitro and in vivo. Biol. Bull. 190, 385-395.

Dunn B.P., and Fee, J. (1979). Polycyclic aromatic hydrocarbon carcinogens in commercial seafoods. J. Fish. Res. Bd. Can. 36, 1469-1476.

Eickhoff C.V., Cretney W, & Law F.C.P. (1995) Use of synchronous fluorescence spectrometry for detecting conjugated monohydroxypyrene in fish bile and dungeness crab haemolymph. Abstracts, 16th Annual Meeting SETAC, Vancouver, BC. November 5-9, 1995, p. 272.

Eickhoff, C.V., He, S.X., Gobas F.A.P.C., and Law, F.C.P. (2003a) Determination of polycyclic aromatic hydrocarbons in dungeness crabs (*Cancer magister*) near an aluminium smelter in Kitimat Arm, BC. Environ. Toxicol. Chem. 22, 50-58.

Eickhoff, C.V., Gobas, F.A.P.C., and Law, F.C.P. (2003b) Screening pyrene metabolites in the haemolymph of dungeness crabs (*Cancer magister*) using synchronous fluorescence spectrometry: method development and application. Environ. Toxicol. Chem. 22, 59-66.

Erickson, R.J., and McKim, J.M. (1990a) A simple flow-limited model for exchange of organic chemicals at fish gills. Environ. Toxicol. Chem. 9, 159-165.

Erickson, R.J., and McKim, J.M. (1990b) A model for exchange of organic chemicals at fish gills: flow and diffusion limitations. Aquat. Toxicol. 18, 175-198.

EVS. (1991) Integrated review: Alcan Marine Impact Studies Volume II: Polycyclic Aromatic Hydrocarbons (PAH). EVS Environment Consultants Ltd. North Vancouver, BC, Canada.

EVS. (1992) Integrated review: Alcan marine impact studies volume II: Polycyclic aromatic hydrocarbons (PAH). EVS Environment Consultants Ltd. North Vancouver, BC, Canada. 1991 Report No. 3/045-11.

EVS. (1995) 1994 Alcan Marine Monitoring Program Intensive Study; Raw Data Volume. EVS Consultants, North Vancouver, BC, Canada, Project No. 3/045-11.

EVS. (1998) Alcan Marine Monitoring Program 1997 Intensive Study. Final Draft, March 1998. EVS Environment Consultants, North Vancouver, BC, Canada, Report No. 3/045-18.

Fisheries and Oceans (DFO). (1989) Backgrounder. Shellfish Closures and Consumption Advisories: Coastal B.C. Sites. November 1989.

Fisheries and Oceans (DFO). (1996) Backgrounder. Reduced Dioxin Levels Lead to Further Crab Fishery Re-openings. April 18, 1996.

Fong, A.T., Hendricks, J.D., and Bailey, G.S. (1988) Carcinogenicity and DNA binding of benzo-a-pyrene and 7 12 dimethylbenz-a-anthracene in rainbow trout by controlled laboratory exposure. 196th American Chemical Society National Meeting, Los Angeles, California, USA, September 196:75.

Fragoso N.M., Hodson, P.V., Kozin, I.S., Brown, R.S., Parrott, J.L. (1999) Kinetics of mixed function oxygenase induction and retene excretion in retene-exposed rainbow trout (*Oncorhychus mykiss*). Environ Toxicol Chem 18 (10), 2268-2274.

Gelboin, H. (1980). Benzo[a]pyrene metabolism, activation, and carcinogenesis: role and regulation of mixed-function oxidases and related enzymes. Phys. Rev. 60 (4), 1106-1166.

Gerlowski, L.E., and Jain, R.K. (1983) Physiologically based pharmacokinetic modeling: principles and applications. J. Pharma. Sci. 72 (10), 1103-1127.

Gibaldi, M., and Perrier, D. (1975) Drugs and the Pharmaceutical Sciences Volume 1 Pharmacokinetics. Marcel Dekker, Inc., New York.

Gibson, R. (1979). The decapod hepatopancreas. Oceanogr. Mar. Biol. Ann. Rev., 17, 285-346.

Giger, W., Blumer, M. (1974) Polycyclic aromatic hydrocarbons in the environment; isolation and characterization by chromatography, visible, ultraviolet and mass spectrometry. Anal Chem 46, 1663-1671.

Gobas, F.A.P.C., and MacKay, D. (1986) Dynamics of hydrophobic organic chemical bioconcentration in fish. Env. Toxicol. Chem. 6, 495-504.

Gobas, F.A.P.C., Zhang, X., and Wells, R. (1993) Gastrointestinal Magnification; The mechanism of biomagnification and food chain accumulation of organic chemicals. Env. Sci. Technol. 27, 2855-2883.

Gobas, F.A.P.C., Pasternak, J.P. Lien, K. and Duncan R.K. (1998) Development & Field-Validation of a multi-media exposure assessment model for waste load allocation in aquatic ecosystems: application to TCDD and TCDF in the Fraser River Watershed. Environ. Sci. Tech. 32, 2442-2449.

Hale, R.C. (1988) Disposition of polycyclic aromatic hydrocarbons in blue crabs, *Callinectes sapidus*, from the Southern Chesapeake Bay. Estuaries 11 (4), 255-263.

Harris, G.E. (1999) Assessment of the Assimilative Capacity of Kitimat Arm, British Columbia: A Case Study Approach to the Sustainable Management of Environmental Contaminants. School of Resource and Environmental Management Ph.D. Thesis.

Hawkins, W.E., Walker, W.W., Overstreet, R.M., Lytle, T.F., Lytle, J.S. (1988) Dose-related carcinogenic effects of water-borne benzo[a]pyrene on livers of two small fish species. Ecotoxicol. Environ. Saf. 16, 219-231.

Hayes, A. Wallace, Ed. (1989) Principles and Methods of Toxicology Second Edition. Raven Press, New York.

Hayton, W.L. and Barron, M.G. (1990) Rate-Limiting Barriers to Xenobiotic Uptake by the Gill. Environ. Toxicol. and Chem. 9, 151-157.

Hellou, J., Upshall, C., Taylor, D., O'Keefe, P., O'Malley, V., and Abrajano, T. (1994) Unsaturated hydrocarbons in muscle and hepatopancreas of two crab species, *Chionoecetes opilio* and *Hyas coarctatus*. Mar. Pollut. Bull. 28, 482-488.

Humason A.W., and Gadbois, D.F. (1982) Determination of polynuclear aromatic hydrocarbons in the New York Bight Area. Bull Environ. Contam. Toxicol. 29, 645-650.

James, M.O. and Little, P.J. (1984) 3-Methylcholanthrene does not induce in vitro xenobiotic metabolism in spiny lobster hepatopancreas, or affect in vivo disposition of benzo[a]pyrene. Comp. Biochem.Physiol. 78C (1), 241-245.

James, M.O. (1987) Conjugation of organic xenobiotics in aquatic animals. Environ. Health. Perspect. 71, 91-103.

James, M.O. (1989) Biotransformation and disposition of PAH in aquatic invertebrates In: Metabolism of polycyclic aromatic hydrocarbons in the aquatic environment, Ed. U. Varanasi, CRC Press, Boca Raton FL.

James, M.O., Altman, A.H., Li, C-L, J. and Schell J.D. Jr. (1995) Biotransformation, hepatopancreas DNA binding and pharmacokinetics of benzo[a]pyrene after oral and parenteral administration to the American lobster, *Homarus americanus*. Chem.-Biol. Interact. 95, 141-160.

Jepson, GW., Hoover, D.K., Black, R.K., McCafferty, J.D., Mahle, D.A. and Gearhart, J.M. (1994) A partition coefficient determination method for nonvolatile chemicals in biological tissues. Fund. Appl. Toxicol. 22 (4), 519-524.

Jernström, B., Martinez, M., Meyer, D.J., and Ketterer, B. (1985) Glutathione conjugation of the carcinogenic and mutagenic electrophile (±)-7β,8α-oxy-7,8,9,10-tetrabhydrobenzo[a]pyrene catalysed by purified rat liver glutathione transferases. Carcinogenesis 6 (1), 85-89.

Kayal, S., and Connell, D.W. (1995) Polycyclic aromatic hydrocarbons in biota from the Brisbane River Estuary, Australia. Estuar. Coast. Shelf Sci. 40, 475-493.

Kennedy, C.J, Gill, K.A., and Walsh, P.J. (1989) Thermal modulation of benzo[a]pyrene metabolism by the gulf toad-fish Opsanus beta. Aquat. Toxicol. 15, 331-344.

Kennedy, C.J. (1990) Toxicokinetic studies of chlorinated phenols and polycyclic aromatic hydrocarbons in rainbow trout (*Oncohynchus mykiss*) Ph.D. Thesis, Simon Fraser University, B.C. Canada.

Keeran, W.S. and Lee, R.F. (1987) The purification and characterisation of glutathione S-transferase from the hepatopancreas of the blue crab, *Callinectes sapidus*. Arch. Biochem. Biophys. 255 (2), 233-243.

Kitamaat Village Council (1996) Haisla First Nation, Haisla Diet Study - Interim Report. (Unpublished Report). Prepared by Pamela Winquist, B.Sc. RDN. Revised June 1996,

Krahn, M.M., Burrows, D.G., MacLeod, W.D. Jr., and Malins, D.C. (1987) Determination of individual metabolites of aromatic compounds in hydrolyzed bile of English sole (*Parophrys vetulus*) from polluted sites in Puget Sound, Washington. Arch Environ. Contam. Toxicol. 16, 511-522.

Krahn, M..M.., Kittle, L.J. Jr., and MacLeod, W.D. Jr.. (1986) Evidence for exposure of fish to oil spilled into the Columbia River. Mar. Environ. Res. 20, 291-298.

Krahn, M..M.., Myers, M.S., Burrows, D.G., and Malins, D.C. (1984) Determination of metabolites of xenobiotics in the bile of fish from polluted waterways. Xenobiotica 14 (8), 633-646.

Krahn, M..M.., Rhodes, L.D., Myers, M.S., Moore, L.K., MacLeod, W.D. Jr., and Malins, D.C. (1986) Associations between metabolites of aromatic compounds in bile and the occurrence of hepatic lesions in English sole (*Parophrys vetulus*) from Puget Sound, Washington. Arch. Environ. Contam. Toxicol. 15, 61-67.

Law, F.C.P. and Gudiatis, J.A. (1994) A Preliminary Assessment of Human Health Risks due to Consumption of Fish Contaminated by Dioxins and Furans in the Fraser and Thompson Rivers. Chemosphere 28 (6), 1079-1086.

Law, F.C.P., Abedini, S. and Kennedy, C.J. (1991) A biologically based toxicokinetic model for pyrene in rainbow trout. Toxicol. Appl. Pharmacol. 110, 390-402.

Law, F.C.P. (1999) A physiologically based pharmacokinetic model for predicting the withdrawal period of oxytetracycline in cultured Chinook salmon (Onchorhychus tshawytscha). In Xenobiotics in Fish. Eds. Smith, D., Gingerich, W.H, and Beconi-Barker, M.G. Kluwer Academic/Plenum Publishers, New York. 105-121.

Lee, R.F., and Conner, J.W. (1982) Cytochrome P-450 dependent mixed function oxygenase systems in marsh crabs In Vernberg WB, Calabrese A, Thurberg FP, Vernberg FJ, eds, Physiological Mechanisms of Marine Pollutant Toxicity. Academic Press, New York, NY, USA, pp. 146-155.

Lee, R.F., Ryan, C., and Neuhauser, M.L. (1976) Fate of petroleum hydrocarbons taken up from food and water by the blue crab *Callinectes sapidus*. Mar. Biol. 37, 363-370.

Lemaire, P., Lemaire-Gony, S., Berhaut, J., and Lafaurie, M. (1992) The uptake, metabolism, and biological half-life of benzo[a]pyrene administered by force-feeding in sea bass (*Dicentrarchus labrax*). Ecotoxicol. Environ. Saf. 23, 244-251.

Li, C.J., and James, M.O. (1993) Glucose and sulfate conjugations of phenol, β-naphthol and 3-hydroxybenzo[*a*]pyrene by the American lobster (*Homarus americanus*). Aquat. Toxicol. 26, 57-72.

Li C.L.J., James M.O. (2000) Oral Bioavailability and Pharmacokinetics of Elimination 9-hydroxybenzo(a)pyrene and its Glucoside and Sulfate Conjugates After Administration to the American Lobster, Homarus Americanus. Toxicol. Sci., 57,75-86.

Lin, E.L.C., Cormier, S.M., and Racine, R.N. (1994) Synchronous fluorometric measurement of metabolites of polycyclic aromatic hydrocarbons in the bile of brown bullhead. Environ. Toxicol. Chem. 13 (5), 707-715.

Loke, M.L., Tjornelund, J., and Halling-Sorensen, B. (2002) Determination of the distribution coefficient (log Kd) of oxytetracycline, tylosin A, olaquindox and metronidazole in manure. Chemosphere 48 (3), 351-61.

Mackay, D., Shiu, W.Y., and Ma, K.C. (1991) Illustrated handbook of physical-chemical properties and environmental fate for organic chemicals. Volume II; Polynuclear aromatic hydrocarbons, polychlorinated dioxins, and dibenzofurans. Lewis Publishers, Ann Arbor, MI, USA.

Marion, S.A., Mathias, R.G., and Huynh, M.D. (1996) The distribution of crab hepatopancreas consumption in specific populations in Greater Vancouver. Unpublished report commissioned by Fisheries and Oceans (DFO).

Marsaglia, G. and Zaman, A. (1991) A New Class of Random Number Generators. Ann. Appl. Prob. 1 (3), 462-480.

McDonald, D.G., Wood, C..M., and McMahon, B.R. (1980). Ventilation and oxygen consumption in the dungeness crab, *Cancer magister*. J. Exp. Biol. 213, 123-136.

McElroy, A.E. and Sisson, J.D. (1989) Trophic transfer of benzo[a]pyrene metabolites between benthic marine organisms. Mar. Environ. Res. 28, 265-269.

McGaw, I.J., Airriess, C.N., and McMahon, B.R. (1994) Patterns of haemolymph-flow variation in decapod crustaceans. Mar. Biol. 121, 53-60.

McGaw, I.J., and McMahon, B.R. (1996) Cardiovascular responses resulting from variation in external salinity in the dungeness crab, Cancer magister. Phys. Zool. 69 (6), 1384-1401.

McGaw, I.J., Reiber, C.L., and Guadagnoli, J.A. (1999) Behavioral physiology of four crab species in low salinity. Biol. Bull. 196, 163-176.

McGaw, I.J., and McMahon, B.R. (2003) Balancing Tissue Perfusion Demands: Cardiovascular Dynamics of Cancer magister During Exposure to Low Salinity and Hypoxia. J. Exp. Zool. 295A, 57-70.

McGroddy S.E., and Farrington, J.W. (1995) Sediment porewater partitioning of polycyclic aromatic hydrocarbons in three cores from Boston Harbor. Massachusetts. Environ. Sci. Technol. 29, 1542-1550.

McLaughlin, M. (1998) UrandomLib: The Ultimate Macintosh Random-Number Generator. MacTech 14 (10). http://www.mactech.com/articles/mactech/Vol.14/14.10/URandomLib/index.html

McMahon, B.R., and Burnett, L.E. (1990) The crustacean open circulatory system: a reexamination. Phys. Zool. 63 (1), 35-71.

McMahon, B.R., McDonald, D. G. and Wood, C.M. (1979) Ventilation, oxygen uptake and haemolymph oxygen transport, following enforced exhausting activity in the dungeness crab, *Cancer magister*. J. Exp. Biol. 80, 271-285.

McMahon, B.R., Sinclair, F., Hassal, C. D., deFur, P.L., and Wilkes, P.R.H. (1978) Ventilation and control of acid-base status during temperature acclimation in the crab, *Cancer magister*. J. Comp. Physiol. 128, 109-116.

Michel, X.R., Beasse, C. and Narbonne, J.F. (1995) In vivo metabolism of benzo[a]pyrene in the mussel *Mytilus galloprovincialis*. Arch. Environ. Contam. Toxicol. 28, 215-222.

Morgan, M.G., and Henrion, M. (1990). Uncertainty, A Guide to Dealing with Uncertainty in Quantitative Risk and Policy Analysis, Cambridge University Press, NY, NY.

Morrison, H.A., Gobas, F.A.P.C., Lazar, R., Whittle, D.M., and Haffner, G.D. (1996) Development and verification of a bioaccumulation model for organic contaminants in benthic invertebrates. Environ. Sci. Tech. 30, 3377-3384.

Mothershead, R.F., Hale, R.C., and Graves, J. (1991) Xenobiotic compounds in blue crabs from a highly contaminated urban subestuary. Environ. Toxicol. Chem. 10 (10), 1341-1349.

Næs, K., Hylland, K., Oug, E., Förlin, L., and Ericson, G. (1999) Accumulation and effects of aluminium smelter-generated polycyclic aromatic hydrocarbons on soft-bottom invertebrates and fish. Environ. Toxicol. Chem. 18 (10), 2205-2216.

Namdari, R. (1994) Pharmacokinetics of pyrene and oxytetracycline in salmonids. M.Sc. Thesis. Simon Fraser University, B.C. Canada.

Namdari, R. (1998). A physiologically based toxicokinetic model of pyrene and its major metabolites in Starry flounder (*Platichthys stellatus*). Ph. D. Thesis. Simon Fraser University, B.C. Canada.

National Academy of Sciences (NAS) (1983) Risk Assessment in the Federal Government: Managing the Process. NAS, Washington, D.C. In: Paustenbach D.J. (2002) Human and Ecological Risk Assessment Theory and Practice. John Wiley and Sons Inc., NY.

National and Trends Program (2000). Mussel Watch Project http:// vertigo.hsrl. rutgers. edu/NST.html

Newman, M.C., Dixon, P.M., Looney, B.B., and Pinder, J.E. III. (1989) Estimating mean and variance for environmental samples with below detection limit observations. Water Res. Bull. 25, 905-916.

Nichols, J.W., McKim, J.M., Andersen, M.E., Gargas, M.L., Clewell, H.J., III and Erickson, R.J. (1990) A physicologically based toxicokinetic model for uptake and disposition of waterborne organic chemicals in fish. Toxicol. Appl. Pharm. 106, 433-447.

Nichols, J.W., McKim, J.M., Lien, G.J., Hoffman, A.D., Bertelsen, S.L. and Elonen, C.M. (1996) A physiologically based toxicokinetic model for dermal absorption of organic chemicals by fish. Fund. Appl. Toxicol. 31, 229-242.

Nisbet, I.C.T. and LaGoy, P.K. (1992) Toxic Equivalency Factors (TEFs) for Polycyclic Aromatic Hydrocarbons (PAHs). Reg. Tox. and Pharmacol. 16, 290-300.

Nishimoto, M., Yanagida, G.K., Stein, J.E., Baird, W.M., and Varanasi, U. (1992) The metabolism of benzo[a]pyrene by the English sole (*Parophrys vetulus*): comparison between isolated hepatocytes *in vitro* and liver *in vivo*.

Notari, R. E. (1980) Biopharmaceutics and Clinical Pharmacokinetics an Introduction Third Edition Revised and Expanded. Marcel Dekker Inc. New York.

O'Flaherty, E.J. (1987) Modeling: and introduction. In: Pharmacokinetics in Risk Assessment, Drinking Water and Health Volume 8. Workshop Proceedings. National Academy Press, Washington, D.C., 27-35.

Ontario Ministry of Environment (1997) Scientific Criteria Document for Multimedia Standards Development Polycyclic Aromatic Hydrocarbons (PAH) Part 1: Hazard Identification and Dose-Response Assessment. Queen's Printer for Ontario.

Ott, W. R. (1995) Environmental Statistics and Data Analysis. CRC Press Inc. Boca Raton, Florida.

Paine, M.D., Chapman, P.M., Allard, P.J., Murdoch, M.H., and Minifie, D. (1996) Limited bioavailability of sediment PAH near an aluminum smelter: contamination does not equal effects. Environ. Toxicol. Chem. 15 (11), 2003-2018.

Pancirov R.J., and Brown, R.A. (1977) Polynuclear aromatic hydrocarbons in marine tissues. Environ. Sci. and Technol. 11, 989-991.

Parsons A. H., Huntley, S.L., Ebert, E.S., Algeo, E.R., and Keenan, R.E. (1991) Risk Assessment for Dioxin in Columbia River Fish. Chemosphere 23 (11-12), 1709-1717.

Pauley, G.B., Armstrong, D.A., and Heun, T.W. (1986) Species profile: life histories and environemental requirements of coastal fishes and invertebrates (Pacific NW) dungeness crab. US Fish and Wildlife Service Biological Report 82(11.63).

Petry, T., Schmid, P., and Schlatter, C., (1996) The use of toxic equivalency factors in assessing occupational and environmental health risk associated with exposure to airborne mixtures of polycyclic aromatic hydrocarbons (PAHs). Chemosphere 32 (4), 639-648.

Porter P.S., Ward, R.C., and Bell, H.F. (1988) The detection limit: water quality monitoring data are plagued with levels of chemicals that are too low to be measured precisely. Environ. Sci. Technol. 22, 856-861.

Price, P. S., Curry, C. L., Goodrum, P. E., Gray, M. N., McCrodden, J. I., Harrington, N.W., Carlson-Lynch, H., and Keenan, R. E. (1996) Monte Carlo Modeling of Time-Dependent Exposures Using a Micro-exposure Approach," Risk Anal. 16 (3), 339-348.

PTI Environmental Services (1991) Puget Sound Estuary Studies Dioxin and furan concentrations in Puget Sound crabs, Draft. Prepared for U.S. Environmental Protection Agency, Doc. No. EPA 910/9-01-040. 43 pages plus appendices.

Ramsey, J. C., and Andersen, M. E. (1984). A physiologically based description of the inhalation pharmacokinetics of styrene in rats and humans. Toxicol. Appl. Pharmacol. 73, 159-175.

Santana Rodriguez J.J., Hernandez Garcia, J., Bernal Suarez, M.M., Bermejo Martin-Lazaro, A. (1993) Analysis of mixtures of polycyclic aromatic hydrocarbons in sea-water by synchronous fluorescence spectrometry in organized media. Analyst 118, 917-921.

Sato, A., and Nakajima. T. (1979) Partition coefficients of some aromatic hydrocarbons and ketones in water, blood, and oil. Brit. J. Ind. Med. 36, 231-234 in: Andersen, M.E., Gargas, M.L. and Ramsey, J.C. (1984) Inhalation pharmacokinetics: Evaluating systemic extraction, total in vivo metabolism, and the time course of enzyme induction for inhaled styrene in rats based on arterial blood:inhaled air concentration ratios. Toxicol. and Appl. Pharmacol. 73, 176-187.

Shugart, L., MacCarthy, J., Jimenez, B., and Daniels, J. (1987). Analysis of adduct formation in the bluegill sunfish (Lepomis macrochirus) between benzo[a]pyrene and DNA of the liver and haemoglobin of the erythrocyte. Aquat. Toxicol. 9, 319-325.

Sigma. (1994) Sigma quality control test procedure; enzymatic assay of β-glucosidase (EC 3.2.1.21) Sigma Chemical Company. Saint Louis, MI.

Simpson, C.D., Mosi, A.A., Cullen, W.R., and Reimer, K.J. (1996) Composition and distribution of polycyclic aromatic hydrocarbon contamination in surficial marine sediments from Kitimat Harbor, Canada. Sci. Total. Environ. 181, 265-278.

Simpson, C.D. (1997) Some aspects of the distribution and fate of polycyclic aromatic hydrocarbon contamination in the Kitimat fjord system. Ph.D. Thesis. University of British Columbia, BC, Canada.

Spacie, A., Landrum, P.F., and Leversee, G.J. (1983) Uptake, depuration, and biotransformation of anthracene and benzo[a]pyrene in bluegill sunfish. Ecotoxicol. Environ. Saf. 7, 330-341.

Stevens, B.G., Armstrong, D.A., and Hoeman, J.C. (1984) Diel activity of an estuarine population of dungeness crabs, *Cancer magister*, in relation to feeding and environmental factors. J. Crust. Biol. 4, 390-403.

Steward, A.R., Kandaswami, C., Chidambaram, S. Ziper, C. Rutkowski, J.P., and Sikka, H.C. (1991) Disposition and metabolic fate of benzo[a]pyrene in the common carp. Aquat. Toxicol. 20, 205-218.

Stroomberg, G.J., De Knecht, J.A., Ariese, F., Van Gestel, C.A.M., Velthorst, N.H. (1999) Pyrene metabolites in the hepatopancreas and gut of the isopod *Porcellio scaber*, a new biomarker for polycyclic aromatic hydrocarbon exposure in terrestrial ecosystems. Environ. Toxicol. Chem. 18 (10), 2217-2224.

Seubert, J.M. and Kennedy, C.J. (1997) The toxicokinetics of benzo[a]pyrene in juvenile coho salmon, Oncorhynchus kisutch, during smoltification. Fish Physiol Biochem. 16, 437-447.

Taylor, H.H., (1990) Pressure-flow characteristics of crab gills: implications for regulation of haemolymph pressure. Physiol. Zool. 63 (1), 72-89.

Thompson, K.M., Burmaster, D.E., and Crouch, E.A.C. (1992) Monte Carlo Techniques for Quantitative Uncertainty Analysis in Public Health Risk Assessments. Risk Anal. 12 (1), 53-63.

US EPA (U.S. Environmental Protection Agency) (1984) The EPA 600 Series Methods, Methods for the determination of organic compounds in industrial and municipal wastewater discharges. in: Guidelines Establishing Test Procedures for the Analysis of Pollutants under the Clean Water Act; Final Rule and Proposed Rule. 40 CFR Part 136. Fed. Reg. 49, 175-179.

US EPA (U.S. Environmental Protection Agency). (1989) Risk Assessment Guidance for Superfund Volume 1 Human Health Evaluation Manual (Part A) Interim Final.

US EPA (U.S. Environmental Protection Agency). (1991a) Drinking Water Criteria Document for PAH. Prepared by the Office of Health and Environmental Assessment, Environmental Criteria and Assessment Office, Cincinnati, OH for the Office of Water Regulations and Standards, Washington, DC.

US EPA (U.S. Environmental Protection Agency). (1991b) Risk Assessment: Technical Guidance Manual. EPA Region III Guidance on Handling Chemical Concentration Data Near the Detection Limit in Risk Assessments. URL: http://www.epa.gov/reg3hwmd/risk/guide3.htm.

US EPA (U.S. Environmental Protection Agency). (1994) Method 8290 Polychlorinated dibenzodioxins (PCDDs) and polychlorinated dibenzofurans (PCDFs) by high-resolution gas chromatography/high-resolution mass spectrometry (HRGC/HRMS) In Methods for Evaluating Solid Waste. SW-846. Washington DC, USA.

US EPA (U.S. Environmental Protection Agency). (1998) Integrated Risk Information System (IRIS) Benzo[a]pyrene Carcinogenicity Assessment for Lifetime Exposure URL: http: //www.epa.gov /ngispgm3 /iris/index.html Last Update: May 14, 1998.

van de Wiel, J.A.G., Fijneman, P.H.S., Duijf, C.M.P., Anzion, R.B.M., Theuws, J.L.G. and Bos, R.P. (1993) Excretion of benzo[a]pyrene and metabolites in urine and feces of rats: influence of route of administration, sex, and long-term ethanol treatment. Toxicology, 80, 103-115.

Varanasi, U., Nishimoto, M., Reichert, W.L., and Stein, J.E. (1982) Metabolism and subsequent covalent binding of benzo[a]pyrene to macromolecules in gonads and liver of ripe english sole (*Parophrys vetulus*). Xenobiotica 12 (7), 417-425.

Varanasi, U., Nishimoto, M., Reichert, W.L., and Eberhart, B.T. (1986). Comparative metabolism of benzo[a]pyrene and covalent binding to hepatic DNA in english sole, starry flounder, and rat. Cancer Res. 46, 3817-3824.

Vose, D. (1996) Quantitative Risk Analysis; A Guide to Monte Carlo Simulation Modelling. John Wiley and Sons, New York.

Welling, P.G. (1986) Pharmacokinetics processes and mathematics. ACS Monograph 185, American Chemical Society, Washington.

Wheatly, M.G., (1985) The role of the antennal gland in ion and acid-base regulation during hyposaline exposure of the dungeness crab *Cancer magister* (Dana). J. Comp. Physiol. B:155, 445-454.

Winquist, P., B.Sc., RDN. 1998. Personal communication.

Winston, G.W., Mayeaux, M.H. and Heffernan, L.M. (1998) Benzo[a]pyrene metabolism by the intertidal sea anemone, *Bundosoma cavernata*. Mar. Environ. Res. 45 (1), 89-100.

Wiseman, C.L.S. (1997) A risk balance analysis of dioxin and furan related shellfish closures for aboriginal costal communities in British Columbia. Research Project. Simon Fraser University, B.C. Canada.

Yates, F.E. (1978) Good manners in good modelling: mathematical models and computer simulations of physiological systems. Amer. J. of Phys. 3, R159-R160.

Yunker, M.B and Cretney, W.J. 1996. Dioxins and furans in crab hepatopancreas: use of principal components analysis to classify congener patterns and determine linkages to contamination sources. *In* M.R. Servos, K.R. Munkittrick, J.H. Carey, and G.J. van der Kraak (Eds.) Environmental Fate and Effects of Pulp and Paper Mill Effluents. St. Lucie Press, Delray Beach, FL. Pp. 315-325.

Yunker M.B., Cretney W.J., and Ikonomou M.G. 2002. Assessment of chlorinated dibenzo-p-dioxin and dibenzofuran trends in sediment and crab hepatopancreas from pulp mill and harbor sites using multivariate- and index-based approaches. Environ Sci Technol; 36 (9),1869-78.

Zaharko, D.S., Dedrick, R.L. and Oliverio, V.T. (1972) Prediction of the distribution of methotrexate in the sting rays *Dasyatidae sabina* and sayi by use of a model developed in mice. Comp. Biochem. Physiol. 42A, 183-194.

APPENDICES

Appendix A
Concentrations of PAH in Tissues of Crabs Collected in Kitimat Arm

Tables A-1 to A-6 present the concentrations of PAH determined in crab tissue samples. Non-detected concentrations are represented by the ESSDL, na = samples that were not analysed. Concentrations are ng/g wet weight.

Table A-1. Concentrations of PAH in hepatopancreas of crabs collected from Hospital Beach

Sample	ACN	PHEN	ANTH	FLR	PYR	BA	CRY	BF	BAP
KIT2-01	na	0.03	0.7	4.3	0.7	0.1	0.1	2.1	0.5
KIT2-02	na	0.1	1.0	6.8	1.2	8.7	12.3	4.2	0.2
KIT2-03	na	0.1	2.0	4.7	3.7	0.1	0.1	0.6	0.9
KIT2-04	na	0.04	2.1	3.8	1.2	0.1	0.1	1.3	1.4
KIT2-05	na	0.03	1.1	4.7	2.2	0.1	0.1	2.3	0.3
KIT2-06	na	0.04	1.5	5.6	1.1	4.6	5.2	2.3	0.3
KIT2-07	na	0.03	1.2	4.6	1.0	2.6	3.3	2.0	0.1
KIT2-08	na	0.04	1.3	3.5	1.4	0.1	0.7	1.4	0.1
KIT2-09	na	0.1	4.2	6.3	1.2	21.2	12.1	2.9	0.2
KIT2-10	na	0.03	0.1	0.7	0.6	0.2	0.5	0.8	0.5
KIT2-11	na	0.1	2.3	1.4	1.1	0.1	0.1	0.5	0.2
KIT2-12	na	0.0	0.8	1.9	1.1	0.2	0.7	1.5	4.5
KIT2-13	na	0.1	2.3	11.6	1.3	6.6	4.8	2.4	0.2
KIT2-14	na	0.03	3.7	4.4	2.4	0.1	0.2	1.4	1.1
KIT2-15	na	0.1	4.2	2.2	1.1	3.8	1.5	1.1	1.0
KIT2-16	na	0.03	1.6	1.7	0.5	0.1	1.3	1.1	0.8

Sample	ACN	PHEN	ANTH	FLR	PYR	BA	CRY	BF	BAP
KIT2-17	na	0.1	4.9	9.0	3.3	6.4	7.3	5.0	4.8
KIT2-18	na	0.1	7.8	15.4	1.3	9.4	7.0	2.3	0.3
KIT2-19	na	0.02	0.4	1.9	0.7	0.2	0.5	0.9	0.8
KIT2-20	na	0.05	2.9	6.7	0.1	12.1	15.6	4.6	1.4
KIT2-21	0.3	2.6	1.9	0.5	0.9	0.1	1.0	0.8	0.01
KIT2-22	9.4	3.3	1.5	16.8	3.5	0.0	0.5	0.8	6.3
KIT2-23	0.3	17.8	0.9	1.0	0.7	0.1	0.2	0.9	0.5
KIT2-24	0.0	1.7	0.1	1.4	0.8	0.3	0.5	0.7	0.7
KIT2-25	0.3	13.9	0.3	0.6	0.1	0.2	0.5	0.4	0.4
KIT2-26	0.4	21.1	0.6	0.9	1.0	0.1	1.7	0.7	0.4
KIT2-27	5.9	5.2	1.1	5.3	3.6	0.2	0.4	1.5	2.0
KIT2-28	0.3	19.3	0.9	0.7	0.9	0.1	0.7	0.9	0.4
KIT2-29	0.3	29.3	2.2	1.4	1.2	0.1	0.1	0.8	0.5
KIT2-30	0.3	30.8	2.0	3.7	0.9	0.1	2.9	2.1	0.3
KIT2-31	0.3	20.3	0.8	0.7	0.8	0.1	0.6	0.9	0.4
KIT2-32	0.1	31.9	1.0	1.0	0.8	0.2	0.6	0.3	0.3
KIT2-33	0.3	19.4	0.3	1.4	0.8	3.4	0.01	0.8	0.5
KIT2-34	6.6	4.5	1.1	4.1	1.9	0.1	4.1	1.8	2.5
KIT2-35	9.5	1.8	1.2	2.6	0.6	0.4	0.6	1.0	2.3
KIT2-36	2.1	1.2	0.6	0.2	1.0	0.2	0.1	0.1	0.5
KIT2-37	19	4.1	1.4	3.0	2.0	0.03	2.2	1.7	0.5
KIT2-38	2.6	2.7	1.2	13.3	0.9	0.1	3.4	1.7	0.3
KIT2-39	599	31.4	7.3	22.2	2.7	4.7	7.5	1.7	0.4
KIT2-40	77	4.3	3.0	0.4	0.5	2.2	2.1	1.1	0.4
KIT2-41	0.1	25.3	3.6	1.6	0.5	0.03	0.1	0.9	0.4
KIT2-42	8.5	5.8	1.7	11.4	5.0	1.0	3.9	2.4	1.7
KIT2-43	4.3	3.6	0.7	1.6	1.2	0.2	0.5	0.7	0.7
KIT2-44	0.6	35	0.9	1.1	1.9	0.2	1.0	1.1	0.5
KIT2-45	0.2	17	1.4	0.5	0.6	0.3	0.4	1.1	0.3
KIT2-46	8.8	3.0	0.7	1.2	0.9	0.3	0.5	0.1	0.7
KIT2-47	0.3	2.2	0.9	4.7	3.3	0.05	1.3	5.8	5.2

Sample	ACN	PHEN	ANTH	FLR	PYR	BA	CRY	BF	BAP
KIT2-48	0.1	7.5	12	12	0.3	0.2	2.1	1.9	1.4
KIT2-49	0.1	87	20	46	36	0.1	13	8.7	3.2
KIT2-50	0.4	3.9	1.4	3.4	2.9	0.04	0.7	2.4	0.1
KIT2-51	0.4	1.8	0.8	0.0	0.3	0.03	0.5	0.5	0.2
KIT2-52	0.5	6.2	14	10.5	1.1	0.1	14	2.7	0.1
KIT2-53	0.3	1.8	0.7	1.2	1.5	0.2	0.1	1.4	0.9
KIT2-54	0.3	4.1	2.0	1.6	1.9	0.02	0.5	1.1	0.7
KIT2-55	0.4	2.2	2.4	4.0	0.9	0.1	0.1	1.5	0.6
KIT2-56	0.4	3.5	1.7	4.9	6.0	0.05	0.5	4.8	0.4
KIT2-57	0.3	92	12	11	9.0	1.1	4.5	2.4	0.2
KIT2-58	0.1	1.1	0.6	0.7	0.5	0.1	0.6	0.5	0.1
KIT2-59	0.5	3.4	4.2	3.2	1.9	0.3	1.6	1.7	0.7
KIT2-60	0.6	1.9	2.0	1.2	0.7	0.1	0.3	1.2	0.7
KIT2-61	0.5	1.3	0.8	1.0	0.5	0.04	0.1	1.2	0.5
KIT2-62	0.6	30	6.2	42	33	5.4	26	11	0.1
KIT2-63	1.0	2.2	3.6	1.5	1.0	0.1	0.7	0.7	0.2
KIT2-64	0.4	232	43	429	211	52	340	0.3	0.3
KIT2-65	0.6	5.1	11	2.3	1.4	0.1	0.2	1.0	0.4
KIT2-66	0.5	3.6	4.2	5.2	1.2	0.1	2.9	1.5	0.8
KIT2-01	na	0.03	0.7	4.3	0.7	0.1	0.1	2.1	0.5
KIT2-02	na	0.1	1.0	6.8	1.2	8.7	12.3	4.2	0.2

Table A-2. Concentrations of PAH in hepatopancreas of crabs collected from Kitamaat Village site

Sample	ACN	PHEN	ANTH	FLR	PYR	BA	CRY	BF	BAP
KVC-01	na	2.1	1.9	0.4	0.4	0.1	0.1	0.4	0.3
KVC-02	na	6.8	0.8	1.9	1.5	0.1	0.2	0.6	0.4
KVC-03	na	1.7	0.4	0.3	0.4	0.3	0.4	0.3	0.2
KVC-04	na	2.0	0.7	0.4	0.6	0.2	0.5	0.5	0.3
KVC-06	na	2.1	0.6	0.9	0.9	0.1	0.1	0.5	0.3
KVC-07	na	2.3	1.8	0.8	0.8	0.4	0.9	0.4	0.4
KVC-08	na	1.2	0.3	0.04	0.04	0.1	0.3	0.3	0.2
KVC-08	na	0.0	0.4	0.2	0.4	0.2	0.4	0.5	0.4
KVC-09	na	2.2	0.9	0.8	0.8	0.2	0.5	0.5	0.3
KVC-10	na	1.8	0.6	0.4	0.6	0.2	0.5	0.5	0.3
KVC-11	na	2.5	1.1	1.0	0.7	0.1	0.1	0.5	0.1
KVC-12	na	2.5	0.8	0.9	0.7	0.0	0.1	0.6	0.4
KVC-13	na	1.9	2.0	0.6	0.7	0.3	0.9	0.5	0.4
KVC-14	na	1.7	0.5	0.5	0.6	0.2	0.5	0.5	0.4
KVC-15	na	2.2	0.4	0.4	0.7	0.3	0.6	0.4	0.3
KVC-16	na	2.4	0.1	0.6	0.7	0.3	1.3	0.8	0.4
KVC-17	na	2.5	1.2	1.2	1.0	0.3	0.8	0.6	0.4
KVC-18	na	4.6	2.7	2.2	1.6	0.1	0.8	0.7	0.4
KVC-19	na	1.7	0.7	0.6	0.6	0.3	0.7	0.5	0.4
KVC-20	na	1.5	0.5	0.5	0.5	0.2	0.8	0.5	0.3
KIT3-01	na	0.1	0.2	1.2	0.8	0.1	3.7	0.7	0.1
KIT3-02	na	0.1	0.7	0.4	0.5	0.1	0.4	0.1	0.2
KIT3-03	na	0.04	0.05	0.2	0.3	0.1	0.3	0.3	0.1
KIT3-04	na	0.1	0.2	0.4	0.3	0.1	0.7	0.5	0.3
KIT3-06	na	0.03	0.3	0.3	0.4	0.1	0.6	0.3	0.8
KIT3-08	na	0.1	0.3	0.8	0.5	0.1	1.0	0.5	0.2
KIT3-10	na	0.0	0.5	1.1	0.7	0.04	0.3	0.5	0.2
KIT3-11	na	0.1	0.3	0.4	0.7	3.1	1.7	0.7	0.2

Sample	ACN	PHEN	ANTH	FLR	PYR	BA	CRY	BF	BAP
KIT3-12	na	0.04	0.5	1.3	0.9	0.3	0.8	0.4	0.1
KIT3-13	na	0.1	0.2	0.6	0.5	0.01	0.6	0.3	0.3
KIT3-14	na	0.03	0.2	0.7	0.6	0.1	0.1	0.3	0.2
KIT3-15	na	0.1	1.1	0.2	0.2	0.1	0.1	0.3	0.4
KIT3-16	na	0.03	0.4	0.4	0.4	0.1	0.5	0.3	0.1
KIT3-17	na	0.05	1.9	0.5	0.5	0.3	0.9	0.4	0.2
KIT3-18	na	0.1	0.6	1.0	0.4	0.2	0.3	0.4	0.2
KIT3-19	0.4	0.7	0.1	0.5	0.4	0.4	0.4	0.4	0.2
KIT3-20	0.3	1.0	0.2	0.6	1.1	0.3	0.6	0.6	0.4
KIT3-21	0.2	1.2	0.04	0.5	0.5	0.2	0.5	0.4	0.3
KIT3-22	0.1	5.3	12.5	1.7	1.0	0.1	1.2	0.6	0.2
KIT3-23	0.4	7.6	4.2	4.3	2.4	0.04	0.01	0.3	0.4
KIT3-24	0.6	5.7	4.8	3.1	2.0	0.1	0.4	0.6	0.3
KIT3-25	0.5	2.8	0.5	0.8	0.6	0.2	0.5	0.6	0.5
KIT3-26	0.6	1.9	0.3	0.4	0.5	0.3	0.5	0.6	0.3
KIT3-27	0.4	2.9	3.6	1.7	1.3	0.1	0.7	0.6	0.2
KIT3-28	0.4	1.5	2.7	0.7	0.0	0.2	0.6	0.6	0.2
KIT3-29	0.5	1.2	0.2	0.5	0.1	0.2	0.4	0.5	0.2
KIT3-30	0.1	21	39	2.6	1.3	0.1	3.6	0.6	0.3
KIT3-31	0.4	1.8	0.8	0.6	0.2	0.1	0.9	0.4	0.2
KIT3-32	0.6	4.1	5.8	1.0	1.5	0.04	1.1	0.6	0.1
KIT3-33	0.4	6.0	12.1	0.2	0.2	0.1	0.1	0.4	0.2
KIT3-34	0.6	7.7	20	2.6	0.9	0.1	4.0	0.7	0.2
KIT3-35	0.5	5.7	3.1	2.0	1.4	0.1	0.7	0.7	0.2
KIT3-36	0.3	5.9	6.3	1.8	1.6	0.1	0.3	0.6	0.2

Table A-3. Concentrations of PAH in hepatopancreas of crabs collected from Wathlsto Creek site

Sample	ACN	PHEN	ANTH	FLR	PYR	BA	CRY	BF	BAP
KIT4-01	na	0.02	0.1	0.4	0.6	0.1	0.2	0.3	0.3
KIT4-03	na	0.02	0.6	0.0	0.0	0.1	0.4	0.3	0.3
KIT4-05	na	0.02	0.2	0.4	0.4	0.1	0.4	0.4	0.2
KIT4-06	na	0.05	0.05	0.3	0.5	0.1	0.4	0.3	0.2
KIT4-07	na	0.03	0.4	0.2	0.1	0.1	0.1	0.1	0.1
KIT4-08	na	0.01	0.1	0.1	1.1	0.1	0.3	0.3	0.4
KIT4-10	na	0.02	0.1	0.6	0.7	0.04	0.3	0.2	0.1
KIT4-11	na	0.02	0.2	0.6	0.6	0.1	0.3	0.2	0.2
KIT4-12	na	0.01	0.1	0.4	0.4	0.2	0.6	0.5	0.4
KIT4-13	0.4	0.05	0.3	0.6	0.5	0.3	0.7	0.3	0.3
KIT4-14	0.3	0.02	0.3	1.0	0.7	0.3	0.6	0.5	0.2
KIT4-15	0.3	0.1	0.2	0.5	0.6	0.3	0.6	0.5	0.3
KIT4-16	0.3	0.1	0.4	0.5	1.0	0.1	0.4	0.6	0.2
KIT4-17	0.5	1.0	0.1	0.5	0.5	0.3	0.2	0.4	0.3
KIT4-18	0.2	0.1	0.2	0.3	0.4	0.2	0.04	0.3	0.4
KIT4-19	0.6	2.4	0.4	0.5	0.4	0.2	0.4	0.5	0.2
KIT4-20	0.4	1.2	0.2	0.2	0.3	0.1	0.4	0.5	0.3

Table A-4. Concentrations of PAH in hepatopancreas of crabs collected from Kildala Arm site

Sample	ACN	PHEN	ANTH	FLR	PYR	BA	CRY	BF	BAP
KIL-01	0.6	2.1	0.2	1.1	1.0	0.8	0.3	2.3	2.6
KIL-02	0.2	2.4	0.2	1.3	1.0	0.4	0.4	0.9	0.9
KIL-03	0.1	1.2	0.0	0.4	0.5	0.1	0.4	0.3	0.3
KIL-04	0.2	0.1	1.6	0.7	0.7	0.3	0.2	0.9	0.9
KIL-05	0.3	0.5	0.2	0.1	0.4	0.1	0.4	0.6	0.8
KIL-06	0.3	1.2	0.1	0.3	0.5	0.2	0.2	0.3	0.4
KIL-07	0.1	1.5	0.1	0.4	0.6	0.1	0.3	0.4	0.3
KIL-08	0.2	0.1	0.1	0.8	1.0	0.2	0.5	0.4	0.2
KIL-09	0.2	1.7	0.1	0.3	0.5	0.2	0.1	0.4	0.3
KIL-10	0.1	0.8	0.1	0.6	0.5	0.2	0.4	0.4	0.3
KIL-11	0.2	0.1	0.1	0.3	0.6	0.2	0.6	0.3	0.2
KIL-12	0.2	1.2	0.1	0.5	0.8	0.2	0.6	0.3	0.3
KIL-13	0.2	1.5	0.1	0.4	0.4	0.1	0.1	0.5	0.2
KIL-14	0.4	1.6	0.1	0.2	0.4	0.2	0.1	0.4	0.3
KIL-15	0.2	1.4	0.1	0.2	0.7	0.1	0.7	0.6	0.2
KIL-16	0.4	1.2	0.1	0.4	0.4	0.04	0.3	0.4	0.1
KIL-17	0.6	1.4	0.1	0.05	0.5	0.1	0.5	0.4	0.1
KIL-18	0.4	1.0	0.1	0.3	0.3	0.2	0.5	0.4	0.1
KIL-19	0.5	1.5	0.02	0.2	0.6	0.1	0.3	0.4	0.1
KIL-20	0.5	1.6	0.02	0.1	0.4	0.1	0.4	0.4	0.1
KIL-21	0.4	0.9	0.03	0.1	0.3	0.1	0.3	0.4	0.2
KIL-22	0.5	1.6	0.1	0.3	0.1	0.1	0.4	0.4	0.1
KIL-23	0.5	1.6	0.1	0.1	0.2	0.1	0.1	0.2	0.1
KIL-24	0.6	1.6	0.0	0.1	0.3	0.1	0.4	0.3	0.2
KIL-25	0.5	1.5	0.0	0.4	0.1	0.1	0.4	0.4	0.3
KIL-26	0.5	2.2	0.1	0.4	0.5	0.1	0.4	0.4	0.1
KIL-27	0.6	1.8	0.1	0.1	0.04	0.1	0.5	0.3	0.1
KIL-28	0.5	1.0	0.04	0.3	0.3	0.1	0.3	0.3	0.2
KIL-29	0.5	1.7	0.1	0.3	0.4	0.1	0.2	0.3	0.2
KIL-30	0.4	1.0	0.1	0.2	0.2	0.2	0.9	0.3	0.2

Table A-5. Concentrations of PAH in hepatopancreas of crabs collected from Kitkiatka Inlet site

Sample	ACN	PHEN	ANTH	FLR	PYR	BA	CRY	BF	BAP
KIT-01	na	2.1	0.2	0.6	0.5	0.5	1.0	0.4	0.6
KIT-02	na	1.6	0.01	0.4	0.3	0.2	0.6	0.3	0.1
KIT-03	na	1.2	0.02	0.4	0.4	0.2	0.3	0.1	0.3
KIT-04	na	3.6	0.2	1.0	0.8	0.4	0.7	0.3	0.7
KIT-05	na	1.7	0.04	0.4	0.4	0.4	0.8	0.4	0.4
KIT-06	na	2.4	0.04	0.5	0.5	0.4	0.5	0.4	0.5
KIT-07	na	1.5	0.3	1.0	0.7	0.2	0.7	0.5	0.8
KIT-09	na	1.9	0.1	0.5	0.5	0.5	0.9	0.6	0.6
KIT-10	na	2.4	0.03	0.6	0.5	0.1	0.0	0.3	0.3
KIT-11	na	3.3	0.2	0.6	0.7	0.4	0.8	0.5	0.4
KIT-12	na	1.4	0.1	0.3	0.4	0.1	0.2	0.2	0.1
KIT-13	na	1.7	0.1	0.5	0.5	0.3	0.5	0.6	0.3
KIT-14	na	2.4	0.2	0.6	0.4	0.03	0.3	0.5	0.4
KIT-15	na	2.4	0.2	0.9	0.6	0.2	0.04	0.7	0.4

Table A-6. Concentrations of PAH in muscle of crabs collected from Hospital Beach and Kitamaat Village sites

Sample	PHEN	ANTH	FLR	PYR	BA	CRY	BF	BAP
KIT2-08M	1.2	0.1	0.4	0.4	0.1	0.4	na	0.1
KIT2-09M	1.4	0.2	0.5	0.4	0.1	0.4	na	0.1
KIT2-11M	1.3	0.1	0.3	0.3	0.2	0.3	na	0.3
KIT2-15M	1.3	1.1	0.3	0.3	0.1	0.2	na	0.2
KIT2-17M	1.5	0.2	0.5	0.5	0.3	0.4	na	0.8
KIT2-18M	1.1	0.9	0.4	0.3	0.2	0.3	na	0.3
KIT2-34M	1.2	0.1	0.6	0.0	0.1	0.4	na	0.6
KIT2-39M	1.1	0.4	0.2	0.3	0.0	0.3	0.2	0.2
KIT2-42M	1.5	0.1	0.6	0.6	0.2	0.5	na	0.7
KIT2-46M	1.3	0.2	0.3	0.4	0.2	0.3	na	0.3
KIT2-50M	11	3.1	2.7	2.3	0.0	1.5	na	1.2
KIT2-56M	3.6	0.1	1.4	2.5	0.0	0.3	0.2	0.2
KIT2-57M	11	1.6	0.6	0.9	0.0	0.6	0.2	0.3
KIT2-62M	2.1	0.4	1.0	1.0	0.1	0.2	0.4	0.5
KIT2-64M	12	2.7	11	6.0	2.4	8.9	6.1	5.8
KIT3-16M	1.0	0.0	0.3	0.4	0.2	0.2	na	0.2
KIT3-30M	1.5	0.7	0.2	0.2	0.0	0.1	0.0	0.0
KVC-07M	1.4	0.1	0.5	0.5	0.2	0.4	na	0.2
KVC-11M	1.1	0.1	0.2	0.2	0.1	0.2	na	0.2

Appendix B
Concentrations of Hydroxypyrene equivalents Determined by SFS

Table B-1 presents concentrations of 1-OH pyrene equivalents (1-OHP) determined in the haemolymph of crabs collected from sites in Kitimat Arm. Concentrations are expressed in ng pyrene equivalents/ml haemolymph.

Table B-1. Concentrations of 1-hydroxypyrene equivalents in haemolymph of crabs collected from Hospital Beach.

Sample	1-OHP	Sample	1-OHP	Sample	1-OHP	Sample	1-OHP
KIT2-02	0.34	KIT2-21	0.67	KIT2-37	0.93	KIT2-53	0.38
KIT2-05	0.83	KIT2-22	1.04	KIT2-38	1.05	KIT2-54	0.30
KIT2-06	0.37	KIT2-23	0.40	KIT2-39	3.19	KIT2-55	0.56
KIT2-07	0.70	KIT2-24	0.88	KIT2-40	1.09	KIT2-56	0.48
KIT2-08	0.52	KIT2-25	0.60	KIT2-41	0.28	KIT2-57	0.72
KIT2-09	0.22	KIT2-26	0.46	KIT2-42	1.01	KIT2-58	0.42
KIT2-10	0.26	KIT2-27	0.86	KIT2-43	0.24	KIT2-59	0.59
KIT2-11	0.46	KIT2-28	0.60	KIT2-44	0.34	KIT2-60	0.69
KIT2-12	0.54	KIT2-29	0.67	KIT2-45	0.35	KIT2-61	0.02
KIT2-13	1.65	KIT2-30	0.75	KIT2-46	0.36	KIT2-62	1.15
KIT2-14	0.60	KIT2-31	0.41	KIT2-47	0.57	KIT2-63	0.43
KIT2-15	0.54	KIT2-32	0.35	KIT2-48	3.37	KIT2-64	4.49
KIT2-16	0.62	KIT2-33	0.56	KIT2-49	0.18	KIT2-65	0.96
KIT2-17	0.63	KIT2-34	0.81	KIT2-50	0.72	KIT2-66	0.98
KIT2-18	2.00	KIT2-35	0.81	KIT2-51	0.37		
KIT2-19	0.47	KIT2-36	0.91	KIT2-52	2.16		

Table B-2. Concentrations of 1-hydroxypyrene equivalents in haemolymph of crabs collected from Kitamaat Village.

Sample	1-OHP	Sample	1-OHP	Sample	1-OHP	Sample	1-OHP
KVC-01	0.04	KVC-15	0.04	KIT3-12	0.27	KIT3-25	0.29
KVC-02	0.02	KVC-16	0.11	KIT3-13	0.18	KIT3-26	0.18
KVC-03	0.02	KVC-17	0.02	KIT3-14	0.69	KIT3-27	0.31
KVC-04	0.05	KVC-18	0.05	KIT3-15	0.64	KIT3-28	0.44
KVC-07	0.02	KVC-19	0.04	KIT3-16	0.23	KIT3-29	0.26
KVC-08	0.05	KIT3-01	0.28	KIT3-17	0.12	KIT3-30	0.32
KVC-08	0.07	KIT3-02	0.28	KIT3-18	0.18	KIT3-31	0.09
KVC-09	0.33	KIT3-03	0.41	KIT3-19	0.18	KIT3-32	0.33
KVC-10	0.07	KIT3-04	0.24	KIT3-20	0.38	KIT3-33	0.83
KVC-11	0.19	KIT3-06	0.21	KIT3-21	0.42	KIT3-34	0.23
KVC-12	0.10	KIT3-08	0.49	KIT3-22	0.45	KIT3-35	0.53
KVC-13	0.02	KIT3-10	0.33	KIT3-23	0.22	KIT3-36	0.10
KVC-14	0.06	KIT3-11	0.04	KIT3-24	0.25		

Table B-3. Concentrations of 1-hydroxypyrene equivalents in haemolymph of crabs collected from Wathlsto Creek.

Sample	1-OHP	Sample	1-OHP	Sample	1-OHP	Sample	1-OHP
KIT4-01	0.73	KIT4-07	0.68	KIT4-13	0.32	KIT4-17	0.32
KIT4-03	0.21	KIT4-08	0.58	KIT4-14	0.17	KIT4-18	0.25
KIT4-05	0.29	KIT4-10	0.27	KIT4-15	0.34	KIT4-19	0.09
KIT4-06	0.34	KIT4-12	0.53	KIT4-16	0.29	KIT4-20	0.21

Table B-4. Concentrations of 1-hydroxypyrene equivalents in haemolymph of crabs collected from Kildala Arm.

Sample	1-OHP	Sample	1-OHP	Sample	1-OHP	Sample	1-OHP
KIL-01	0.27	KIL-09	0.29	KIL-17	0.33	KIL-25	0.14
KIL-02	0.03	KIL-10	0.37	KIL-18	0.34	KIL-26	0.23
KIL-03	0.06	KIL-11	0.24	KIL-19	0.12	KIL-27	0.27
KIL-04	0.29	KIL-12	0.33	KIL-20	0.36	KIL-28	0.25
KIL-05	0.17	KIL-13	0.36	KIL-21	0.16	KIL-29	0.38
KIL-06	0.37	KIL-14	0.27	KIL-22	0.10	KIL-30	0.23
KIL-07	0.38	KIL-15	0.40	KIL-23	0.27		
KIL-08	0.51	KIL-16	0.32	KIL-24	0.15		

Table B-5. Concentrations of 1-hydroxypyrene equivalents in haemolymph of crabs collected from Kitkiatka Inlet.

Sample	1-OHP	Sample	1-OHP	Sample	1-OHP	Sample	1-OHP
KIT-03	0.19	KIT-06	0.18	KIT-10	0.42	KIT-13	0.43
KIT-04	0.35	KIT-07	0.98	KIT-11	0.25	KIT-14	0.22
KIT-05	0.14	KIT-09	0.15	KIT-12	0.25	KIT-15	0.30

Appendix C
PBTK Model Equations

The following mass balance differential and algebraic equations are used in the PBTK model to simulate the disposition of benzo[a]pyrene in the dungeness crab.

E.1 Equations which describe the uptake of benzo[a]pyrene into the gut compartment from the oral dose

First order uptake in the gut is described by the following functions:

$$UR_o = -k_o * e^{(-k_o t)} \quad \text{(E1)}$$

$$RSTOM = UR_o(A_o)D \quad \text{(E2)}$$

$$dCGT/dt = (QGT(CBA - CGT/RGT) + (-RSTOM))/VGT \quad \text{(E3)}$$

where UR_o and k_o are the first order uptake rate and rate constant respectively, RSTOM is the amount remaining in the stomach, A_o is the bioavailability constant and D is the dose. The concentration, partition coefficient and volume parameters for the gut are represented by CGT, RGT and VGT.

E.2 Equations which describe the uptake of benzo[a]pyrene into the gill compartment from the water

The flux of chemical in the gill is described by the following equations:

$$dCGL/dt = ((Qt\ (CBV - CGL/RGL) + (Cw(Qw)(A_b)UR))/VGL \quad \text{(E4)}$$

where the first order uptake function is described by:

$$UR = k_b * e^{(-k_b t)} \quad \text{(E5)}$$

The uptake of benzo[a]pyrene in the gill is regulated by the water concentration, Cw, venous haemolymph concentration, CBV, gill ventilation rate, Qw, cardiac output, Qt, partition coefficient, RGL first order uptake rate constant, k_b, and branchial bioavailability constant, A_b.

E 3 Equations which describe the concentration of benzo[a]pyrene in the remaining tissue compartments:

Arterial Haemolymph:

$$dCBA/dt = Qt(CGL/RGL - CBA)/VB \quad \text{(E6)}$$

where: CBA is the arterial haemolymph concentration, Qt is cardiac output, CGL is the gill compartment concentration, RGL is the gill partition coefficient, and VB is the volume of haemolymph compartment.

Hepatopancreas:

$$dCL/dt = (CBA(QL - QGT) + QGT(CGT/RGT) - QL(CL/RL) - ((Vmax(CL/RL)VL)/(Km + CL/RL)) - KL(CL/RL))/VL \quad \text{(E7)}$$

where: CL is the concentration of the hepatopancreas compartment, QL is the flow to the hepatopancreas, QGT is the flow to the gut, CGT is the concentration of the gut compartment, RGT is the gut partition coefficient, RL is the hepatopancreas partition coefficient, and the volume of the compartment is VL. Hepatic clearance is denoted by KL and the Michaelis-Menten rate constants are V_{max} and K_m.

Muscle:

$$dCM/dt = QM(CBA - CM/RM)/VM \quad \text{(E8)}$$

where: CM is concentration in the muscle, QM is the flow to the muscle, RM is the muscle partition coefficient, and VM is the volume of the muscle.

Carcass:

$$dCCdt = QC(CBA - CC/RC)/VC \quad \text{(E9)}$$

where: CC is the concentration of the carcass compartment, QC is the flow to the carcass, RC is the carcass partition coefficient, and VC is the volume of the carcass.

Bladder:

$$dCK/dt = (QK(CBA - CK/RK) - KK(CK/RK))/VK \quad \text{(E10)}$$

where: CK is the concentration in the bladder, QK is the flow to the bladder, KK is the bladder elimination constant, RK is the bladder partition coefficient, and VK is the volume of the compartment.

Venous Haemolymph:

$$dCBV/dt = (QL(CL/RL) + QM(CM/RM)$$

$$+ QC(CC/RC) + QK(CK/RK) - (QT)(CBV))/Qt \quad \text{(E11)}$$

where: CBV is the concentration in the venous haemolymph.

Appendix D
Visual Basic Code for Micro-exposure Event Stochastic Risk Assessment Model

The Visual Basic® macro that is built into the Excel® spreadsheet for calculating stochastic micro-exposure event risk estimates is presented below.

Model Code

```
'Monte Carlo Modelling of time-Dependent Exposures Using a Micro-exposure event
approach for ingestion of crab.
'This model is the result of a labour of love of computer modelling by Thomas
Achenbach and Curtis Eickhoff, and the lab and field work of Curtis Eickhoff
'This model is copyright ©1998-2004 and may be used and distributed for educational
purposes only.
'This Model contains code from other sources.
'The normal distribution function is from code by Dr. Michael P. McLaughlin from his
Urandom library which is a Macintosh implementation of Ultra pseudo-random number
generator by Dr. George Marsaglia and co – workers in the Dept. of Statistics, Florida
State University
'information on Urandom can be found at
http://www.mactech.com/articles/mactech/Vol.14/14.10/URandomLib/index.html

Option Explicit
Dim Bodywtaverage As Single
Dim a As Single, dose As Single, bodyweight As Single,
bodywtsum As Single, maxpeople As Integer, gender As Boolean
Dim age As Integer, femalepercent As Single, gmaleagemean As
Integer, gmaleagesd As Integer
Dim gfemaleagemean As Integer, gfemaleagesd As Integer
Const male = 1
Const female = 0
Dim gcrabmassmean As Single, gcrabmassSD As Single,
ghcrabconcmean As Single, ghcrabconcSD As Single,
gmcrabconcmean As Single, gmcrabconcSD As Single
Dim gSchldIR As Single, musclepercent As Single,
hepatopercent As Single
Dim gSjuvIR As Single, gSadltIR As Single, gSmturIR As
Single, gwchldIR As Single, gwjuvIR As Single, gwadltIR As
Single, gwmturIR As Single
Dim gmchldmean As Single, gmchldsd As Single, gmjuvmean As
Single, gmjuvsd As Single, gmadltmean As Single, gmadltsd As
Single
```

```
Dim gmmturmean As Single, gmmtursd As Single, gfchldmean As
Single, gfchldsd As Single, gfjuvmean As Single, gfjuvsd As
Single, gfadltmean As Single, gfadltsd As Single, gfmturmean
As Single, gfmtursd As Single
Dim ghconcmax As Single, ghconcmin As Single, gmconcmax As
Single, gmconcmin As Single, gcrabmassmin As Single,
gcrabmassmax As Single
Dim CV As Single
Dim ageoption As Integer
Dim siteindex As Integer
Dim risk As Single, csf As Single, cf As Single
Dim averageintake As Single

Dim Ran0Y As Double
Dim Ran0V(97) As Double

Dim aa, m, q, r As Integer
Dim invm As Double
Dim rndindex As Integer

Private Sub initialize()

'Initial parameters

rndindex = Range("rndindex")
maxpeople = Range("maxpeople")
musclepercent = Range("musclepercent")
hepatopercent = Range("hepatopercent")
femalepercent = Range("femalepercent")
'Range("age").Value = femalepercent
CV = Range("CV").Value
csf = Range("csf").Value
cf = Range("cf").Value

'this defines a named range of cells used for storing the
output
           Names.Add "LADDdata", "=output!R2C2:R" &
maxpeople + 1 & "C" & 6 & ""
  siteindex = Range("siteindex")

gcrabmassmean = Range("crabmassmean")
gcrabmassSD = Range("crabmassSD")
gcrabmassmin = Range("crabmassmin")
gcrabmassmax = Range("crabmassmax")

ghcrabconcmean = Range("crabconcdata").Cells(1,
siteindex).Value
ghcrabconcSD = Range("crabconcdata").Cells(4,
siteindex).Value
gmcrabconcmean = Range("crabconcdata").Cells(1, siteindex +
4).Value
```

```
gmcrabconcSD = Range("crabconcdata").Cells(4, siteindex +
4).Value
ghconcmax = Range("crabconcdata").Cells(3, siteindex).Value
ghconcmin = Range("crabconcdata").Cells(2, siteindex).Value
gmconcmax = Range("crabconcdata").Cells(3, siteindex +
4).Value
gmconcmin = Range("crabconcdata").Cells(2, siteindex +
4).Value

gmaleagemean = Range("maleagemean")
gmaleagesd = Range("maleagesd")
gfemaleagemean = Range("femaleagemean")
gfemaleagesd = Range("femaleagesd")
gmchldmean = Range("mchldmean")
gmchldsd = Range("mchldsd")
gmjuvmean = Range("mjuvmean")
gmjuvsd = Range("mjuvsd")
gmadltmean = Range("madltmean")
gmadltsd = Range("madltsd")
gmmturmean = Range("mmturmean")
gmmtursd = Range("mmtursd")
gfchldmean = Range("fchldmean")
gfchldsd = Range("fchldsd")
gfjuvmean = Range("fjuvmean")
gfjuvsd = Range("fjuvsd")
gfadltmean = Range("fadltmean")
gfadltsd = Range("fadltsd ")
gfmturmean = Range("fmturmean")
gfmtursd = Range("fmtursd")
gSchldIR = Range("SchldIR")
gSjuvIR = Range("SjuvIR")
gSadltIR = Range("SadltIR")
gSmturIR = Range("SmturIR")
gwchldIR = Range("wchldIR")
gwjuvIR = Range("wjuvIR")
gwadltIR = Range("wadltIR")
gwmturIR = Range("wmturIR")
ageoption = Range("ageoption")
End Sub

Private Sub MainCalc(IR As Single)
Dim crab As Single, muscle As Single, hepato As Single,
tCrabmass As Single
Dim Cmcrab As Single, Chcrab As Single, Muscleconc As
Single, Hepatoconc As Single

tCrabmass = 0
Do
    crab = crabmass
    Cmcrab = crabmconc
    Chcrab = crabhconc
```

```
    muscle = crab * musclepercent
    hepato = crab * hepatopercent
    'if concentration is different in muscle and hepato then
change this

    Muscleconc = Cmcrab '* muscle
    Hepatoconc = Chcrab '* hepato

    dose = dose + muscle * Muscleconc + hepato * Hepatoconc
    tCrabmass = tCrabmass + (muscle + hepato) * CV

Loop Until tCrabmass >= IR
End Sub

Private Function crabmass()
'make function get crab mass

crabmass = lograndom(gcrabmassmean, gcrabmassSD,
gcrabmassmin, gcrabmassmax) 'put proper values here

End Function

Private Function crabhconc()
'make function get crab Concentration

crabhconc = lograndom(ghcrabconcmean, ghcrabconcSD,
ghconcmin, ghconcmax)

If crabhconc < 0 Then crabhconc = 0
End Function
Private Function crabmconc()
'make function get crab Concentration

crabmconc = lograndom(gmcrabconcmean, gmcrabconcSD,
gmconcmin, gmconcmax)

If crabmconc < 0 Then crabmconc = 0
End Function
Private Function getgender()
Dim a As Single

getgender = female
Randomize
a = Rnd
If a > femalepercent Then getgender = male
'Make function get gender

End Function

Private Function getage(gender)
'make function get age
```

```
'add stuff here if this is not a normal distribution
    Select Case gender
        Case male
        'get age using male data
        getage = Int(random(gmaleagemean, gmaleagesd, 0,
75))
        Case female
        'get age using female data
        getage = Int(random(gfemaleagemean, gfemaleagesd, 0,
75))
     End Select

End Function

Private Function getbodywt(gender, age)

  Select Case gender
     'get bodywt using male age
        Case male
            Select Case age
                Case 1 To 11
                     getbodywt = lograndom(gmchldmean,
gmchldsd, 18, 45)
                Case 12 To 17
                     getbodywt = lograndom(gmjuvmean,
gmjuvsd, 43, 118)
                Case 18 To 49
                     getbodywt = lograndom(gmadltmean,
gmadltsd, 64, 126)
                Case Is > 49
                     getbodywt = lograndom(gmmturmean,
gmmtursd, 76, 108)

            End Select

        'get bodywt using female age
        Case female

        Select Case age
                Case 1 To 11
                     getbodywt = lograndom(gfchldmean,
gfchldsd, 21, 52)
                Case 12 To 17
                     getbodywt = lograndom(gfjuvmean,
gfjuvsd, 39, 60)
                Case 18 To 49
                     getbodywt = lograndom(gfadltmean,
gfadltsd, 55, 100)
                Case Is > 49
                     getbodywt = lograndom(gfmturmean,
gfmtursd, 64, 102)
```

```
            End Select
     End Select
End Function

Private Sub getnewperson(gender, age, bodyweight)
    gender = getgender
    Do
    age = getage(gender)
    Loop Until age > 0
    Do
    bodyweight = getbodywt(gender, age)
    Loop Until bodyweight > 0

End Sub
Private Function NewsummerIR(gender)
Dim probability As Single
    Randomize
    probability = Int((100 - 0 + 1) * Rnd)
    Select Case gender
    Case female
        Select Case probability
            Case 0 To 7
            NewsummerIR = 59
            Case 8 To 20
            NewsummerIR = 104
            Case 21 To 27
            NewsummerIR = 118
            Case 28 To 73
            NewsummerIR = 237
            Case 74 To 80
            NewsummerIR = 327
            Case 81 To 100
            NewsummerIR = 710
        End Select
    Case male
      Select Case probability
            Case 0 To 3
            NewsummerIR = 59
            Case 4 To 14
            NewsummerIR = 118
            Case 15 To 28
            NewsummerIR = 237
            Case 29 To 36
            NewsummerIR = 327
            Case 37 To 56
            NewsummerIR = 473
            Case 57 To 92
            NewsummerIR = 710
            Case 93 To 94
            NewsummerIR = 946
```

```
            Case 95 To 100
            NewsummerIR = 1420
        End Select
    End Select
End Function
Private Function summerexposurefr(gender)
Dim probability As Single
    Randomize
    probability = Int((100 - 0 + 1) * Rnd)
    Select Case gender
    Case female
        Select Case probability
            Case 0 To 54
            summerexposurefr = 0
            Case 55 To 62
            summerexposurefr = 1
            Case 63 To 85
            summerexposurefr = 2
            Case 86 To 98
            summerexposurefr = 4
            Case 99 To 100
            summerexposurefr = 8
        End Select
    Case male
      Select Case probability
            Case 0 To 31
            summerexposurefr = 0
            Case 32 To 51
            summerexposurefr = 1
            Case 52 To 75
            summerexposurefr = 2
            Case 76 To 87
            summerexposurefr = 3
            Case 88 To 97
            summerexposurefr = 4
            Case 98 To 100
            summerexposurefr = 8
        End Select
    End Select
End Function
Private Function NewWinterIR(gender)
Dim probability As Single
    Randomize
    probability = Int((100 - 0 + 1) * Rnd)
    Select Case gender
    Case female
        Select Case probability
            Case 0 To 4
            NewWinterIR = 15
            Case 5 To 18
            NewWinterIR = 59
```

```
            Case 19 To 39
            NewWinterIR = 118
            Case 40 To 68
            NewWinterIR = 237
            Case 69 To 71
            NewWinterIR = 327
            Case 72 To 93
            NewWinterIR = 473
            Case 94 To 96
            NewWinterIR = 654
            Case 97 To 100
            NewWinterIR = 710
        End Select
    Case male
      Select Case probability
            Case 0 To 7
            NewWinterIR = 59
            Case 8 To 14
            NewWinterIR = 104
            Case 15 To 24
            NewWinterIR = 118
            Case 25 To 48
            NewWinterIR = 237
            Case 49 To 62
            NewWinterIR = 327
            Case 63 To 83
            NewWinterIR = 473
            Case 84 To 86
            NewWinterIR = 654
            Case 87 To 97
            NewWinterIR = 946
            Case 98 To 100
            NewWinterIR = 1420
        End Select
    End Select
End Function
Private Function Winterexposurefr(gender)
Dim probability As Single
    Randomize
    probability = Int((100 - 0 + 1) * Rnd)
    Select Case gender
    Case female
        Select Case probability
            Case 0 To 42
            Winterexposurefr = 0
            Case 43 To 76
            Winterexposurefr = 1
            Case 77 To 94
            Winterexposurefr = 2
            Case 94 To 100
            Winterexposurefr = 3
```

```
        End Select
    Case male
      Select Case probability
            Case 0 To 48
            Winterexposurefr = 0
            Case 49 To 69
            Winterexposurefr = 1
            Case 70 To 86
            Winterexposurefr = 2
            Case 87 To 95
            Winterexposurefr = 3
            Case 96 To 98
            Winterexposurefr = 4
            Case 99 To 100
            Winterexposurefr = 8
        End Select
    End Select
End Function
Private Function summerIR(age As Integer)
    'function to determine summerIR
    Select Case age
                Case 1 To 11
                     summerIR = gSchldIR
                Case 12 To 17
                     summerIR = gSjuvIR
                Case 18 To 49
                     summerIR = gSadltIR
                Case Is > 49
                     summerIR = gSmturIR
            End Select
End Function

Private Function WinterIR(age As Integer)
'function to determine winterIR
    Select Case age
                Case 1 To 11
                     WinterIR = gwchldIR
                Case 12 To 17
                     WinterIR = gwjuvIR
                Case 18 To 49
                     WinterIR = gwadltIR
                Case Is > 49
                     WinterIR = gwmturIR

            End Select
End Function

Sub Main()
Cells(2, 1).Value = Now
Dim IR As Single, people As Integer, startage As Integer,
count As Integer
```

```
   'initialize all the variables
    initialize
    'set people to zero hence we are starting the model
    people = 0

    'This DO loop does the life cycles of the number of
persons defined on the spreadsheet
    Do
        people = people + 1
        getnewperson gender, age, bodyweight

        'checks to see if we want to start our population as
babies

        If ageoption = True Then age = 1
        startage = age
        dose = 0
        bodywtsum = 0
        averageintake = 0

        'This DO loop does the life cycle of a person till
they are 76
        Do

        'If the age is 12, 18 or 49 we need to find a new
body weight
        Select Case age
                Case 12, 18, 49
                     bodyweight = getbodywt(gender, age)

            End Select

        'add bodyweight for calculation of risk
        bodywtsum = bodywtsum + bodyweight
        'Determine summer intake rate

        IR = 0
        For count = 1 To 6
        IR = IR + NewsummerIR(gender) *
summerexposurefr(gender)
        Next count
        MainCalc (IR)
        averageintake = averageintake + IR

        'Determine winter intake rate

         IR = 0
        For count = 1 To 6
        IR = IR + NewWinterIR(gender) *
Winterexposurefr(gender)
        Next count
```

```
        MainCalc (IR)
        averageintake = averageintake + IR
        age = age + 1

        'age is 76 since we want to include the 75 th year

        Loop Until age >= 76

        If age <> startage Then
        Bodywtaverage = bodywtsum / (age - startage)
        averageintake = averageintake / (age - startage)
        Else '<-this else is here to catch people who
started off at age 75
        Bodywtaverage = bodywtsum
        averageintake = averageintake
        End If

    DetermineLADD people
    Loop Until people = maxpeople
    Cells(3, 1).Value = Now
End Sub
Private Sub DetermineLADD(people As Integer)
Dim ladd As Single
'is this bodywtaverage or bodywtsum
    ladd = 1 / (75 * 365) * 1 / Bodywtaverage * dose
    ' add a storage routine for storing LADD (array or on
spreadsheet

    Select Case gender

                Case False
                     Range("LADD").Cells(people, 1).Value =
"female"
               Case Else
                    Range("LADD").Cells(people, 1).Value =
"male"

            End Select

   Range("LADD").Cells(people, 2).Value = ladd
   risk = ladd * csf * cf
Range("LADD").Cells(people, 3).Value = risk
Range("LADD").Cells(people, 4).Value = averageintake
Range("ladd").Cells(people, 5).Value = crabmconc
Range("ladd").Cells(people, 6).Value = crabhconc
End Sub
Function random(mean, sd, min, max)
Dim sigma, zeta As Double

Select Case rndindex
 Case 3
```

```
Case Else
 random = normal(mean, sd, min, max)
 End Select
End Function
Private Function normal(mean, sd, min, max)
Dim u, v, r, sigma, zeta As Single, z As Double
Do
Do
Select Case rndindex

Case 1
      u = -1 + 2 * Rnd
      v = -1 + 2 * Rnd
Case 2
      u = -1 + 2 * RandShuffle(1)
      v = -1 + 2 * RandShuffle(1)

End Select

      '{see if it is in the unit circle  }
      r = u * u + v * v
 Loop Until (r < 1 And r <> 0)
  z = u * Sqr(-2# * Log(r) / r)
normal = Exp(sd * z + mean)
 Loop Until (normal < max) And (normal > min)

End Function

Function lograndom(mean, sd, min, max)
 Select Case rndindex
 Case 3

'Range("crystalballrndoutput").Activate
'cb.DefineAssumND cbDfaLognormal, mean, sd, min, max
'lograndom = Range("crystalballrndoutput").Value
Case Else
 lograndom = lognormalcalc(mean, sd, min, max)
 End Select
End Function
Function lognormalcalc(mean, sd, min, max)
'This function returns a random number from a lognormal
distribution.

 'One thing to note is that the incoming mean and SD are
arithmic and we convert to normal distribution return log

Dim u, v, r, normal, sigma, zeta As Single, z As Double

'this code here converts from arithmic to normal
```

```
sigma = Sqr(Log(1 + sd ^ 2 / mean ^ 2))
zeta = Log(mean) - 0.5 * sigma ^ 2

Do
Do
Select Case rndindex

Case 1
      u = -1 + 2 * Rnd
      v = -1 + 2 * Rnd
Case 2
      u = -1 + 2 * RandShuffle(1)
      v = -1 + 2 * RandShuffle(1)


End Select

      '{see if it is in the unit circle  }
      r = u * u + v * v
 Loop Until (r < 1 And r <> 0)
  normal = u * Sqr(-2# * Log(r) / r)
  lognormalcalc = Exp(sigma * normal + zeta)
 Loop Until (lognormalcalc < max) And (lognormalcalc > min)
End Function

Sub testtest()
Dim i As Integer, j As Integer, probability As Integer,
crabmass As Single

  Randomize

  rndindex = Range("rndindex")

  RandShuffle (-3)
  For j = 1 To 1
  For i = 1 To 1


    'crabmass = newlog(1.191, 1.773, 0.03, 9.907)
    'Range("crystalballrndoutput").Activate
    'cb.DefineAssumND cbDfaLognormal, 1.191, 1.773, , 0.03,
9.9, "Fred"

    'crabmass = lograndom(1.191, 1.773, 0.03, 9.907)
    'crabmass = newlog(0.288, 0.188, 0.013, 0.843)
Cells(i, j).Value = crabmass
Next i
Next j
End Sub
```

```
'this function generates a random number from a normal
distribution with a Mean and SD
'This is the old method of use
Private Function oldrandom(mean, sd, min, max)
Dim n As Single, j As Integer
Do
Randomize
n = 0
For j = 1 To 12
n = n + Rnd
Next j
random = (n - 6) * sd + mean
Loop Until (random < max) And (random > min)

End Function
Private Function oldlograndom(mean, sd, min, max)
Dim n As Double, j As Integer, lsd As Double, lmean As
Double, lrandom As Double
'remember in visual basic log = ln

lsd = Sqr(Log(1 + sd ^ 2 / mean ^ 2))
lmean = Log(mean) - 0.5 * lsd ^ 2
Randomize
Do
n = 0
For j = 1 To 12
n = n + Rnd
Next j
lrandom = (n - 6) * lsd + lmean
lograndom = Exp(lrandom)
 Loop Until (lograndom < max) And (lograndom > min)
End Function


'this function stores 100 random numbers and then picks and
replaces that random number, this prevents any artefacts of
the newly
'generated number having dependencies on the previous number
which is known to occur in Excel's Random number generator

Function RandShuffle(idum As Integer)
    Dim dum As Double
    Dim j As Integer
    If idum < 0 Then
        Randomize (-idum)
        For j = 1 To 97
            dum = Rnd()
        Next
        For j = 1 To 97
            RanOV(j) = Rnd()
        Next
```

```
        Ran0Y = Rnd()
    End If
    Ran0Y = Rnd()
    j = 1 + Int(97 * Ran0Y)
    If (j > 97) Or (j < 1) Then
        MsgBox "Error"
    End If
    Ran0Y = Ran0V(j)
    RandShuffle = Ran0Y
    Ran0V(j) = Rnd()
End Function
```